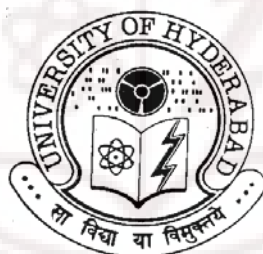


# **STRUCTURAL AND THERMAL ANALYSIS OF ORGANIC SOLIDS**

**A Thesis  
Submitted for the Degree of  
Doctor of Philosophy**

**By  
BIPUL CH. SARMA**



**School of Chemistry  
University of Hyderabad  
Hyderabad 500 046  
India**

**July 2009**

# **STRUCTURAL AND THERMAL ANALYSIS OF ORGANIC SOLIDS**

**A Thesis  
Submitted for the Degree of  
Doctor of Philosophy**

**By  
BIPUL CH. SARMA**



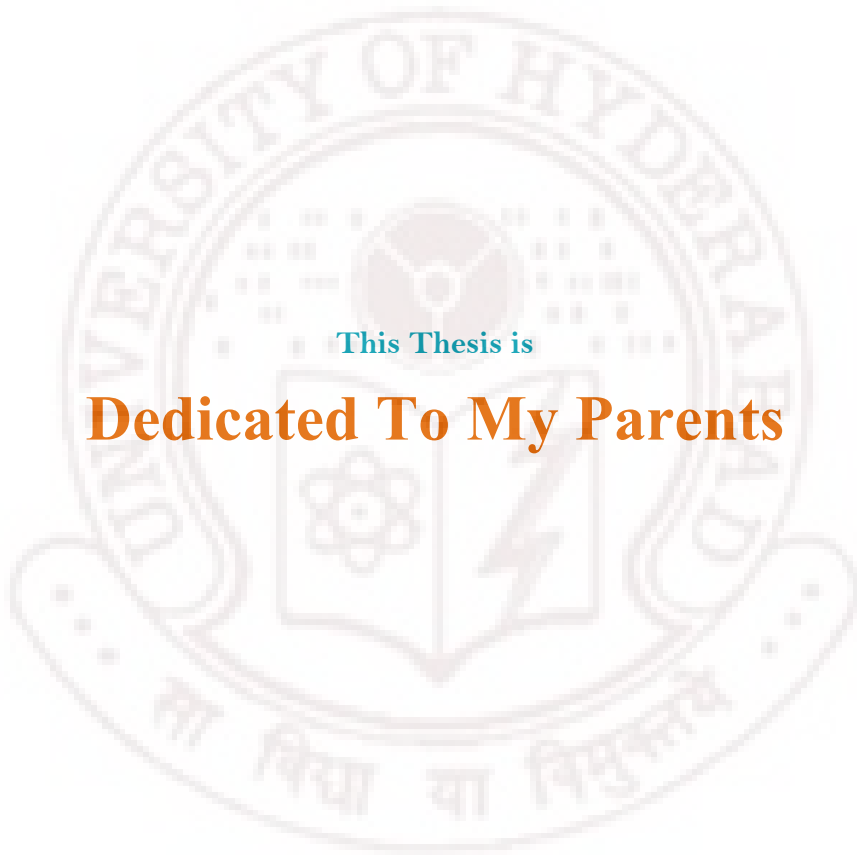
**School of Chemistry  
University of Hyderabad  
Hyderabad 500 046  
India**

**July 2009**

## **DEDICATION**

**This Thesis is**

**Dedicated To My Parents**



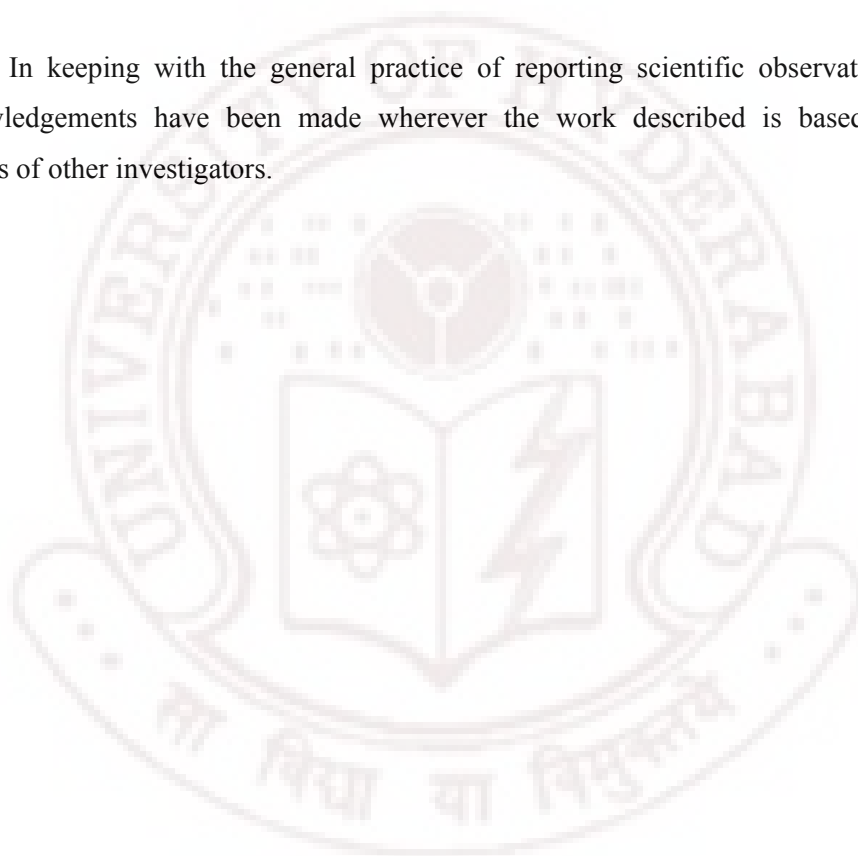




# STATEMENT

I hereby declare that the matter embodied in this thesis entitled **“STRUCTURAL AND THERMAL ANALYSIS OF ORGANIC SOLIDS”** is the result of investigations carried out by me in the School of Chemistry, University of Hyderabad under the supervision of **Prof. Ashwini Nangia**.

In keeping with the general practice of reporting scientific observations due acknowledgements have been made wherever the work described is based on the findings of other investigators.



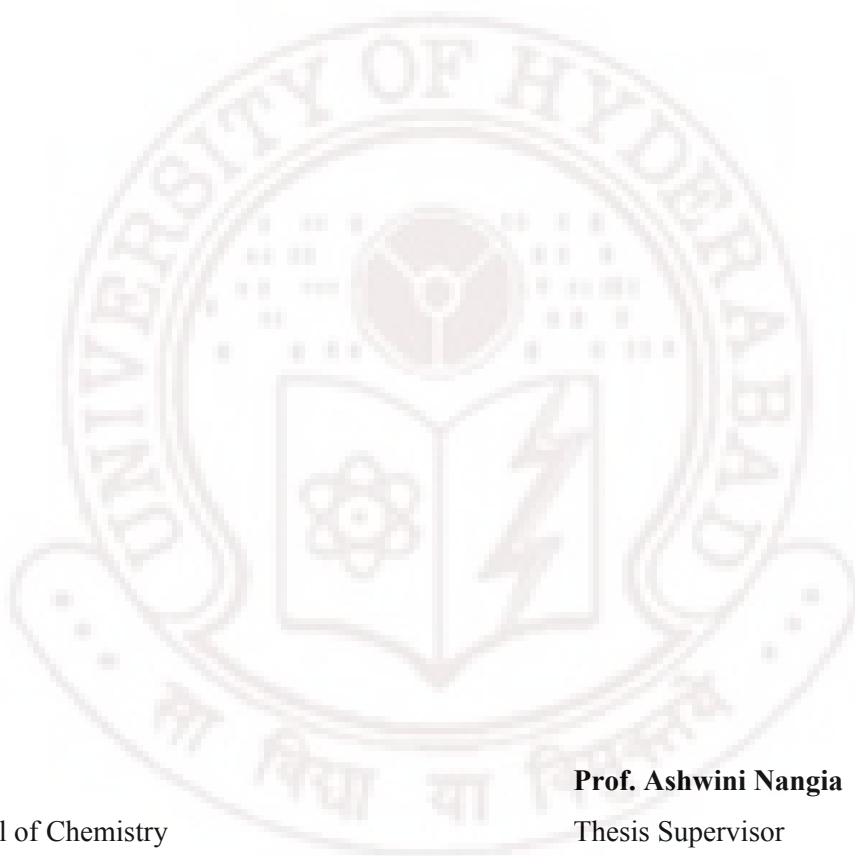
Hyderabad  
July 2009

**Bipul Ch. Sarma**



# CERTIFICATE

Certified that the work “**STRUCTURAL AND THERMAL ANALYSIS OF ORGANIC SOLIDS**” has been carried out by Bipul Ch. Sarma under my supervision and that the same has not been submitted elsewhere for a degree.



**Dean**  
School of Chemistry

**Prof. Ashwini Nangia**  
Thesis Supervisor



# ACKNOWLEDGEMENT

I express my deep sense of gratitude and profound thanks to **Prof. Ashwini Nangia** for his inspiring guidance and constant encouragement throughout the course of this research work. I have been able to learn a great deal in this fascinating field of research through his inspiring lectures and thought provoking discussions, and I consider my association with him a rewarding experience.

I thank Prof. D. Basavaiah, Dean, School of Chemistry, former Deans Prof. M. Periasamy, Prof. E. D. Jemmis, and faculty members for their co-operation, helpful discussion and providing facilities in the School.

I would like to acknowledge Dr. László Fábián, Cambridge Crystallographic Data Centre (CCDC), UK, for providing software to calculate Isostructurality Index.

My sincere thank to Prof. Jubaraj B. Baruah, IIT Guwahati and Subrata Baruah, B. Barooah College, Guwahati, Assam. I am also thankful to all other teachers and lecturers who taught me throughout my career and their constant encouragement.

I am grateful to CSIR, New Delhi, for providing fellowship support. I thank DST for providing single crystal X-ray diffractometer facility and UPE programme of UGC for infrastructure facilities at the school.

I thank each and every non-teaching staff of the School of Chemistry, CIL, COSIST building and the Computer Centre for their assistance on various occasions. Much of the research displayed in this thesis comes from single crystal X-ray diffraction, IR and PXRD techniques. I take this opportunity to thank Dr. P. Raghavaiah, Ayesa Parwez, Mr. Nageshwara Rao for their kind help in acquiring the data with great deal of expertise and care. I thank Mr. Sathyanarayana, Mr. Bhaskar Rao, Smt. Vijayalakshmi for their help in recording NMR spectra. I thank Mr. Shetty, Mr. Vijay Bhaskar, Mr. Dilip, Mr. Sai, Mr. Sharma, Mr. Jayaram, Mr. Desbandu, Mr. Durgesh, Mr. Shetty, Mr. Joseph for their cooperation.

I wish to thank my friendly and cooperative lab mates Dr. S. George, Dr. V. R. Vangala, Dr. S. Atipamula, Dr. Bala Krishna Reddy, Dr. S. Basavoju, Dr. B. K. Saha, Dr. D. Das, Dr. R. Banerjee, Dr. C. Malla Reddy, Dr. L. S. Reddy, Dr. A. Dey, Dr. V. Aparna, Dr. S. Panigrahi, Dr. S. Roy, Dr. P. M. Bhatt, Dr. T. Thakur, Dr. N. J. Babu, Dr.

Y. Azim and Mr. Sairam, Sreekanth, Naba, Ranjit, Palash, Suryanarayan, Rajesh and Kalyan for creating a cheerful working atmosphere in the lab. I also thank Pati, Sanjeev and Sandeep for their help on various occasions.

My heartfelt thank to my seniors Dr. Gokul Baishya, Dr. Ashok Basak, Pranjal Saikia and Pankaj Bharali. A special thanks to Babita, Lakshidra, Sangeeta, Mausam, Kajal, Rajib, Bishnu, Parag, Hemanta, Tiken, Kamalesh and Gitartha.

My pleasant association with Abhik, Moloy, Subhash, Sunirbaan, Manab, Sandy, Tamal, Prasun, Bisharoop, Anirudha, Shatabdi, Kedar, Abhijit, Utpal, Ghona, Pradip, and Masum is just unforgettable. My stay in the campus a memorable one because of them and I will cherish each and every moment I spent with them throughout my life.

I would like to thank Tridib, Satyajit, Pabitra, Alankar, Premanka, Rabha, Gaurang, Mondal, Tapta, Arindam, Arun, Ghanta, Dinu, Sandip, Sudhanshu, Mehboob, Nayan, Tanmoy, Mousumi, Bhaswati, Vasudhara, Saonti, Nilanjana, Monima, Swarnalee, Anindita, Rumpa, Suparna, Susmita, Tulika, and Sanghamitra for many reasons. I am also thankful to Anup, Param, Pavan, Gupta, Venkatesh, Balaraman, Ramesh Reddy, Shekhar Reddy, Satish, Selva, Bhuvan, Phani, Ramsuresh, Venu, Anji, Ramesh, Narahari, Rajeshwar, Satpal, Rajesh, Ravi, Srinivas, G.D.P, Rambabu, Armuganathan, Bharath, D.K., Ramu, Chaitanya, Vikram, Biju, Shiva, Venkatesh, Kishore, Ram Kumar, Murali, Anil & Sunil, Raju, Ashok and all others whose names are not mentioned due to limited space.

I would like to thank all my family members, Binita, Pooja, Moina, Laku for their love, constant support and guidance. My special thanks to our relatives, friends and all others who have made a contribution to my life. I would like to express my love and gratitude to god for giving me patience and persistent determination to endure challenges in my life. The unconditional love of my parents and their blessings made me what I am today and I owe everything to them. Dedicating this thesis to them is a minor recognition for their relentless support and love.

**Bipul Ch. Sarma**

# SYNOPSIS

This thesis entitled “**STRUCTURAL AND THERMAL ANALYSIS OF ORGANIC SOLIDS**” consists of seven chapters.

## CHAPTER ONE

### Crystal Engineering

Crystal engineering relies on non-covalent bonding in the solid state with desired properties and functions mainly focused on the use of more directional hydrogen bonds. It is the synthesis of supramolecular structures in the solid state which has now become an interdisciplinary subject dealing with the self-assembly of molecular crystals using hydrogen bonding, electrostatics,  $\pi$ -stacking, halogen bonding, van der Waals interactions, and metal-coordination bonding. The Cambridge Structural Database (CSD) of nearly 4,70,000 crystal structures provides an excellent tool for accessing the efficiency and reproducibility of a particular supramolecular synthon. Design of new molecular solids with predictable synthon becomes more difficult in multi-functional molecules because of competition between multiple donor/acceptor groups. The subject of crystal engineering deals with various solid forms like polymorphs, host-guest complexes, network solids, salts, hydrates, cocrystals, more preferably pharmaceutical cocrystals, and this chapter will cover a brief foundation of various organic solid-state forms.

The ability of a compound to exist in more than one crystalline modification is known as polymorphism, a phenomenon with tremendous importance in pharmaceutical development and materials science as it can alter physical and chemical properties. It is therefore important to know the correct crystalline modification in active pharmaceutical ingredients (APIs) to enable formulation of drug substances. The presence of different conformers of the same molecule in different crystal structures is termed as conformational polymorphism. Polymorphism tends to be prominent in molecules that contain multifunctional groups thereby forming multiple supramolecular synthons known as synthon polymorphism. However the exact molecular features for a compound for it to be polymorphic are still elusive. Among the various analytical methods used for

the characterization of polymorphs, thermal analysis (i.e. differential scanning calorimetry, thermogravimetry, hot stage microscopy), spectroscopy (FT-IR, NIR, Raman etc.), in-situ variable temperature powder X-ray diffraction and finally single crystal X-ray diffraction have received considerable attention. Thermal relation among kinetic/thermodynamic polymorphs, such as enantiotropic or monotropic, and their stability must be understood. Understanding the recurrence of more than one molecule or conformation (i.e.  $Z' > 1$ ) in the crystal lattice has drawn chemists and crystallographers interest. Our recent study shows higher probability of occurrence of  $Z' > 1$  structure using high temperature crystallization methods: melt and sublimation.

The rational construction of novel open-framework organic solids has received particular interest because of their diverse applications such as chemical separation, drying agents, reactions and catalysis in a microcavity and for electro optic, nonlinear and magnetic materials. Hydration of molecules in the crystal structure is a common phenomenon, especially in pharmaceuticals. Apart from polymorphs and hydrate structures, organic salts and cocrystals can show effective advantages over neutral APIs. Cocrystal is a multi-component crystal structure in which two or more compounds coexist through hydrogen bonds or non-covalent interactions. If the reactants are solids at ambient conditions, the multi-component crystalline materials are cocrystals and those composed of one or more solids and a liquid are known as solvates or pseudopolymorphs. The multi-component system is known as “molecular salt” or “organic salt” if proton is transferred from acid to base in ionic state. Common problems encountered with Active Pharmaceutical Ingredients (APIs), in terms of their solubility, dissolution rates, and stability can be solved by making salt, cocrystal etc. without the need to make or break covalent bonds.

## CHAPTER TWO

### Conformational and Synthon Polymorphism in Host Compounds

1,1-Bis-(4-hydroxyphenyl)cyclohexane (**1**) is a very good host molecule as more than 31 solvates/cocrystal structures are reported. However its pure host form was never crystallized. Crystallization of **1** from several solvents was attempted to get a guest-free form; only solvent inclusion crystals or ill-defined powders were obtained. We successfully isolated the guest-free form of popular host **1** and could isolate two



polymorphs by using solvent-free methods, melt crystallization and sublimation. These techniques are further employed to generate new polymorphs of isomeric dihydroxybenzoic acids (**2**, **3**, **4**, **5**, **6**, and **7**). These compounds are prone to give solvate/hydrate forms upon crystallization. Two polymorphs of 3,5-dihydroxybenzoic acid (**2**), a new polymorph of 2,3-dihydroxybenzoic acid (**3**) and guest free form of 3,4-dihydroxybenzoic acid (**4**) were crystallized by melting and sublimation.

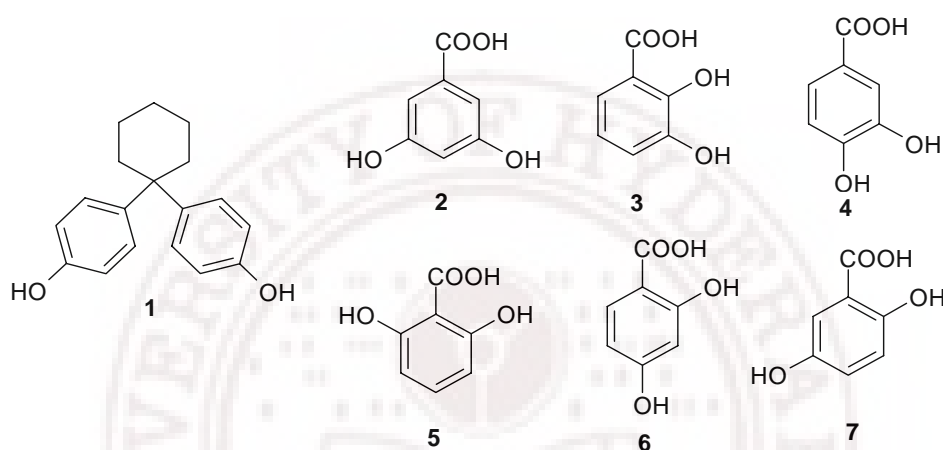


Figure 1: Popular host 1,1-bis-(4-hydroxyphenyl)cyclohexane (**1**) afforded guest free form and conformational polymorphism on melting and sublimation and validated these solvent free methods successfully on isomeric dihydroxybenzoic acid molecules (**2**, **3**, **4**, **5**, **6**, **7**).

A new hydrate polymorph of 3,4-dihydroxybenzoic acid was isolated along with tetrahydrofuran, acetylacetone and dioxane solvates of 3,5-dihydroxybenzoic acid (**2**•THF, **2**•Acac and **2**•Diox) to confirm that they are prone to form solvates. **5**, **6** and **7** gave either decomposed polyphenols or reported forms in the literature. Polymorphs of **1** differ in the conformations of OH groups which lead to the difference in molecular arrangement in crystalline lattice. Polymorphs of isomeric dihydroxybenzoic acid differ in nature of hydrogen bond synthons in their crystal structures however two hydrate polymorphs of **4** show differences in packing. Two solvent free methods to obtain guest free forms of molecules that are prone to give solvent/water included structures on crystallization were investigated. These methods show potential to generate new polymorphic modifications. Phase transition from metastable to stable polymorph was

explained in detail by differential scanning calorimetry (DSC), hot stage microscopy (HSM) and hydrogen bonding changes in **1**.

## **CHAPTER THREE**

### **High $Z'$ Structures by Solvent Less Methods**

Crystal structures with multiple  $Z'$  (= number of molecules in the asymmetric unit) are now being intensely studied to understand the factors leading to high  $Z'$  crystal structures. A Cambridge Structural Database (CSD) search on structures crystallized using solvent free methods such as melt and sublimation was carried out. It is found that solvent-free crystallization methods show a much higher probability of multiple  $Z'$  structures compared to overall CSD trends on  $Z'$  frequencies. Crystal structure having  $Z' > 1$  is <12%. Carbamazepine is a notable example for which  $Z' = 1$  from solution crystallization (3 polymorphs) whereas  $Z' = 4$  when it is crystallized from melting. Generation of high  $Z'$  structures by melting and sublimation crystallization can be understood as rapid cooling of the hot liquid or vapor in the open flask or on the cold finger is a kinetic phase and the conditions under which hydrogen-bonded clusters are likely to condense in a pseudo-symmetric crystalline arrangement. 1,1-bis-(4-hydroxyphenyl)cyclohexane is a remarkable example to illustrate how close packing conflicts in a metastable  $Z' = 2$  structure are resolved in the thermodynamic  $Z' = 1$  polymorph.

## **CHAPTER FOUR**

### **Polymorphism and Phase Transition in Phenylbenzenesulfonamides**

Analysis of structures and phase relationship between different crystalline modifications of the same molecule will help us to understand more about polymorphism. A thorough screening for all the possible polymorphs is considered an essential step in pharmaceutical industry to choose the best drug formulation with desirable properties. The original antibacterial sulfonamides i.e. sulfa drugs are synthetic antimicrobial agents (sulfathiazole, sulfapyridine, sulfadiazine etc.) that contain the sulfonamide functionality (primary or secondary). Our objective is to compare molecular packing, nature of different types of non-covalent interaction like hydrogen bonds, and halogen interactions, isostructurality of polymorphs and more important solvent effect on

polymorphism and complete spectroscopic analysis. A systematic study on polymorphism gives insight into structural relationship and the mechanism of phase transition between crystalline modifications.

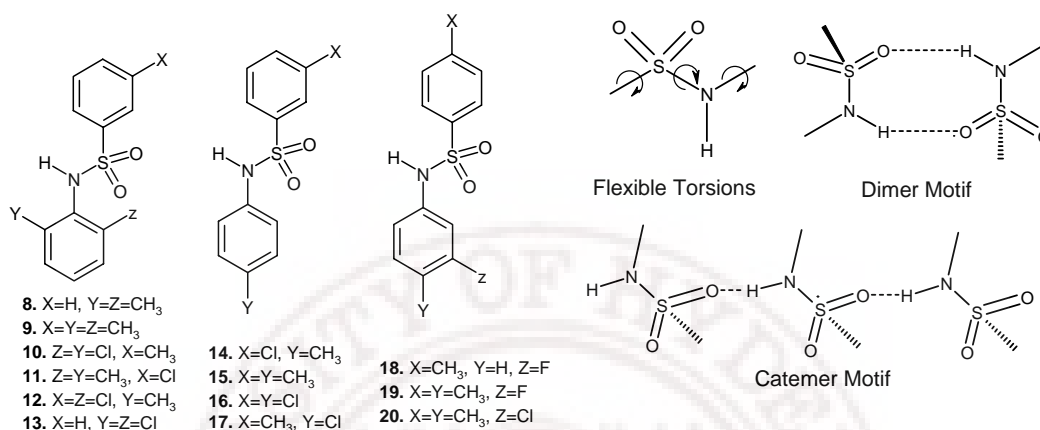


Figure 2(a): Phenylbenzenesulfonamides, (b) Torsion flexibility, dimer or catemer hydrogen bond motifs and other weak interactions ( $C-H\cdots O$ ,  $C-H\cdots\pi$ ,  $\pi\cdots\pi$  interactions) play a role in polymorph structures in phenylbenzenesulfonamides.

Six molecules from a set of thirteen (8–20) are found to be polymorphic and all are well characterized by powder X-ray diffraction, single crystal X-ray diffraction, thermal analysis, hot stage microscopy, Raman, FT-IR, NIR spectroscopy, manual heating/grinding experiment etc. Phase transition from metastable to stable polymorph was examined by HSM and DSC in two systems further confirmed by powder X-ray pattern and unit cell parameter determination.  $N-H\cdots O$  catemer and dimer motif of sulfonamide group (Figure 2b) is seen as the main difference in two systems (8 and 10) however  $C-H\cdots O$ ,  $C-H\cdots\pi$ ,  $C-H\cdots X$ ,  $Cl\cdots Cl$  interaction play a role in differentiating other polymorphic systems. Solvent plays significant role in the nucleation of polymorphic crystals. Reasons for nearly equal preference for the formation of  $N-H\cdots O$  homo dimer and catemer synthons in phenylbenzenesulfonamides are discussed.

## CHAPTER FIVE

### Tetrahedral and H-shaped Host Tectons

Tetrahedral molecular scaffolds are versatile building blocks for the directed organization of host–guest and/or interpenetrated networks. Tetrahedral molecules are

normally organized in predictable diamondoid, rhombohedral or columnar type packing motifs. Tetraphenyl methanes and silanes with boronic acid group have the potential of exchange in guest inclusion and predictable porous architectures includes guest species to the extent of 60-65% in inter-connected channels. Tetraphenylmethane tetrasulfonic acid was synthesized (TPM-SO<sub>3</sub>H, **21**, Figure 3a) and crystallized from MeOH to analyze structural and thermal behavior as the structural chemistry of sulfonic acid group has not been explored in tetrahedral molecules. Colorless needle-shaped crystals of TPM-SO<sub>3</sub>H crystallized in tetragonal space group *I4*(1)/*a* contains ¼ TPM-SO<sub>3</sub>H molecule and 3 water molecules in its asymmetric unit giving a host: guest ratio of 1:12 (Figure 3b).

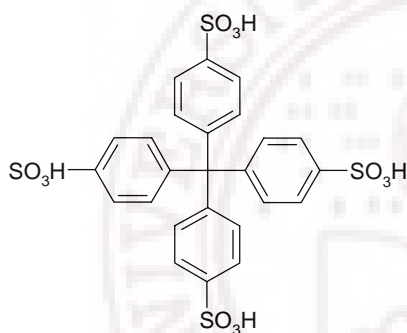


Figure 3: (a) Tetrakis(4-sulfophenyl) methane (**21**)

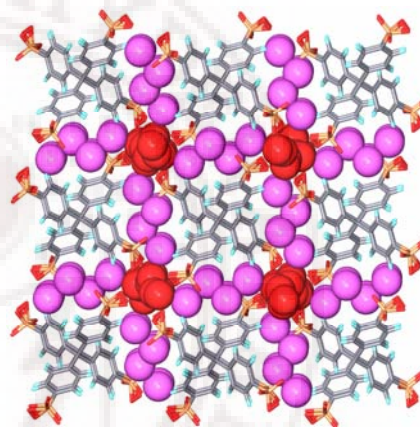


Figure 3: (b) Two types of water molecules are sitting in square (red) and irregular interconnected channels (pink) in the crystal structure

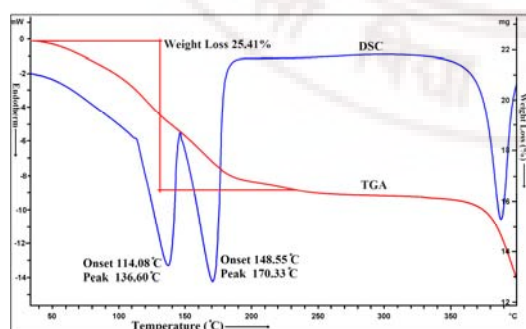


Figure 3: (c) DSC and TGA curves of TPM-SO<sub>3</sub>H. The values are in accordance with the X-ray crystal structure.

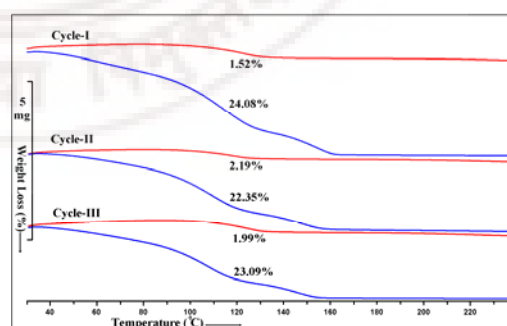


Figure 3: (d) Water loss and uptake is reversible in 3 successive cycle in TGA

TGA and X-ray crystal structure are consistent with 1:12 host: water stoichiometry (observed: 25.41%, calculated: 25.23%, Figure 3c). Two endothermic steps in DSC show water is lost in two stages. TPM-SO<sub>3</sub>H can reversibly uptake water from atmosphere. This loss/reuptake of water is quantitative and selective in successive cycles (Figure 3d). Compounds having properties of reversible, quantitative and selective uptake of water/solvent can have potential applications in dehydrating agents and organic zeolites. Structural part includes water helices, interconnected channels, hydrogen bonding pattern on TPM-SO<sub>3</sub>H are analyzed.

Porous architectures and network solids have important applications. H-shaped molecule 1,4-di[bis(4'-hydroxyphenyl)methyl]benzene (**22**) and its octamethyl derivative (**23**) were synthesized (Figure 4) and crystallized in solvated and guest-free forms to analyze the occurrence of specific network architectures.

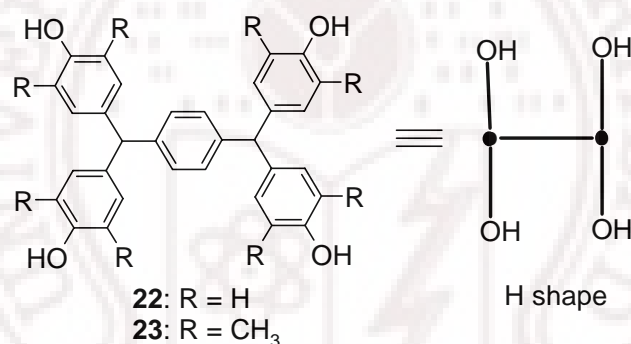


Figure 4: Simple H-shaped molecule and octamethyl derivative (**22** and **23**) are synthesized and crystallized in solvated and guest free form. **22**• CH<sub>3</sub>NO<sub>2</sub> and **23**• CHCl<sub>3</sub> show rare pentagonal (5,<sub>4</sub><sup>3</sup>) net.

Doubly interpenetrated 1D ladder is observed in the guest-free form of **22**. Crystallization of **22** from CH<sub>3</sub>NO<sub>2</sub> with varying amount of CF<sub>3</sub>CH<sub>2</sub>OH afforded two CH<sub>3</sub>NO<sub>2</sub> solvate polymorphs as plate-shaped crystals in space group *Pbca* and block crystals in space group *P2<sub>1</sub>/c* having different network topologies. *Pbca* form shows polycatenated porous hexagonal sheets with degree of catenation 2/2. However *P2<sub>1</sub>/c* polymorph shows rare pentagonal layer tiling of (5,<sub>4</sub><sup>3</sup>) nets extending in third dimension. Molecule **23** upon crystallization from CHCl<sub>3</sub> solvents also afforded the same rare (5,<sub>4</sub><sup>3</sup>) net of contiguous pentagons in 2D sheet. The tetrahedral carbon centers are 3-connected

nodes and hydrogen bonding OH groups are 4-center nodes of congruent cyclopentanoid rings. The first examples of pentagon layer tiling in a lattice inclusion organic host are reported.

## CHAPTER SIX

### Synthon Competition and Cooperation in Cocrystals and Salts

The study of supramolecular synthons between common functional groups is a key step in crystal engineering. Hydrogen bond synthon competition and cooperation was studied when four functionalities: carboxylic acid, pyridine, amine, and hydroxyl are simultaneously present in the supramolecular system. Isomeric and substituted hydroxybenzoic acids and isomeric aminopyridines were selected to prepare 11 cocrystals from methanol solvent (Figure 5) and their structures were characterized by X-ray diffraction.

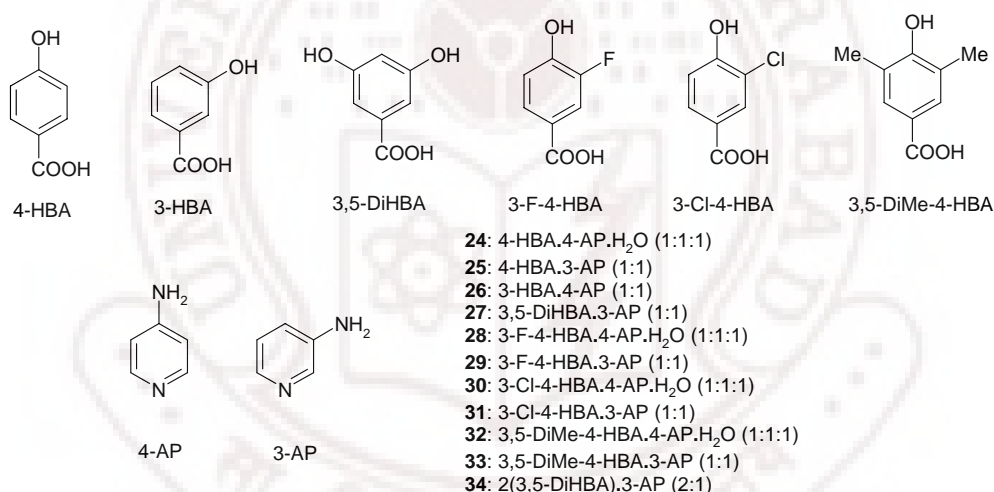


Figure 5: Hydroxybenzoic acids (HBA) cocrystallized with aminopyridines (AP) and the resulting organic salt composition (24-34). Four are hydrate (24, 28, 30, 32) structures.

Proton transfer from COOH to pyridyl N acceptor (PyN) occurred in all 11 molecular salts (24-34) leading to a  $\text{PyNH}^+\cdots\text{OOC}^-$  ionic synthon in 10 structures (24-33) and  $\text{PyNH}^+\cdots\text{O}=\text{C}$  hydrogen bond in 34. The observed hydrogen bonds were analyzed between  $\text{COO}^-$ , OH,  $\text{NH}_2$ ,  $\text{PyNH}^+$ , and  $\text{H}_2\text{O}$  functional groups in these 11 structures, of which 4 are hydrates (24, 28, 30, 32). Synthons in this study are compared with statistics extracted from the Cambridge Structural Database to summarize trends



and predict hydrogen bonding in new cocrystal and salt structures. We show that hydrogen bonding functional groups such as OH and NH<sub>2</sub> promote persistent formation of ionic PyNH<sup>+</sup>...<sup>-</sup>OOC synthon in the same supramolecular system. However the  $\Delta pK_a$  rule for predicting neutral or ionic O-H...N/N<sup>+</sup>-H...O<sup>-</sup> hydrogen bonds is found to be inadequate in this system. Even as bioavailability of a drug is intimately related to its formulation; neutral (cocrystal) or ionic (salt), there is no easy way to know the answer before structure determination.

## CHAPTER SEVEN

### Conclusion and Future Prospects

The immense importance of polymorphism in the formulation of APIs is because they can alter the physical and chemical properties. Therefore it is crucial to screen for all possible polymorphs of a drug and chose the right one, preferably the most stable polymorph with desirable properties for product formulation after a complete thermal profile. Melt and sublimation crystallization are used to generate guest-free host structures and polymorphs. Two conformational polymorphs of the popular host 1,1-bis(4-hydroxyphenyl)cyclohexane (**1**) and synthon polymorphs of 3,5-dihydroxybenzoic acid (**2**), 2,3-dihydroxybenzoic acid (**3**) and pure 3,4-dihydroxybenzoic acid (**4**) were generated by sublimation and melting. Stability relationship of the two conformational polymorphs of **1** is established. Melt crystallization and sublimation are likely to give high *Z'* structures. Our results were compared with overall *Z'* frequencies in CSD statistics in chapter 3. A series of secondary sulfonamide molecules were synthesized and screened and found six polymorphic systems from solvent crystallization and melting. Solid to solid state phase transition was observed and confirmed by spectroscopic techniques and thermal analysis. An organic host tetraphenylmethane tetraphenylsulfonic acid was synthesized and detail structural and thermal analysis was carried out. This compound shows reversible and selective guest release and uptake properties that can have potential application in organic zeolite and in dehydrating agents. The organic phenol host 1,4-di[bis(hydroxyphenyl)methyl]benzene and its octamethyl derivative were synthesized and crystallized in solvated and guest free forms. Supramolecular network includes

interpenetrated ladders, polycatenated (6,3) net, rare pentagonal ( $5, \frac{3}{4}$ ) net are observed. Important biological phenomenon of proton transfer dependence on  $pK_a$  and functional groups present on salt formation was carried out by studying a set of 11 molecular salts between isomeric hydroxybenzoic acid and isomeric amino pyridines. Cocrystals, pharmaceutical cocrystals, salts, hydrates are also having substantial importance in pharmaceutical industry to modify the properties of drugs. Salts and cocrystals have the potential to be much more useful in pharmaceutical products than solvates or hydrates because the number of pharmaceutically acceptable solvents is very small, and moreover solvents tend to undergo dehydration/desolvation in the solid dosage forms. Crystal engineering has significant contribution and overlap with like organic chemistry, inorganic chemistry, supramolecular chemistry, X-ray crystallography, materials research, computational chemistry and pharmaceutical chemistry and in current times it is moving from structure design to functional control.

Salient crystallographic details of the crystal structures discussed in this thesis have been given in an appendix at the end of the thesis. A full list of atomic coordinates has been deposited with the University of Hyderabad and is available upon request from Prof. Ashwini Nangia ([ashwini.nangia@gmail.com](mailto:ashwini.nangia@gmail.com)).



# CONTENTS

|                      |         |
|----------------------|---------|
| Statement.....       | v       |
| Certificate.....     | vii     |
| Acknowledgement..... | ix-x    |
| Synopsis.....        | xi - xx |

## CHAPTER ONE

### CRYSTAL ENGINEERING 1-38

|      |  |    |
|------|--|----|
| 1.1  | Introduction.....  | 1  |
| 1.2  | Intramolecular Interactions and Supramolecular Synthons.....     | 2  |
| 1.3  | Organic Solid-State Forms.....                                   | 6  |
| 1.4  | Polymorphism.....  | 10 |
| 1.5  | Enantiotropic and Monotropic Related Polymorphs.....             | 13 |
| 1.6  | Isostructurality.....  | 15 |
| 1.7  | Polymorphism and High Z' Structures in Solvent Less Methods..... | 19 |
| 1.8  | Salt Cocrystal Continuum.....                                    | 21 |
| 1.9  | Pharmaceutical Cocrystals.....                                   | 23 |
| 1.10 | Hydrates and Host-Guest Compounds.....                           | 25 |
| 1.11 | Network Solids.....  | 27 |
| 1.12 | Conclusions.....   | 29 |
| 1.13 | References.....  | 30 |

## CHAPTER TWO

### CONFORMATIONAL AND SYNTHON POLYMORPHISM IN HOST COMPOUNDS 39-72

|     |  |    |
|-----|--|----|
| 2.1 | Introduction.....                                    | 39 |
| 2.2 | Conformational and Synthon Polymorphism.....         | 40 |
| 2.3 | Methods for Obtaining Guest Free Host Structure..... | 43 |
| 2.4 | 1,1-Bis-(4-hydroxyphenyl)cyclohexane.....            | 44 |
| 2.5 | Lattice and Conformer Energy.....                    | 47 |

|        |  |    |
|--------|--|----|
| 2.6    | Phase Transition.....  | 48 |
| 2.7    | High $Z'$ Structures and CSD Trends.....                     | 51 |
| 2.8    | Synthon Polymorphism in Isomeric Dihydroxybenzoic Acids..... | 53 |
| 2.9    | Results and Discussions.....                                 | 54 |
| 2.9.1  | Solvates of 3,5-Dihydroxybenzoic Acid.....                   | 55 |
| 2.9.2  | Polymorphs of 3,5-Dihydroxybenzoic Acid.....                 | 56 |
| 2.9.2a | Structure Analysis.....                                      | 57 |
| 2.9.2b | Thermal Analysis.....  | 60 |
| 2.9.3  | Polymorphs of 2,3-Dihydroxybenzoic Acid.....                 | 61 |
| 2.9.4  | Guest Free Structure of 3,4-Dihydroxybenzoic Acid.....       | 62 |
| 2.9.5  | New Hydrate Polymorph of 3,4-Dihydroxybenzoic Acid.....      | 63 |
| 2.10   | Cambridge Structural Database (CSD).....                     | 65 |
| 2.11   | Summary and Conclusions.....                                 | 66 |
| 2.12   | Synthesis of 1,1-Bis-(4-hydroxyphenyl)cyclohexane.....       | 68 |
| 2.13   | References.....  | 68 |

### CHAPTER THREE

#### HIGH $Z'$ STRUCTURES BY SOLVENT LESS METHODS 73-90

|     |   |    |
|-----|---|----|
| 3.1 | Introduction.....   | 73 |
| 3.2 | Multiple Molecules in Asymmetric Unit ( $Z' > 1$ ).....   | 74 |
| 3.3 | Pseudosymmetry.....                                       | 76 |
| 3.4 | Awkward Shapes, Molecular Helices and Kinetic Effect..... | 77 |
| 3.5 | Chirality and Strong Hydrogen Bond.....                   | 78 |
| 3.6 | Polymorphs and Modulated Structures.....                  | 79 |
| 3.7 | Crystal Structure with $Z' > 1$ Solvent Less Methods..... | 82 |
| 3.8 | Conclusions.....  | 86 |
| 3.9 | References.....   | 87 |

### CHAPTER FOUR

#### POLYMORPHISM AND PHASE TRANSITION IN PHENYLBENZENESULFONAMIDES 90-130

|      |   |     |
|------|---|-----|
| 4.1  | Introduction.....                                     | 91  |
| 4.2  | Results and Discussion.....                           | 93  |
| 4.3  | Crystal Structure Analyses.....                       | 95  |
| 4.4  | Chloro-Methyl Exchange Rule and Isostructurality..... | 103 |
| 4.5  | Solvent Influence on Polymorphs.....                  | 106 |
| 4.6  | Spectroscopic Analysis: IR, NIR and Raman .....       | 109 |
| 4.7  | Thermal Analysis and Phase Transition.....            | 113 |
| 4.8  | Cambridge Structural Database (CSD).....              | 118 |
| 4.9  | Summary and Conclusions.....                          | 121 |
| 4.10 | Experimental Section.....                             | 122 |
| 4.11 | References.....                                       | 125 |

## CHAPTER FIVE

### TETRAHEDRAL AND H-SHAPED HOST TECTONS 131-162

|         |   |     |
|---------|---|-----|
| 5.1     | Introduction.....   | 131 |
| 5.2     | Results and Discussion.....   | 134 |
| 5.2.A   | Tetrakis-(4-sulfophenyl)methane: An Organic Host Hydrate.....   | 134 |
| A.(i)   | Tetrahedral Tecton.....   | 134 |
| A.(ii)  | Synthesis and Structural Analysis.....  | 136 |
| A.(iii) | Cambridge Structural Database Analysis.....   | 139 |
| A.(iv)  | Differential Scanning Calorimetry, Thermogravimetry and XRPD...   | 141 |
| A.(v)   | Summary.....  | 144 |
| 5.2.B   | H-Shaped Aromatic Phenol Host.....  | 144 |
| B.(i)   | Introduction.....   | 144 |
| B.(ii)  | 1,4-Di[bis(4'-hydroxyphenyl)methyl]benzene and its Octamethyl<br>derivative.....                        | 145 |
| B.(iii) | Construction of Rare Pentagonal Net.....  | 146 |
| B.(iv)  | Solvate Polymorphism, Interpenetration, Catenation, and<br>Rare (5 <sub>4</sub> <sup>3</sup> ) Net..... | 148 |
| B.(v)   | Summary.....  | 154 |
| 5.3     | Conclusions.....  | 154 |

|     |                          |     |
|-----|--------------------------|-----|
| 5.4 | Experimetal Section..... | 156 |
| 5.5 | References.....          | 157 |

## CHAPTER SIX

### SYNTHON COMPETITION AND COOPERATION IN COCRYSTALS AND SALTS 163-198

|     |   |     |
|-----|---|-----|
| 6.1 | Introduction.....                         | 163 |
| 6.2 | Results and Discussion.....               | 167 |
| 6.3 | Structural Analysis.....                  | 175 |
| 6.4 | Proton Transfer: Cocrystal or Salt.....   | 181 |
| 6.5 | SPARC <i>p</i> Ka Calculator.....         | 185 |
| 6.6 | Cambridge Structural Database Search..... | 187 |
| 6.7 | Coclusions.....                           | 189 |
| 6.8 | Experimental Section.....                 | 190 |
| 6.9 | References.....                           | 193 |

## CHAPTER SEVEN

### CONCLUSIONS AND FUTURE PROSPECTS 199-209

|     |  |     |
|-----|--|-----|
| 7.1 | Guest free Host Structure by Solvent Less Methods.....           | 199 |
| 7.2 | Polymorphism and Phase Transition.....                           | 200 |
| 7.3 | Reasons For High <i>Z'</i> Structures: Solvent Less Methods..... | 202 |
| 7.4 | A Host Hydrate: Organic Zeolite.....                             | 203 |
| 7.5 | Rare Hydrogen Bond Network: Pentagonal Tiling.....               | 204 |
| 7.6 | Synthon Competition and Cooperation in Cocrystals and Salts..... | 206 |
| 7.7 | References.....  | 208 |

## APPENDIX 211-222

|                                       |     |
|---------------------------------------|-----|
| Salient Crystallographic Details..... | 211 |
| About the Author.....                 | 219 |
| List of Publications.....             | 221 |

---

## CRYSTAL ENGINEERING

---

### 1.1 Introduction

Supramolecular chemistry<sup>1</sup> is a new and rapidly progressing field on the crossroads between chemistry, biology, physics and materials science. It is the chemistry of molecular assemblies (beyond molecules) and of intermolecular interactions (non covalent bonds). This not only provides the basis for revolutionizing numerous branches of industry but also improves our understanding of the functioning of living organisms and of the origin of life. Designing a new supramolecular system with desired properties will provide us a better understanding about non-covalent interactions between molecules within the molecular aggregates and it will transform the pharmaceutical industry and medicine by developing new ways of drug administration and new composite biocompatible materials which will serve as implants of new generation. The existence of intermolecular forces was first postulated by Johannes Diderik van der Waals in 1873. In the early twentieth century noncovalent bonds were understood in greater detail, with the hydrogen bond being first described by Latimer and Rodebush<sup>2a</sup> in 1920 and later by Linus Pauling in an extended treatment.<sup>2b,c</sup> The importance of supramolecular chemistry was established by the 1987 Nobel Prize for Chemistry being awarded to Donald J. Cram, Jean-Marie Lehn, and Charles J. Pedersen in recognition of their work in the development and synthesis of shape and ion selective receptors or "host-guest" complexes. Afterwards it took a rapid pace with the concepts of mechanically-interlocked molecular architectures, crystal engineering and supramolecular materials coming within its fold. In the 1990s, supramolecular chemistry became even more sophisticated. The science of nanotechnology also had a strong influence on the subject, with building blocks such as fullerenes, nanoparticles, and dendrimers becoming part of synthetic systems.

Within the realm of supramolecular chemistry another well-defined area is *crystal engineering*,<sup>3</sup> devoted to the design and studies of crystals built of two or more components with desirable properties. Pepinsky first introduced the term “Crystal Engineering” in 1955 and the subject was elaborated by Schmidt<sup>4</sup> during 1950 to 1970 to address the issue of crystal packing in the context of organic solid state photochemical reactions of cinnamic acids and amides. A general meaning of the term was proposed by Desiraju<sup>3a</sup> of Crystal Engineering as *"the understanding of intermolecular interactions in the context of crystal packing and the utilization of such understanding in the design of new solids with desired physical and chemical properties"*. Crystal engineering is a mainline interdisciplinary subject today that was started with organic solids and now deals with the self-assembly of molecular crystals, metal–organic architectures, nanostructures, and coordination polymers using hydrogen bonding, electrostatic, van der Waals interactions, and metal coordination bonding. It is an interdisciplinary field that seeks to develop protocols for predicting and controlling the structure and functional properties of solids. Catalysis, optical materials, conducting and magnetic materials, nanotechnology, electronic materials and sensors, nano and microporous materials, supramolecular devices, protein-receptor binding, molecular modeling, drug design and improving properties of existing APIs are some of the key research areas within the realm of crystal engineering.

## 1.2 Intermolecular Interactions and Supramolecular Synthons

Crystal, the supramolecule *par excellence*,<sup>5</sup> is an assembly of millions of molecules held together in a periodic arrangement at an amazing level of precision by intermolecular interactions, guided by molecular recognition and organized self assembly. Intermolecular interactions include ion-ion, ion-dipole, dipole-dipole interactions, hydrogen bonding, London forces, etc. The close packing principle of Kitaigorodskii<sup>6</sup> postulates that molecules in a crystal pack such that the projections of one molecule dovetail into the hollows of its neighbour, i.e. bumps fit into hollows just like lock and key, so that the maximum numbers of intermolecular contacts are achieved. The crystal structure of a molecule is the free energy minimum resulting from the optimization of several attractive and repulsive intermolecular interactions with varying

strengths, directional preferences and distance-dependence properties. Therefore understanding the nature and strength of intermolecular interactions is of fundamental importance in supramolecular chemistry. Intermolecular forces are mainly of two types, (i) isotropic or non-directional ( $C\cdots C$ ,  $C\cdots H$ ,  $H\cdots H$  interactions) that defines the shape, size and close packing and (ii) anisotropic or directional<sup>3a</sup> as hydrogen bonds, charge transfer interactions, halogen interaction, and heteroatom interactions (e.g.  $O-H\cdots O$ ,  $N-H\cdots O$ ,  $C-H\cdots O$ ,  $C-H\cdots N$ ,  $O-H\cdots \pi$ , halogen $\cdots$ halogen, nitrogen $\cdots$ halogen, sulfur $\cdots$ halogen etc). Long range dispersion forces and short range repulsive forces are isotropic. These interactions vary with  $r^{-n}$ , where  $r$  is the distance between relevant non-bonded atoms and  $n$  is a positive integer. The attractive forces vary from  $r^{-1}$  to  $r^{-6}$  depending upon the interaction type and short range exchange repulsion varies with  $r^{-12}$ . Among all intermolecular interactions hydrogen bonding is the most reliable directional interaction and it has a fundamental role in crystal engineering.<sup>3a</sup> Hydrogen bonds are classified into three categories based on their strength as very strong, strong and weak hydrogen bonds (Table 1).<sup>7</sup> The properties of a crystalline material are the result of molecular arrangement in the crystal lattice, which is controlled by intermolecular interactions.

**Table 1** Some properties of very strong, strong and weak H-bonds.

| Properties                                | Very strong  | Strong  | Weak   |
|---|--|---|--|
| Bond energy<br>(-kcal mol <sup>-1</sup> ) | 15–40  | 4–15  | <4   |
| Examples                                  | $[F\cdots H\cdots F]^-$<br>$[N\cdots H\cdots N]^+$<br>$P-OH\cdots O=P$ | $O-H\cdots O=C$<br>$O-H\cdots O=C$<br>$O-H\cdots O-H$ | $C-H\cdots O$<br>$O-H\cdots \pi$<br>$Os-H\cdots O$ |
| Red shift in IR                           | >25%   | 5–25%   | <5%  |
| $D(X\cdots A)$ (Å)                        | 2.2–2.5  | 2.5–3.2   | 3.0–4.0  |
| $D(H\cdots A)$ (Å)                        | 1.2–1.5  | 1.5–2.2   | 2.0–3.0  |
| $\theta(X-H\cdots A)$ (°)                 | 175–180  | 130–180   | 90–180   |
| Covalency                                 | Pronounced   | Weak  | Vanishing  |
| Electrostatic                             | Significant  | Dominant  | Moderate   |

From crystal engineering point of view the strong, directional forces are more helpful to design target crystal structures. The interaction motifs for designing crystals

are termed as *supramolecular synthons*<sup>8a,b</sup> and Desiraju defined it as “*supramolecular synthons are structural units within supermolecules which can be formed and/or assembled by known or conceivable synthetic operations involving intermolecular interactions.*” The concept is widely used in the design of solids which are important from scientific and commercial viewpoints. The synthesis of supramolecular structures in the solid state dealing with the self-assembly of molecular crystals using hydrogen bonding, electrostatics,  $\pi$ -stacking, halogen bonding, van der Waals interactions, and metal-coordination bonding. Crystal engineering is effectively like supramolecular synthesis in the solid state, and there is a direct analogy between the *supramolecular synthon* and the *molecular synthon*<sup>8c,d</sup> that was originally proposed for organic synthesis by E. J. Corey<sup>8c</sup> in 1967. The advantage of using the synthon approach is that it offers a simplification in the understanding of crystal structures. Zaworotko sub-classified synthons as homosynthons and heterosynthons based on the interacting functional groups. If supramolecular synthon is formed between the same functional group it is a homosynthon, if it forms between two different functional groups it is called as heterosynthon.<sup>9</sup> Some of the well known homosynthons are COOH $\cdots$ COOH, CONH<sub>2</sub> $\cdots$ CONH<sub>2</sub>, OH $\cdots$ OH, NH<sub>2</sub> $\cdots$ NH<sub>2</sub>, halogen $\cdots$ halogen, etc. which are between similar functional groups and COOH $\cdots$ pyridine, CONH<sub>2</sub> $\cdots$ pyridine, COOH $\cdots$ CONH<sub>2</sub>, OH $\cdots$ NH<sub>2</sub>, CONH<sub>2</sub> $\cdots$ N-oxide, halogen bonds, etc. are heterosynthons (Figure 1).

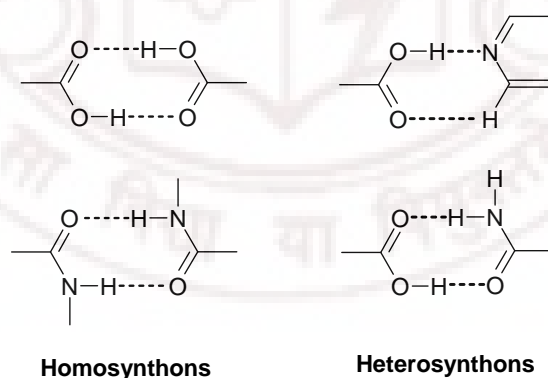


**Figure 1** Examples of homosynthons and heterosynthons.

Similar to hydrogen bonds, halogen bonds<sup>10</sup> are the noncovalent interaction between halogen atoms (Lewis acids) and neutral or anionic Lewis bases, emerging as prototype to hydrogen bonding. The interaction energy for halogen bond spans over a



wide range from 1 to 35 kcal mol<sup>-1</sup>. The weak Cl $\cdots$ Cl interaction between chlorocarbons and the very strong I $\cdots$ I<sub>2</sub> interaction in I<sub>3</sub><sup>-</sup> being the extremes. Weak interactions<sup>11</sup> that include C–H $\cdots$ O and C–H $\cdots$ N hydrogen bonds,<sup>11a</sup> C–H $\cdots\pi$ ,<sup>11i</sup> halogen $\cdots$ halogen interactions<sup>10</sup> etc. are important in crystal design. C–H $\cdots$ O and C–H $\cdots$ N hydrogen bonds are electrostatic in nature and have long-range distance character that have importance in wide variety of chemical and biological systems. C–H $\cdots$ O hydrogen bonds are capable of exhibiting all the properties<sup>11e</sup> that are similar to strong hydrogen bonds such as dependence on the acidity and basicity of donor and acceptor strengths and near linearity of the interaction and lone-pair directionality of the acceptor.

Identification of molecular functionalities that will generate predictable or robust intermolecular interactions/ synthons is the key step of crystal engineering. The situation will become more complicated in multi-functional molecules because of competition between similar strength donor/acceptor groups. To understand hydrogen bonding and its competition in organic compounds, Etter proposed<sup>12</sup> three hydrogen bond rules as, (a) *“all acidic hydrogens available in a molecule will be used in hydrogen bonding in the crystal structure of that compound,”* (b) *“all good proton acceptors will be used in hydrogen bonding when there are available hydrogen-bond donors,”* and the third rule is that (c) *“the best hydrogen-bond donor and the best hydrogen acceptor will preferentially form hydrogen bonds to one another.”* These rules provide useful information about the preferred connectivity patterns, hydrogen bond competition and stereoelectronic properties of hydrogen bonds for a particular functional group or for sets of functional groups. The methods of ranking solid-state hydrogen bond preferences are based on functional group competitions in homomeric crystals or heteromeric cocrystals. These rules involved in analyzing which donors are selected by a limited number of acceptors or *vice versa* during crystallization. The analysis of hydrogen bonds and other weak interactions and its cooperation and competition will guide the construction of target architectures and functions. A huge storehouse of crystal structures in the Cambridge Structural Database (CSD)<sup>13</sup> of nearly 4,83,000 crystal structures up to May 2009 (compared to very small sized 2000 entries in 1965) provides an excellent tool for accessing the efficiency and reproducibility of a particular supramolecular synthon in molecular crystals. A study on the probabilities of occurrence of supramolecular

synthons in a supramolecular system in presence or absence of second competing functionality is discussed in Chapter 6 with a detailed chronological literature survey. Our synthon analysis study<sup>14</sup> of carboxylic acid, pyridine, amine, and hydroxyl functional groups while present in same supramolecular system is discussed in Chapter 6.

Bernstein<sup>15</sup> developed geometrical notations to recognize the hydrogen bond patterns that are known as Graph Set Notation. Graph set approach is nothing but to analyze the hydrogen-bond patterns from a complicated networks structure to a reduced simple pattern. There are combinations of four, each specified by a designator: chains (**C**), rings (**R**), intramolecular hydrogen-bonded patterns (**S**), and other finite patterns (**D**). Specification of a pattern is augmented by a subscript designating the number of hydrogen-bond donors **d** and a superscript giving the number of hydrogen-bond acceptors **a**. In addition, the number of atoms **n** in the pattern is called the degree of the pattern and is specified in parentheses. The graph set descriptor is then given as  $[G_d^a(n)]$ , where **G** represents one of the four possible designators. Some examples are given in Figure 2.

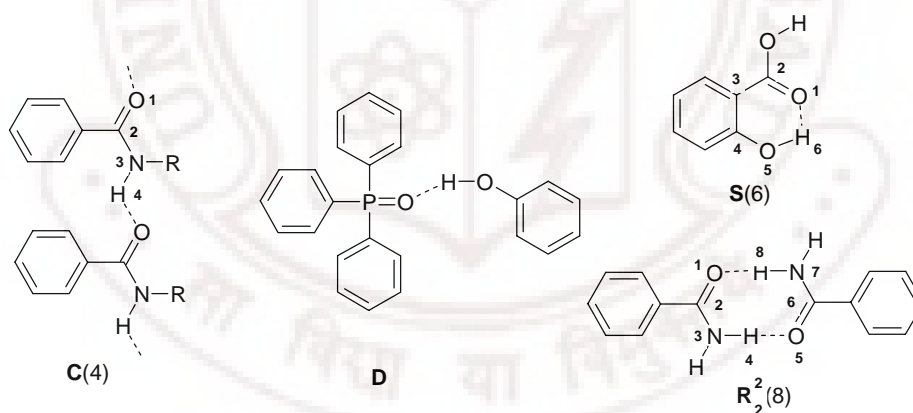


**Figure 2** Examples of various graph set descriptors.

### 1.3 Organic Solid-State Forms

A crystal is "a three dimensional atomic, ionic, or molecular structure consisting of periodically repeated, identically constituted, congruent unit cells"<sup>16a</sup> and the process of the formation of solid crystals from the homogeneous solution, melt or by direct vapor

deposition is known as crystallization.<sup>16b</sup> Crystal is a well-defined pattern, or structure, dictated by forces acting at the molecular level and during its formation process the solute concentration should reach a certain critical value, before changing status otherwise solid formation is impossible below the solubility threshold at the given temperature and pressure conditions. Crystallization process consists of two main events, (i) nucleation and (ii) crystal growth. Nucleation is the step where the solute molecules dispersed in the solvent start to assemble into clusters, on the nanometer scale (elevating solute concentration in a small region), that becomes stable under that conditions. The stable clusters constitute the nuclei otherwise they re-dissolve and form the stable once again. Supersaturation is the driving force for initial nucleation step. The nuclei are stable only when they reach a critical size and such critical size is dictated by the operating conditions (temperature, supersaturation, etc.). Single crystal X-ray diffraction and powder X-ray diffraction are two very powerful techniques to determine crystal structures. Crystal structures offer an understanding of various forces responsible for holding the organic crystalline solids that can be engineered to have desired properties. The nature of crystallization process is governed by thermodynamic and kinetic factors (Figure 3). Several research groups studied crystal growth aspect.<sup>17</sup> Davey *et. al.*<sup>17a,b</sup> and Desiraju *et. al.*<sup>17c</sup> studied nucleation and crystal growth on the crystal formation pathway of tetrolic acid and Na(saccharinate).nH<sub>2</sub>O systems respectively. These are some of the typical studies to understand primary stage of crystallization. Ostwald<sup>18</sup> stated that a system moves to equilibrium from an initial high-energy state through minimal changes in free energy. Therefore the structure that crystallizes first is one which has the lowest energy barrier (highest energy, kinetically metastable). This form would then transform to the next lower energy polymorph until a thermodynamically stable state is reached, the so-called Ostwald's Law of Stages (Figure 4).

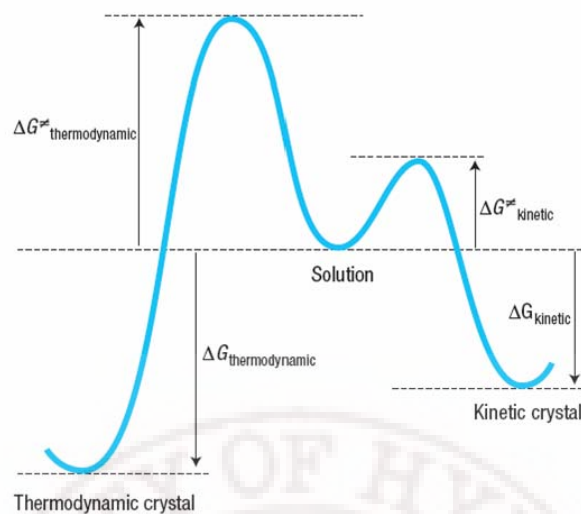


**Figure 3** Hypothetical transitions from solution to thermodynamic and kinetic crystals. Small difference between  $\Delta G^{\ddagger}_{\text{thermodynamic}}$  and  $\Delta G^{\ddagger}_{\text{kinetic}}$  determines formation of kinetic crystals.

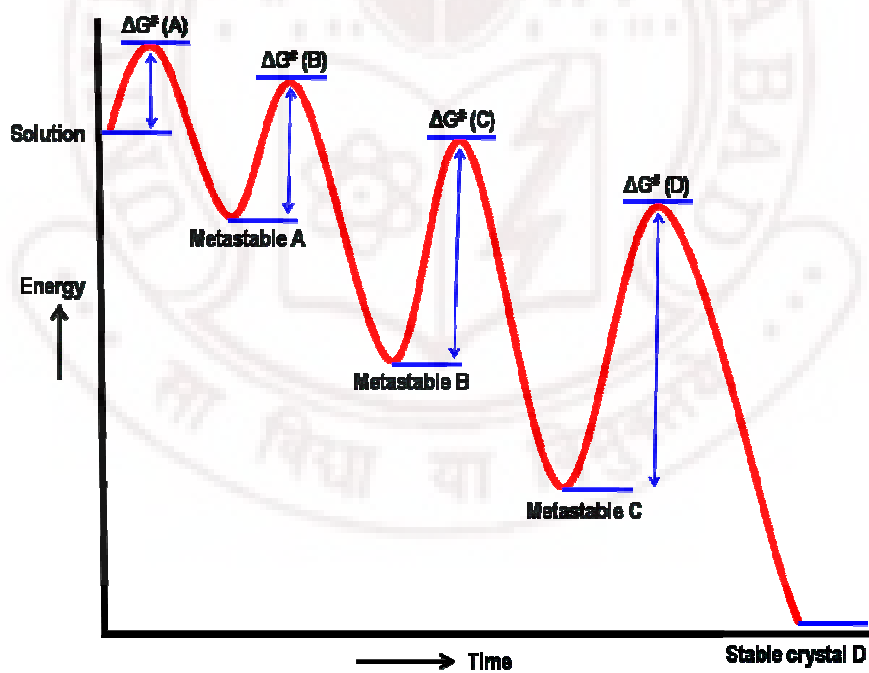


**Figure 4** Ostwald's Rule of Stages. Initial high-energy state (metastable A) through minimal changes in free energy crystallizes first is one which has the lowest energy barrier. Metastable A form will then transform to the next lower energy polymorph (metastable B) and so on (metastable C) until thermodynamically stable crystal D.

Crystal engineering deals with various solid forms. It includes polymorphs, host-guest complexes, network solids, salts, hydrates, cocrystals, more preferably pharmaceutical cocrystals, and this chapter will cover a brief introduction to various organic solid-state forms and the concept and its importance. When a compound crystallized in two or more different crystalline modifications, they are known as polymorphs and the phenomenon is polymorphism.<sup>19</sup> Cocrystals<sup>20</sup> can be defined as multiple-component crystal structure in which two or more compounds coexist through hydrogen bonds or non-covalent interactions. If the reactants are solids at ambient conditions, the multi-component crystalline materials are cocrystals and those composed of one or more solids and a liquid are known solvates or pseudopolymorphs<sup>21</sup> and hydrates<sup>22</sup> when solvent is water. However the multi-component system is known as molecular salt/ salt<sup>14,23</sup> if proton is transferred from acid to base and retains as ionic state. Thus salts and cocrystals are multicomponent crystals that can be distinguished by the location of the proton between an acid and a base. Cartoon depictions of all these solid phases are illustrated in Figure 5.

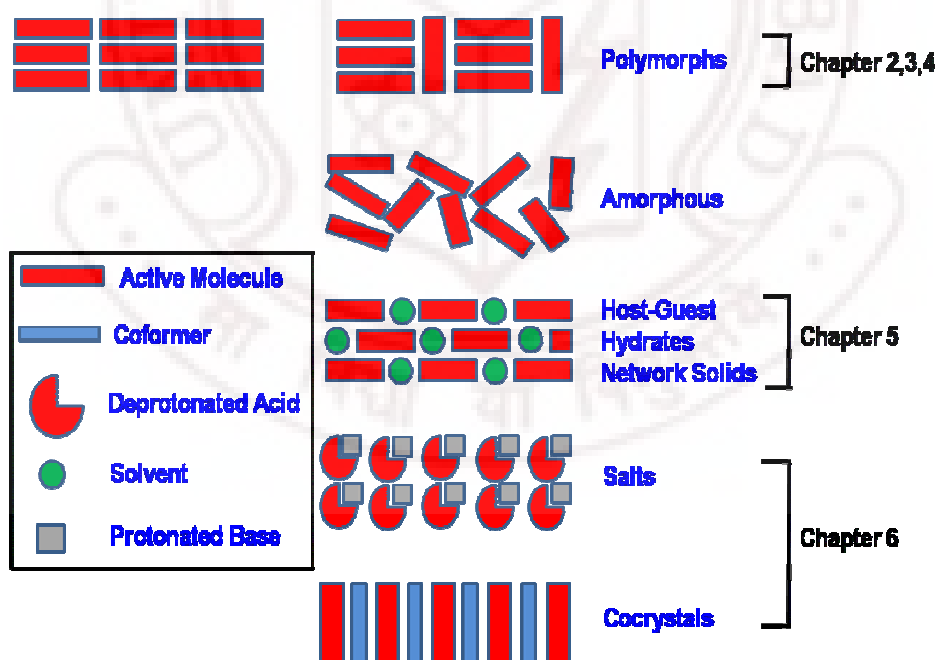


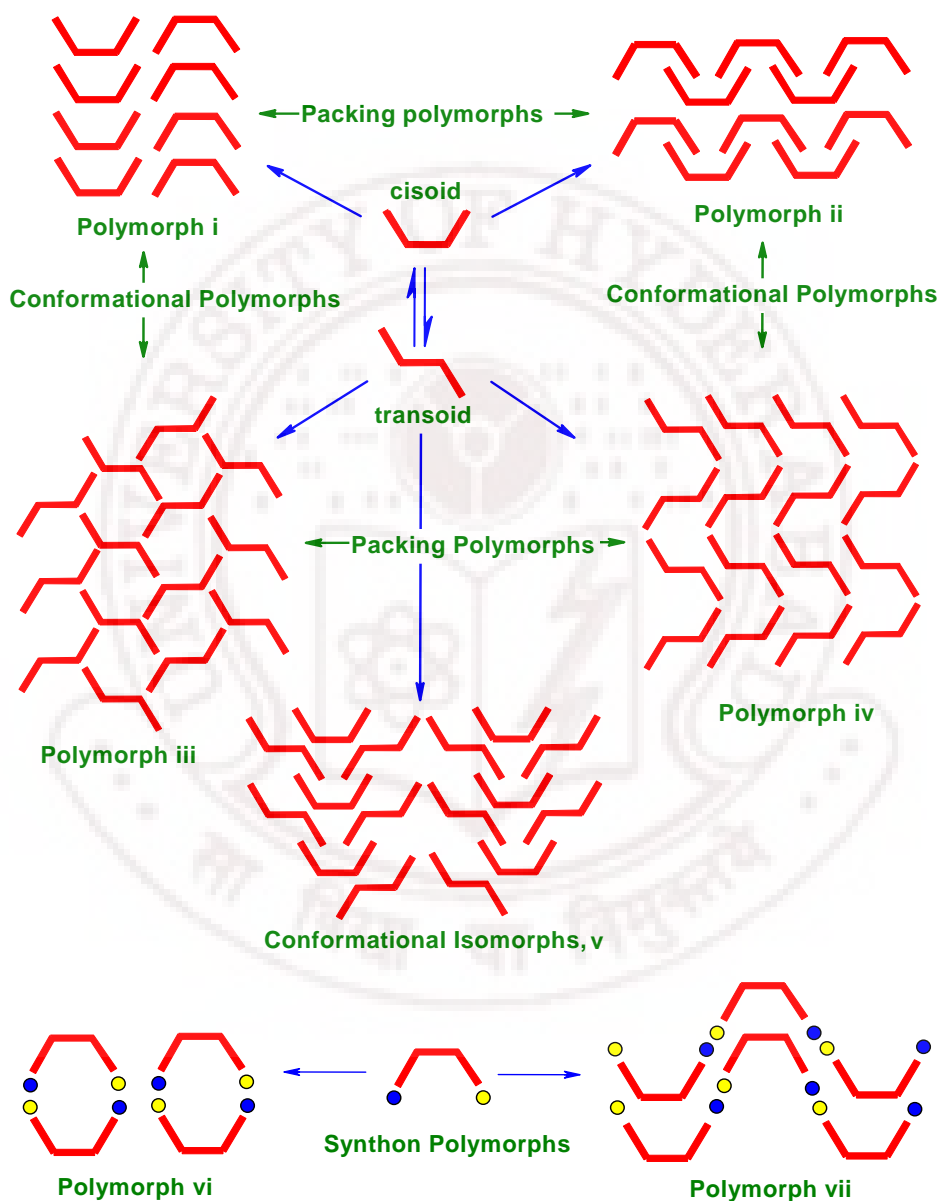
**Figure 5** Cartoon depictions of various organic solid forms and discussed in the corresponding Chapters.

## 1.4 Polymorphism

The word ‘*Polymorphism*’ originally comes from the Greek literature (*poly* = many, *morph* = form). Polymorphism was first realized in 1798, when the German chemist Martin Heinrich Klaproth discovered calcite minerals and aragonite had the same chemical composition ( $\text{CaCO}_3$ ). Mitscherlich first documented polymorphism in 1822 in the context of crystallography<sup>24a</sup> of arsenate and phosphate salts that can exist as different crystal forms. Ostwald’s work<sup>18</sup> on the relative stability of different crystal structures of the same compound was a major development in polymorphism. Polymorphism acquired potential importance after Buerger and McCrone’s work<sup>24c</sup> on change in properties like melting point and solubility of different crystal forms of the same chemical compound. The existence of different crystal structures for the same element or atom is known as allotrope first described by Berzelius.<sup>24d</sup> Allotropes are at the elemental (e.g. C, S, P, Sn etc.) level whereas polymorphism is used to refer structural diversity of molecular compounds.<sup>24e</sup> For example carbon has three allotropes, diamond, graphite and fullerene. Depending on the atomic arrangement in their lattice they show quite different properties. A widely accepted definition of polymorphism was given by McCrone<sup>24f</sup> which states that “*a solid crystalline phase of a given compound resulting from the possibility of at least two crystalline arrangements of the molecules of that compound in the solid state*”. Buerger<sup>24g</sup> tried to simplify the definition limiting only for *solids composed of one component*, but the concept was confusing and misleading as polymorphism can exist in multi-component system as well.

Polymorphism may occur due to various reasons, packing of molecules, conformational or molecular flexibilities, supramolecular synthon competitions are the main reasons and subsequently they are called as packing, conformational and synthon polymorphs<sup>19,25</sup> (Scheme 1). Packing polymorphism exists when the molecule is mostly rigid. Conformationally flexible molecules have greater scope for their polymorphic occurrence because of large number of degrees of freedom as the energy differences between conformational polymorphs lies in a small window of  $0.5\text{--}3\text{ kcal mol}^{-1}$ . A metastable conformation may be stabilized by stronger hydrogen bonds in the crystal structure while a stable conformer may not be able to form strong hydrogen bonds, although they lead to a balance of energy state and the overall stability of a polymorph is accounted by measuring conformation energy and lattice energy. The energy

compensation towards overall energy of a polymorphic system and the phenomenon known as systematic effect was recently reviewed by Nangia<sup>25c</sup> with several examples of conformational polymorphs. Our result on conformational and synthon polymorphism is discussed in Chapter 2 and 4.



**Scheme 1** Schematic illustrations of different arrangement of molecules in the crystalline lattice that leads to different kinds of polymorphism. This scheme is culled from A. Nangia *Acc. Chem. Res.* **2008**, *41*, 595.



Different polymorphs have different physical and chemical properties (Table 2). Thus characterization of all polymorphs through polymorph screening using various methods like solvent less methods of melt and sublimation via green methodology, solution crystallization etc. and then identification of stable form and control over the preparation of that particular form has become a major goal for academic (crystal engineering and solid-state chemistry) and industry research.<sup>19,26a</sup> Polymorphism of drugs is of central interest after the Norvir and Zantac<sup>26</sup> incidents in the last decade. Dissolution profile of Ritonavir polymorphs shows a significant difference with unique crystal structures. Polymorph I is almost five times more soluble compared with Polymorph II which is almost insoluble. Thus a thorough screening and complete characterization of all possible polymorphs is considered an essential step in pharmaceutical industry to choose the best drug formulation with desirable properties. The extensive study on polymorphism gives fundamental understanding on molecular recognition, crystal nucleation, and structure–property relationships.<sup>27</sup> Among the various methods of polymorph generation, solution crystallization and/or high-throughput crystallization<sup>28</sup> are default. Recent approaches for polymorph generation include crystallization with structurally related additives,<sup>29a,b</sup> epitaxial growth,<sup>29c</sup> laser induced nucleation,<sup>29d</sup> crystallization in capillaries,<sup>29e</sup> confinement within porous materials,<sup>29f</sup> using polymers as heteronuclei,<sup>29g,h</sup> mechanical grinding,<sup>29i</sup> using supercritical liquids,<sup>29j</sup> using self assembled monolayer with different functional moieties,<sup>29k</sup> potentiometric cycling<sup>29m</sup> etc. Recently melting and sublimation, the two solvent less high temperature techniques to afford guest free host structures were explored<sup>25d</sup> by our group and those techniques were employed to generate new polymorphs of compound that are prone to give guest included crystal on solution crystallization with very good probabilities.



**Table 2** Properties that can be different for polymorphs. This table is culled from, S. Dutta, D. J. W. Grant, *Nat. Rev. Drug Discovery*, **2004**, 3, 42.

|  |   |
|--|---|
| <b>Packing properties</b>              | <b>Thermodynamic properties</b>                       |
| • Molar volume and density             | • Melting and sublimation temperatures                |
| • Refractive index, optical properties | • Internal energy                                     |
| • Conductivity, electrical and thermal | • Enthalpy  |
| • Hygroscopicity                       | • Heat capacity                                       |
| <b>Kinetic properties</b>              | • Entropy   |
| • Dissolution rate                     | • Free energy and chemical potential                  |
| • Rates of solid state reactions       | • Thermodynamic activity                              |
| • Stability                            | • Vapour pressure                                     |
| <b>Surface properties</b>              | • Solubility  |
| • Surface free energy                  | <b>Spectroscopic properties</b>                       |
| • Interfacial tensions                 | • Electronic transitions, ultraviolet-visible spectra |
| • Habit                                | • Vibrational transitions, infrared and Raman spectra |
| <b>Mechanical properties</b>           | • Rotational transitions                              |
| • Hardness                             | • Nuclear magnetic resonance chemical shifts          |
| • Tensile strength                     |   |
| • Compactibility, tabletability        |   |
| • Handling, flow and blending          |   |

## 1.5 Enantiotropic and Monotropic Related Polymorphs

The thermodynamics of polymorphs of molecular crystals can be represented by pressure-temperature or commonly used energy-temperature phase diagram that are helpful for characterizing and understanding polymorphic behavior of a compound. Polymorphism exists in the solid state and natural physical process phase transition between polymorphs is a common phenomenon. The stability relationship of polymorphs of a molecule can be established by measuring their enantiotropic or monotropic relationship.<sup>9a</sup> The two polymorphic modifications are said to be enantiotropic when the transition point between the two phases is found at a temperature below the melting point of either of them (Figure 6a). When there is no transition point below the melting point

of the two polymorphs then the two forms are monotropically related (Figure 6b). This is known as *heat-of-transition rule*.<sup>9a</sup> The *heat-of-fusion rule* states that in an enantiotropic system higher melting polymorph will have the lower heat of fusion. If the higher melting polymorph has a higher heat of fusion the two polymorphs are monotropically related. Solid and liquid will be in equilibrium at melting point and Gibbs free energy will be zero for two phases. The entropy of fusion can be expressed as,

$$\Delta S_f = \Delta H_f / T_f$$

*Entropy of fusion rule* states that two modifications are enantiotropically related if polymorph with higher melting point has the lower entropy of fusion and monotropically related if lower melting polymorph has lower entropy of fusion. eg. for a dimorphic system (Figure 6a) it is seen that the thermodynamic transition point  $T_{p,I/II}$  defined by the point at which  $G_I$  and  $G_{II}$  cross, falls at a temperature below the melting point of lower melting form,  $mp_{II}$  and hence enantiotropically related. However the free energy curves do not cross at a temperature below the two melting points (Figure 6b) and so they are monotropically related.

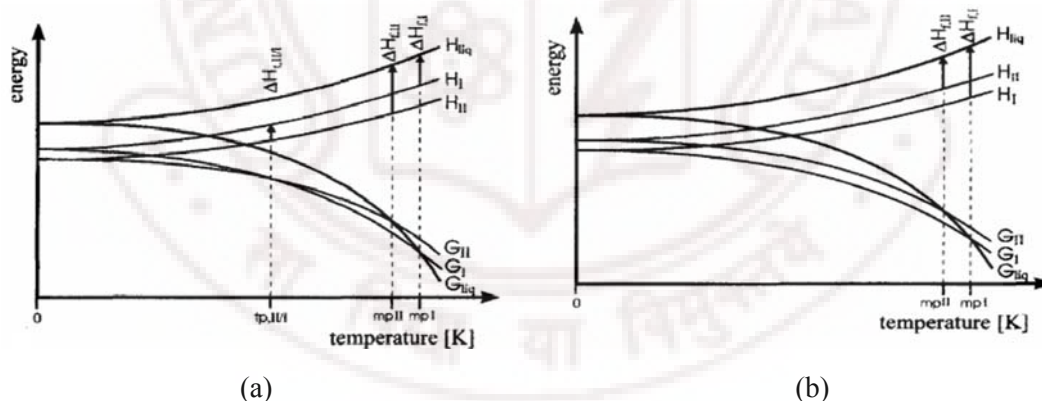


**Figure 6** (a) Fundamental E/T diagram for dimorphic enantiotropic system. Form I is stable below transition point. Above transition point Form II is stable. (b) Fundamental E/T diagram for dimorphic monotropic system. Form I is more stable at all temperature below melting point than form II.

Several analytical techniques are being used to establish the thermodynamic behaviour of polymorphs, eg. Optical and/ or Hot Stage Microscopy (HSM), Differential Scanning Calorimetry (DSC) etc. HSM can be used to obtain qualitative information on polymorphic behaviour however thermal analysis (DSC or DTA) provides quantitative

information about the relative stability of polymorphic modifications, the energies involved in phase changes between them and the monotropic and enantiotropic nature of those transitions. Tolbutamide [1-butyl-3-(4-methylphenylsulfonyl)urea], an oral hypoglycaemic agent exists in four polymorphic modifications. Polymorph I is stable and phase transition from polymorph III, II and IV can clearly be described by DSC thermograms (Figure 7). Transitions III→I, II→I, IV→I show those pairs are enantiotropically related. Monotropic and enantiotropic relation between polymorphs in several instances are observed and discussed in Chapter 2 and 4 with the help of HSM, DSC and X-ray diffractions. For characterization of polymorphs spectroscopic methods that include infrared (FT-IR), near infrared (NIR) and Raman spectroscopy etc., thermal analysis (DSC, TGA, HSM etc) and finally X-ray diffraction (single crystal and powder X-ray diffraction) are used.

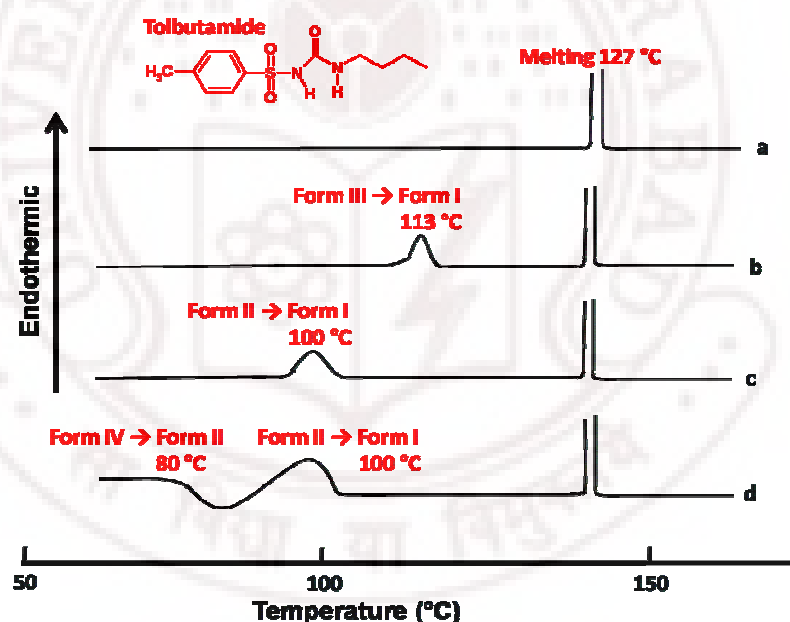


**Figure 7** DSC thermogram of Tolbutamide polymorphs: (a) Form I, (b) Form II, (c) Form III and (d) Form IV. The polymorph conversions from other forms to Form I are shown. These transitions are enantiotropically related.

## 1.6 Isostructurality

Geometrical properties like shape, size and chemical like electronegativity, polarizability of functional group influence crystal packing. Kitaigorodskii has given

importance to the volume and shape of functional groups in crystal packing,<sup>6</sup> however the electronic properties of functional groups cannot be over looked.<sup>30a,b</sup> As the size of the molecule increases the significance of geometric effects becomes important. A given packing motif may be able to tolerate small changes in the molecular structure without a considerable change in the close-packed crystal structure. These changes are minor alterations in substitution and/or epimerization. The tolerance may be ascribed to the presence of ~30% free space in close-packed structures because the packing coefficients of organic crystals are generally about 70%.<sup>30d</sup> The phenomenon by which different molecules pack in a similar fashion to produce similar crystal structures is called isostructurality and the structures are called isostructural<sup>30e</sup> and is inversely related to the phenomenon of polymorphism. Isostructurality and Isomorphism are two commonly used terms in literature. Two crystals are said to be *isomorphous*<sup>31a</sup> if (a) they have the same space group and unit-cell dimensions and (b) the types and the positions of atoms in both are same except for a replacement of one or more atoms in one structure with different types of atoms in the other (*isomorphous replacement*), such as heavy atoms, or the presence of one or more additional atoms in one of them (*isomorphous addition*). The substances are so closely similar that they can form a continuous series of solid solutions. On the other hand, two crystals are said to be *isostructural*<sup>31b</sup> if they have the same structure, but not necessarily the same cell dimensions nor the same chemical composition, and with a comparable variability in the atomic coordinates to that of the cell dimensions and chemical composition. e.g. calcite (CaCO<sub>3</sub>), sodium nitrate (NaNO<sub>3</sub>) and iron borate (FeBO<sub>3</sub>) are isostructural. The phenomenon of isomorphism is known for more than two centuries with the growth of potassium alum crystals from a saturated solution of ammonium alum. Kitaigorodskii<sup>6</sup> was the first to review isostructurality in organic molecular crystals. Kálmán et al. have divided isostructurality into two categories—isostructural crystals or main-part isostructuralism of related molecules and homeostructural crystals and proposed two descriptors to quantify isostructurality. They are unit-cell similarity index  $\Pi$  and isostructurality index  $I_i(n)$ <sup>30e</sup> and can be defined as the following equations. When the related molecules differing by substitutions on more than one atomic site have similar packing, it is called homeostructural crystals.

$$\Pi = \left| \frac{a+b+c}{a'+b'+c'} \right| - 1 \cong 0$$

where  $a, b, c$  and  $a', b', c'$  are orthogonalized lattice parameters of the related structures. For a pair of completely isostructural crystals  $\Pi$  should be close to zero.

$$I_i(n) = \left[ 1 - \left( \frac{\sum_i \Delta R_i^2}{n} \right)^{1/2} \right] \times 100$$

The isostructurality index,  $[I_i(n)]$  is a measure of the degree of internal isostructurality where  $n$  is the number of distance differences ( $\Delta R_i$ ) between the absolute coordinates of identical non-hydrogen atoms within the same section of asymmetric units of related structures.  $I_i(n)$  should be close to 100% for isomorphous crystals.

Isostructurality in three dimensions means the complete crystal packing. However one- and two dimensional isostructurality<sup>32</sup> is documented. When two structures show similar infinite two-dimensional molecular arrangements they are called as two-dimensionally isostructural. Accordingly similar arrangement of molecules in 1D is one-dimensionally isostructural. It is important to have some knowledge about which groups are interchangeable and under which circumstances to see the isostructural behavior between two structures. Kitaigorodskii<sup>33</sup> has ranked them as, (i) the halogens Cl, Br, I; (ii) O and S; (iii) C, quadrivalent Si, Ge, Sn and Pb. There are some examples where strong hydrogen bonding functional groups, such as  $-\text{OH}$ ,  $-\text{NH}_2$ ,  $=\text{O}$ , can also replace hydrogen to produce isostructural crystals (Figure 8). Isostructurality phenomenon was investigated for steroids by Kálmán with an exchange of functional groups (gamabufotalin/arenobufagin) or by epimerization ( $5\alpha$ - and  $5\beta$ -androstane-3  $\alpha,17\beta$ -diol).<sup>34</sup> 2-oxa-4-androstene-3,17-dione is isostructural with  $6\alpha$ -hydroxy analogue, replaced  $\text{C}-\text{H}\cdots\text{O}$  interaction by  $\text{C}-\text{O}-\text{H}\cdots\text{O}$  hydrogen bond is an example of 1D isostructurality from our group (Figure 8b).<sup>32b,c</sup> The fact that these two compounds form solid solution validates the isomorphous replacement of  $\text{C}-\text{H}$  atom by  $\text{C}-\text{OH}$  group (Figure 8d, 8e).

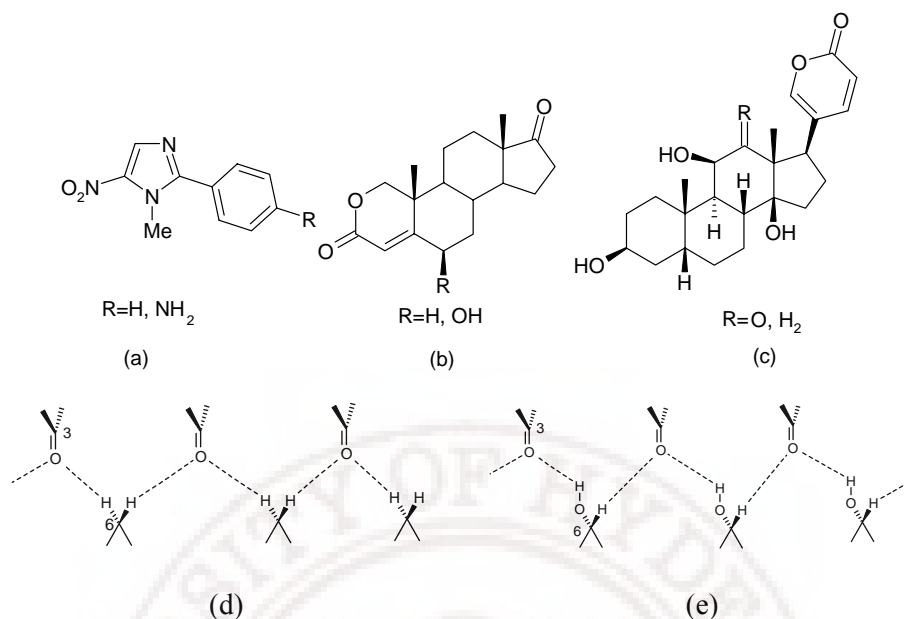


**Figure 8** (a) H/NH<sub>2</sub> exchange forms isostructural crystals. (b) In 6α-Hydroxy-2-oxa-4-androstene-3,17-dione, H/OH exchange produces isostructural crystals. (c) H<sub>2</sub>/O exchange generates isostructurality. (c) via C–O–H...O synthon in (d) without disturbing the overall arrangement of molecules; (d) Hydrogen bonding of 2-oxa-4-androstene-3,17-dione when R = H and (e) R = OH. Identical *a*-axis and the similarity in hydrogen bonding and arrangement of molecule in both structures lead to isostructural, due to replacement of C–H...O synthon by C–O–H...O.

Triiodoresorcinol and triiodophloroglucinol are rare case of examples which are both polymorphic and isostructural recently reported from our group.<sup>35a</sup> They crystallized as orthorhombic ( $P2_12_12_1$ ) and monoclinic ( $P2_1/n$ ) polymorphs and the orthorhombic polymorphs of both compounds are isostructural and correspondingly monoclinic polymorphs are also identical. These examples illustrate isostructurality via C–H  $\leftrightarrow$  C–OH replacements. Another example that shows both polymorphism and isostructurality is 2-amino-4-chloro-6-morpholinepyrimidine and 2-amino-4-chloro-6-piperidino pyrimidine.<sup>35b</sup> Exceptions are also reported. For example room temperature form of 2,6-dichloro-N-phenylformaide and 2-chloro-6-methyl N-phenylformaide (both orthorhombic) are isomorphous<sup>35c</sup> but their high temperature forms (both in monoclinic) are not isomorphous. 2-Amino-4-chloro-6-morpholinopyrimidine is dimorphic with  $Z' = 2$  and 1 in space group  $P2_1/c$ . The  $Z' = 2$  polymorph is isostructural with 2-Amino-4-chloro-6-piperidinopyrimidine that has only one crystal structure with  $Z' = 2$  showing O

$\Leftrightarrow$  CH<sub>2</sub> replacement. Chloro–methyl exchange is well known and this rule states that when the geometry of the groups governs the crystal packing they produce isostructural crystals due to their similar size and shape (Cl 20 Å<sup>3</sup> and Me 24 Å<sup>3</sup>),<sup>35d</sup> discussed thoroughly and calculated isostructurality index and unit cell similarity index of newly synthesized series of similar phenylbenzenesulfonamides and its polymorph structures that is covered in Chapter 4. Isostructurality in organic solids is well documented in literature.<sup>35</sup> There is a report on bromide and nitrate exchange in isostructural crystals in spite of their different shapes where both of the anions make strong H-bonds with the cation counter part.<sup>35e</sup> Above all these groups, the halogen exchange,<sup>35f</sup> specially Cl, Br and I to produce isostructurality, are more frequent. Propargylammonium halides (Cl<sup>−</sup>, Br<sup>−</sup>, I<sup>−</sup>) are isostructural where halide ions accept three H-bonds from ammonium group and one from terminal alkyne group. Another interesting isostructurality has been reported by Bar et al.<sup>35g</sup> in *para* substituted X–C<sub>6</sub>H<sub>4</sub>–CH=N–C<sub>6</sub>H<sub>4</sub>–X' molecules. When X = X' = Cl or Br, the molecules are not isostructural, but molecule with X = Cl and X' = Br is isostructural to the dichloro compound. On the other hand X = Br and X' = Cl substituted molecule is isostructural to dibromo derivative. It indicates the importance of halogens as well as the position of substitution in the molecules. In principle, two isostructural compounds are expected to yield the similar polymorphs<sup>35q</sup> and the idea is similarly applicable for multi-component systems like solvate, salt and cocrystals etc. Isostructural crystals often lead to similar kind of properties.<sup>35r,s</sup>

## 1.7 Polymorphism and High Z' Structures in Solvent Less Methods

Awkward molecular shape, OH, NH<sub>2</sub>, SO<sub>3</sub>H like sticky functional groups, ionic nature etc. are some of the factors for hydration and/or solvent inclusion complexes of organic molecules, especially APIs. In drug industry, solvent inclusion complexes are not advisable because of the toxic vapor nature of most solvents. Thus the synthesis and characterization of guest-free crystalline forms has gained importance but difficult to crystallize because, in general a solvent or water molecule acts as a crystallization aid or filler in the voids of the host. Methods that have been used to obtain guest free structure of lattice inclusion host compounds and discussed in Chapter 2. Temperature lowering, isothermal evaporation and isothermal diffusion crystallization techniques are common



methods to grow single crystals. Some popular methods to produce guest free host crystal structure are (a) misfit size and/or shape<sup>36a</sup> of the guest molecule to the void formed by the host, (b) using an appropriate dual-nature solvent or unfavourable electrostatic interactions,<sup>36b,c</sup> (c) layer-by-layer conversion of particles from the outside in as guest is leached out,<sup>36d</sup> (d) recrystallization with a solvent-nonsolvent<sup>36e</sup> system, (e) sonication,<sup>36f</sup> (f) gradual pH change<sup>36g</sup> etc. High temperature crystallization methods melting and sublimation<sup>36h,i</sup> were explored recently from our group. The two high temperature solvent less methods of green methodology generate guest free structures of well known host 1,1-bis-(4-hydroxyphenyl)cyclohexane<sup>j</sup> and further illustrated with isomeric dihydroxybenzoic acid molecules and successfully isolated guest free forms and new polymorphic modification of other cases are covered.

$Z'$  ( $Z'$  prime)<sup>37a,b</sup> is the number of symmetry independent or crystallographic unique molecules in a crystal lattice. Structure with  $Z' = 1$  means that each molecule is surrounded by like molecules, however,  $Z' > 1$  structure means each molecule is surrounded by molecules that are crystallographically different. The occurrence and reasons behind high  $Z'$  structures have attracted attention of crystallographers and now being intensely studied to understand the factors leading to high  $Z'$  crystal structures even as occurrence of high  $Z'$  structures is still not properly understood. Steed<sup>37a</sup> showed presence of pseudosymmetry, awkward shape, formation of molecular helices via hydrogen bond or other interactions, strong hydrogen bonds, chirality, kinetic or temperature effect are different reasons for high  $Z'$  structures are elaborately discussed in Chapter 3. Our observation<sup>25d</sup> is the frequent occurrence of high  $Z'$  structures in high temperature solvent less methods of melt and sublimation and compared with Cambridge Structural Database (CSD). It is found that solvent-free crystallization methods show a much higher probability of multiple  $Z'$  structures (~18%) compared to overall CSD trends on  $Z'$  frequencies (<12%). Generation of high  $Z'$  structures by melting and sublimation crystallization can be understood as rapid cooling of the hot liquid or vapor in the open flask or on the cold finger is a kinetic phase and the conditions under which hydrogen-bonded clusters are likely to condense in a pseudo-symmetric crystalline arrangement. Popular host 1,1-bis-(4-hydroxyphenyl)cyclohexane is found to be a remarkable example to illustrate the occurrence of high  $Z'$  structure in metastable polymorph by melting. Solvent less methods when used to generate guest free host

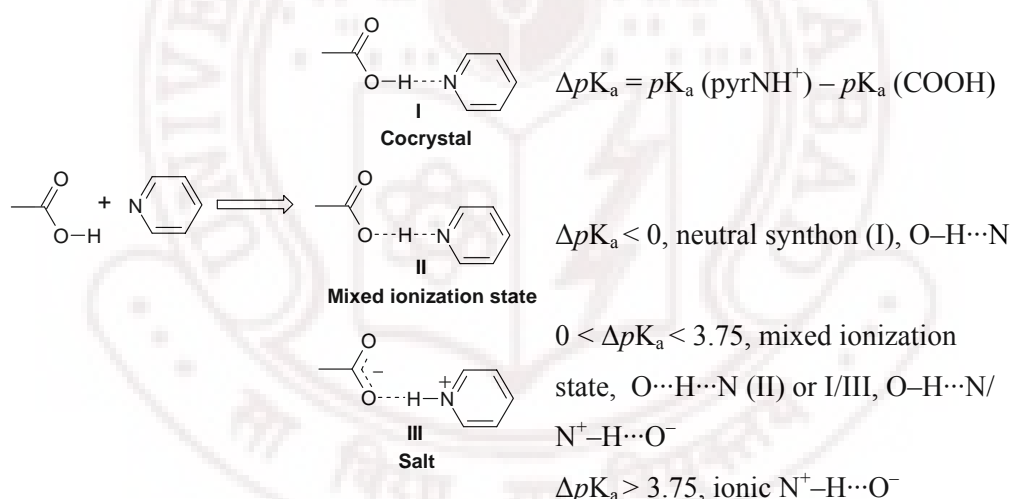


structures of isomeric dihydroxybenzoic acids,  $Z' > 1$  structure is observed commonly discussed in Chapter 2 and 3. Carbamazepine<sup>37c</sup> is another exciting example for which  $Z' = 1$  from solution crystallization (3 polymorphs) whereas  $Z' = 4$  when it is crystallized from melting.

## 1.8 Salt Cocrystal Continuum

It is a must to label and classify crystalline solid forms in order to characterize them and then make comparisons. There has been a long standing and lively debate on the nomenclature issues in crystal engineering, starting from what is a cocrystal, or co-crystal/salts, to the definition of pseudopolymorph, solvate, host–guest compounds etc. In general, molecular crystals can be classified broadly into single-component and multiple-component crystals. Salts and cocrystals are multi-component crystals there exists a continuum linking cocrystals and salts based on the extent of proton transfer between the components. Cocrystals can be defined as multiple-component crystal structure in which two or more compounds coexist through hydrogen bonds or non-covalent interactions. If the reactants are solids at ambient conditions, the multi-component crystalline materials are cocrystals and those composed of one or more solids and a liquid are known solvates or pseudopolymorphs.<sup>21</sup> However the multi-component system is known as molecular salt/ salt if proton is transferred from acid to base in the ionic state. If a solution containing an organic acid and an organic base deposits a crystalline solid containing both components, the result can be a molecular salt or a cocrystal. If the proton resides on the base, then proton transfer has occurred and the crystalline acid-base complex is a molecular salt. If proton transfer has not occurred and the proton remains on the acid, then it is a cocrystal.<sup>21,38a</sup> The propensity of an acid to give up a proton is represented by its  $pK_a$ , the negative logarithm of the dissociation constant.  $pK_a$  relates to the equilibrium behavior in aqueous solution and measured  $pK_a$  values will vary depending on measurement technique, solvent, temperature, and other factors. The extent of proton transfer depends on the magnitude of the difference of  $pK_a$  values of the reacting acid and base. It is generally accepted that reaction of an acid with a base will be expected to form a salt if the  $\Delta pK_a$  [ $\Delta pK_a = pK_a(\text{base}) - pK_a(\text{acid})$ ] is greater than 3.75, which is an essential criteria while selecting the appropriate counter ions to the preparation of salts of API in order to improve its properties like solubility.

For acid-base complexes with similar  $pK_a$  values the  $\Delta pK_a$  value and the crystalline environment determine the extent of proton transfer. Johnson and Rumon studied<sup>38b</sup> the type of hydrogen bonding interaction as a function of  $\Delta pK_a$ , where  $\Delta pK_a$  refers to the difference in  $pK_a$  of pyridinium ion ( $BH^+$ ) and the benzoic acid ( $AH$ ) in water via infrared spectra of solid state complexes of benzoic acid and substituted benzoic acids with pyridine and substituted pyridines. Extensive study by Nangia *et. al.*<sup>39</sup> based on the analysis of several cocrystals and salts, concluded that the carboxylic acid–pyridine  $O\cdots H\cdots N$  interaction will be neutral when  $\Delta pK_a < 0$  and it will have an intermediate H bond character,  $O\cdots H\cdots N$  and/or  $N^+-H\cdots O^-$ , when the transition range  $0 < \Delta pK_a < 3.75$ . The interaction will be ionic  $N^+-H\cdots O^-$  when  $\Delta pK_a > 3.75$  (Scheme 2). Similar observation was noted by Childs and Stahly<sup>38</sup> in their analysis of 20 complexes of theophylline with COOH partners, which resulted in 16 salts, 2 cocrystals and 2 mixed ionizations states with transition range  $0 < \Delta pK_a < 2.5$ .



**Scheme 2** The  $pK_a$  rule thumb to predict the H-bonding motifs in multi-component crystals.

Although the contribution from Aakeroy, Black, Price, Tocher *et. al.*<sup>39</sup> is worthy, it is really difficult to predict any general conclusions about proton transfer in acid-base systems. A detailed discussion is recently reported from our group and presented in Chapter 6. The  $pK_{HB}$  scale, proposed by Laurence,<sup>40</sup> measures the free energy of hydrogen bonded complex ( $1.364 pK_{HB} = -\Delta G_{HB}$  in  $\text{kcal mol}^{-1}$ ) could be a better guide in predicting H-bond pairing compared to  $pK_a$  values as it deals with sharing of H atom

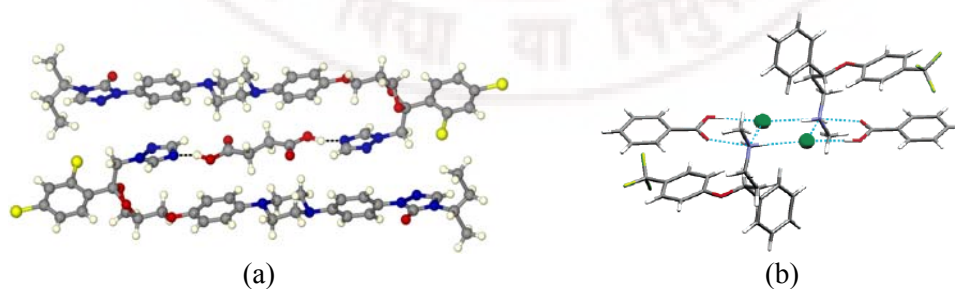
between two electronegative atoms, while the  $pK_a$  scale considers only the ability of the proton to be transferred from acid to base. The  $pK_{HB}$  values are quite sensitive to factors that modify H-bonding ability, *e.g.* inductive/resonance effects, steric hindrance, lone-pair repulsion, and intramolecular H-bonding.

## 1.9 Pharmaceutical Cocrystals

Cocrystals and salts are very useful in designing extended supramolecular architectures; prepare NLO materials, solid-state photodimerisation reactions, enantio separation of racemic compounds, pharmaceutical developments etc. Cocrystallization is a very important technique to develop new pharmaceutical phases of active pharmaceutical ingredients (APIs). Pharmaceutical cocrystals are crystalline molecular complexes of an Active Pharmaceutical Ingredient (API) with another pharmaceutically acceptable molecule or Generally Regarded As Safe (GRAS) chemicals. Food additives, preservatives, excipients, vitamins, minerals, amino acids, bio-molecules, and other APIs can be selected as cocrystal formers (CCF). Zaworotko *et al.* stated<sup>41</sup> that polymorphs, pseudopolymorphs, salts, molecular complexes and cocrystals of APIs can modify chemical and physical properties that may lead to extended patent coverage and consequent legal protection of products. Several pharmaceutical crystals are known to undergo a variety of phase transformations. Phase transformations during processing and formulation can affect the stability and bioavailability of drugs. Crystalline APIs are strongly preferred due to their relative ease of isolation, the rejection of impurities inherent to the crystallization process and the physico-chemical stability that the crystalline solid state affords. Crystal engineering affords a paradigm for rapid development of APIs, that of pharmaceutical cocrystals and salts which can be rationally designed. Recent articles<sup>42</sup> emphasize the development and importance of pharmaceutical cocrystals. For example, cocrystallization of aspirin, *rac*-ibuprofen, and *rac*-flurbiprofen with 4,4'-bipyridine by Zaworotko;<sup>42a</sup> Fluoxetine hydrochloride with pharmaceutically acceptable carboxylic acids (Figure 9b) by Childs;<sup>42b</sup> several drug molecules with Saccharine as API saccharinate salts by Desiraju;<sup>42c,d</sup> Itraconazole with 1,4-dicarboxylic acids by Remenar;<sup>42e</sup> Carbamazepine with Saccharin as saccharinate salts<sup>42f</sup> etc. were the well known strategies to deal with inadequate solubility, dissolution

rate, absorption, physical stability, complexation etc. of APIs. Extremely water insoluble nature of Itraconazole, an antifungal agent, is solved by making itraconazole–succinic acid cocrystals (Figure 9a) as oral formulation. Cocrystal of carbamazepine and saccharin (CBZ–SAC) appears to be superior to existing crystal forms of CBZ with respect to stability, favourable dissolution, suspension stability, and favourable oral absorption profile. Hydration behaviour of caffeine and theophylline was controlled by their 1:1 cocrystals with oxalic and other diacids. These cocrystals or salts exhibit physical properties different from those of the parent compounds as a direct result of hydrogen-bonding interactions between the binary components of the crystals. However, the utility of cocrystal formers in pharmaceutical products is limited by their pharmacological and toxicological properties.

Cocrystallization of polymorphic APIs may provide a route to obtain a single pharmaceutical phase by controlled formation of specific supramolecular synthons between functional groups. For example, Cocrystals of a polymorphic drug Piracetam and Gentisic acid, *p*-hydroxybenzoic acids as cocrystal formers which are also polymorphic and APIs were synthesized *via* acid-amide heterosynthon (Figure 9c).<sup>42i</sup> The cocrystals do not exhibit polymorphism. However polymorphism in cocrystals or multi-component systems is not so uncommon.<sup>43</sup> A recent study from our group<sup>25b</sup> showed<sup>43</sup> there are 33 cocrystal polymorph sets up to the January 2008 release of the CSD when compared to more than 1600 polymorphic systems of single component crystals with our own results on cocrystal polymorphs of Temozolamide and bipyridine-N-oxide. The cocrystal former strategy is being applied for the optimization of the drug design, processing, and delivery procedures.



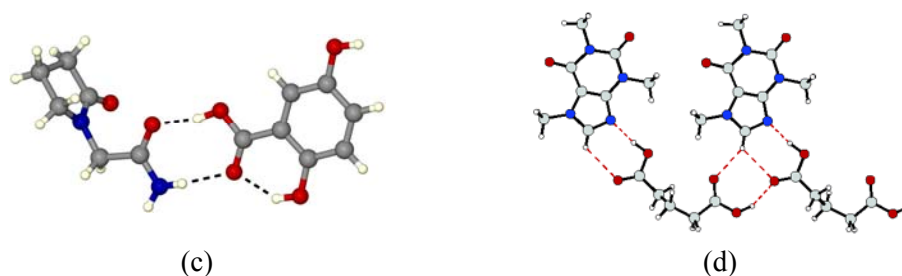


**Figure 9** (a) Structure of *cis*-itraconazole and succinic acid cocrystal. Succinic acid molecule is closely fitting between the two itraconazole molecules *via* O–H...N hydrogen bonding. (b) Hydrogen bonds between fluoxetine cations, benzoic acids and chloride ions in the cocrystals of fluoxetine hydrochloride with benzoic acid to improve physical properties of fluoxetine. (b) Cocrystals of piracetam with gentisic acid *via* acid–amide heterosynthon to control polymorphism. (d) Caffeine–glutaric acid cocrystals to solve hydration.

Salts and cocrystals have the potential to be much more useful in pharmaceutical products than solvates or hydrates. But it is also true that making cocrystal or salt may have adverse effects on physiological systems. For example nearly 4000 deaths of pets occurred due to the renal failure is due to the additive in food. Melamine–cyanuric acid cocrystal was given as protein additive.<sup>44</sup> Investigations concluded the presence of cyanuric acid as another co-contaminant along with melamine causes intratubular precipitation of cocrystal leading to the kidney failure and the death of animals. Crystal engineering of melamine and cyanuric acid (1:1 molar ratio) cocrystals show two-dimensional networks in the solid-state that is highly insoluble in water and causes immediate precipitation, which was the reason for deaths of animals.

## 1.10 Hydrates and Host Guest Compounds

Hydration of molecules in the crystal structure is a common phenomenon, especially in pharmaceutical industries. Hydrated structures received considerable attention because of its different topologies in the structure, conformations and functions. Hydrates are commonly used in pharmaceutical solids because of its abundance, flexibility, small size and ability to act as both a strong hydrogen bond donor and acceptor and obviously its non toxic nature.<sup>45</sup> The study of different water clusters is also important to understand the bulk properties of water and its role in different biological processes, such as protein–DNA binding, ion transport, protein folding–defolding,

structure determination of the fibrous proteins, etc. Included water molecules can form discrete and extended motifs, e.g. finite and infinite chains, ring motifs and different topologies. In biological systems water channels have been found and water topology is widely studied because of its application in water and ion transport.<sup>46</sup> In red blood cells and the renal tubules water can rapidly and selectively cross the plasma membrane. Thus water release from the interface, in general, is favored entropically but enthalpically unfavorable. Infantes and co-workers<sup>47</sup> showed that 6.6% of organic compounds are hydrated and this value increases to 75% for bioactive pharmaceutical compounds or APIs and categorized and given rank for different functional groups that promote hydration. Molecules containing charged or strong H-bonding functional groups favor entrapment of waters into its crystalline lattice. Many fundamental biological processes depend on potentially important water chains.<sup>48</sup> Water chain motif is responsible in proton transport in Gramicidin-A.<sup>48d</sup> Buchanan,<sup>48e</sup> Ripmeester<sup>48f</sup> and others have studied water chains that can serve as a model for biological proton wires or water transport. Henry showed that water can act also as templating nanoporous material.<sup>49</sup> Due to the difficulties in studying the role of water molecules in macromolecular systems, entrapment of water in small molecular environment and then study has become an interesting topic in recent solid state supramolecular chemistry.

Davy's discovery<sup>50</sup> of chlorine hydrate in 1811 can be recognized as the origin of host-guest chemistry as well supramolecular chemistry. But the field took a rapid pace after the seminal contribution from Busch, Curtis, Jägar, Pederson, and then Lehn's work towards host-guest compounds in the development and synthesizing shape and ion selective receptors with macrocyclic ligands (Figure 10). The host-guest relationships involve a complementary stereoelectronic arrangement of binding sites between host and guest. The host component is defined as an organic molecule or ion whose binding sites converge in the complex and the guest component are any molecule, ion whose binding sites diverge in the complex. Host guest chemistry has received particular interest because of their diverse applications in chemical separation, reactions and catalysis in a microcavity, and for electrooptic, nonlinear and magnetic materials.<sup>51</sup> Hydrogen bonds or other weak interactions mediated self-assembly and directional metal-ligand coordination bonding are used to synthesize porous materials or low density frameworks.<sup>52</sup>



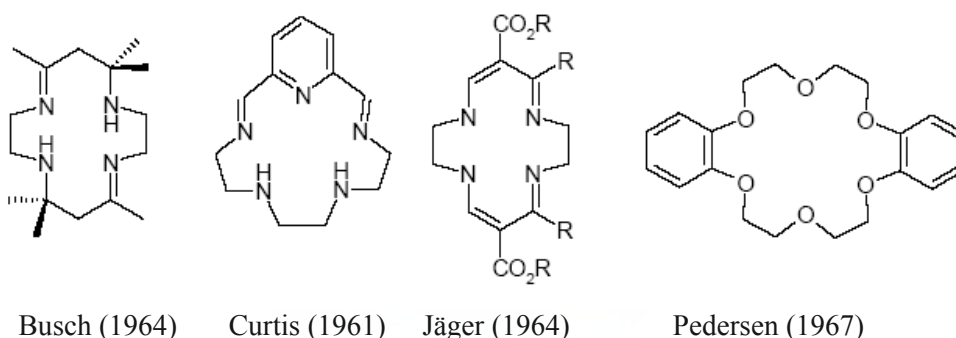
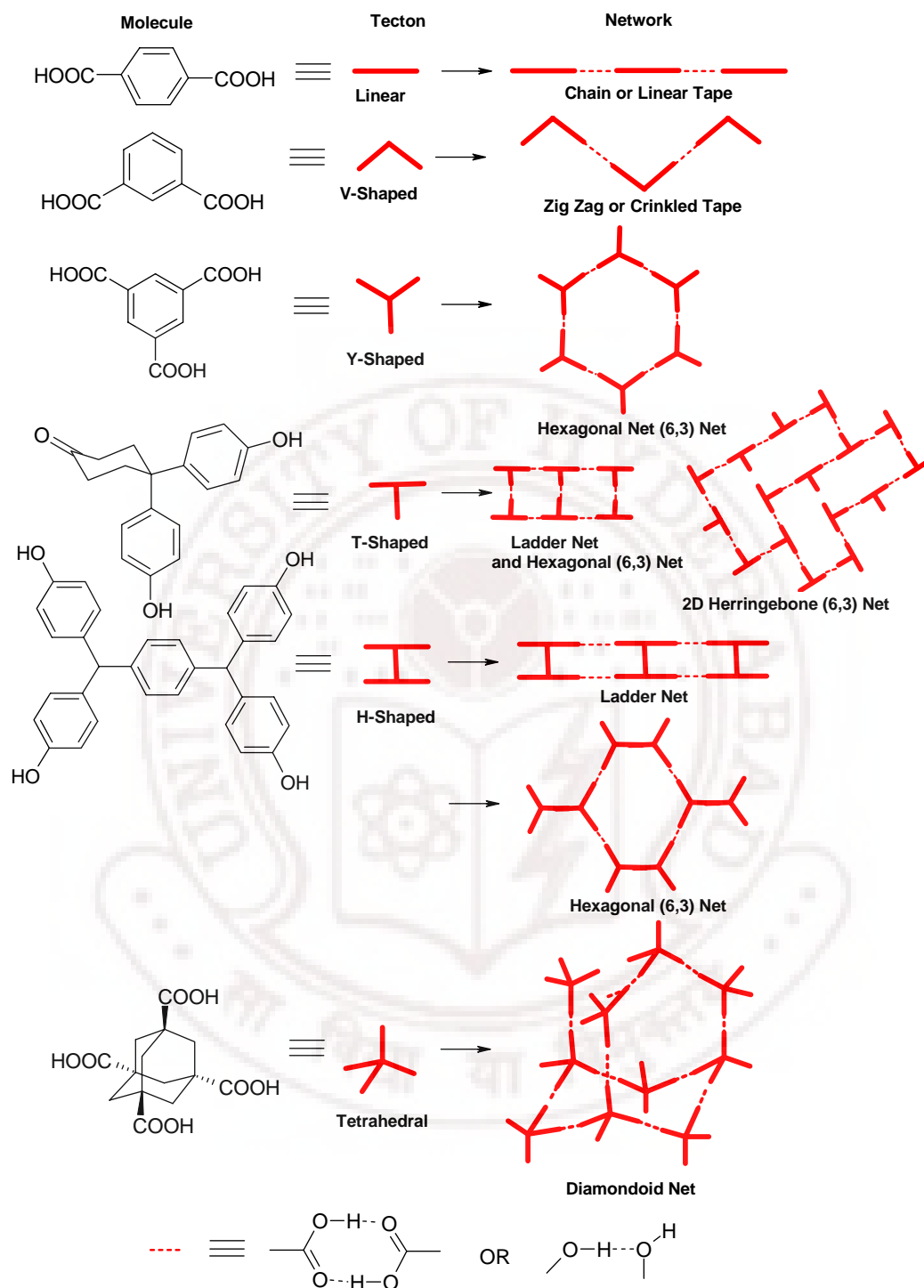


**Figure 10** The macrocyclic ligands are synthesized by Busch, Curtis, Jager and Pedersen.

Host-guest compounds are mainly divided into Cavitands and Clathrands based on the nature of the host. Cavitands are intra-molecular cavities however clathrands are hosts with extra-molecular cavities resulted from aggregation of more than one molecule.<sup>51c</sup> Based on the size of porosity, open frameworks are divided into three categories, such as nanoporous or microporous (<15 Å), mesoporous (15–500 Å) and macroporous (>500 Å) materials.<sup>51a,h</sup> The cavities formed by host molecules can either be of zero dimensional (cage), one dimensional (channel) or two dimensional (layered). To design porous solids various methods have been developed based on crystal engineering principles and hydrogen bonds or metal coordination bonds. Weber rules<sup>53</sup> for designing host framework are discussed in Chapter 5. Bulky shape, rigid framework structure, strong and directional bonding properties are some requirements to construct host-guest crystals.

### 1.11 Network Solids

The rational construction of novel open-framework organic solids<sup>8</sup> has received considerable attention because of their diverse applications. One of the main challenges in the approaches of constructing host-guest compounds is to prevent interpenetration to obtain open frameworks. Selection of suitable building blocks is must to construct a particular architecture. In supramolecular chemistry building architectures is important and the molecular building blocks are known as “molecular tectonics” defined by Wuest.<sup>54</sup> The word “tecton” is taken from Greek for “builder.”



**Scheme 3** Examples of molecule to supermolecule relationship and showed how linear, trigonal and tetrahedral tectons produce one-, two- and three dimensional networks. H-tecton can afford either ladders or (6,3) hexagonal nets.



This approach is a modular, programmed build up from molecule to crystal—rod type molecules form linear aggregates, chiral and  $C_2$ -symmetry molecules lead to helical networks,  $C_3/D_3$  symmetry molecules produce honeycomb grid or hexagonal layer structures, and  $T_d/S_4$  symmetry tectons self-assemble as adamantane or diamondoid networks.<sup>55</sup> H-shaped 1,4-di[bis(4'-hydroxyphenyl)methyl]benzene and its  $\text{CH}_3$  and  $\text{CH}_3\text{O}$  derivatives are synthesized and used to construct a diverge network topologies recently reported from our group.<sup>56</sup> The ability to predict the network architecture from the shape and symmetry of the functionalized tecton is fundamental to crystal design. For instance benzoic, terephthalic, trimesic and adamantane-1,3,5,7-tetracarboxylic acids produce zero-, one-, two- and three-dimensional supramolecular structures respectively, based on molecular geometry and carboxylic acid dimer synthon (Scheme 3). Our results of ladder networks, (6,3) hexagonal network, rare pentagonal tiling by superposition of two (6,3) hexagonal net, interpenetration and catenation are discussed in Chapter 5.

## 1.12 Conclusions

Single-component crystals (polymorphs) and multi-component crystals (salts, solvates, hydrates, cocrystals and their polymorphs) are equally important to modify the physical and chemical properties of drugs. Unsolvated forms are advisable because most solvents are toxic and volatile in nature. Melt and sublimation are two high temperature solvent less methods explored by our group to find guest free structures of those compounds that are prone to give solvates upon solution crystallization. Thus a thorough screening of all possible forms of API is considered to be very important step in pharmaceutical industry. Single crystal X-ray diffraction, powder XRD diffraction, FT-IR, NIR, Raman Spectroscopy, DSC, TGA and other thermal methods, Microscopy and Solid-state NMR spectroscopy techniques are currently used to characterize these various crystalline phases. Solving the crystal structure from powder X-ray diffraction data is slowly becoming a solvable problem.<sup>57</sup>

To summarize, crystal engineering is an emerging and interdisciplinary subject of chemistry, physics, biology, materials and pharmaceutical science. This involves synthesis, crystallography, crystal structure analysis, analysis of all kinds of interactions, property study, and computation. Study on the molecular recognition events during nucleation and growth, crystal engineering has acquired control over the internal

structure and symmetry of crystals and of producing materials with modified chemical and physical properties. Recent literature reflects the advances in crystal engineering and its success. This subject is successfully emerged in several exciting new areas of research, such as catalysis, electronic materials, magnetic sensors, non-linear optics, nanotechnology, protein-receptor binding, microporous materials, supramolecular devices, molecular modelling and drug design.

### 1.13 References

1. (a) J. -M. Lehn, *Supramolecular Chemistry*, Wiley-VCH, 1995; (b) G. R. Desiraju, (Eds.), *The Crystal as a Supramolecular Entity; Perspectives in Supramolecular Chemistry*, Wiley: Chichester, 1996, Vol. 2; (c) J. W. Steed, J. L. Atwood, *Supramolecular Chemistry*, Wiley, Chichester, 2000.
2. (a) W. M. Latimer, W. H. Rodebush, *J. Am. Chem. Soc.* **1920**, 42, 1419; (b) L. Pauling, *The Nature of the Chemical Bond*, Cornell University Press, 1939; (c) L. Pauling, *The Nature of the Chemical Bond and the Structure of Molecules and Crystals: An Introduction to Modern Structural Chemistry*, Third edition, Ithaca, NY, Cornell University Press, 1960.
3. (a) G. R. Desiraju, *Crystal Engineering: The Design of Organic Solids*, Elsevier, Amsterdam, 1989; (b) E. Weber (Eds.), *Design of Organic Solids*, Springer-Verlag, Berlin, 1998; (c) E. R. T. Tiekink, J. J. Vittal (Eds.), *Frontiers in Crystal Engineering*, Wiley, 2006.
4. (a) M. D. Cohen, G. M. J. Schmidt, F. I. Sonntag, *J. Chem. Soc.* **1964**, 2000; (b) L. Leiserowitz, G. M. J. Schmidt, *J. Chem. Soc. A* **1969**, 2372.
5. J. D. Dunitz, *Pure Appl. Chem.* **1991**, 63, 177.
6. A. I. Kitaigorodskii, *Molecular Crystals and Molecules*, Academic Press, New York, 1973.
7. (a) G. R. Desiraju, T. Steiner, *The Weak Hydrogen Bond in Structural Chemistry and Biology*, Oxford University Press, Oxford, **1999**; (b) G. R. Desiraju, *Acc. Chem. Res.* **2002**, 35, 565
8. (a) G. R. Desiraju, *Angew. Chem. Int. Ed. Engl.* **1995**, 34, 2311; (b) A. Nangia, G. R. Desiraju, *Top. Curr. Chem.* **1998**, 198, 57; (c) E.J. Corey, *Pure Appl.*

- Chem.* **1967**, *14*, 19; (d) E. J. Corey, X. -M. Cheng, *The Logic of Chemical Synthesis*, 1989, Wiley, New York.
9. (a) R. D. B. Walsh, M. W. Bradner, S. Fleishman, L. A. Morales, B. Moulton, N. Rodríguez-Hornedo, M. J. Zaworotko, *Chem. Commun.* **2003**, 186; (b) S. G. Fleischman, S. S. Kuduva, J. A. McMahon, B. Moulton, R. D. B. Walsh, N. Rodríguez-Hornedo, M. J. Zaworotko, *Cryst. Growth Des.* **2003**, *3*, 909.
  10. (a) P. Metrangolo, H. Neukirch, T. Pilati, G. Resnati, *Acc. Chem. Res.* **2005**, *38*, 386; (b) E. Corradi, S. V. Meille, M. T. Messina, P. Metrangolo, G. Resnati, *Angew. Chem. Int. Ed.* **2000**, *39*, 1782; (c) N. Ramasubbu, R. Parthasarathy, P. M. -Rust, *J. Am. Chem. Soc.* **1986**, *108*, 4308. (d) S. L. Price, A. J. Stone, J. Lucas, R. S. Rowland, A. E. Thornley, *J. Am. Chem. Soc.* **1994**, *116*, 4910.
  11. (a) R. Boese, M. T. Kirchner, W. E. Billups, L. R. Norman, *Angew. Chem. Int. Ed.* **2003**, *42*, 1961; (b) R. Taylor, O. Kennard, *J. Am. Chem. Soc.* **1982**, *104*, 5063; (c) Z. S. Derewenda, L. Lee, U. Derewenda, *J. Mol. Biol.* **1995**, *252*, 248; (d) G. R. Desiraju, *Acc. Chem. Res.* **1996**, *29*, 441; (e) G. R. Desiraju, *Acc. Chem. Res.* **2002**, *35*, 565; (f) G. R. Desiraju, *Chem. Commun.* **2005**, 2995; (g) M. C. Wahl, M. Sundaralingam, *Trends Biochem. Sci.* **1997**, *22*, 97; (h) Y. M. -Gutfreund, H. Margalit, R. L. Jernigan, V. B. Zhurkin, *J. Mol. Biol.* **1998**, *277*, 1129; (i) M. Nishio, M. Hirota, Y. Umezawa, *The C-H/ $\pi$  Interaction*, Wiley, New York, 1988; (j) M. Nishio, *CrystEngComm* **2003**, *7*, 130; (k) H. Suezawa, T. Yoshida, S. Ishihara, Y. Umezawa, M. Nishio, *CrystEngComm* **2003**, *7*, 514.
  12. (a) M. C. Etter, *J. Am. Chem. Soc.* **1982**, *104*, 1095; (b) M. C. Etter, *Acc. Chem. Res.* **1990**, *23*, 120; (c) M. C. Etter, *J. Phys. Chem.* **1991**, *95*, 4601.
  13. (a) Cambridge Structural Database, CSD, version 5.30, ConQuest 1.11, August 2008 release, May 2009 update; (b) F. H. Allen, *Acta Crystallogr.* **2002**, *B58*, 380; (c) A. Nangia, *CrystEngComm* **2002**, *4*, 93; (d) F. H. Allen, R. Taylor, *Chem. Soc. Rev.* **2004**, *33*, 463; (e) F. H. Allen, W. D. S. Motherwell, *Acta Crystallogr.* **2002**, *B58*, 407.
  14. B. Sarma, L. S. Reddy, A. Nangia, *Cryst. Growth Des.* **2008**, *8*, 4546.
  15. J. Bernstein, R. E. Davis, L. Shimoni, N. L. Chang, *Angew. Chem. Int. Ed. Engl.* **1995**, *34*, 1555.

16. (a) *American Heritage Dictionary of the English Language*, American Heritage Publishing Co, and Houghton Mifflin Company, Boston, 1973, pg 319; (b) <http://en.wikipedia.org/wiki/Crystallization>
17. (a) S. Parveen, R. J. Davey, G. Dent, R. G. Pritchard, *Chem. Commun.* **2005**, 1531; (b) R. J. Davey, G. Dent, R. K. Mughal, S. Parveen, *Cryst. Growth Des.* **2006**, 6, 1788; (c) R. Banerjee, P. M. Bhatt, M. T. Kirchner, G. R. Desiraju, *Angew. Chem. Int. Ed.* **2005**, 44, 2515; (d) J. Hulligar, *Angew. Chem. Int. Ed.* **1994**, 33, 143; (e) S. X. M. Boerrigter, F. F. A. Hollander, J. van de Streek, P. Bennem, H. Meekes, *Cryst. Growth Des.* **2002**, 2, 51; (f) J. Lu, X. -J. Wang, C. -B. Ching, *Cryst. Growth Des.* **2003**, 3, 83; (g) A. L. Rohl, *Current Opinion in Solid State and Materials Science* **2003**, 7, 21; (h) H. M. Cuppen, G. M. Day, P. Verwer, H. Meekes, *Cryst. Growth Des.* **2004**, 4, 1341; (i) R. Hiremath, S. W. Varney, J. A. Swift, *Chem. Commun.* **2004**, 2676.
18. W. F. Ostwald, *Z. Phys. Chem.* **1897**, 22, 289.
19. (a) J. Bernstein, *Polymorphism in Molecular Crystals*, Clarendon, Oxford, 2002; (b) R. Hilfiker, *Polymorphism in the Pharmaceutical Industry*, Wiley-VCH, Weinheim, Weinheim, 2006; (c) H. G. Brittan, *Polymorphism in Pharmaceutical Solids*, Marcel Dekker, New York, 1999; (d) S. R. Byrn, R. R. Pfeiffer and J. G. Stowell, *Solid-State Chemistry of Drugs*, West Lafayette, IN, 1999; (e) T. L. Threlfall, *Analyst* **1995**, 120, 2435; (f) B. Rodríguez-Spong, C. P. Price, A. Jayashankar, A. J. Matzger, N. Rodríguez-Hornedo, *Adv. Drug. Del. Rev.* **2004**, 56, 241; (g) J. Bernstein, R. J. Davey, J. -O. Henck, *Angew. Chem. Int. Ed.* **1999**, 38, 3440.
20. (a) G. R. Desiraju, *CrystEngComm* **2003**, 5, 466; (b) J. D. Dunitz, *CrystEngComm* **2003**, 5, 506; (c) A. D. Bond, *CrystEngComm* **2007**, 9, 833; (d) J. Z. Schpector, E. R. T. Tiekink, *Z. Kristallogr.* **2008**, 223, 233.
21. (a) A. Nangia, G. R. Desiraju, *Chem. Commun.* **1998**, 605; (b) A. L. Bingham, D. S. Hughes, M. B. Hursthouse, R. W. Lancaster, S. Tavener, T. L. Threlfall, *Chem. Commun.* **2001**, 603; (c) A. Nangia, *Cryst. Growth Des.* **2006**, 6, 2; (d) A. Nangia, *Cryst. Growth Des.* **2008**, 8, 1079; (e) G. R. Desiraju, *CrystEngComm* **2003**, 5, 466; (f) J. D. Dunitz, *CrystEngComm* **2003**, 5, 506; (g) A. D. Bond, *CrystEngComm* **2007**, 9, 833.

22. (a) L. Infantes, J. Chisholm, S. Motherwell, *CrystEngComm* **2003**, 5, 480; (b) A. Gillon, N. Feeder, R. J. Davey, R. Storey, *Cryst. Growth Des.* **2003**, 3, 663; (c) G. R. Desiraju, *J. Chem. Soc.* **1991**, 6, 426.
23. (a) S. L. Childs, K. I. Hardcastle, *Cryst. Growth Des.* **2007**, 7, 1291; (b) S. L. Childs, G. P. Stahly, A. Park, *Mol. Pharmaceutics* **2007**, 4, 323.
24. (a) E. Mitscherlich, *Abhl. Akad. Berlin* **1822-1823**, 43; (b) M. J. Buerger, M. C. Bloom, *Z. Kristallogr.* **1937**, 96, 182; (c) J. Haleblian, W. C McCrone, *J. Pharma. Sci.* **1969**, 58, 911; (d) J. Berzelius, *Jahresbericht* **1844**, 23, 44; (e) W. B. Jensen, *J. Chem. Educ.* **1998**, 75, 817; (f) W. C. McCrone, in *Physics and Chemistry of the Organic Solid State*, Vol. 2, eds. D. Fox, M. M. Labes and A. Weissberger, Wiley Interscience, New York, 1965, pp. 725-767; (g) A. Buerger, in *Topics in pharmaceutical science*, (Eds.) D. D. Breimer, P. Speiser, Elsevier, Lausanne, 1983, pp 347-358.
25. (a) V. S. S. Kumar, A. Anthony, A. Nangia, W. T. Robinson, C. K. Broder, R. Mondal, I. R. Evans, J. A. K. Howard, F. H. Allen, *Angew. Chem. Int. Ed.* **2002**, 41, 3848; (b) N. J. Babu, L. S. Reddy, S. Aitipamula, A. Nangia, *Chem Asian J.* **2008**, 3, 1122; (c) A. Nangia, *Acc. Chem. Res.* **2008**, 41, 595; (d) B. Sarma, S. Roy, A. Nangia, *Chem. Commun.* **2006**, 4918; (e) B. Sarma, A. Nangia, *Acta Crystallogr.* **2008**, A64, C449; (f) B. Sarma, A. Nangia (unpublished results).
26. (a) J. A. Bis, M. J. Zaworotko, *Cryst. Growth Des.* **2005**, 5, 1169; (b) S. R. Chemburkar, J. Bauer, K. Deming, H. Spiwek, K. Patel, J. Morris, R. Henry, S. Spanton, W. Dziki, W. Porter, J. Quick, P. Bauer, J. Donaubauer, B. A. Narayanan, M. Soldani, D. Riley, K. McFarland, *Org. Process Res. Dev.* **2000**, 4, 413; (c) J. Bauer, S. Spanton, R. Henry, R. Quick, W. Dziki, W. Porter, J. Morris, *Pharm. Res.* **2001**, 18, 859; (d) K. Knapman, *Mod. Drug. Disc.* **2000**, 3, 53; (e) S. Datta, D. J. W. Grant, *Nat. Rev. Drug. Disc.* **2004**, 3, 42; (f) Glaxo Inc. V. Novapharm Ltd. *52F3d 1043, 34 U. S. P. Q. 2d* (BNA), 1565 (fed. Cir. 1995).
27. (a) C. M. Reddy, K. A. Padmanabhan, G. R. Desiraju, *Cryst. Growth Des.* **2006**, 6, 2720; (b) C. M. Reddy, S. Basavoju, G. R. Desiraju, *Chem. Commun.* **2005**, 19, 2439; (c) J. Bernstein, *Nat. Mater.* **2005**, 4, 427.

28. (a) S. L. Morissette, Ö. Almarsson, M. L. Peterson, J. F. Remenar, M. J. Read, A. V. Lemmo, S. Ellis, M. J. Cima, C. R. Gardner, *Adv. Drug. Del. Rev.* **2004**, 56, 275; (b) A. Linás, J. M. Goodman, *Drug. Disc. Today* **2008**, 13, 198.
29. (a) P. K. Thallapally, R. K. R. Jetti, A. K. Katz, H. L. Carrell, K. Singh, K. Lahiri, S. Kotha, R. Boese, G. R. Desiraju, *Angew. Chem. Int. Ed.* **2004**, 43, 1149; (b) C. -H. Gu, K. Chatterjee, V. Young Jr, D. J. W. Grant, *J. Cryst. Growth* **2002**, 235, 471; (c) C. A. Mitchell, L. Yu, M. D. Ward, *J. Am. Chem. Soc.* **2001**, 123, 10830; (d) X. Sun, B. A. Garetz, A. S. Myerson, *Cryst. Growth Des.* **2006**, 6, 684; (e) J. L. Hilden, C. E. Reyes, M. J. Kelm, J. S. Tan, J. G. Stowell, K. R. Morris, *Cryst. Growth Des.* **2003**, 3, 921; (f) G. Di Profio, S. Tucci, E. Curcio, E. Drioli, *Cryst. Growth Des.* **2007**, 7, 526 (g) M. D. Lang, A. L. Grzesiak, A. J. Matzger, *J. Am. Chem. Soc.* **2002**, 124, 14834; (h) C. P. Price, A. L. Grzesiak, A. J. Matzger, *J. Am. Chem. Soc.* **2005**, 127, 5512; (i) A. V. Trask, N. Shan, W. D. S. Motherwell, W. Jones, S. Feng, R. B. H. Tan, K. J. Carpenter, *Chem. Commun.* **2005**, 880; (j) A. Bouchard, N. Jovanović, G. W. Hofland, E. Mendes, D. J. A. Crommelin, W. Jiskoot, G. Witkamp, *Cryst. Growth Des.* **2007**, 7, 1432; (k) R. Hiremath, J. A. Basile, S. W. Varney, J. A. Swift, *J. Am. Chem. Soc.* **2005**, 127, 18321; (m) A. Llinás, K. J. Box, J. C. Burley, R. C. Glen, J. M. Goodman, *J. Appl. Crystallogr.* **2007**, 40, 379.
30. (a) A. Kálmán, L. Fábián, G. Argay, *Chem. Commun.* **2000**, 2255; (b) A. Nangia, G. R. Desiraju, *Acta Crystallogr.* **1998**, A54, 934; (c) G. R. Desiraju, *Chem. Commun.* **1997**, 1475; (d) L. Fábián, A. Kálmán, *Acta Crystallogr.* **1999**, B55, 1099; (e) A. Kálmán, L. Párkányi, G. Argay, *Acta Crystallogr.* **1993**, B49, 1039.
31. (a) [http://reference.iucr.org/dictionary/Isomorphous\\_crystals](http://reference.iucr.org/dictionary/Isomorphous_crystals)  
(b) [http://reference.iucr.org/dictionary/Isostructural\\_crystals](http://reference.iucr.org/dictionary/Isostructural_crystals)
32. (a) L. Fábián, A. Kálmán, *Acta Crystallogr.* **2004**, B60, 547; (b) A. Anthony, M. Jaskólski, A. Nangia, G. R. Desiraju, *Chem. Commun.* **1998**, 2537; (c) A. Anthony, M. Jaskólski, A. Nangia, *Acta Crystallogr.* **2000**, B56, 512.
33. A. I. Kitaigorodskii, *Organic Chemical Crystallography*, New York, 1961.



34. (a) G. Argay, A. Kálmán, B. Ribár, S. Vladimirov, D. Zivanov-Stackic, *Acta Crystallogr.* **1987**, C43, 922; (b) A. Kálmán, G. Argay, D. Zivanov-Stackic, S. Vladimirov, B. Ribár, *Acta Crystallogr.* **1992**, C48, 812.
35. (a) N. K. Nath, B. K. Saha, A. Nangia, *New J. Chem.* **2008**, 32, 1693; (b) K. F. Bowes, C. Glidewell, J. N. Low, M. Melguizo, A. Quesada, *Acta Crystallogr.* **2003**, C59, o4; (c) B. Omondi, M. A. fernandes, M. Layh, D. C. Levendis, J. L. Look, T. S. P. Mkwizu, *CrystEngComm* **2005**, 7, 690; (d) G. R. Desiraju, J. A. R. P. Sarma, *Proc. Ind. Acad. Sci. Chem. Sci.* **1986**, 96, 599; (e) L. -P. Zhang, T. C. W. Mak, *J. Mol. Struct.* **2004**, 693, 1; (f) T. Steiner, *J. Mol. Struct.* **1998**, 443, 149; (g) I. Bar, J. Bernstein, *Tetrahedron*, **1987**, 43, 1299; (h) T. A. Olszak, O. M. Peeters, N. M. Blaton, C. J. de Ranter, *Acta Crystallogr.* **1994**, C50, 761; (i) L. Prasad, E. J. Gabe, *Acta Crystallogr.* **1983**, C39, 273; (j) S. S. C. Chu, V. Napoleone, A. I. Jr. Ternay, S. Chang, *Acta Crystallogr.* **1982**, B38, 2508; (k) M. Chakravarty, P. Kommana, K. C. K. Swamy, *Chem. Commun.* **2005**, 5396; (m) P. K. Thallapally, K. Chakraborty, H. L. Carrell, S. Kotha, G. R. Desiraju, *Tetrahedron* **2000**, 56, 6721; (n) P. G. Jones, F. Vancea, *CrystEngComm* **2003**, 5, 303; (o) G. P. Bettinetti, M. R. Caira, M. Sorrenti, L. Catenacci, M. Ghirardi, L. Fábíán, *J. Therm. Anal. Cal.* **2004**, 77, 695; (p) H. Karfunkel, H. Wilts, Z. Hao, A. Iqbal, J. Mizuguchi, Z. Wu, *Acta Crystallogr.* **1999**, B55, 1075; (q) N. Panina, F. J. Leusen, F. B. J. Jassen, P. Verwer, H. Meekes, E. Vleig, G. Deroover, *J. Appl. Cryst.* **2007**, 40, 105.
36. (a) E. B. Brouwer, K. A. Udachin, G. D. Enright, J. A. Ripmeester, K. J. Ooms, P. A. Halchuk, *Chem. Commun.* **2001**, 565; (b) P. O. Brown, G. D. Enright, J. A. Ripmeester, *CrystEngComm* **2006**, 8, 381; (c) B. K. Saha, A. Nangia, *Chem. Commun.* **2006**, 1825; (d) P. S. Sidhu, G. D. Enright, K. A. Udachin, J. A. Ripmeester, *Chem. Commun.* **2005**, 2092; (e) E. B. Brouwer, G. D. Enright, K. A. Udachin, S. Lang, K. J. Ooms, P. A. Halchuk, J. A. Ripmeester, *Chem. Commun.* **2003**, 1416; (f) J. L. Atwood, L. J. Barbour, G. O. Lloyd, P. K. Thallapally, *Chem. Commun.* **2004**, 922; (g) G. D. Enright, K. A. Udachin, I. L. Moudrakovski, J. A. Ripmeester, *J. Am. Chem. Soc.* **2003**, 125, 9896; (h) J. L. Atwood, L. J. Barbour, A. Jerga, B. L. Schottel, *Science* **2002**, 298, 1000; (i) B. K. Saha, A. Nangia, *CrystEngComm* **2006**, 8, 440.

37. (a) J. W. Steed, *CrystEngComm* **2003**, 5, 169; (b) G. R. Desiraju, *CrystEngComm* **2007**, 9, 91; (c) K. M. Anderson, J. W. Steed, *CrystEngComm* **2007**, 9, 328.
38. (a) S. L. Childs, G. P. Stahly, A. Park, *Mol. Pharmaceutics* **2007**, 4, 323; (b) S. L. Johnson, K. A. Rumon, *J. Phys. Chem.* **1965**, 69, 74.
39. (a) C. B. Aakeröy, D. J. Salmon, *CrystEngComm* **2005**, 7, 439; (b) B. R. Bhogala, S. Basavoju, A. Nangia, *CrystEngComm* **2005**, 7, 551; (c) B. R. Bhogala, S. Basavoju, A. Nangia, *Cryst. Growth Des.* **2005**, 5, 1683; (d) A. V. Trask, W. D. S. Motherwell, W. Jones, *Cryst. Growth Des.* **2005**, 5, 1013; (e) X. Gao, T. T. Friščić, L. R. MacGillivray, *Angew. Chem. Int. Ed.* **2004**, 43, 232; (f) B. R. Bhogala, A. Nangia, *Cryst. Growth Des.* **2003**, 3, 547; (g) C. B. Aakeröy, A. M. Beatty, B. A. Helfrich, *Angew. Chem. Int. Ed.* **2001**, 40, 3240; (h) B. R. Bhogala, A. Nangia, *New. J. Chem.* **2008**, 32, 800; (i) P. Vishweshwar, A. Nangia, V. M. Lynch, *J. Org. Chem.* **2002**, 67, 556; (j) S. Mohamed, D. A. Tocher, M. Vickers, P. G. Karamertzanis, S. L. Price, *Cryst. Growth Des.* **2009**, 9, 2881.
40. C. Laurence, H. Berthelot, *Perspect. Drug. Discovery Des.* **2000**, 18, 39.
41. Ö. Almarsson, M. J. Zaworotko, *Chem. Commun.* **2004**, 1889.
42. (a) R. D. B. Walsh, M. W. Bradner, S. Fleischman, L. A. Morales, B. Moulton, N. Rodríguez-Hornedo, M. J. Zaworotko, *Chem. Commun.* **2003**, 186; (b) L. Childs, L. J. Chyall, J. T. Dunlap, V. N. Smolenskaya, B. C. Stahly, P. G. Stahly, *J. Am. Chem. Soc.* **2004**, 126, 13335; (c) P. M. Bhatt, N. V. Ravindra, R. Banerjee, G. R. Desiraju, *Chem. Commun.* **2005**, 1073; (d) R. Banerjee, P. M. Bhatt, N. V. Ravindra, G. R. Desiraju, *Cryst. Growth Des.* **2005**, 5, 2299; (e) J. F. Remenar, S. L. Morissette, M. L. Peterson, B. Moulton, J. M. MacPhee, H. R. Guzman, Ö. Almarsson, *J. Am. Chem. Soc.* **2003**, 125, 8456; (f) M. B. Hickey, M. L. Peterson, L. A. Scoppettuolo, S. L. Morissette, A. Vetter, H. Guzmán, J. F. Remenar, Z. Zhang, M. D. Tawa, S. Haley, M. J. Zaworotko, Ö. Almarsson, *Eur. J. Pharm. Biopharm.* **2007**, 67, 112; (g) S. L. Morissette, Ö. Almarsson, M. L. Peterson, J. F. Remenar, M. J. Read, A. V. Lemmo, S. Ellis, M. J. Cima, C. R. Gardner, *Adv. Drug Delivery Rev.* **2004**, 56, 275; (h) G. Bettinetti, M. R. Caira, A. Callegari, M. Merli, M. Sorrenti, C. Tadini, *J. Pharm. Sci.* **2000**, 89, 478; (i)



- P. Vishweshwar, J. A. McMahon, M. L. Peterson, M. B. Hickey, T. R. Shattock, M. J. Zaworotko, *Chem. Commun.* **2005**, 4601; (j) A. V. Trask, W. D. S. Motherwell, W. Jones, *Cryst. Growth Des.* **2005**, *5*, 1013; (k) A. Nangia, N. Rodríguez-Hornedo, *Cryst. Growth Des.* **2009**, DOI: 10.1021/cg900554h
43. (a) B. R. Sreekanth, P. Vishweshwar, K. Vyas, *Chem. Commun.* **2007**, 2375; (b) J. A. Bis, P. Vishweshwar, R. A. Middleton, M. J. Zaworotko, *Cryst. Growth Des.* **2006**, *6*, 1048; (c) S. L. Childs, K. I. Hardcastle, *Cryst. Growth Des.* **2007**, *7*, 1291; (d) J. A. Bis, P. Vishweshwar, D. Weyna, M. J. Zaworotko, *Mol. Pharma.* **2007**, *4*, 401; (e) W. W. Porter III, S. C. Elie, A. J. Matzger, *Cryst. Growth Des.* **2008**, *1*, 14.
44. (a) C. T. Seto, G. M. Whitesides, *J. Am. Chem. Soc.* **1990**, *112*, 6409; (b) N. Shan, M. J. Zaworotko, *Drug. Disc. Today* **2008**, *13*, 440.
45. (a) R. K. Khankari, D. J. W. Grant, *Thermochim. Acta.* **1995**, 61; (b) A. L. Gillon, N. Feeder, R. J. Davey, R. Storey, *Cryst. Growth Des.* **2003**, *3*, 663.
46. (a) R. Custelcean, C. Afloroaei, M. Vlassa, M. Polverejan, *Angew. Chem. Int. Ed.* **2000**, *39*, 3094; (b) R. Ludwig, *Angew. Chem. Int. Ed.* **2001**, *40*, 1808; (c) R. Ludwig, *Angew. Chem. Int. Ed.* **2003**, *42*, 258.
47. (a) L. Infantes, J. Chisholm, S. Motherwell, *CrystEngComm* **2003**, *5*, 480; (b) L. Infantes, L. Fábíán, W. D. S. Motherwell, *CrystEngComm* **2007**, *9*, 65.
48. (a) B. Sarma, A. Nangia, *CrystEngComm* **2007**, *9*, 65; (b) B. K. Saha, A. Nangia, *Chem. Commun.* **2005**, 3024; (c) A. Mukherjee, M. K. Saha, M. Nethaji, A. R. Chakravarty, *Chem. Commun.* **2004**, 716; (d) F. Kovacs, J. Quine, T. A. Cross, *Proc. Natl. Acad. Sci. USA*, **1999**, *96*, 7910; (e) L. E. Cheruzel, M. S. Pometun, M. R. Cecil, M. S. Mashuta, R. J. Wittebort, R. M. Buchanan, *Angew. Chem. Int. Ed.* **2003**, *42*, 5452; (f) P. S. Sidhu, K. A. Udachin, J. A. Ripmeester, *Chem. Commun.* **2004**, 1358; (g) A. Wakahara, T. Ishida, *Chem. Lett.* **2004**, *33*, 354.
49. M. Henry, F. Taulelle, T. Loiseau, L. Beitone, G. Férey, *Chem. Eur. J.* **2004**, *10*, 1366.
50. H. Davey, *Philos. Trans. R. Soc. Lond.* **1811**, *101*, 155.
51. (a) M. E. Davis, *Nature* **2002**, *417*, 813; (b) R. E. Morris, P. S. Wheatley, *Angew. Chem. Int. Ed.* **2008**, *47*, 4966; (c) A. Nangia, *Nanoporous Materials: Science and Engineering*, Eds. G. Q. Lu, X. S. Zhao, Imperial College Press,

- London, 2004, pp. 165; (d) L. R. MacGillivray, J. L. Atwood, *Angew. Chem. Int. Ed.* **1999**, 38, 1018; (e) P. J. Langley, J. Hulliger, *Chem. Soc. Rev.* **1999**, 28, 279; (f) Y. Aoyama, *Top. Curr. Chem.* **1998**, 198, 131; (g) M. D. Hollingsworth, *Science* **2002**, 295, 2410; (h) A. Nangia, *Curr. Opin. Solid State Mater. Sci.* **2001**, 5, 115.
52. (a) S. L. James, *Chem. Soc. Rev.* **2003**, 32, 276; (b) S. A. Barnett, N. R. Champness, *Coord. Chem. Rev.* **2003**, 246, 145; (c) N. W. Ockwig, O. Delgado-Friedrichs, M. O’Keeffe, O. M. Yaghi, *Acc. Chem. Res.* **2005**, 38, 176; (d) S. Kitagawa, K. Uemura, *Chem. Soc. Rev.* **2005**, 34, 109.
53. E. Weber, in *Comprehensive Supramolecular Chemistry*; (Eds.), D. D. MacNicol, F. Toda, R. Bishop, Pergamon: Oxford, 1996, vol. 6.
54. (a) M. Simard, D. Su, J. D. Wuest, *J. Am. Chem. Soc.* **1991**, 113, 4696; (b) J. D. Wuest, *Chem. Commun.* **2005**, 5830 and references therein.
55. (a) A. F. Wells, *Three-Dimensional Nets and Polyhedra*, Wiley, New York, 1977; (b) S. R. Batten, R. Robson, *Angew. Chem. Int. Ed.* **1998**, 37, 1460; (c) L. Carlucci, G. Ciani, D. M. Proserpio, *Coord. Chem. Rev.* **2003**, 246, 247; (d) L. Carlucci, G. Ciani, D. M. Proserpio, *CrystEngComm* **2003**, 5, 269; (e) G. R. Desiraju, *Chem. Commun.* **1997**, 1475; (f) B. Moulton, M. J. Zaworotko, *Chem. Rev.* **2001**, 101, 1629; (g) M. W. Hosseini, *CrystEngComm* **2004**, 6, 318; (h) R. E. Melendez, C. V. K. Sharma, M. J. Zaworotko, C. Bauer, R. D. Rogers, *Angew. Chem. Int. Ed. Engl.* **1996**, 35, 2213; (i) R. K. R. Jetti, P. K. Thallapally, F. Xue, T. C. W. Mak, A. Nangia, *Tetrahedron* **2000**, 56, 6707; (j) T. C. W. Mak, F. Xue, *J. Am. Chem. Soc.* **2000**, 122, 9860; (k) R. K. R. Jetti, P. K. Thallapally, A. Nangia, C. -K. Lam, T. C. W. Mak, *Chem. Commun.* **2002**, 952; (m) S. Furukawa, M. Obha, S. Kitagawa, *Chem. Commun.* **2005**, 865.
56. (a) S. Aitipamula, A. Nangia, *Supramol. Chem.* **2005**, 17, 17; (b) R. Thakuria, B. Sarma, A. Nangia, *Cryst. Growth Des.* **2008**, 8, 1471; (c) R. Thakuria, B. Sarma, A. Nangia, *New J. Chem.* **2009** (in press).
57. K. D. M. Harris, E. Y. Cheung, *Chem. Soc. Rev.* **2004**, 33, 526.

## CONFORMATIONAL AND SYNTHON POLYMORPHISM IN HOST COMPOUNDS

### 2.1 Introduction

Long-range periodicity of the molecules in crystalline solids results in substantial differences in physical and chemical properties.<sup>1</sup> Majority of drugs are administered as solids and are preferred in their crystalline forms because of superior stability over amorphous solids. Crystal structure, polymorphism, morphology, shape and size have economical and practical impact on all active substances at all stages of development from research to commercialization. Crystalline forms of solid compounds may either exist as single molecular entities or multi-component species. The contribution from various possible intermolecular interactions like van der Waals, ionic, hydrogen bonding etc. will be different in different polymorphs means that their physical and chemical properties will be different. Polymorphism<sup>2</sup> is defined as the phenomenon by which a given compound may exist in more than one distinct crystal structure, an extremely important phenomenon in single molecular entities, which can occur in multi-component species also. Multi-component crystals include salts, hydrates, solvates and cocrystals of a molecule where a second component (counter-ion, water, solvent or a cocrystal former respectively) is incorporated into the crystalline lattice. Cocrystals and salts of an API (with a non-toxic chemical to the human body Generally Regarded As Safe chemicals, GRAS<sup>3</sup> approved by the Food and Drug Administration, FDA) and hydrates are preferable formulations in drug development. Their physico-chemical properties also differ from those of polymorphs and amorphous form. Growing a new and selective crystalline modification, understanding polymorphism, phase transformations between polymorphs has become everybody's concern especially in pharmaceutical developments.<sup>4</sup> Thus it is essential to screen all possible polymorphs of a

drug molecule and choose the right candidate preferably the most stable polymorph. This led to an increased interest on developing methods to control the outcome of crystallization in producing desired polymorphs. Computational approach, Crystal Structure Prediction (CSP)<sup>5</sup> can help to identify crystal structures of either some or all of the polymorphs available for a given compound. To screen all polymorphic modification of a molecule several methods are used. Control over the formation of different polymorphic structures during production is desirable, especially to avoid concomitant polymorphism<sup>4f,g</sup> because this would result in a product with ill-defined properties. The relative stability of polymorphs is defined by thermodynamics, but the structure that will actually form, depends also on kinetics, that is, competitive nucleation and growth rates. Different condition in the crystallization process is the main reason responsible for the crystallization of different polymorphic forms is discussed in chapter 4.

## 2.2 Conformational and Synthon Polymorphism

Polymorphism is a major challenge in the fundamental understanding of crystallization and received immense practical importance in pharmaceuticals as each polymorph can exhibit different chemical and physical properties including dissolution rate, oral absorption, bioavailability, stability, melting point, solubility, optical and mechanical properties, vapor pressure, etc. When different conformers (flexible torsions) of the same molecule occur in different crystal forms, the phenomenon is termed as conformational polymorphism.<sup>6</sup> Polymorphism perhaps tends to be prominent in molecules that contain multifunctional groups, thereby forming multiple supramolecular synthons known as synthon polymorphs. Sulfathiazole, an anti-bacterial and antimicrobial sulfa drug<sup>7</sup> has five polymorphs containing different hydrogen bonding patterns (Figure 1). Competition between N–H···O and N–H···N hydrogen bond synthons leads to difference in molecular arrangements in their polymorphic structures and they are synthon polymorphs. One will realize the importance of polymorphism by looking at the dissolution (or bioavailability) profile of the two conformational polymorphs of Ritonavir, the anti-HIV drug (Figure 2).<sup>8</sup> Form I of Ritonavir is about five times more soluble than form II indicates more bioavailability of the original polymorph. A general discussion about polymorphism was covered in Chapter 1.

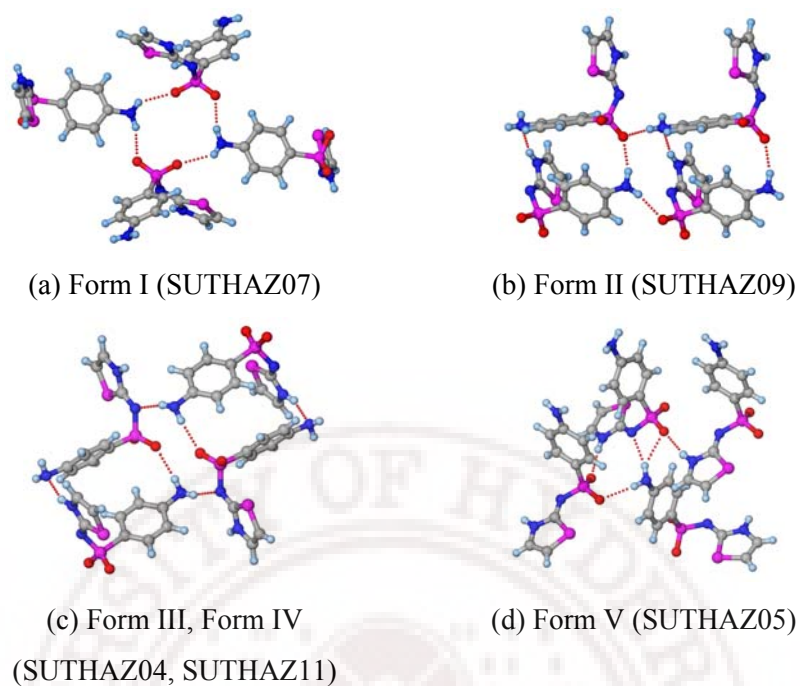


**Figure 1** Synthon polymorphism in anti bacterial drug sulfathiazole.

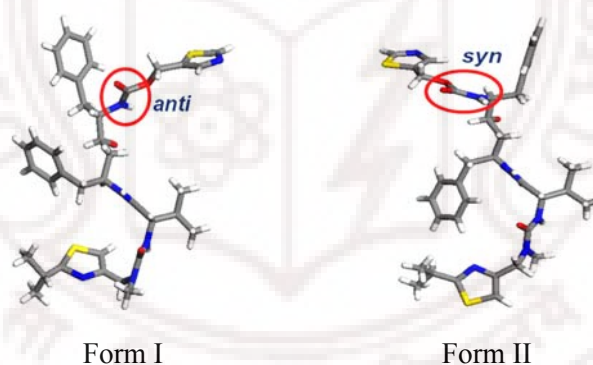


**Figure 2** Two conformational polymorphs of anti HIV drug Ritonavir.

Selective growing of a polymorph is an important goal for the pharmaceutical chemist. This led to an increased interest on developing methods to control the outcome of crystallization in producing desired polymorphs. In anti-solvent crystallization,<sup>9</sup> a solution of the compound that has to be crystallized is mixed with an antisolvent. Mixed solvent lowers the solubility of the compound compared to the original solution which creates a driving force for supersaturation by changing the interfacial energy between

solution and crystal. The increase in supersaturation ratio results in a decrease of the nucleation, while the increase of the interfacial energy results in an increase of the nucleation. Antisolvent crystallization of L-Histidine<sup>9c</sup> from aqueous solution with ethanol as antisolvent the polymorphic fraction of the metastable polymorph B increased with increasing supersaturation ratio. Rapid cooling and different cooling rates can also results in new polymorphic modification. The use of structurally similar additives that direct the nucleation process of a synthon through habit modification in the supersaturated solution has been recognized as a new entry toward manipulating new crystalline modification and growth. Additive induced polymorphism or cocrystallization<sup>10</sup> are explored recently and there are many instances of new polymorphs being discovered as unintended outcomes of cocrystallization experiments. Polymorphs of benzidine,<sup>10a</sup> acridine,<sup>10b</sup> pentafluorophenol,<sup>10c</sup> are some interesting examples of additive induced polymorphism. Lian Yu has ascribed in detail the cross nucleation<sup>11</sup> process for generating new polymorphs. By pseudoseeding<sup>12</sup> the supersaturated solution with the  $\delta$ -form seed crystals of an analogous compound, the desired  $\delta$ -form crystals of  $\pm$ -[2-[4-(3-ethoxy-2-hydroxypropoxy)phenyl]carbonyl]ethyl] dimethylsulfonium-*p*-toluenesulfonate could be obtained as a pure single phase. Otherwise nucleation of the undesired stable  $\alpha$ -polymorphic form was common. Kofler preparations,<sup>13</sup> change in pH<sup>14</sup> can also lead to a new polymorphic outcome. Solution crystallization<sup>15</sup> by slow evaporation at different temperature condition is default crystallization technique to screen for new polymorphic modifications. Preparation of slice crystals<sup>16</sup> with a regular shape by the physical vapor transport method, where molecules are packed in layer-by-layer mode with the same molecular orientation, and in one molecular layer, the molecules are packed in a “brick wall” motif can result different crystalline modifications, which may differ from the crystal appeared in solution crystallization. Fabricated patterned self-assembled monolayers (SAM) substrates made from functionalized metallic islands are being used to generate multiple crystal forms in a single experiment in a given solvent system and this technique has become attractive to screen out polymorphs. More common and current approaches for discovery and selection of polymorphic forms of a compound include crystallization with tailor made soluble additives,<sup>10</sup> epitaxial growth,<sup>17</sup> laser induced nucleation,<sup>18</sup> crystallization in capillaries,<sup>19a,b</sup> confinement within porous materials,<sup>20</sup> and more traditional methods,



such as varying solvent, temperature, and extent of supersaturation. Most high throughput polymorph generation is limited to combinatorially changing solvent, temperature, and supersaturation conditions.<sup>21</sup> Such approaches do not explicitly address the vital role of nucleation despite the fact that this is the decisive step in controlling polymorphism. Moreover, heterogeneous nucleation, the process by which nucleation occurs due to foreign particles or surfaces that are not chemically identical to the nucleated material, is generally believed to be responsible for the majority of crystallizations conducted on the laboratory scale.<sup>22</sup> Methodology to control the phenomenon of crystal polymorphism through the use of diverse libraries of polymer heteronuclei<sup>23</sup> including both commercially available polymers and combinatorially synthesized cross-linked polymers are also available in literature. We explored melting and sublimation, the two solvent less high temperature techniques to afford guest-free host structures and employed to generate new polymorphs of compound that are prone to give guest included crystal on solution crystallization with very good probabilities.

### 2.3 Methods for Obtaining Guest-Free Host Structure

In general, the awkward shape/size and sticky functional moieties (like OH, NH<sub>2</sub>, SO<sub>3</sub>H etc) of most of the organic molecules distinctly APIs are responsible for solvent inclusion complexes upon crystallization from solution which is not advisable in drug industries because most solvents exhibit toxicity. Hydrates are useful but limited due to stability and solubility reasons. The synthesis and characterization of guest-free crystalline forms of host molecules is generally difficult because they do not crystallize in the absence of a second component, usually a solvent and/or water molecule, which acts as a crystallization aid or filler in the voids. Recent literature shows various methods have been used to obtain guest-free structure of lattice inclusion host compounds. Efforts to grow single crystals of organic compounds commonly include temperature lowering, isothermal evaporation, and isothermal diffusion crystallization techniques. Misfit size and/or shape<sup>24a-c</sup> of the guest molecule to the void formed by the host can lead to the guest-free host structure. The bowl-shaped *p*-*tert*-butylcalix[4]arene host with small organic guest molecules have been studied extensively. Ripmeester<sup>24a</sup> showed that the increase in linear hydrocarbon (guest) chain length with the host changes the host:guest ratio from 1:1 to 2:1 and finally long chain tetradecane solvent afforded guest-free

crystals. Similar idea has been employed to get pure host structure of *c*-methylpyrogall[4]arene,<sup>24b</sup> a well known host. Dibromophloroglucinol<sup>24c</sup> from CHCl<sub>3</sub> and EtOAc mixture afforded an anhydrous crystalline form however aq. CH<sub>3</sub>OH affords only hydrate structure. Crystallization of clathrate host molecules, using an appropriate dual-nature solvent or unfavourable electrostatic interactions<sup>25</sup> can afford growth of pure host crystals by exclusion of guest. Another possibility for guest-free host crystals is a layer-by-layer conversion of particles from the outside in as guest is leached out,<sup>26a</sup> with the inclusion crystal acting as a template. Depending on the details of the technique employed, desolvation of inclusion compounds<sup>27a-d</sup> leads to either a dense, or low dense guest-free polymorphs. Recrystallization with a solvent-nonsolvent<sup>28a</sup> system, sonication,<sup>28b</sup> etc. are other methods used to crystallize guest-free host. Very recently enzymatic route that promotes the precipitation of drug in anhydrous form by a gradual pH change has been reported<sup>28c</sup>. However the high temperature crystallization methods melting<sup>29a</sup> and sublimation<sup>29b,c</sup> are also used in fewer instances. This chapter discusses<sup>6c,42</sup> how successfully the two high temperature solvent less methods of green methodology<sup>30</sup> generate guest-free structures of well known host 1,1-bis-(4-hydroxyphenyl)cyclohexane (**1**, Figure 3). The idea of employing high temperature solvent free crystallization techniques are further illustrated with isomeric dihydroxybenzoic acid molecules (**2-7**) and successfully isolated guest-free forms and new polymorphic modification in multiple numbers of cases. Phase transition from metastable to a stable polymorphic modification in molecule **1** is studied through microscopy, thermal methods and X-ray diffraction.

## 2.4 1,1-Bis-(4-hydroxyphenyl)cyclohexane

1,1-Bis-(4-hydroxyphenyl)cyclohexane (**1**) is a very good host molecule that entraps solvent molecule upon solution crystallization. More than 31 solvates and cocrystal structures were reported.<sup>31</sup> Getting an anhydrous crystal of this molecule from solution media was a real trouble. The compound 1,1-bis-(4-hydroxyphenyl)cyclohexanone<sup>32</sup> has also shown as a good host property and cocrystallizing agent. Compound **1** was synthesized (Experimental section) and attempted to crystallize from several common laboratory solvents (including trifluorotoluene)<sup>26b</sup> to obtain a guest-free form; only solvent inclusion crystals or ill-defined powders were obtained. Host **1** is



hydrogen bonded to solvent or partner molecules either as donor ( $\text{O}_{\text{phenol}}-\text{H}\cdots\text{O}/\text{N}_{\text{solvent}}$ ), or acceptor ( $\text{O}/\text{N}_{\text{solvent}}-\text{H}\cdots\text{O}_{\text{phenol}}$ ), or both, as is common in phenolic host molecules.

Upon sublimation of **1** at 150-175 °C for 6 h or 140-150 °C at 0.2 Torr vacuum pressure for 2 h afforded thin plate and fine needle shaped crystals on the cold finger of sublimation apparatus. When the sample was heated to 180-190 °C and the resulting neat liquid phase was rapidly cooled (by bathing the outer wall of the test tube with volatile solvents like hexane, acetone etc), crystals of plate and block morphology were obtained. Single crystal X-ray diffraction confirmed that the sublimed and melt phase crystals, **1s** and **1m**, are indeed polymorphs of pure host. The isolation of pure **1** dimorphs will allow us to study desolvation pathways of its host–guest complexes, analogous to the versatile *p*-*tert*-butylcalix[4]arene host. Sublimed crystals (**1s**) crystallizes in triclinic space group  $P\bar{1}$  with one symmetry independent molecule ( $Z' = 1$ ) in its crystalline lattice and the structure of melt crystals (**1m**) is orthorhombic space group *Pbca* with  $Z' = 2$ . The crystal data for both polymorphs are summarized in Appendix. The three conformers of the two polymorphs of **1** overlay nicely except for the different orientation of OH groups (Figure 3b); OH groups are oriented *syn* in the triclinic polymorph conformer and one of the orthorhombic conformer (A) of **1m** whereas they are *anti* in the second conformer (B). One of the OH group in **1s** is connected via a chain of O–H $\cdots$ O hydrogen bonds along [010] (Figure 4a) and the second hydroxyl group engages in an O–H $\cdots$  $\pi$  interaction<sup>33</sup> (O1–H $\cdots$ O2 1.84 Å, 172.5°; O2–H $\cdots$  $\pi$  2.42 Å, 134.7°,  $\pi$  = Phenyl ring centroid). Hydrogen bond parameters are summarized in Table 1. In orthorhombic polymorph (**1m**), molecule A has O–H $\cdots$ O chain along [010] and O–H $\cdots$  $\pi$  interaction with a B molecule (O1A–H $\cdots$ O2A 1.95 Å, 172.9°; O2A–H $\cdots$  $\pi$ B 2.99 Å, 152.5°) (Figure 4b). Molecule B uses both hydroxyl groups in a cooperative chain of hydrogen bonds (Figure 5a) along [100] (O1B–H $\cdots$ O2B 1.91 Å, 172.8°; O2B–H $\cdots$ O1B 1.88 Å, 176.5°) that make microporous molecular ladders (Figure 5b). Microporous cavities in this polymorph have potential application in H<sub>2</sub> storage technology.<sup>34</sup> The diol orientation and hydrogen bonding motif in **1m** are related: the *syn* conformer participates in O–H $\cdots$ O chain and O–H $\cdots$  $\pi$  interaction whereas the *anti* conformer makes O–H $\cdots$ O chains on both sides. However conformer A makes O–H $\cdots$ O chain and O–H $\cdots$  $\pi$  interaction similar to **1s**. The infinite O–H $\cdots$ O chain motif in **1m** is rationalized by the presence of such hydrogen

bonded oligomers in the neat liquid, which solidify upon immediate cooling to polymorph **1m**.

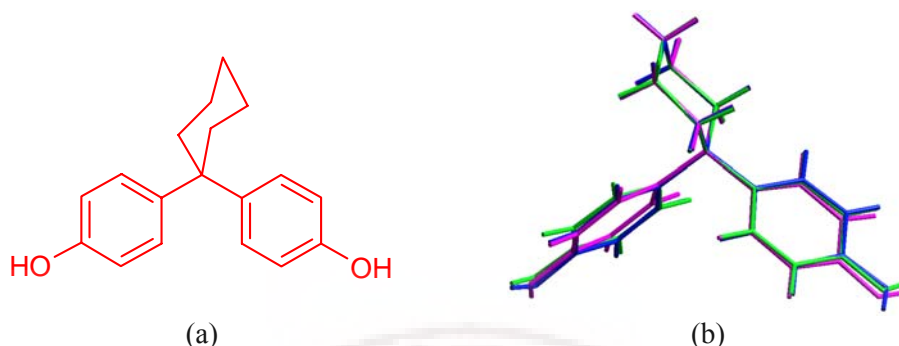


**Figure 3** (a) 1,1-Bis-(4-hydroxyphenyl)cyclohexane (**1**). (b) Molecular overlay of the two polymorphs of **1**. 1s = magenta, A (**1m**) = blue, B (**1m**) = green. OH groups are syn in conformer 1s and A (**1m**) and anti in B (**1m**).

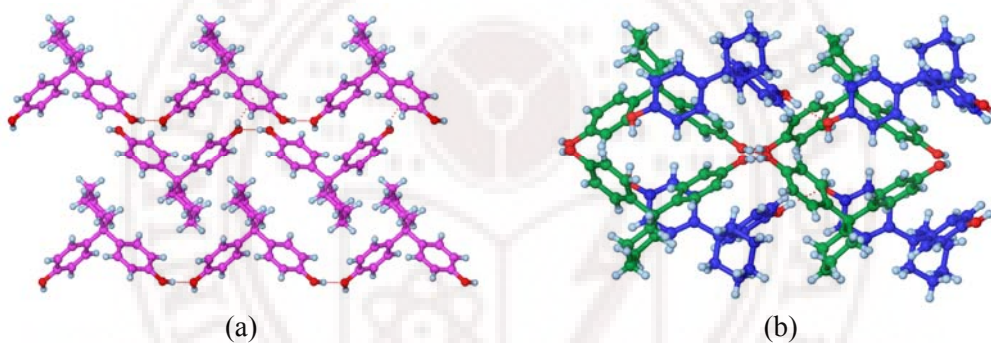


**Figure 4** (a) O-H...O chain along [010] in triclinic polymorph (**1s**) and O-H... $\pi$  interactions stabilizes the 3D structure, (b) Two symmetry independent molecules in **1m**. The A conformer (blue) have O-H...O hydrogen bonding down [100] similar to **1s** polymorph.

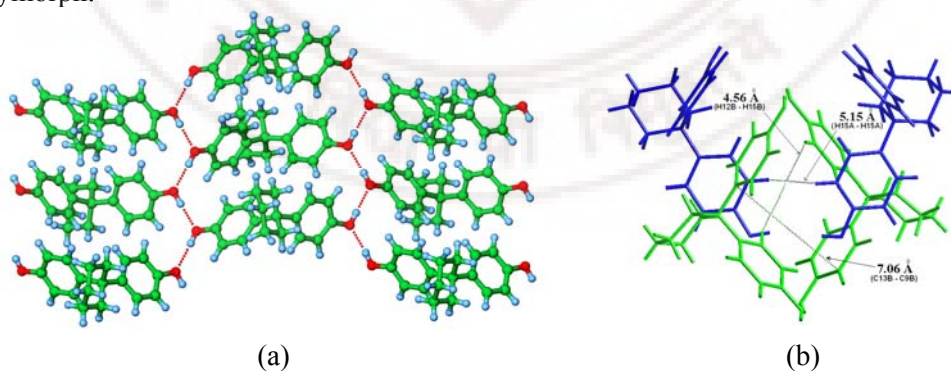


**Figure 5** (a) Cooperative O-H...O bonds along [100] in the ladder network of B molecules (green) in orthorhombic polymorph (**1m**). (b) Available pore dimensions in **1m** are 3.66 Å (= 7.06 – 3.40 Å), 2.26 Å (= 4.66 – 2.40 Å) and 2.75 Å (= 5.15 – 2.40 Å) [after removing the van der Waal distances for  $\pi$ -ring and H atoms. The rectangular voids in the molecular ladders of B conformer (green) is along [010].

**Table 1** Neutron normalised hydrogen bond parameter for **1m** and **1s**

|           | Interaction  | $d / (\text{\AA})$ | $D / (\text{\AA})$ | $\theta / (^\circ)$ |
|-----------|--------------|--------------------|--------------------|---------------------|
| <b>1m</b> | O1–H1...O2   | 1.85               | 2.829(2)           | 172.4               |
|           | O3–H3A...O4  | 1.77               | 2.747(2)           | 172.3               |
|           | C24–H24...O1 | 2.39               | 3.268(3)           | 137.7               |
|           | O4–H4A...O3  | 1.77               | 2.752(2)           | 176.2               |
| <b>1s</b> | O1–H1...O2   | 1.84               | 2.754(2)           | 173.1               |
|           | C9–H9...O1   | 2.49               | 3.342(2)           | 145.8               |

## 2.5 Lattice and Conformer Energy

Polymorph stability is of special interest because their energy differences are relatively small and inter-conversion is very common. A conformational energy change or the rotation about single bonds (torsion) of a molecule is within a small window of 1-3 kcal mol<sup>-1</sup> or it can go up to 7-8 kcal mol<sup>-1</sup> that may lead to conformational polymorphs. The energies of intramolecular torsions and intermolecular non-bonded interactions lie in the same range (0.5-10 kcal mol<sup>-1</sup>). Therefore, there is an immediate possibility that conformationally flexible systems are prone to polymorphism. Molecular conformer and crystal lattice energies of **1s** and **1m** were computed<sup>6b</sup> in Gaussian 03 (DFT, B3LYP/6-31G)<sup>35a</sup> and Cerius<sup>2</sup> COMPASS<sup>35b</sup> for **1s** and **1m**. Molecule conformer energy of **1s**, A (**1m**) and B (**1m**) are 0.00, 0.23, 0.29 kcal mol<sup>-1</sup> (relative energies) respectively. Crystal lattice energy of **1s** and **1m** are -37.11, -36.23 kcal mol<sup>-1</sup> (per molecule) respectively. Total crystal energy **1s**, **1m** = conformer + lattice = -37.11, -35.97 kcal mol<sup>-1</sup> (per molecule). Intramolecular and intermolecular energy compensation or systematic effect is absent. More stable conformer is in stable lattice (**1s**) and there is no energy compensation towards the overall stability. The sublimed phase is more stable than the melt form by  $[(-37.11) - (-35.97)] = 1.14$  kcal mol<sup>-1</sup>. Conformer and lattice energy values for **1s** and **1m** (conformer A and B) are summarized in Table 2.

**Table 2** Molecular conformer and crystal lattice energies for **1s** and **1m**

| Polymorphs               | $U_{\text{latt}}$ , COMPASS<br>(kcal mol <sup>-1</sup> ) | $E_{\text{conf}}$ , GAUSSIAN<br>(kcal mol <sup>-1</sup> ) | $E_{\text{total}} = U_{\text{latt}} + E_{\text{conf}}$<br>(kcal mol <sup>-1</sup> ) |
|--------------------------|--|---|---|
| <b>1s</b> (triclinic)    | - 37.11  | 0.00  | - 37.11   |
| <b>1m</b> (orthorhombic) | - 36.23  | + 0.26 (average)  | - 35.97   |

The metastable state of **1m** and its lower crystal density and packing fraction (**1m** 1.261 g cm<sup>-3</sup>, 69.9%; **1s** 1.275 g cm<sup>-3</sup>; 71.1%) may be due to the longer inter-aromatic separation of 3.8 × 2.4 Å (C13B–C9B, C15A–C15A) between B molecules (Figure 5b) compared to no gap in **1s** (C15–C15, after subtracting 3.4 Å =  $\pi$ -plane diameter).

## 2.6 Phase Transition

Crystallization is a supramolecular reaction that leads to kinetic and thermodynamic products through Curtin-Hammett like reaction kinetics.<sup>36a</sup> Kinetic forms nucleate faster over the thermodynamic one because of its strong hydrogen bonding and better close packing. Polymorph interconversion can occur upon heating, grinding, slurry method or by ultrasound is reported in literature (discussed in chapter 4). Kinetic polymorph which normally appears at ambient temperature may be converted to the stable thermodynamic form upon heating or grinding. As different polymorphs have different physical and chemical properties, characterization of all polymorphs (thorough polymorph screening), identification of the stable form and controlled preparation of a particular metastable form has become one of the major challenges in modern crystal engineering and solid-state chemistry. Ostwald's rule<sup>36b</sup> states that "the system moves to equilibrium from an initial high-energy state through minimal changes in free energy". Therefore the structure that crystallizes first is one which has the lowest energy barrier (kinetic or metastable form). This form would then transform to the next lower energy polymorph and so on until a thermodynamically stable state is achieved. The transformation from higher energy state to lower energy is system specific. The structural analysis of various polymorphs at different stages would help us to understand the nature and the extent of self-assembly process that take place during crystallization.<sup>36,37</sup> Lattice and conformer energy correlation indicate melt (**1m**,  $Z' = 2$ ) as metastable polymorph whereas sublimed phase (**1s**,  $Z' = 1$ ) as stable form. Hot stage microscope (HSM) and differential scanning calorimetry (DSC) were used to identify kinetic and thermodynamic forms, monotropic or enantiotropic phases, and mechanism of transformation. Hot stage microscopy shows that the block of the melt crystal begins to melt at 178-182 °C and is completely melted at 183-185 °C. Cooling affords sublimed



crystals of fine needle shape (Figure 6). On the other hand, sublimed crystals **1s** do not show any apparent crystal form change in a similar heat-cool cycle on the hot stage.

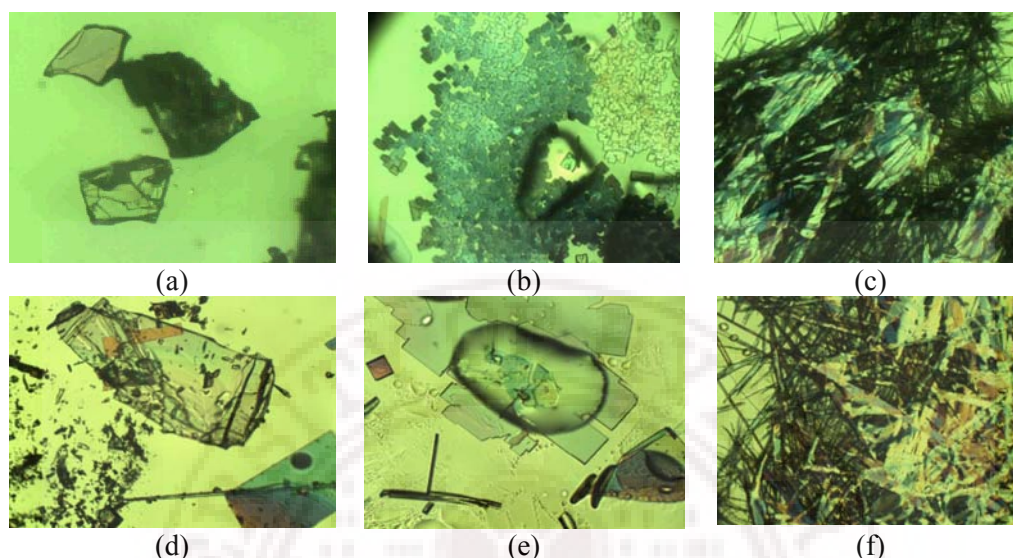


**Figure 6** HSM frames. **1m**: (a) at 25 °C, (b) 181-182 °C, (c) cool to room temperature. **1s**: (d) at 25 °C, (e) 183-184 °C, (f) cool to room temperature. (a) to (c) represents phase transition of a block crystal of **1m** to **1s** needle fibre. A plate-like crystal of **1s** shows change to needle morphology (d-f) but retains the same form.

Differential scanning calorimetry thermogram of **1s** has a single broad endotherm at  $\sim 184$  °C ( $T_{\text{peak}}$ ) but **1m** shows two sharp endotherms at 183 °C and 188 °C, which are assigned to melting of **1m**, then solidification (exotherm) to **1s** phase, followed by fusion of the sublimed form. After a heat-cool-heat cycle in DSC both melt and sublimed phase exhibit a single endotherm (Figure 7). Sublimation occurs in both **1s** and **1m** (after phase transition at 183-185 °C) confirmed with TG-IR (thermal gravimetry–infrared spectroscopy, Figure 8a, b, c) of the evolved vapor. The single endotherm peak after reheating is ascribed to the stable sublime phase. DSC, HSM and computation indicate that **1m** is the kinetic polymorph and **1s** is the thermodynamic phase ( $T_{1m} = 183 \pm 1$  °C;  $T_{1s} = 188 \pm 1$  °C). Conformational polymorphs **1m** and **1s** are monotropic up to 160 °C and enantiotropic between 180-200 °C.

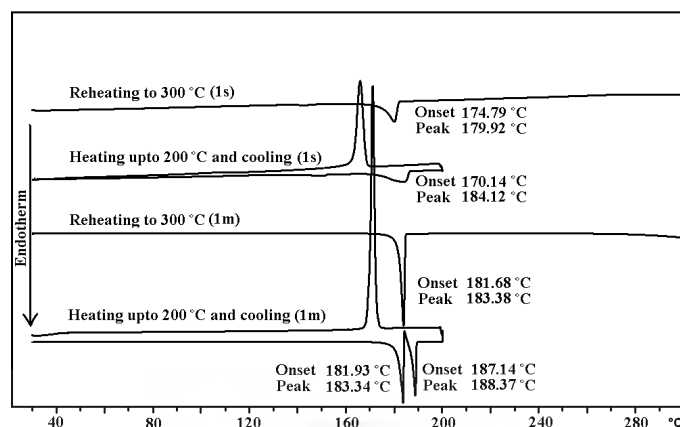
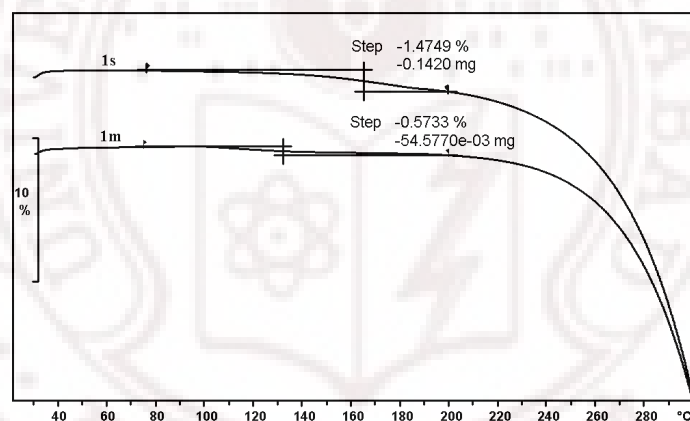
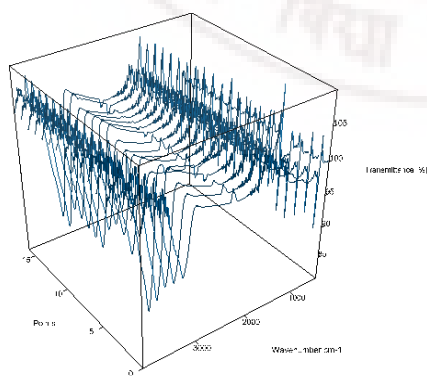


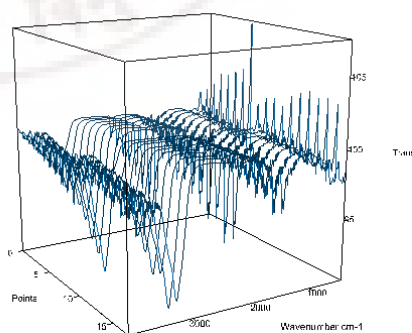
**Figure 7** DSC of **1m** and **1s** polymorphs. Metastable phase **1m** shows phase transition to the sublimation polymorph **1s** and transformation to the thermodynamic form upon heating up to 200 °C. Polymorph **1s** does not show phase changes under the same conditions except the sublimation endotherm. The reheating cycle endotherm is shifted to ~5 °C lower *T* than the first heating cycle due to more efficient contact of the sample with the pan.



(a)



(b)



(c)

**Figure 8** Thermal gravimetric analysis (a) and infrared spectrum of the evolved vapor of **1s** (b) and **1m** (c) polymorphs. 8-12 mg of the sample was heated at 10 °C/min and dry N<sub>2</sub> gas purged at 100 mL/min. The evolved vapor from TGA was passed through a heated transfer line at 100 °C and IR recorded using DLaTGS detector. The up peaks in the spectrum are due to incomplete cancellation of background air. TG-IR is used to characterize sublimation in polymorphs. Sublimation is known to occur even when there is marginal to nil weight loss in TGA as observed in (a).

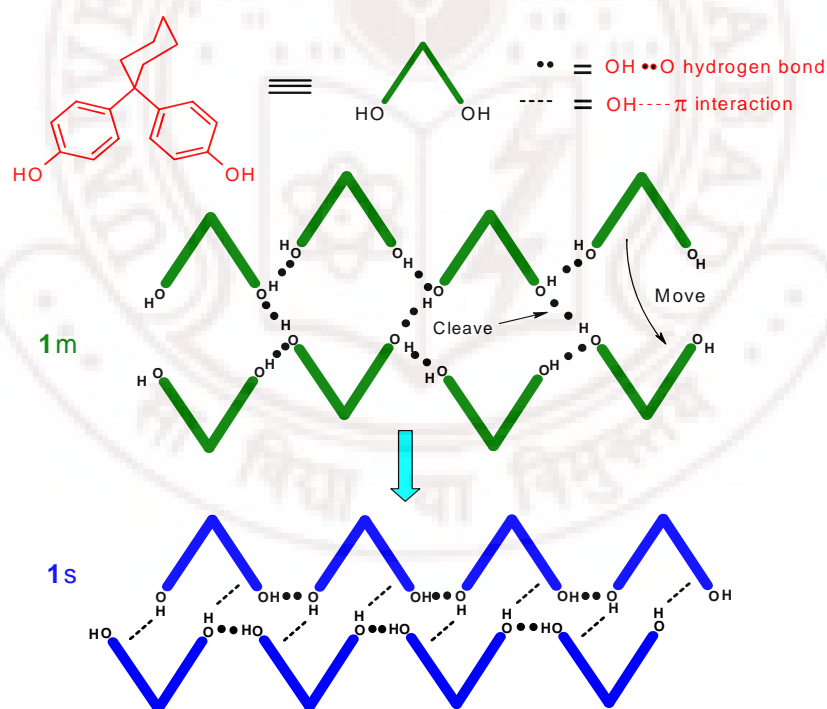
The transitions from metastable to stable phase are normally dependent on heating-rate, grinding (solid state grinding, solvent drop grinding), slurry methods, etc. HSM data provide visual evidence for the presence of these transitions. Phase transition is a common phenomenon in APIs. Polymorphic transformation of Nifedipine,<sup>38</sup> a drug for calcium channel blocker from a kinetic to a thermodynamic stable form upon heating at 110°C was recently reported and established by thermal analysis and variable temperature powder X-ray diffraction (VT-PXRD) study. Studies on premafloxacin, a potent antibiotic have revealed three anhydrous polymorphic modifications. Form III appears to be more stable however other two, Form I and Form II undergoes phase transition under variety of conditions well characterized with various physical methods like optical microscopy, thermomicroscopy, powder X-ray diffraction, differential scanning calorimetry etc. Variety of tools exists nowadays, that allow giving a sharp definition of a solid. Such characterization of solid-state forms encompass microscopy, infrared (IR) spectroscopy, differential scanning calorimetry (DSC), thermogravimetric analysis (TGA), Karl Fischer titration, X-ray powder diffraction analysis, single-crystal X-ray diffraction. More examples on phase transition phenomenon are discussed in chapter 4. Analyzing the hydrogen bond pattern in two polymorphs a structural model for the phase transition of the microporous structure of **1m** to the close-packed structure of **1s** on the basis of breaking of O–H···O bond and forming O–H··· $\pi$  interaction is proposed in the following Scheme 1. This is a remarkable example to illustrate how close packing conflicts<sup>39</sup> in a metastable  $Z' = 2$  structure are resolved in the thermodynamic  $Z' = 1$  polymorph.

## 2.7 High $Z'$ Structures and CSD Trends

Occurrence of  $Z'$  in organic crystals crystallized ‘from the melt’, ‘by sublimation’ and ‘overall statistics’ in the CSD was compared and complete analysis is



discussed in chapter 3. There is an increase in  $Z' > 1$  frequency for solvent less methods compared to solution crystallization. Cambridge Structural Database (CSD version 5.30, ConQuest 1.10, November 2008 release, May 2009 update) was used<sup>40</sup> in all searches and crystal structures were visualized in Mercury CSD 2.2 (Build RC5). CSD shows 4-5% organic compounds, 5.5% organometallics and 2.1% of coordination compounds are polymorphic, however pharmaceutically active molecules show a greater probability of 30-50% in drug substances of  $<600 \text{ g mol}^{-1}$  molecular weight. This phenomenon is more common in conformationally flexible molecules and/or multiple functional groups capable of forming hydrogen bonds. The comparison of polymorphic structures comes in their difference in molecular conformations, hydrogen bonding, packing arrangements, and lattice energies. The occurrence of symmetry-independent B conformer is consistent with recent results that implicate strong  $\text{O-H}\cdots\text{O}$  hydrogen bonding in multiple  $Z'$  crystal structures,<sup>6b,c</sup> discussed in chapter 3.



**Scheme 1** Cleavage of  $\text{O-H}\cdots\text{O}$  hydrogen bonds down  $[100]$  of B molecules in **1m** and movement of hydrogen bonded chains along  $[010]$  towards each other results in an  $\text{O-H}\cdots\pi$  interaction and filling of the voids to give a close-packed structure similar to **1s**.

## 2.8 Synthron Polymorphism in Isomeric Dihydroxybenzoic Acids

Chapter 1 gives an introduction to polymorphism, its occurrence and importance in commercial and industrial implications in various fields such as drugs and pharmaceuticals, agrochemicals, pigments, dyes and explosive devices etc. Polymorphism perhaps tends to be prominent in molecules that contain multifunctional groups thereby forming multiple supramolecular synthons and molecules with conformational flexibility. Supramolecular synthon approach and careful observation extend these ideas to multi-component solids like cocrystals, solvates, and salts. Dihydroxybenzoic acid (DHB now on) molecules are easily available and have biological interest.<sup>38</sup> Six isomeric dihydroxybenzoic acids are considered (Figure 9) for polymorphism study as these molecules show very good host property. 2,3-DHB is a salicylate metabolite. 2,5-DHB (Gentisic acid), 3,4-DHB and 3,4,5-trihydroxybenzoic acid (Gallic acid) have antioxidant activity. They are responsible for apoptosis or cell death that is characterized by DNA cleavage. Being two established high temperature solvent free methods in our hand to generate guest-free form of host molecule with a good probability to isolate new polymorphic modification, we employed the same in this series of molecules to validate the idea of generating guest-free form of host compound and search for new polymorphs.

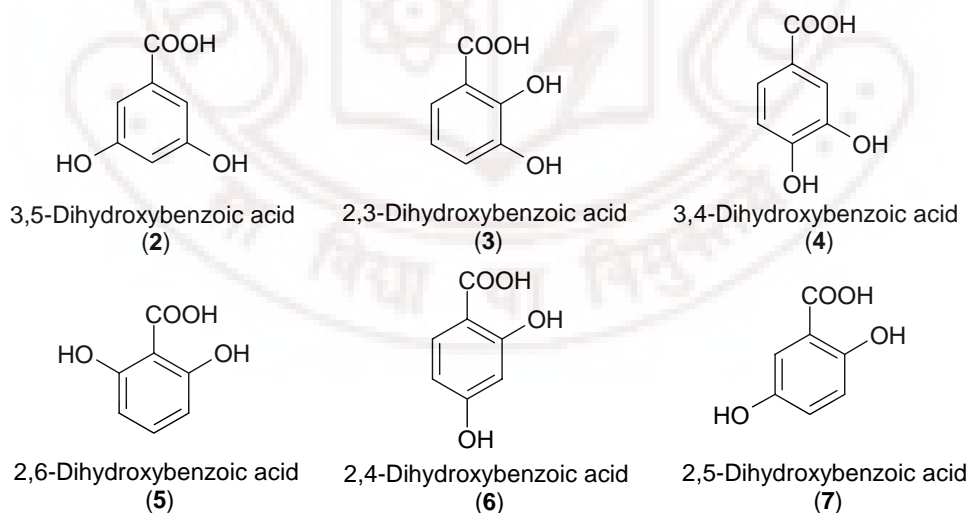


**Figure 9** Isomeric dihydroxybenzoic acids

These compounds are prone to give solvate/hydrate upon solution crystallization. Multiple functionalities on these molecules like –OH and –COOH offer hydrogen bond synthon competition in the crystal structures. Solvent free conditions can afford guest-free structures and polymorphs of molecules. These high temperature solvent less techniques are now employed to generate new polymorphs of 2,3-, 2,4-, 2,5-, 2,6-, 3,4-, and 3,5-positional isomers of dihydroxybenzoic acids. Two polymorphs of 3,5-DHB, a new polymorph of 2,3-DHB and guest-free form of 3,4-DHB were crystallized by melting and sublimation.<sup>41</sup> A new hydrate polymorph of 3,4-DHB was also isolated when crystallized from water in refrigerator at 0-5°C. These polymorphs differ in the nature of hydrogen bond synthons in their crystal structure. Structural and thermal characterization of polymorphic phases having multiple *Z'* is presented. Anti-inflammatory drug 2-(2-Methyl-3-chloroanilino)-nicotinic acid (BIXGIY, BIXGIY02, BIXGIY03, and BIXGIY04),<sup>42a</sup> Oxalic acid,<sup>42b</sup> Tetrolic acid<sup>42c</sup> are remarkable examples that show synthon polymorphism. All compounds are purchased from Sigma Aldrich and used directly for experiments.

## 2.9 Results and Discussion

Crystal structures of two polymorphs of pure 2,6-DHB (**5**) or  $\gamma$ -resorcylic acid, (refcodes LEZJAB, LEZJAB01)<sup>43a</sup> and a 2,6-DHB hydrate (LEZJEF) structure was reported. The hydrogen of carboxylic acid group is flanked towards the phenolic OH via O–H $\cdots$ O intramolecular hydrogen bond and as a result the carboxylic acid dimer is absent in form I of **5**, however form II shows carboxylic acid dimer synthon. Recently Wilson reported<sup>43b</sup> a second polymorph of 2,4-DHB (**6**) (ZZZEEU01). Cooperative hydrogen bonding between the intermolecular carboxylic acid dimer and intramolecular hydrogen bonds is present in this structure. A single polymorph of this compound was previously reported in 1956 (ZZZEEU)<sup>43c</sup> with little structural information other than unit-cell parameters made available without 3D coordinate. A hydrate structure of **6** was also reported (QIVTUK). The report on two polymorphs of 2,5-DHB (**7**) (BESKAL, BESKAL01)<sup>43d,e</sup> was first published in 1982 and their structures were redetermined recently. Slow evaporation of aqueous solutions afforded a polymorph II of **7**. Crystals of polymorph I was obtained from a mixed solution of chloroform and acetone (3:1 in

volume). The modes of molecular packing are divided into two types, parallel and alternate. Form II belongs to the parallel modes of stacking and the form I belongs to the alternate modes of stacking. There is remarkable similarity of the crystal structures of benzoic acid and the form II, salicylic acid and form I. Only the hydrogen bonding of the phenolic OH plays an additional role in determining the structure. 3,5-DHB (**2**) is a tricky molecule has high propensity to include solvents on crystallization. This molecule is crystallized from several common solvents e.g. water, ethylacetate, ethanol, methanol, acetone, dioxane, tetrahydrofuran, dimethylsulfoxide, acetic acid etc. Only solvent inclusion crystals were obtained. In consequence three solvated structures of compound **2** are considered to demonstrate here the structural and thermal behaviour. They are acetyl acetone, tetrahydrofuran, dioxane solvates of **2** (**2**•Acac, **2**•THF, **2**•Dioxane).

### 2.9.1 Solvates of 3,5-Dihydroxybenzoic Acid (**2**)

When **2** is crystallized from acetylacetone (**2**•Acac) and few drops of methanol, at ambient condition, slow evaporation of solvent afforded suitable crystals for single crystal X-ray diffraction. Structure solution and refinement showed four molecules of **2**, four molecules of water and one molecule of acetyl acetone in the asymmetric unit. The host molecules are arranged in layer structures through carboxylic acid homo dimer and hydroxyl group O—H...O hydrogen bonding (O6—H9...O2, 2.648(3) Å, 174°; O5...O1, 2.628 Å, O7—H11...O4, 2.738(3) Å, 169°; O3—H3A...O8, 2.687(3) Å, 162°). The hydrogen between O5 and O1 in the acid homo dimer could not be located from Fourier map. Acetyl acetone and two water molecules reside in the hexagonal channel formed by the host layers (Figure 10).

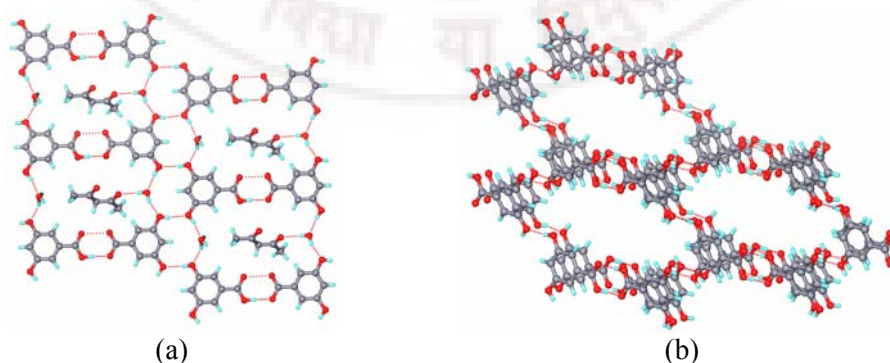


**Figure 10** (a) Water and Acetyl acetone solvent molecules are sitting in the hexagonal channel (b) formed by host in **2**•Acac.

Crystallization of **2** from tetrahydrofuran (**2**•THF) afforded single crystals which is refined and solved with four molecules of the host, four molecules of waters and one THF molecule in its asymmetric unit. THF solvate shows similar structural pattern as discussed above for **2**•Acac. The host molecules are arranged in a layer through carboxylic acid dimer and O–H···O hydrogen bonds forming hexagonal channels. THF and water guest molecules occupy the void space. One water molecule acts as the linker between two host layers (Figure 11a). Crystallization of **2** from dioxane afforded block crystals (**2**•Dioxane). 1:1 ratio of host to guest is present in the asymmetric unit. The crystal structure shows a different molecular arrangement of the host molecule compared with **2**•THF and **2**•Acac. Dioxane acts as a connector between the tapes formed by the host molecules extends it to a layer structure (Figure 11b). Acid homo dimer is absent in this structure.

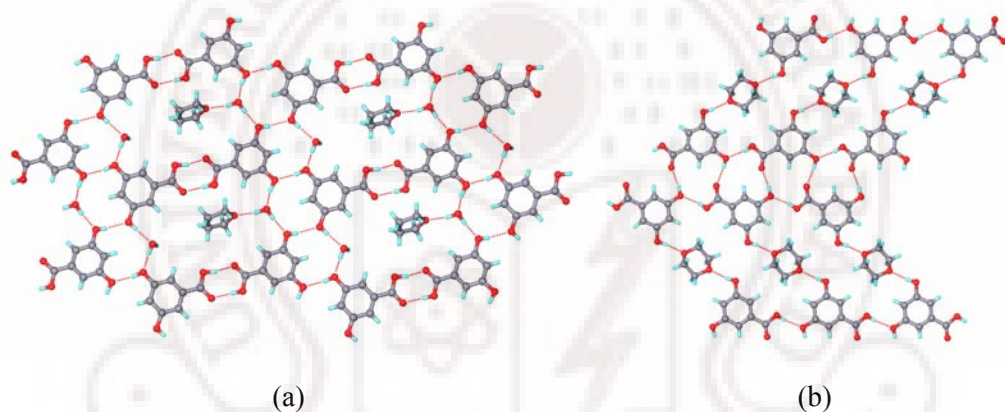
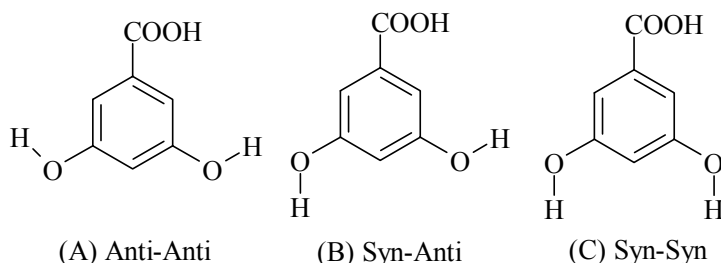


**Figure 11** (a) Formation of hexagonal channel in **2**•THF by host molecule layers. THF and waters are sitting in the channel gives similar packing as **2**•Acac. (b) Dioxane connects the 2D tapes formed by the host molecules in **2**•Diox and extends it into overall layer structure.

### 2.9.2 Polymorphs of 3,5-Dihydroxybenzoic Acid (**2**)

3,5-DHB is good host compound because it includes guest on crystallization. Only 5 cocrystals/salts structures were reported in CSD. Three of them are cocrystals with bipyridyl derivatives (BEQWAV, VEFVEI and VEFVIM) and one amino acid complex (UCEMEV). Presence of several OH groups may offer multiple numbers of conformational states that can causes polymorphic outcome of these compounds. OH orientations of molecule **2** in the crystal structures are shown in Scheme 2 and these

different conformers are found in the reported crystal structures. Carboxylic acid homo dimer is absent in all reported crystal structures of **2**.



**Scheme 2** Three possible orientations of OH group in 3,5-DHB

### (a) Structural Analysis

Upon sublimation of **2** at 170-180 °C for 10 h afforded thin plate and fine needle shaped crystals on the cold finger of sublimation apparatus. When the sample was heated to 235-240 °C and the resulting neat liquid phase was rapidly cooled crystals of plate and block morphology were obtained. Single crystal X-ray diffraction confirmed that the sublimed and melt phase crystals, **2s** and **2m**, are indeed polymorphs of pure host **2**. **2s** crystallizes in the monoclinic space group  $C2/c$  with three symmetry independent molecules ( $Z' = 3$ ) in asymmetric unit however **2m** crystallizes in the same monoclinic space group  $C2/c$  with  $Z' = 0.5$ . Crystal data are summarized in Appendix. Two symmetry independent molecules are hydrogen bonded involves only OH groups via O–H $\cdots$ O hydrogen bond (O12–H12C $\cdots$ O3, 2.689(6) Å, 174.96°; O4–H4A $\cdots$ O11, 2.635(6) Å, 173.34°) leads to 1D tape (Figure 12a) and these tapes are interconnected through carboxylic acid homo dimer (O1–H1A $\cdots$ O10, 2.657(4) Å, 178.75°; O9–H9C $\cdots$ O2, 2.637(5) Å, 164.35°) and extend it into a brick wall like 2D sheet parallel to  $ab$  plane (Figure 12a) in **2s**. The third symmetry independent molecule also forms 1D tape with phenolic OH groups via O–H $\cdots$ O hydrogen bonding (O7–H7B $\cdots$ O8, 2.719(5) Å, 172.27°) which fills the void formed by the stacked brick wall layers moved perpendicular to the  $ab$  plane to complete the 3D packing (Figure 12b). Hydrogen bond parameters are tabulated in Table 3.



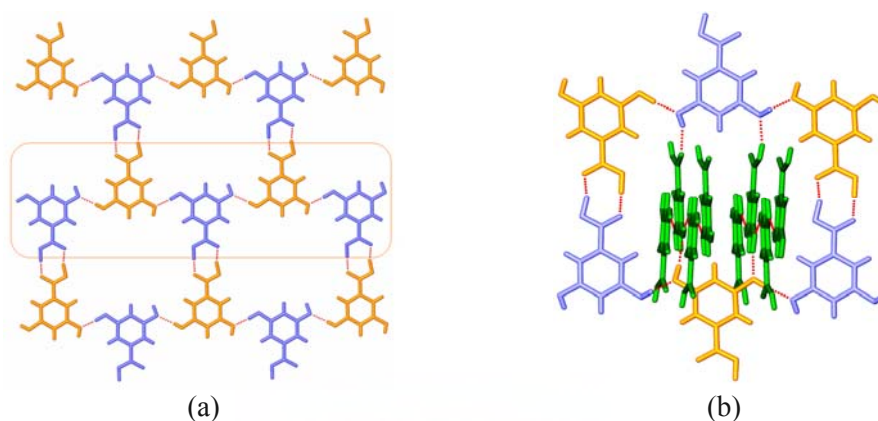


**Figure 12** (a) 1D O–H...O hydrogen bond tape in **2s** (Sublimed polymorph) along [100]. The acid dimers connect two tapes lead to the formation of 2D brickwaal like sheet. (b) Third symmetry independent molecule (green) forms 1D tape via O–H...O hydrogen bond that connects the parallel layers.

**2m** adopts a layered structure via the cyclic synthon formed by one COOH and two OH groups highlighted in Figure 13a. Carboxylic acid homo dimer is absent. Phenolic OH takes an orientation similar to Scheme 2 (A) giving rise to a tandem like situation. 2D layers which are in turn stabilized by  $\pi\cdots\pi$  stacking at 3.01 Å separation (Figure 13b).

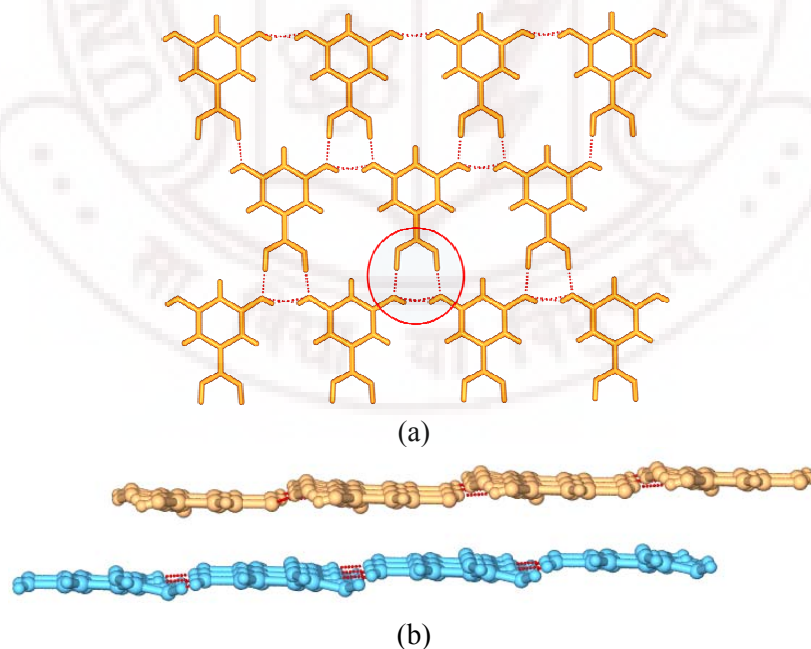


**Figure 13** (a) O–H...O hydrogen bond forms the tape that extends into 2D layer parallel to (001) via cyclic hydrogen bond synthon of two OH groups with COOH in **2m**. (b) 2D layers are stabilized by  $\pi\cdots\pi$  stacking at 3.01 Å separation viewed down [100].



**Table 3** Neutron normalized hydrogen bond parameters.

|               | Interaction    | H...A/ Å | D...A/ Å | ∠D-H...A/° |
|---------------|----------------|----------|----------|------------|
| <b>2s</b>     | O1-H1...O10    | 1.67     | 2.657(4) | 179        |
|               | O3-H3...O7     | 1.81     | 2.766(5) | 162        |
|               | O4-H4...O11    | 1.65     | 2.635(6) | 173        |
|               | O5-H5B...O12   | 1.70     | 2.648(5) | 161        |
|               | O7-H7B...O8    | 1.74     | 2.719(5) | 172        |
|               | O8-H8B...O4    | 1.69     | 2.671(4) | 173        |
|               | O9-H9C...O2    | 1.68     | 2.637(5) | 164        |
|               | O11-H11C...O6  | 1.74     | 2.681(5) | 159        |
|               | O12-H12C...O3  | 1.71     | 2.689(6) | 175        |
| <b>2m</b>     | O1-H1...O2     | 1.73     | 2.713(2) | 177        |
|               | O2-H2...O2     | 1.85     | 2.640(2) | 136        |
| <b>2•Acac</b> | O12-H1...O19   | 1.66     | 2.641(4) | 173        |
|               | O9-H2...O14    | 1.66     | 2.640(3) | 178        |
|               | O3-H3A...O8    | 1.73     | 2.687(3) | 162        |
|               | O11-H4...O15   | 1.73     | 2.695(4) | 168        |
|               | O4-H4A...O20   | 1.70     | 2.661(4) | 165        |
|               | O16-H6...O12   | 1.76     | 2.730(4) | 167        |
|               | O13-H8...O10   | 1.65     | 2.624(3) | 173        |
|               | O8-H8A...O21   | 1.68     | 2.638(4) | 165        |
|               | O6-H9...O2     | 1.67     | 2.648(3) | 174        |
|               | O7-H11...O4    | 1.77     | 2.738(3) | 169        |
|               | O15-H15A...O22 | 1.67     | 2.658(5) | 179        |
|               | O19-H19A...O20 | 1.95     | 2.918(5) | 170        |
|               | O19-H19B...O11 | 1.89     | 2.839(4) | 162        |
|               | O20-H20A...O3  | 1.84     | 2.773(4) | 158        |
|               | O20-H20B...O18 | 1.73     | 2.710(4) | 175        |
|               | O21-H21B...O7  | 1.94     | 2.815(4) | 147        |
|               | O22-H22A...O16 | 2.00     | 2.815(5) | 139        |
|               | O22-H22B...O17 | 2.07     | 2.849(5) | 135        |
| <b>2•THF</b>  | O1-H1A...O14   | 1.70     | 2.652(3) | 163        |
|               | O3-H3A...O18   | 1.69     | 2.649(4) | 163        |
|               | O4-H4A...O15   | 1.77     | 2.748(3) | 172        |
|               | O5-H5A...O12   | 1.79     | 2.762(3) | 169        |
|               | O6-H6A...O17   | 1.66     | 2.627(4) | 165        |
|               | O7-H7A...O10   | 1.67     | 2.651(3) | 178        |
|               | O9-H9A...O8    | 1.64     | 2.600(3) | 166        |
|               | O11-H11A...O6  | 1.73     | 2.704(3) | 171        |
|               | O12-H12A...O19 | 1.72     | 2.690(4) | 171        |
|               | O13-H13A...O2  | 1.63     | 2.615(3) | 176        |
|               | O15-H15A...O21 | 1.70     | 2.659(4) | 163        |
|               | O16-H16A...O3  | 1.74     | 2.725(3) | 176        |
|               | O17-H17A...O20 | 1.75     | 2.698(3) | 161        |
|               | O17-H17B...O5  | 1.90     | 2.874(4) | 171        |
|               | O18-H18A...O19 | 2.11     | 2.979(5) | 147        |

|                                       |                |      |          |     |
|---------------------------------------|----------------|------|----------|-----|
|                                       | O18–H18B...O4  | 1.89 | 2.847(4) | 165 |
|                                       | O19–H19A...O14 | 2.19 | 2.918(5) | 130 |
|                                       | O19–H19B...O11 | 1.74 | 2.718(4) | 172 |
|                                       | O21–H21A...O10 | 1.98 | 2.928(5) | 162 |
|                                       | O21–H21B...O17 | 2.01 | 2.927(5) | 155 |
|                                       | C13–H13...O21  | 2.45 | 3.216(5) | 127 |
| <b>2•Diox</b>                         | O2–H2...O3     | 1.72 | 2.697(4) | 170 |
|                                       | O3–H3...O1     | 1.76 | 2.738(4) | 171 |
|                                       | O4–H4...O5     | 1.74 | 2.701(4) | 165 |
|                                       | C3–H3A...O1    | 2.34 | 3.151(5) | 130 |
| <b>3•Form II</b><br>(monoclinic)      | O2–H2...O1     | 1.68 | 2.661(3) | 178 |
|                                       | O4–H4...O2     | 2.17 | 3.006(3) | 142 |
|                                       | C7–H7...O4     | 2.44 | 3.516(3) | 174 |
| <b>4•Pure</b>                         | O3–H3...O6     | 2.03 | 2.83(4)  | 138 |
|                                       | O4–H4...O12    | 1.80 | 2.77(5)  | 167 |
|                                       | O7A–H7A...O3   | 2.04 | 2.87(5)  | 140 |
|                                       | O8–H8...O3     | 1.84 | 2.77(4)  | 157 |
|                                       | O11A–H11A...O1 | 1.72 | 2.70(6)  | 173 |
|                                       | O12–H12...O11A | 2.01 | 2.73(6)  | 128 |
|                                       | O9–H30...O1    | 1.73 | 2.69(5)  | 166 |
|                                       | O5–H31...O6    | 1.61 | 2.60(5)  | 174 |
|                                       | O2–H32...O10   | 1.63 | 2.61(5)  | 169 |
| <b>4•H<sub>2</sub>O</b><br>monoclinic | O1–H1...O2     | 1.66 | 2.642(5) | 173 |
|                                       | O3–H3A...O3    | 1.86 | 2.778(4) | 155 |
|                                       | O3–H3B...O5    | 1.91 | 2.844(5) | 157 |
|                                       | O4–H4...O5     | 1.75 | 2.730(5) | 171 |
|                                       | O5–H5B...O2    | 2.22 | 3.014(6) | 137 |
|                                       | O5–H5C...O3    | 1.98 | 2.844(5) | 145 |
|                                       | O5–H5C...O4    | 2.32 | 3.036(6) | 129 |

## (b) Thermal Analysis

DSC thermogram of **2s** has a single sharp endotherm at 238.1 °C ( $T_{\text{onset}}$ ) and **2m** shows endotherm at 232.8 °C ( $T_{\text{onset}}$ ). These two synthon polymorphs, **2s** and **2m** are monotropically related up to melting temperature at atmospheric pressure as they do not show phase transition. Stability of polymorphs can be explained in terms of hydrogen bonding, packing fraction, density, melting point and by computation. Due to the positional disorder of OH group of –COOH functionality, the lattice energy value of **2m** is unlikely comparable. Density and packing fraction (**2s**: 1.536 g cm<sup>-3</sup>; 71.0%; **2m**: 1.541 g cm<sup>-3</sup>, 71.6%) from crystal structure did not give a clear indication for stability comparison of **2s** and **2m** although **2s** show ~6 °C higher melting onset.

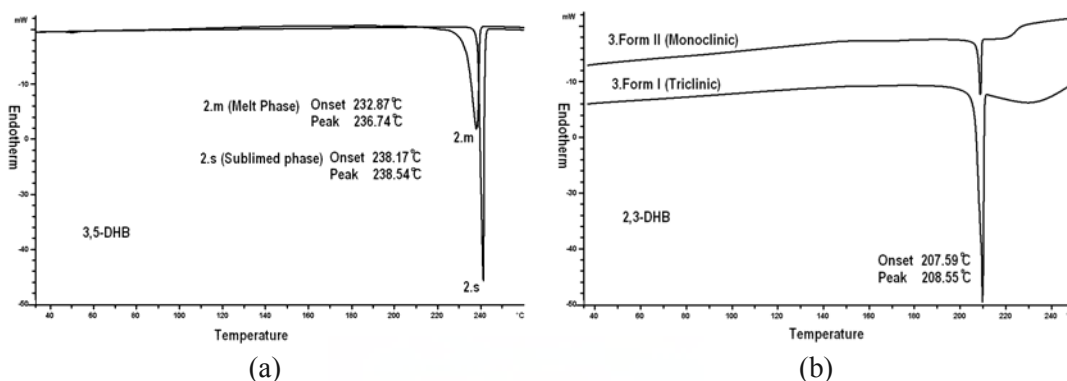


**Figure 14** (a) DSC thermogram shows 6°C higher melting onsets for sublimed (2s) over melt phase (2m). (b) 3.Form I (triclinic) and new 3.Form II (monoclinic) show almost similar melting onset (207.6 °C).

### 2.9.3 Polymorphs of 2,3-Dihydroxybenzoic Acid (3)

Sublimation of **3** afforded block crystals in major amount along with few thin plates on the cold finger of the sublimation apparatus concomitantly. Single crystal X-ray diffraction confirmed that block and thin plate crystals, Form I and Form II are indeed polymorphs of pure host **3**. Form I crystallizes in triclinic space group  $P\bar{1}$  with  $Z' = 2$ , that is reported in literature (refcode CACDAM)<sup>43f</sup>. The new Form II crystallized in monoclinic space group  $P2_1/n$  with  $Z' = 1$ . Melting did not afford good quality single crystals. Carboxylic acid homo dimer is common in both crystal structures. Form I shows a layer structure however Form II shows 3D packing arrangements of host molecules extended via C–H···O hydrogen bonds. The cyclic hydrogen bond synthon highlighted in Figure 15 present in Form I but absent in Form II is the main difference in these two polymorphs. Concomitant polymorphs in sublimation are not common and 11 pairs extracted from the CSD are listed in Table 4.

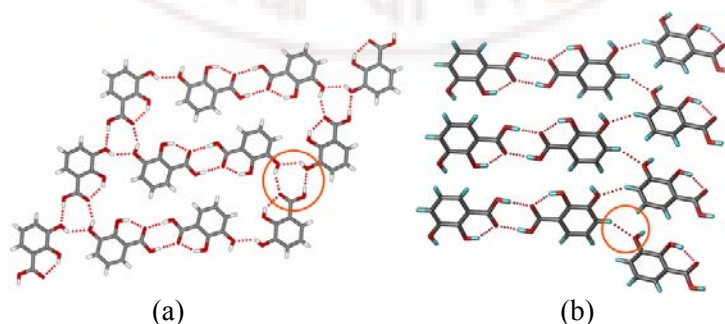


**Figure 15** (a) Form I of **3** show 2D layer structure. (b) New Form II has a 3D structure differing in hydrogen bond synthon (in circle).

**Table 4** CSD refcodes of 11 pairs of concomitant polymorphs crystallized by sublimation

|   |                    |
|---|--------------------|
| BATCAA, BATCAA01                                  | BEZQAZ, BEZQAZ01   |
| GEGXAS, GEGXAS01                                  | HAWRAZ, HAWRAZ01   |
| IFULUQ, IFULUQ01, IFULUQ02,<br>IFULUQ03, IFULUQ04 | KACRUC, KACRUC01   |
| NOLFUP, NOLFUP01                                  | SUWMIG02, SUWMIG03 |
| ZZZIYE05, ZZZIYE06                                | PUCMIJ, PUCMIJ01   |
|   | VARYIW01, VARYIW02 |

As both polymorphs appeared concomitantly by sublimation they are probably equienergetic as indicated by the melting onset temperature of Form I and Form II (Figure 14b). Packing fraction and density (Form I: 1.546 g cm<sup>-3</sup>; 71.8%; Form II: 1.595 g cm<sup>-3</sup>, 74.6%) from crystal structure indicates that Form II is more stable (Table 5).

#### 2.9.4 Guest-Free Structure of 3,4-Dihydroxybenzoic Acid (**4**)

Hydrate of **4** was reported (BIJDON03)<sup>43g</sup> however guest-free **4** is difficult to crystallize from solution crystallization because it adopts guest molecules in its crystalline lattice. Guest-free host crystals were generated from melting that solved and refined in triclinic space group  $P\bar{1}$  with  $Z' = 3$ . Sublimation afforded decomposed product catechol. ORTEP of **4** shows two symmetry independent molecules have orientation disorder (Figure 16a) at the *m*-hydroxy group into two sites (s.o.f 0.3 for H11B, O11B, H20, H11, H7B, O7B and 0.7 for H11A, O11A, H18, O7A, O7B, H13 each). One disordered host molecule forms acid homo dimer with non-disordered symmetry independent molecule that extends into 1D tape through a tetrameric O–H $\cdots$ O hydrogen bond synthon (Figure 16b). The third asymmetry molecule engaged via O–H $\cdots$ O hydrogen bond in the formation of 1D tape is perpendicular to the first tape by forming acid homo dimers.

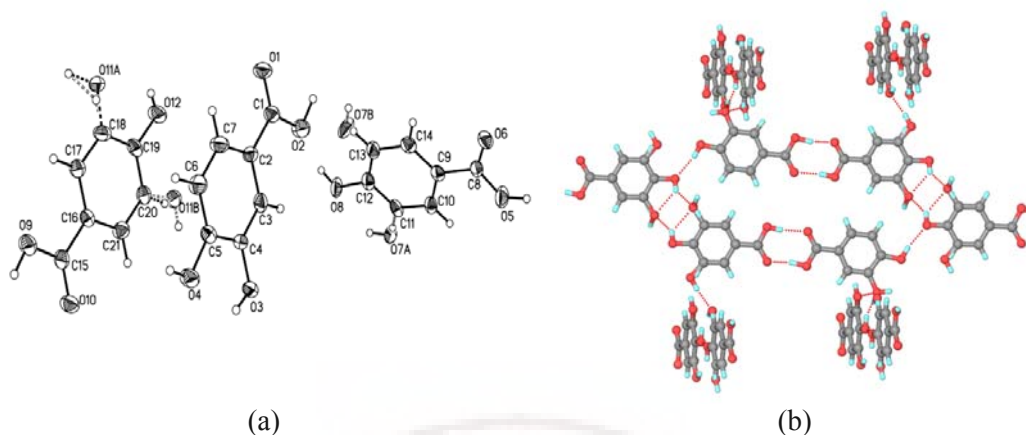


**Figure 16** (a) ORTEP of **4**. (b) Cyclic O–H···O tetrameric synthon connects acid homo dimers formed by two symmetry independent molecules and extends it into a 1D tape like structure. Third symmetry independent molecule connects them into 3D structure.

### 2.9.5 New Hydrate Polymorph of 3,4-Dihydroxybenzoic Acid

A new hydrate polymorph of 3,4-dihydroxybenzoic acid was isolated as needle shaped pale brown crystals by slow evaporation of solvent in domestic refrigerator at  $\sim 5^{\circ}\text{C}$  that solved and refined in space group  $P2_1/c$  with  $Z' = 1$  (**4**·H<sub>2</sub>O monoclinic). At ambient temperature block crystals of the reported triclinic hydrate form (BIJDON03) were reproduced. Carboxylic acid dimer is formed via O–H···O hydrogen bonds and are connected through water molecules in a helical O–H···O hydrogen bond chain (Figure 17a) along [010] leading to a 3D structure. In comparison the reported triclinic hydrate shows 2D layer structure (Figure 17b). Water hydrogens in the monoclinic hydrate form are disordered over three positions with s.o.f of 0.67 each. Packing fraction and density (triclinic:  $1.541\text{ g cm}^{-3}$ ; 73.6%; monoclinic:  $1.540\text{ g cm}^{-3}$ , 73.1%) did not give a clear indication about stability of these two hydrate forms but the higher melting onset and guest release temperature of the triclinic hydrate in DSC (Figure 18, Table 5) show higher stability over the monoclinic hydrate.

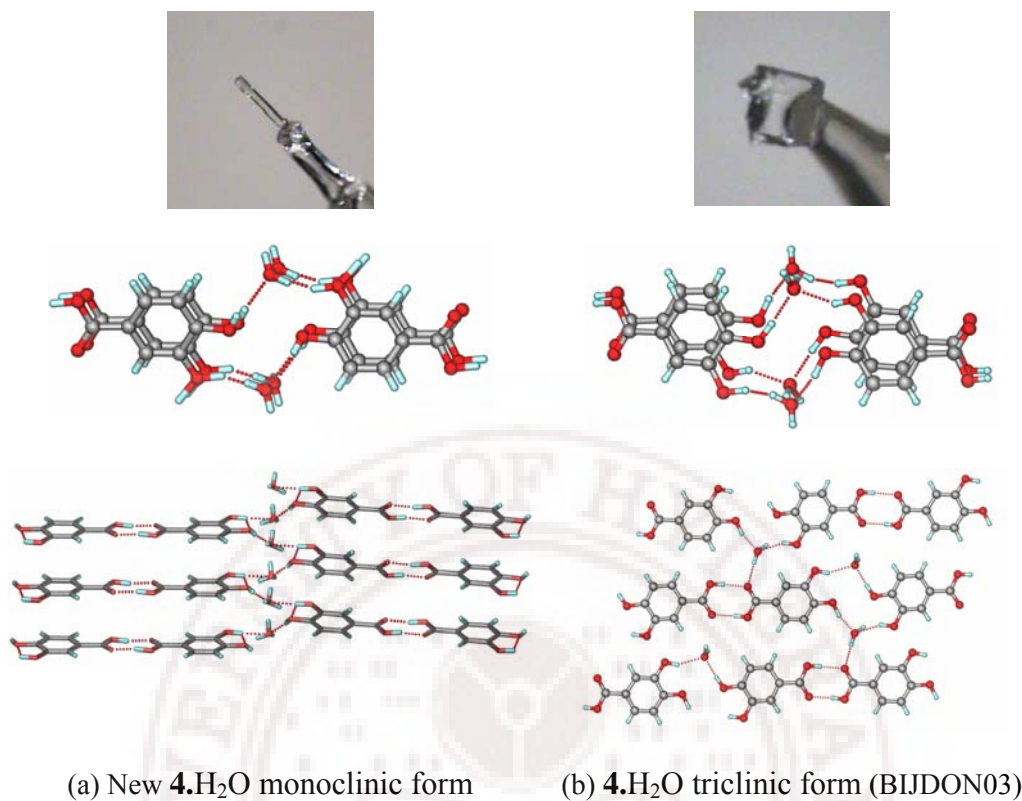


**Figure 17** (a) Thin needle crystals of monoclinic hydrate form show O–H...O hydrogen bonds helically down [010] leading to 3D structure however block crystals of reported triclinic hydrate shows a 2D layer structure.

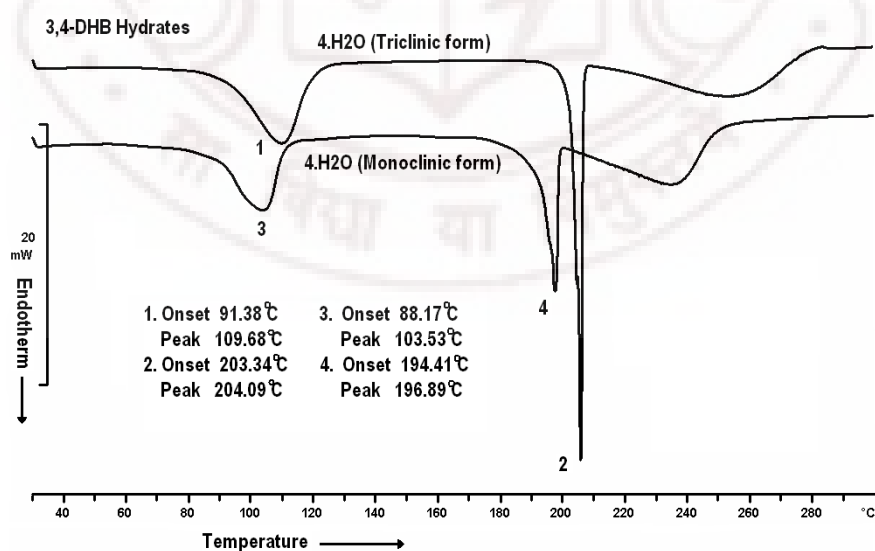


**Figure 18** Higher melting onset and guest release temperature of triclinic hydrate form show higher stability over monoclinic hydrate.



**Table 5** Density, packing fraction and melting point comparison of polymorphic pairs.

|                               | 3      |        |         |         | 4•H <sub>2</sub> O |            |
|-------------------------------|--------|--------|---------|---------|--------------------|------------|
|                               | 2s     | 2m     | Form I* | Form II | Triclinic*         | Monoclinic |
| Density (g cm <sup>-3</sup> ) | 1.536  | 1.541  | 1.546   | 1.595   | 1.541              | 1.540      |
| Packing Fraction (%)          | 71.0   | 71.6   | 71.8    | 74.6    | 73.6               | 73.1       |
| Melting onset/peak (°C)       | 238.2  | 232.9  | 206.4   | 207.6   | 203.34             | 194.41     |
|                               | /238.5 | /236.7 | /208.1  | /208.5  | /204.09            | /196.89    |

\* Reported structure

## 2.10 Cambridge Structural Database

A study has been carried out for polymorphs of organic crystals with the All Text phrase ‘polymorph’, ‘phase’ or ‘form’ having COOH group. The CSD version 5.30, ConQuest 1.11, November 2008 release with May 2009 update was used. The search limits were ‘only organics’ with ‘3D coordinates available’, ‘*R* factor < 0.10’, ‘no disordered’, ‘no error’ and ‘no polymeric’. The lower *R*-factor structure was retained for duplicate refcodes. The results are summarized below,

|   |                          |
|---|--------------------------|
| Number of carboxylic acid polymorphic systems   | 292 hits (135 molecules) |
| Polymorphic systems containing only COOH but no OH  | 114 hits                 |
| Number of polymorphic systems containing both COOH and OH   | 21 hits                  |
| Total systems having different <i>Z'</i> in their polymorphs  | 61 hits                  |
| Number of systems having different <i>Z'</i> in their polymorphs containing only COOH group                       | 53 hits                  |
| Number of systems having different <i>Z'</i> in their polymorphs containing both COOH and OH group                | 8 hits                   |
| Total number of systems containing one polymorph having dimer and the second polymorph having catemer or no dimer | 17 hits                  |
| Number of systems having both COOH and OH groups where one polymorph contains dimer and other one does not.       | 4 hits                   |



This study shows carboxylic acid homo dimer [graph set  $R_2^2(8)$ ] is common in all polymorphic structures generated by solvent less methods except **2m**. Only 17 pairs of carboxylic acid polymorphic systems having 3D coordinate are reported where one polymorph contains acid dimer and absent in the other forms. Oxalic acid (OXALAC04, OXALAC06)<sup>42b</sup> and tetrolic acid (TETROL, TETROL01)<sup>42c</sup> are the only two examples having catemer and dimer motifs of carboxylic acid functionality in their polymorphs. 21 pairs of organic polymorphic systems having both COOH and OH are found (Table 6) in CSD and only 7 pairs show  $Z'$  difference in their structures. Molecule **2**, **3** show different  $Z'$  polymorphs, that is frequent in solvent less methods discussed in Chapter 3, also covers the occurrence of high  $Z'$  structures in isomeric dihydroxybenzoic acids and molecule **1** generated by melt and sublimation. A separate study was done for polymorphs generated by sublimation concomitantly keeping the limits as no error; no polymeric, only organic with 3D coordinate available and all text phrase “sublimation” and refcodes are listed in Table 4.

**Table 6** List of the CSD refcodes of organic polymorphic systems having both COOH and OH groups (21 pairs).

|                               |                       |                       |                       |
|-------------------------------|-----------------------|-----------------------|-----------------------|
| BIDLOP,<br>BIDLOP01           | BESKAL,<br>BESKAL01   | DLMAND02,<br>DLMAND03 | DLMALC,<br>DLMALC11   |
| DEWVOQ,<br>DEWVOQ01           | EWACAG,<br>EWACAG01   | HAKVAR,<br>HAKVAR01   | GORXEQ,<br>GORXEQ01   |
| GORXAM,<br>GORXAM01           | KONTIQ,<br>KONTIQ01   | LEZJAB,<br>LEZJAB01   | PEMZAI01,<br>PEMZAI02 |
| PHOGLY,<br>PHOGLY04           | PIWKOV01,<br>PIWKOV02 | QIJZOY,<br>QIJZOY01   | TARTMM,<br>TARTMM01   |
| TOZKOI,<br>TOZKOI01           | YOYFIB,<br>YOYFIB02   | ZZZSSY01,<br>ZZZSSY02 | ZAJGUM,<br>ZAJGUM01   |
| FAFWIS, FAFWIS01,<br>FAFWIS02 |                       |                       |                       |

## 2.11 Summary and Conclusions

Structural and thermal characterization of polymorphic phases, notably those with multiple  $Z'$  is highly topical because it offers a better understanding of crystal nucleation and a window into the evolution of kinetic and thermodynamic forms. This study show two polymorphs of a popular host compound, 1,1-bis(4-hydroxyphenyl)

cyclohexane (**1**), whose numerous guest inclusion structures were published by Toda and Nassimbeni research groups during the last decade and a half. Yet, the pure host structure(s) are not reported until our study. The guest-free form of popular host **1** and could isolated two polymorphs by using solvent-free methods, melt crystallization and sublimation. They are conformational polymorphs after solving the crystal structures. These solvent less techniques are further employed to generate new polymorphs of isomeric dihydroxybenzoic acids (molecule **2**, **3**, **4**, **5**, **6**, and **7**). These compounds are prone to give solvate/hydrate forms upon crystallization. Two polymorphs of 3,5-dihydroxybenzoic acid (**2s** and **2m**), a new polymorph of 2,3-dihydroxybenzoic acid (**3**.Form II, monoclinic) and guest-free form of 3,4-dihydroxybenzoic acid (**4**.pure) were crystallized by melting and sublimation. Polymorphs of isomeric dihydroxybenzoic acid differ in nature of hydrogen bond synthons i.e. synthon polymorphs in their crystal structures. It was showed that the advantage of melt and sublimation crystallization to get (1) guest-free forms of a host molecule through a green methodology, and (2) high  $Z'$  crystal structures in good probability. Thermal analysis, X-ray crystallography and computation indicate that the kinetic polymorph (**1m**,  $Z' = 2$ ) transforms to the thermodynamic phase (**1s**,  $Z' = 1$ ) at 180-200 °C. Polymorph **1s** with one strong and one weak hydrogen bond is more stable than **1m** with 1.5 O–H $\cdots$ O and 0.5 O–H $\cdots\pi$  hydrogen bonds (per molecule) because the latter structure has less efficient close packing. Microporous cavities in the metastable polymorph have potential application in H<sub>2</sub> storage technology. The difference in conformation of OH groups and overall packing of **2s** and **2m** and the method of preparation are summarized in Figure 19.

A new hydrate polymorph of 3,4-dihydroxybenzoic acid (monoclinic hydrate form) was also isolated along with tetrahydrofuran, acetylacetone and dioxane solvates of 3,5-dihydroxybenzoic acid (**2**•THF, **2**•Acac and **2**•Diox) to confirm that they are prone to form solvates upon solution crystallization. Use of solvent less method in **5**, **6** and **7** gave either decomposed polyphenols or reported structures. In summary, two solvent free methods were investigated to get guest-free forms of molecules that are prone to give solvent/water included structures on crystallization and successfully isolated pure host structures in multiple cases. These methods show potential to generate new polymorphic modifications and high  $Z'$  structures. Phase transition from metastable

to stable polymorph was explained in detail by differential scanning calorimetry, hot stage microscopy and hydrogen bonding changes for molecule **1**.

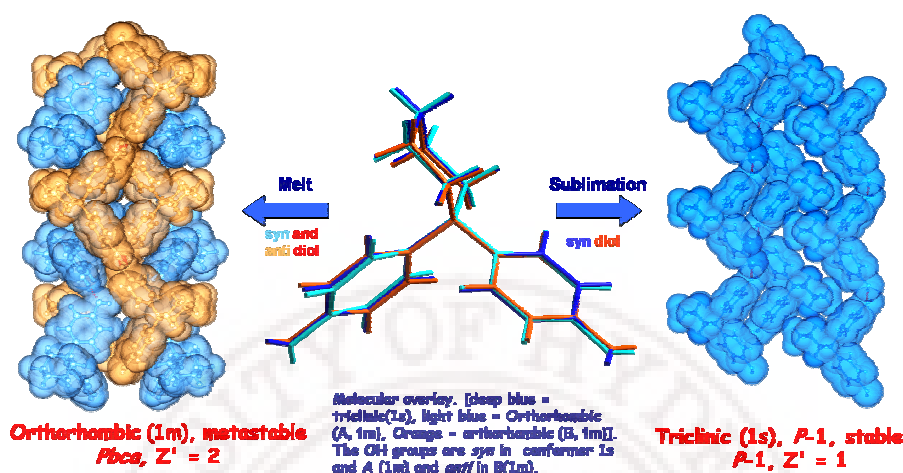


**Figure 19** High temperature crystallization methods: melting and sublimation afforded guest-free structures of host 1,1-bis-(4-hydroxyphenyl)cyclohexane (**1**) and they are conformational polymorphs depending on the phenolic OH orientations with a high probability of  $Z' > 1$  structures. Molecular packing of both polymorphs in the crystalline lattice is shown.

## 2.12 Synthesis of 1,1-Bis(4-hydroxyphenyl)cyclohexane (**1**)

A mixture of cyclohexanone (0.490 g, 5 mmol), phenol (0.940 g, 10 mmol) in dioxane (10 ml) and water (10 ml) at 0 °C was treated dropwise with conc.  $\text{H}_2\text{SO}_4$  (6 ml). The reaction mixture was stirred for 1 hr at 0 °C then at room temperature for 5 hrs. Neutralized the reaction mixture with  $\text{NaHCO}_3$  solution and extracted the product with diethylether. Purification carried out using column chromatography taking 8 % ethyl acetate/hexane solvent mixture as eluent.

Yield = 1.11g (83%), Melting point = 183–186 °C.

$^1\text{H-NMR}$  ( $\text{CDCl}_3$ ):  $\delta$  7.10 (d,  $J = 8\text{Hz}$ , 4H), 6.72 (d,  $J = 8\text{Hz}$ , 4H), 4.78 (s, 2H), 1.53 (s, 10H); IR (KBr,  $\text{cm}^{-1}$ ): 3493, 3375, 2935, 2858, 1610, 1595, 1510, 1452, 1361, 1238.

## 2.13 References

1. S. R. Byrn, R. R. Pfeiffer, J. G. Stowell, *Solid-State Chemistry of Drugs*; SSCI: West Lafayette, IN, 1999.
2. J. Bernstein, *Polymorphism in Molecular Crystals*; IUCR Monographs on

- Crystallography 14; Oxford Science Publications: OUP, Oxford, U.K. 2002.
3. GRAS chemicals list is available at <http://www.cfsan.fda.gov/~dms/eafus.html>.
  4. (a) R. Hilfiker, *Polymorphism in the Pharmaceutical Industry*, Wiley-VCH, Weinheim, Weinheim, 2006; (b) H. G. Brittan, *Polymorphism in Pharmaceutical Solids*, Marcel Dekker, New York, 1999; (c) T. L. Threlfall, *Analyst* **1995**, *120*, 2435; (d) B. R. -Spong, C. P. Price, A. Jayashankar, A. J. Matzger, N. Rodriguez-Hornedo, *Adv. Drug. Del. Rev.* **2004**, *56*, 241; (e) J. Bernstein, R. J. Davey, J. -O. Henck, *Angew. Chem. Int. Ed.* **1999**, *38*, 3440; (f) I. S. Lee, A. Y. Lee, A. S. Myerson, *Pharma. Res.* **2008**, *25*, 4.
  5. (a) G. Fillipini, A. Gavezotti, *J. Am. Chem. Soc.* **1995**, *117*, 12299; (b) T. Beyer, G. M. Day, S. L. Price, *J. Am. Chem. Soc.* **2001**, *123*, 5086.
  6. (a) J. Bernstein, R. J. Davey, J. -O. Henck, *Angew. Chem. Int. Ed.* **1999**, *38*, 3440; (b) A. Nangia, *Acc. Chem. Res.* **2008**, *41*, 595; (c) B. Sarma, S. Roy, A. Nangia, *Chem. Commun.* **2006**, 4918.
  7. (a) D. S. Hughes, M. B. Hursthouse, T. Threlfall, S. Tavener, *Acta. Crystallogr.* **1999**, *C55*, 1831; (b) T. Gelbrich, D. S. Hughes, M. B. Hursthouse, T. L. Threlfall, *CrystEngComm* **2008**, *10*, 1328.
  8. J. Bauer, S. Spanton, R. Henry, J. Quick, W. Dziki, W. Porter, J. Morris, *Pharm. Res.* **2001**, *18*, 859.
  9. (a) W. Beckmann, *J. Cryst. Growth* **1999**, 198/199, 1307; (b) J. Toth, A. K. -Fodor, S. H. -Peterfi, *Chem. Eng. Process.* **2004**, *44*, 193; (c) C. P. M. Roelands, S. Jiang, M. Kitamura, J. H. Horst, H. J. M. Kramer, P. J. Jansens, *Cryst. Growth Des.* **2006**, *6*, 955.
  10. (a) M. Rafilovich, J. Bernstein, *J. Am. Chem. Soc.* **2006**, *128*, 12185; (b) X. Mei, C. Wolf, *Cryst. Growth Des.* **2004**, *4*, 1099; (c) M. T. Kirchner, D. Bläser, R. Boese, G. R. Desiraju, *CrystEngComm* **2009**, *11*, 229; (d) N. J. Babu, A. Nangia, *Cryst. Growth Des.* **2006**, *6*, 1995.
  11. (a) J. Tao, K. J. Jones, L. Yu, *Cryst. Growth Des.* **2007**, *7*, 2410; (b) L. Yu, *J. Am. Chem. Soc.* **2003**, *125*, 6380; (c) S. Chen, H. Xi, L. Yu, *J. Am. Chem. Soc.* **2005**, *127*, 17439; (d) C. Stoica, P. Tinnemans, H. Meekes, E. Vlieg, P. J. C. M. van Hoof, F. M. Kaspersen, *Cryst. Growth Des.* **2005**, *5*, 975; (e) J. Tao, L. Yu, *J. Phys. Chem. B* **2006**, *110*, 7097.

12. H. Miura, T. Ushio, K. Nagai, D. Fujimoto, Z. Lepp, H. Takahashi, R. Tamura, *Cryst. Growth Des.* **2003**, 3, 959.
13. L. Kofler, E. Lindpaintner, *Mikrochemie* **1938**, 24, 52.
14. I. S. Lee, K. T. Kim, A. Y. Lee, A. S. Myerson, *Cryst. Growth Des.* **2008**, 8, 108.
15. (a) D. E. Braun, T. Gelbrich, R. K. R. Jetti, V. Kahlenberg, S. L. Price, U. J. Griesser, *Cryst. Growth Des.* **2008**, 8, 1977; (b) R. J. Davey, N. Blagden, S. Righini, H. Alison, E. S. Ferrari, *J. Phys. Chem. B* **2002**, 106, 1954; (c) C. Cashell, D. Corcoran, B. K. Hodnett, *Chem. Commun.* **2003**, 374, 375; (d) E. S. Ferrari, R. J. Davey, *Cryst. Growth Des.* **2004**, 4, 1061.
16. Z. Xie, H. Wang, F. Li, W. Xie, L. Liu, B. Yang, L. Ye, Y. Ma, *Cryst. Growth Des.* **2007**, 7, 2512.
17. (a) S. J. Bonafede, M. D. Ward, *J. Am. Chem. Soc.* **1995**, 117, 7853; (b) C. A. Mitchell, L. Yu, M. D. Ward, *J. Am. Chem. Soc.* **2001**, 123, 10830.
18. J. Zaccaro, J. Matic, A. S. Myerson, B. A. Garetz, *Cryst. Growth Des.* **2001**, 1, 5.
19. (a) L. J. Chyall, J. M. Tower, D. A. Coates, T. L. Houston, S. L. Childs, *Cryst. Growth Des.* **2002**, 2, 505; (b) J. L. Hilden, C. E. Reyes, M. J. Kelm, J. S. Tan, J. G. Stowell, K. R. Morris, *Cryst. Growth Des.* **2003**, 3, 921.
20. J. M. Ha, J. H. Wolf, M. A. Hillmyer, M. D. Ward, *J. Am. Chem. Soc.* **2004**, 126, 3382.
21. M. L. Peterson, S. L. Morissette, C. McNulty, A. Goldsweig, P. Shaw, M. LeQuene, J. Monagle, N. Encina, J. Marchionna, A. Johnson, J. Gonzalez-Zugasti, A. V. Lemmo, S. J. Ellis, M. J. Cima, O. Almarsson, *J. Am. Chem. Soc.* **2002**, 124, 10958.
22. J. W. Mullin, *Crystallization*, 4th Ed. Oxford, England, 2001.
23. C. P. Price, A. L. Grzesiak, A. J. Matzger, *J. Am. Chem. Soc.* **2005**, 127, 5512.
24. (a) E. B. Brouwer, K. A. Udachin, G. D. Enright, J. A. Ripmeester, K. J. Ooms, P. A. Halchuk, *Chem. Commun.* **2001**, 565; (b) P. O. Brown, G. D. Enright, J. A. Ripmeester, *CrystEngComm* **2006**, 8, 381; (c) B. K. Saha, A. Nangia, *Chem. Commun.* **2006**, 1825.
25. (a) J. L. Atwood, J. E. D. Davies, D. D. MacNicol, (Eds.), *Inclusion Compounds*, Academic Press, London, 1984, vol. 1–3; (b) J. L. Atwood, J. E. D. Davies, D.

- D. MacNicol, (Eds.), *Inclusion Compounds*, Oxford University Press, Oxford, 1991, vol. 4–5.
26. (a) P. S. Sidhu, G. D. Enright, K. A. Udachin, J. A. Ripmeester, *Chem. Commun.* **2005**, 2092; (b) R. Bishop, A. N. M. M. Rahman, J. Ashmore, D. C. Craig, M. L. Scudder, *CrystEngComm* **2002**, 4, 605.
  27. (a) E. B. Brouwer, G. D. Enright, K. A. Udachin, S. Lang, K. J. Ooms, P. A. Halchuk, J. A. Ripmeester, *Chem. Commun.* **2003**, 1416; (b) J. L. Atwood, L. J. Barbour, G. O. Lloyd, P. K. Thallapally, *Chem. Commun.* **2004**, 922; (c) G. D. Enright, K. A. Udachin, I. L. Moudrakovski, J. A. Ripmeester, *J. Am. Chem. Soc.* **2003**, 125, 9896; (d) R. Banerjee, P. M. Bhatt, G. R. Desiraju, *Cryst. Growth Des.* **2006**, 6, 1468.
  28. (a) C. C. Rusa, T. A. Bullions, J. Fox, F. E. Porbeni, X. Wang, A. E. Tonelli, *Langmuir* **2002**, 18, 10016; (b) J. W. Chung, T. J. Kang, S. -Y. Kwak, *Langmuir* **2007**, 23, 12366; (c) I. Aranaz, M. C. Gutierrez, L. Yuste, F. Rojo, M. L. Ferrera, F. del Monte, *J. Mater. Chem.* **2009**, 19, 1576.
  29. (a) G. S. McGrady, M. Odlyha, P. D. Prince, J. W. Steed, *CrystEngComm* **2002**, 4, 271; (b) J. L. Atwood, L. J. Barbour, A. Jerga, B. L. Schottel, *Science* **2002**, 298, 1000; (c) B. K. Saha, A. Nangia, *CrystEngComm* **2006**, 8, 440.
  30. J. Ulrich, *Cryst. Growth Des.* **2004**, 4, 879.
  31. (a) F. Toda, K. Tanaka, T. Fujiwara, *Angew. Chem. Int. Ed. Engl.* **1990**, 29, 662; (b) M. R. Caira, A. Horne, L. R. Nassimbeni, F. Toda, *J. Mater. Chem.* **1998**, 8, 1481; (c) Z. U. -Lipkowska, K. Yoshizawa, S. Toyota, F. Toda, *CrystEngComm* **2003**, 5, 114.
  32. S. Aitipamula, A. Nangia, *Chem. Eur. J.* **2005**, 11, 6727.
  33. E. Weber, K. Skobridis, A. Wierig, L. R. Nassimbeni, L. Johnson, *J. Chem. Soc., Perkin Trans. 2*, **1992**, 2123.
  34. (a) M. E. Davis, *Nature* **2002**, 417, 813; (b) R. E. Morris, P. S. Wheatley, *Angew. Chem. Int. Ed.* **2008**, 47, 4966.
  35. (a) Gaussian 03, Version 6.0, (b) Cerius<sup>2</sup> Materials Studio, [www.accelrys.com](http://www.accelrys.com). (c) S. Roy, R. Banerjee, A. Nangia, G. J. Kruger, *Chem. Eur. J.* **2006**, 12, 3777;.
  36. (a) G. R. Desiraju, *Nat. Mater.* **2002**, 1, 77; (b) W. F. Ostwald, *Z. Phys. Chem.* **1897**, 22, 289.



37. (a) J. W. Steed, *CrystEngComm* **2003**, 5, 169; (b) G. R. Desiraju, *CrystEngComm* **2007**, 9, 91; (c) W. Clegg, G. S. Nichol, *Acta Crystallogr.* **2004**, E60, 1433; (d) H. -J. Lehmler, L. W. Robertson, S. Parkin, C. P. Brock, *Acta Crystallogr.* **2002**, B58, 140; (e) C. P. Brock, *Acta Crystallogr.* **2002**, B58, 1025; (f) D. Das, R. Banerjee, R. Mondal, J. A. K. Howard, R. Boese, G. R. Desiraju, *Chem. Commun.* **2006**, 555; (g) R. J. Davey, K. Allen, N. Blagden, W. I. Cross, H. F. Lieberman, M. J. Quayle, S. Righini, L. Seton, G. J. T. Tiddy, *CrystEngComm* **2002**, 4, 257; (h) N. Blagden, R. J. Davey, H. F. Lieberman, L. Williams, R. Payne, R. Roberts, R. Rowe, R. Docherty, *J. Chem. Soc. Faraday Trans.* 1998, 94, 1035; (i) T. Hara, Y. Hayashi, M. Kitamura, *Cryst. Growth Des.* **2007**, 7, 147.
38. M. Kawase, N. Motohashi, T. Kurihara, M. Inagaki, K. Satoh, H. Sakagami, *Anticancer Res.* **1998**, 18, 1069, and references therein
39. (a) H. -J. Lehmler, L. W. Robertson, S. Parkin, C. P. Brock, *Acta Crystallogr.* **2002**, B58, 140; (b) C. P. Brock, *Acta Crystallogr.* **2002**, B58, 1025; (c) G. S. McGrady, M. Odlyha, P. D. Prince, J. W. Steed, *CrystEngComm* **2002**, 4, 271.
40. CSD version 5.30, ConQuest 1.10, November 2008 release, May 2009 update.
41. (a) B. Sarma, A. Nangia, *Acta Crystallogr.* **2008**, A64, C449; (b) B. Sarma, A. Nangia, (manuscript in preparation).
42. (a) M. Takasuka, H. Nakai, M. Shiro, *J. Chem. Soc., Perkin Trans.2* **1982**, 1061; (b) V. R. Thalladi, M. Nüsse, R. Boese, *J. Am. Chem. Soc.* **2000**, 122, 9227; (c) V. Benghiet, L. Leiserowitz, *J. Chem. Soc. Perkin Trans.2* **1972**, 1763.
43. (a) L. R. MacGillivray, M. J. Zaworotko, *J. Chem. Cryst.* **1994**, 24, 703; (b) A. Parkin, M. Adam, R. I. Cooper, D. S. Middlemiss, C. C. Wilson, *Acta Crystallogr.* **2007**, B63, 303; (c) Giacomello, *Nature (London)* **1956**, 177, 944; (d) M. Haisa, S. Kashino, S. -I. Hanada, K. Tanaka, S. Okazaki, M. Shibagaki *Acta Crystallogr.* **1982**, B38, 1480; (e) D. E. Cohen, J. B. Benedict, B. Morlan, D. T. Chiu, B. Kahr, *Cryst. Growth Des.* **2007**, 7, 492; (f) N. Okabe, H. Kyoyama, *Acta Crystallogr.* **2001**, E57, o1224; (g) V. Horneffer, K. Dreisewerd, H. -C. Ludemann, F. Hillenkamp, M. Lage, K. Strupat, *Int. J. Mass Spectrom. Ion. Process.* **1999**, 185, 859.



---

## HIGH $Z'$ STRUCTURES BY SOLVENT LESS METHODS

---

### 3.1 Introduction

The number of symmetry independent or crystallographic unique molecules in a crystal lattice is denoted by parameter  $Z'$  ( $Z$  prime).<sup>1</sup>  $Z'$  may be defined in relation to the number of molecules in the unit cell:  $Z = Z' \times \text{number of lattice points} \times \text{number of symmetry operations}$ .<sup>2</sup> Alternatively the number of formula units in the unit cell divided by the number of independent general positions for that space group is  $Z'$ . Eijck and Kroon<sup>3</sup> introduced the symbol  $Z''$  to denote the number of crystallographically non equivalent molecules for multicomponent systems like cocrystals, salts, hydrates and solvates. Any structure with  $Z' = 1$  means that each molecule is surrounded by like molecules and is therefore self-included. However, any molecular crystal with  $Z' > 1$  is defined as each molecule is surrounded by other molecules that are crystallographically non equivalent, e.g. different conformation or non symmetry-related molecules. Multiple numbers of molecules in the asymmetric unit have attracted attention from the earliest days of crystallography. The occurrence of multiple molecules sometimes makes crystal structure solution and refinement difficult because of pseudosymmetry. Crystallographic difficulties associated with data collection of large unit cells, weak scattering and reflections with very low intensity are other reasons to solve structures. Incorrect assignment of space groups can result in artificially high apparent  $Z'$  values. For example, misassignment of the uncommon  $P1$  instead of much more frequent  $P\bar{1}$  space group immediately results in a doubling of  $Z'$ .<sup>4</sup> The availability of the vast amount of crystallographic data in the easily accessible Cambridge Structural Database (CSD)<sup>5</sup> has given a new impetus to the statistical study of the  $Z'$  frequencies, conformation and packing of the molecules in the crystal structures.

### 3.2 Multiple Molecules in Asymmetric Unit ( $Z' > 1$ )

There is renewed interest on why molecules crystallize with  $Z' > 1$  from a fundamental viewpoint, because the factors leading to its occurrence are still not properly understood.<sup>6</sup> Crystallographer or crystal chemists have been curious over decades for what the reasons to such an occurrence of high  $Z'$ .<sup>2</sup> The formation of crystals under non-equilibrium conditions may be viewed as a fossil relic<sup>2a</sup> of the fastest growing crystal nucleus rather than a thermodynamic minimum structure. A survey on  $Z'$  frequencies by Steed and co-workers<sup>2a,6g</sup> found that 8.8 % crystal structures have  $Z' > 1$ , 66.4 % are  $Z' = 1$  structures however 24.9 % belongs to  $Z' < 1$ . High  $Z'$  structures can be engineered by combining a molecule with one or more resolved chiral centre by a strongly directional supramolecular synthon with a preference for centrosymmetry because, in order to preserve the dimer motif, one or more extra molecules must be introduced into the asymmetric unit. Structures that exhibit  $Z' > 1$  is counter intuitive to the rule of close packing, however it is often observed that molecules crystallizes with  $Z' > 1$  particularly for polymorphic compounds and compounds having awkward shape. A study by Gavezzotti and Filippini showed that polymorphs with one partner having  $Z' = 1$  and at least one partner with  $Z' > 1$  is 28% compare to overall percentage in the Cambridge Structural Database, which is 8.3%.<sup>7</sup>

Several research groups have carried out CSD searches for crystal structures containing more than one molecule in the asymmetric unit ( $Z' > 1$ ) over the last two decades. Padmaja et al. (1990)<sup>8a</sup> reported space group frequencies for the structures in the 1987 version of CSD. The distribution agreed well with that found by Mighell et al.<sup>8b</sup> They observed a significant fraction (8.3%) of high  $Z'$  structures in the database and also analyzed the distribution of organic crystal structures (total 51,611 structures) with more than one formula unit in the asymmetric unit among the 230 space groups by distributing 81% of the total structures in five different space groups as  $P2_1/c$  (27.8%),  $P\bar{1}$  (23.5%),  $P2_1$  (13.8%),  $P1$  (8.5%) and  $P2_12_12_1$  (7.8%). Further reports on  $Z'$  frequency in crystal structures usually appeared in connection with the compilations of space group frequencies. Sona and Gautam (1992)<sup>8c</sup> found about half of the structures belonging to  $P1$  space group have more than one molecule in the asymmetric unit, this proportion drops to around one twentieth for  $P2_12_12_1$  space group. In succession, Wilson

(1993),<sup>8d</sup> Brock and Dunitz (1994),<sup>8e</sup> Zorky (1995)<sup>8f</sup> surveyed  $Z'$  frequencies in crystal structures that were compiled with space group frequencies. Steiner (2000)<sup>8g</sup> analyzed exclusively the frequency of  $Z'$  values in organic and organometallic crystal structures, and more recently Kubicki (2005)<sup>8h</sup> and Steed (2006).<sup>6h,8i</sup> Wilson 1993 paper<sup>8d</sup> discusses the role of variable  $Z'$  in detail. The importance of the variable  $Z'$  was also recognized by Scaringe<sup>8j</sup> and by Chernikova et. al.<sup>8k</sup> Brock and Dunitz showed<sup>8e</sup> that the chiral molecules with no inversion center, mirror and glide planes have sufficiently high  $Z' > 1$  structures than the corresponding centrosymmetric structures. In 2000, Steiner analyzed<sup>8g</sup> the frequency of  $Z'$  values for reported organic and organometallic compounds and found that values of  $Z' = 0.5$ , 1, and 2 were 96.6% and 94.3% of their crystal structures, respectively, and generally structures with internal molecular symmetry have  $Z' < 1$ .  $\text{CBr}_4$  ( $Z' = 4$ ) and Selenourea ( $Z' = 9$ ) are few exceptions of high  $Z'$  structures even though they have internal molecular symmetry. Gavezzotti (2008)<sup>8m</sup> recently compared 5547 organic structures with two molecules in the asymmetric unit ( $Z' = 2$ ) with 45182 crystal structures having one molecule in the asymmetric unit ( $Z' = 1$ ) and concluded as there are no obvious differences between the  $Z' = 1$  and  $Z' = 2$  sets in chemical composition, except for a slightly smaller average size of  $Z' = 2$  molecules and for a slight increase in the frequency of  $Z' = 2$  for alcohols. The frequency of space groups  $P1$ ,  $P2_1$  and  $P\bar{1}$  increase in  $Z' = 2$  crystals, while the frequency of space groups  $P2_1/c$  and  $P2_12_12_1$  decreases. 83% of  $Z' = 2$  structures show the presence of some form of pseudosymmetry. In general organic compounds with  $Z' > 1$  show a frequency of 8.8% on average, but this percentage is raised to 18.8% and 20.8% for steroids, nucleosides & nucleotides.<sup>8g</sup> Similar anomalies have been highlighted in the survey of monoalcohols, phenols, and primary amines.<sup>7b,8e</sup> This indicates a general packing problem of these awkwardly shaped molecules which often cannot crystallize out in simple packing modes with single molecule in the asymmetric unit. The analysis on the proportion of  $Z' > 1$  structures reveals the consistency over the decades (8.3 % in 1990<sup>9a</sup> and 8.8% in 2007<sup>9b</sup> and 8.6% in 2009 CSD May update) even though there is a huge deposition of structures into the CSD during this period. In 1990 the number was 1,03,000 structures which rose to 4,83,000 crystal structures in May 2009 update.

### 3.3 Pseudosymmetry

Pseudosymmetry can be described as a spatial arrangement that pretends a symmetry without fulfilling it.<sup>10</sup> Displacement of pseudosymmetry  $< 0.1 \text{ \AA}$  may represent cases of incorrect space group assignment.<sup>10d</sup> In general structures with  $Z' > 1$  there is some pseudosymmetry. Davies and Wilier showed about 27% of structures with  $Z' > 1$  show approximate symmetry elements. Also it was observed that the incidence of pseudosymmetry is more likely responsible for higher occurrence of  $Z'$  values of 4, 6 and 8 compared to the odd 5, 7 and 9 since the odd numbered arrangements do not even approximate to crystallographic symmetry operations. The frequency of occurrence of structures with  $3 \leq Z' \leq 10$  were extracted from the CSD and shown in Figure 1 as a column chart. Structures with  $Z' > 4$  are extremely rare.

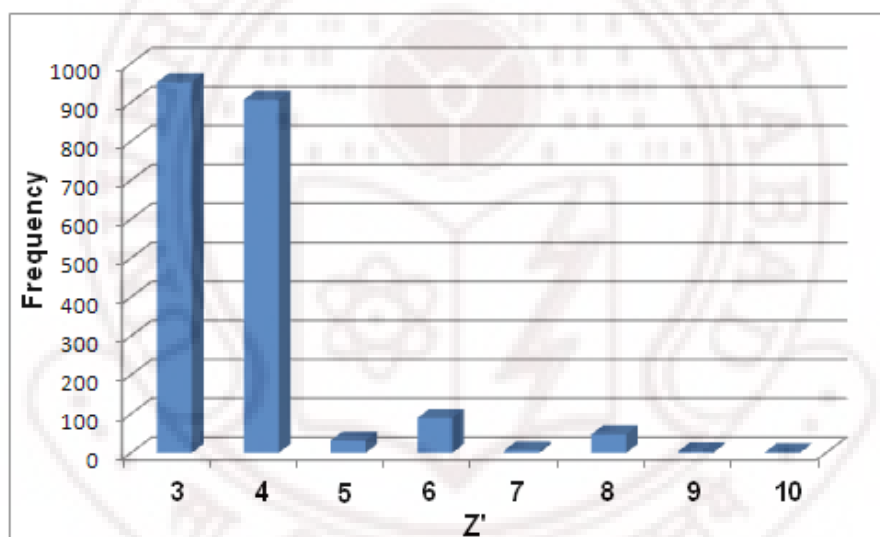


**Figure 1** The columns showing the frequency of occurrence of structures with  $3 \leq Z' \leq 10$  extracted for the organic molecules from CSD version 5.30, ConQuest 1.11, May 2009 update. Structures with  $Z' > 4$  are very small in number.  $Z' = 6, 8$  show slight rise in the column height correspond to the existence of pseudosymmetry however odd  $Z'$  (5, 7, 9) structures are very rare in the database. (This bar chart is culled from the study on  $Z'$  frequencies by Steed<sup>2a</sup> in 2001 and updated with CSD 2009, May update).

Cholesterol and its monohydrate (with  $Z' = 8$  in space group  $P1$ ) are interesting examples.<sup>10b</sup> The high temperature phase of cholesterol with  $Z' = 16$ ,<sup>10e</sup> and hydrated benzene-1,3,5-tricarboxylic acid with  $Z' = 12$  have been determined with great care and pseudosymmetry have been thoroughly analyzed. Chiral elements can be resolved with a

strongly directional supramolecular synthon giving a preference for centrosymmetry such as carboxylic acid dimer in a simple way with  $Z' > 1$ , indeed does exhibit  $Z' = 2$ . Dunitz studied chiral (5S,6S)-5,6-dihydro-5,6-dimethyl-1,3-dithiolo[4,5-b][1,4]dithiin-2-thione which exhibits significant pseudosymmetry.<sup>10f</sup> Ruck,<sup>10a</sup> Desiraju,<sup>10g</sup> Zorky,<sup>10c</sup> Kuleshova,<sup>10d</sup> Dunitz<sup>10f</sup> have commented on the presence of pseudosymmetry in  $Z' > 1$  structures.

### 3.4 Awkward Shapes, Molecular Helices and Kinetic Effect

Formation of molecular helices<sup>11a,b</sup> through hydrogen bond or other dominating interactions leads to the presence of pseudosymmetry result in high  $Z'$  structures. For example 3,5-dimethyl-1,2-tellurazole crystallized in a helical arrangement with  $Z' = 6$  comprising two independent *pseudo*-3<sub>1</sub> helices linked by Te...N interaction (Figure 2a). Awkward molecular shapes that result in the formation of lattice voids and hence host-guest formation leading to the adoption of lower symmetry structures of the enclathrated system. Awkward molecular shapes of biphenyls are the most studied systems by Brock.<sup>11c,d</sup> The non-ortho substituted biphenyl derivatives adopt energetically unfavourable planar conformations because it can adopt more efficient packing modes by stacking. Those where aryl rings are not co-planar frequently exhibit structures with  $Z' > 1$ , e.g. 4-cyano-4'-ethynylbiphenyl ( $Z' = 4$ ),<sup>11e</sup> 4-(dimethylamino)-3-cyanobiphenyl ( $Z' = 8$ ).<sup>11f</sup> The compound 4-chlorobiphen-2'-ol<sup>11g</sup> crystallizes with  $Z' = 4$  at both 293K and 142K and comprises a four-membered hydrogen bonded ring (OH tetramer) that shows the absence of any kind of pseudosymmetry.

The change in temperature can increase or decrease  $Z'$  in the crystal structures. Due to thermal motion of atoms as well as the molecule, the X-ray diffraction measures the average positions and thus it raises the time-averaged crystal symmetry. So the study on high  $Z'$  structures is incomplete without a survey over a range of temperatures. Lowering temperature has a substantial contribution to raising  $Z'$  or vice versa. Phase transition from lower density, high symmetry phase to a higher density phase can also lead to higher  $Z'$ . The reverse examples are also found.<sup>12</sup>

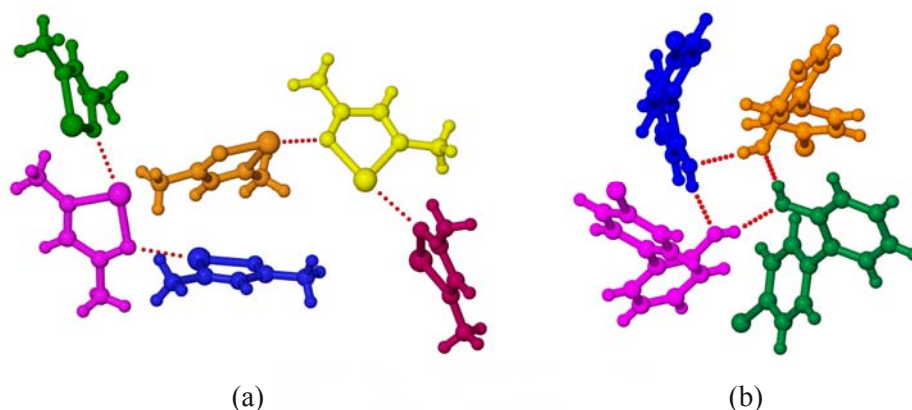


**Figure 2** (a) 3,5-Dimethyl-1,2-tellurazole crystallized in a helical arrangement with  $Z' = 6$  (JOSVAO, symmetry independent molecules are shown in different color code). (b) Four-membered hydrogen bonded ring (OH tetramer via O–H...O hydrogen bonds) in 4-chloro-2-hydroxybiphenyl between four symmetry independent molecules ( $Z' = 4$ , MEZNIO) in the monoclinic space group  $P2_1/c$ .

### 3.5 Chirality and Strong Hydrogen Bond

In a piece of fascinating work in crystal engineering, Steed and Gibson<sup>13</sup> showed how highly stereoselective molecular and crystal synthesis allows the preparation and control of a range of resolved, chiral solid-state compounds with  $Z' > 1$ . This approach makes concrete predictions about the crystal packing mode of all resolved compounds for which the racemate crystallizes in such a way as to demonstrate the nature of homochiral interactions, assuming those interactions to be isolated and dominant and also use chirality to predict and engineer the incidence of structures with  $Z' > 1$ . Thus, a racemate displaying a centrosymmetric intermolecular interaction (e.g., carboxylic acid dimer) must double  $Z'$  upon resolution; that is, a resolved chiral mono carboxylic acid dimer must exhibit  $Z' = 2$  if the racemate exhibits  $Z' = 1$  with the two enantiomers related by inversion symmetry. Many research groups have tried to correlate the occurrence of  $Z' > 1$  with close packing frustration and optimization of intermolecular interactions.<sup>7b</sup> Presence of irregular molecular shape and strong hydrogen bonds associate in nucleosides and nucleotides, steroids, and alcohols is one of the reason of higher  $Z'$ .<sup>7,8g</sup> Brock has noted that around 40% of monoalcohols<sup>8e,10</sup> have  $Z' > 1$ , as compared with 8.3% of the CSD. An elegant explanation as to why these compounds have a higher proportion of  $Z' > 1$  crystal structures when compared with the full database of organic molecular crystals exemplify the tendency of these hydroxy compounds (ROH) to form



cooperative hydrogen bonded chains (O–H $\cdots$ O–H type) is anticipated by the steric demands of the R-groups and the other reason is the crystallization in a higher symmetry system.

It is likely that this behavior is a result of the fact that the hydrogen bonding requirements of the OH group dominate the crystal packing, often resulting in frustration between the conflicting needs to achieve close packing and maximize hydrogen bonding to the lone OH group. Even in the absence of the OH group compounds of type YXPh<sub>3</sub> (Y = halogen, X = group 14 element) exhibit an extremely high incidence of  $Z' > 1$  (42%) as a consequence of weak aryl C–H $\cdots$ Y interactions.<sup>10b</sup> Approximately 50% of cholesterol,<sup>10b,c</sup> 33% of *vic*-diols<sup>10d</sup> have  $Z' > 1$ . Clegg and co-workers<sup>14</sup> recently studied salt of 1,8-bis(dimethylamino)naphthalene systems and reported the importance of weak interaction like C–H $\cdots$ O and  $\pi$ – $\pi$  stacking in crystal packing which result structures of  $Z' > 1$ . Steed *et al* showed that weak interaction C–H $\cdots$ X or C–H $\cdots\pi$  (where X=halogen) and  $\pi$ – $\pi$  stacking can influence molecule in crystallization with more than one molecule in asymmetric unit for the triaryl derivative of group 14 elements and oxo-anion structures.<sup>8i</sup> The weak C–H $\cdots$ O hydrogen bonds follow similar trend like O–H $\cdots$ O hydrogen bonds have been ascribed to multiple  $Z'$  in monoalcohols, phenols and cholesterol. Furthermore, the sterically demanding nature of the system limits the number of possible intermolecular interactions, resulting in a high degree of reproducibility across many structures. The compounds with terminal alkynyl (–C $\equiv$ CH) group show occurrence of high  $Z'$ <sup>15a</sup> structures however 1,2-disubstituted alkynes are below average. Strong hydrogen bonds can facilitate high  $Z'$  through a conflict between their highly directional character and the requirements of close packing. Recently the requirement of  $Z' \geq 2$  for assembling an acid-pyridine trimer synthon in small and nonsymmetric molecules like 5-methylpyrazine-2,3-dicarboxylic acid via O–H $\cdots$ N hydrogen bonds stabilized by C–H $\cdots$ O interactions was reported.<sup>15b</sup>

### 3.6 Polymorphs and Modulated Structures

A recent study by Dunitz, Gavezzotti and Bernstein on polymorphic crystalline systems of organic compounds in which at least one member has  $Z' > 2$  provides improved crystal structure recognition methods and clarifies details of the molecular



organization in crystal structures with high  $Z'$ .<sup>16a</sup> They executed a CSD search on  $Z' > 2$  polymorphs having 3D coordinates and extracted a data set of 138 crystal structures that contain: 38 dimorphic systems, 8 trimorphic systems and 4 tetramorphic systems. The  $\Delta Z'/\Delta V$  plot [where  $\Delta Z'$  is the difference in  $Z'$  between polymorphs and the difference in cell volume per molecule is  $\Delta V$ ] of these polymorphic systems shows a slight apparent tendency for larger volume, lower density with increasing  $Z'$ . The  $\Delta Z'/\Delta E$  plots ( $\Delta E$  is the difference in lattice energy) show no systematic trend in lattice energy as a function of  $Z'$ . In parallel  $\Delta Z'/\Delta R_f$  [ $\Delta R_f$  is the difference in R factor] plot shows no systematic trend in R-factor as a function of  $Z'$ . This imply that the structures with high  $Z'$  does not represent refinement problems which are arising from an unfavorable ratio between number of measured reflections and number of parameters. There could be a tendency for high  $Z'$  crystals to be of poorer quality than their low  $Z'$  polymorphs.<sup>16f</sup> On the other hand, the lower  $Z'$  structures may sometimes be disordered. Occurrence of high  $Z'$  in polymorphic and modulated phases have drawn interest of chemists over the last few years. Nangia and co-workers reported crystal structures with high  $Z'$  values, where all or some of the symmetry independent molecules have significantly different conformations (Figure 3).<sup>16,17</sup> When crystals are cooled below room temperature, additional weak interactions appear in the X-ray diffraction pattern and disappear again on warming. One has to be careful when two structures are very similar and called as polymorphs or merely as modulated and demodulated version of the same basic molecular arrangement. The 1:2 complex of  $\alpha$ -D-glucose and *p*-tolylboronic acid crystallized<sup>16b</sup> in glucofuranose form (Figure 3c) at room temperature in  $P2_12_12_1$  space group with one molecule in the asymmetric unit ( $Z' = 1$ ), however a modulated structure in  $P2_1$  space group was crystallized with  $Z' = 2$  at 100 K. Multiple molecules in asymmetric unit were correlated with C–H $\cdots$ O interactions between symmetry-independent molecules. A series of structurally related compounds  $[M(H_2O)_2(15\text{-Crown-5})](NO_3)_2$ , where M = Cu, Mg, Zn and Co are the remarkable examples<sup>16c</sup> of modulated structures having  $Z' > 1$ . Dichlorofuchsone crystallized in two polymorphic phases.<sup>17a</sup> Solution crystallization afforded form I (in  $C2/c$  space group) with  $Z' = 4$ , however the second form with  $Z' = 1$  in  $P2_1/c$  space group was obtained by sublimation. C–H $\cdots$ O hydrogen bonds and type-1 Cl $\cdots$ Cl interaction are the main interactions in these structures. 4,4-Diphenyl-2,5-cyclohexadienone (Figure 3b) crystallized as four conformational polymorphs<sup>17b,c,d</sup> with

a record number of 19 crystallographically independent molecules [form A ( $P2_1$ ,  $Z' = 1$ ), form B ( $P\bar{1}$ ,  $Z' = 4$ ), form C ( $P\bar{1}$ ,  $Z' = 12$ ), and form D ( $Pbca$ ,  $Z' = 2$ )]. The strength of the C–H $\cdots$ O interaction correlates with the number of symmetry independent conformations ( $Z'$ ) in polymorphs, i.e. a short C–H $\cdots$ O interaction leads to a high  $Z'$  value. The 1,1-bis-(4-hydroxyphenyl) cyclohexane show two polymorphic modifications by solvent less crystallization discussed in Chapter 2 in detail. Sublimation afforded structure with  $Z' = 1$  however  $Z' = 2$  in melt crystals. The phenolic OH group takes different orientation in one of the conformer in melt crystals that result in difference in packing (Figure 3a). Careful observation of the small differences in habit/color for the possibility of different/new crystal forms, benzidine was found to be tetramorphic system.<sup>18</sup> All polymorphs were characterized by a rather unusual number of molecules in the asymmetric unit ( $Z' = 1.5$ , 3, and two forms with 4.5), which are found in only 0.25%, 0.4%, and 0.002% of structures in the CSD (in the November 2005 version). In all forms except Form II ( $Z' = 3$ ), one of the molecules lies on a crystallographic inversion center, requiring the molecule to be planar; other molecules are nonplanar. Recently Bishop has studied<sup>19</sup> false conglomerate materials that have multiple molecules in their asymmetric unit ( $Z' > 1$ ).

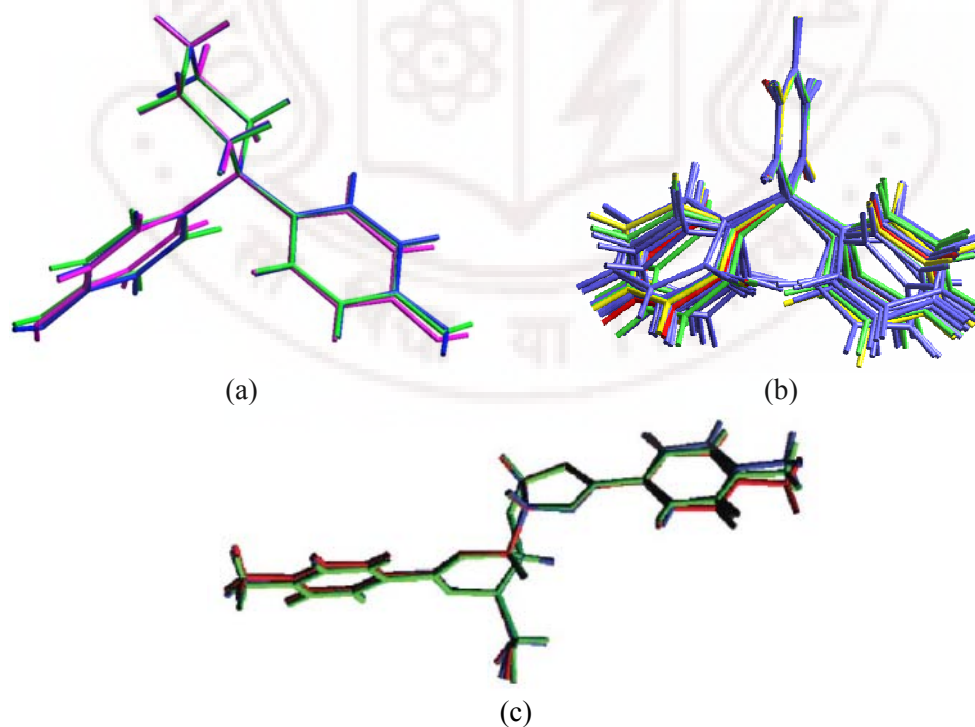


**Figure 3** (a) Molecular overlay of the two polymorphs of 1,1-bis-(4-hydroxyphenyl)cyclohexane.<sup>17c</sup> Sublimed form ( $Z' = 1$ ) in magenta and melt form ( $Z' = 2$ ) in blue & green conformer. OH groups are syn in sublimed polymorph and one conformer (blue conformer) from melt phase and anti in green conformer. (b) Overlay of nineteen crystallographic independent conformations of a tetramorphic 4,4-diphenyl-2,5-cyclohexadienone<sup>17b</sup> (Red, form A,  $Z' = 1$ ; green, form B,  $Z' = 4$ ; blue, form C,  $Z' = 12$ ; yellow, form D,  $Z' = 2$ ). (c) Overlay of symmetry-independent molecules in 1:2 complex of  $\alpha$ -D-glucose and p-tolylboronic acid<sup>17a</sup> by keeping the furanose ring as the fixed fragment. Orthorhombic form = green, monoclinic form = red and blue conformer. Boronate ester on left side overlays nicely but the right side portion has different orientations.

### 3.7 Crystal Structures with $Z' > 1$ by Solvent Less Methods

Our intent was to produce guest free crystal structures of host compounds that often produce solvates by solution crystallization. The popular host 1,1-bis-(4-hydroxyphenyl)cyclohexane<sup>17c</sup> was considered for study. Its guest free crystal structure which was not known at that time was crystallized by solvent free methods. One form is crystallized by sublimation in triclinic space group  $P\bar{1}$  with one symmetry independent molecule ( $Z' = 1$ ). A second polymorph of pure host was isolated by melting in space group  $Pbca$  with two molecules in asymmetric unit ( $Z' = 2$ ). These solvent less high temperature techniques are further employed to generate new polymorphs of isomeric dihydroxybenzoic acids. These compounds are prone to give solvate/hydrate forms upon crystallization. Two polymorphs of pure host 3,5-dihydroxybenzoic acid (sublimed phase  $Z' = 3$ , melt phase  $Z' = 0.5$ ), a new polymorph of 2,3-dihydroxybenzoic acid (monoclinic form by sublimation with  $Z' = 1$ ) and guest free form of 3,4-dihydroxybenzoic acid (by sublimation  $Z' = 3$ ) were crystallized by melting and sublimation.<sup>20</sup> A new hydrate polymorph of 3,4-dihydroxybenzoic acid was also crystallized from water. 1,1-bis-(4-hydroxyphenyl)cyclohexane show conformational polymorphism as the phenolic OH group orientations are different in their polymorphs however isomeric dihydroxybenzoic acids are synthon polymorphs. Conformational and synthon polymorphism on these host molecules including phase transition behavior is discussed in detail in chapter 2. The  $Z'$  frequencies in the guest free structures and polymorphs of 1,1-bis-(4-hydroxyphenyl)cyclohexane and isomeric hydroxybenzoic acids are summarized in Table 1. Literature shows 2,5- dihydroxybenzoic acid (BESKAL, BESKAL01), 2,4 - dihydroxybenzoic acid (ZZZEEU with no 3D and ZZZEEU01) and 2,6-

dihydroxybenzoic acid (LEZJAB, LEZJAB01) are dimorphic from solution crystallization.<sup>21</sup>

**Table 1** Occurrence of  $Z'$  frequencies in the polymorphs of 1,1-bis-(4-hydroxyphenyl) cyclohexane and isomeric hydroxybenzoic acids that are generated by solvent less high temperature methods. Crystal structures are discussed in Chapter 2.

| Compound   | Occurrence of $Z'$ frequencies   |
|--|--|
| 1,1-bis-(4-hydroxy phenyl)cyclohexane ( <b>1</b> ) | <b>1s</b> ( $P\bar{1}$ , $Z' = 1$ , Refcode WETFAD01, by sublimation)<br><b>1m II</b> ( $Pbca$ , $Z' = 2$ , Refcode WETFAD, from melt) |
| 3,5-Dihydroxybenzoic acid ( <b>2</b> )             | <b>2s</b> ( $C2/c$ , $Z' = 3$ , by sublimation)<br><b>2m</b> ( $C2/c$ , $Z' = 0.5$ , from melt)  |
| 2,3-Dihydroxybenzoic acid ( <b>3</b> )             | <b>3</b> .Form I ( $P\bar{1}$ , $Z' = 2$ , Refcode CACDAM by sublimation)<br><b>3</b> .Form II ( $P2_1/c$ , $Z' = 1$ , by sublimation) |
| 3,4-Dihydroxybenzoic acid ( <b>4</b> )             | <b>4</b> .Pure ( $P\bar{1}$ , $Z' = 3$ , from melt)  |

A Cambridge Structural Database (CSD) search on structures crystallized using solvent free methods: melt and sublimation was carried out and analyzed the frequency of  $Z'$  on organic crystal structures generated by these two solvent less methods. Our CSD study on organic crystals till 2006 (CSD version 5.27, ConQuest 1.8, May 2006 update) showed that these kinetic methods of crystallization gave higher probability of occurrence with  $Z' > 1$  (~18 %) in the crystal structures, compared to crystallization from solution (~8.6%). Total 334 and 83 crystal structures were extracted in “sublimation” and “melt” category within the search limits no error, no polymeric and only organic with available 3D coordinates and the occurrences of  $Z'$  is compared with global statistics till May 2006 CSD update<sup>17c</sup> and are summarized in Table 2.

**Table 2** Occurrence of  $Z'$  in organic crystals crystallized ‘from the melt’ (83 hits), ‘by sublimation’ (334 hits), and ‘overall statistics’ in the CSD version 5.27, ConQuest 1.8, May 2006 update. Overall percentages are values from 1,60,850 organic structures.

| $Z'$     | Sublimation(S)<br>% (# hits) | Melt(M)<br>% (# hits) | Overall(O)<br>% | $S+M \div 2 \times O$<br>% values |
|----------|------------------------------|-----------------------|-----------------|-----------------------------------|
| <1       | 29.04 (97)                   | 22.89 (19)            | 17.64           | 1.47                              |
| 1        | 53.89 (180)                  | 59.04 (49)            | 71.88           | 0.78                              |
| >1       | 17.06 (57)                   | 18.07 (15)            | 11.54           | 1.52                              |
| 2        | 12.28 (41)                   | 10.84 (9)             | 10.04           | 1.15                              |
| $\geq 3$ | 3.89 (13)                    | 7.23 (6)              | 1.24            | 4.48                              |
| >3       | 2.99 (10)                    | 3.61 (3)              | 0.69            | 4.78                              |
| 4        | 2.69 (9)                     | 2.40 (2)              | 0.45            | 5.65                              |

The database is now updated with CSD version 5.30, ConQuest 1.11, May 2009 update and extracted additional 121 organic crystal structures generated by sublimation and only 12 from the melt keeping the same search limits. The occurrence of high  $Z'$  ( $Z' > 1$ ) in organic crystals generated from sublimation and melt was found to be ~16% and ~33% respectively during last three years (2006 to 2009) but the number of hits in the melt category is very small (only 12). The overall database show (Table 3) that the solvent-free crystallization methods show a much higher probability (18%) of multiple  $Z'$  structures ( $Z' > 1$ ) compared to overall CSD trends on  $Z'$  frequencies.<sup>17c</sup> The overall database for organic crystal structures show  $Z' > 1$  is only < 12%. In general,  $Z' \leq 1$  is normal. There is an increase in  $Z' > 1$  frequency for solvent-free methods compared to solution crystallization, and the preference (last column ratio, Table 2 and 3) is dramatic for  $Z' \geq 3$ . But the available structures in the CSD with  $Z' \geq 3$  is sparse and a more clear trend will come forth only after more crystal structures are available with time.

**Table 3** Occurrence of  $Z'$  in organic structures generated from sublimation (455 hits) and melt (95 hits) is compared with that of solution crystallization (CSD version 5.30, ConQuest 1.11, May 2009 update)

| $Z'$     | Sublimation(S)<br>% (# hits) | Melt(M)<br>% (# hits) | Overall(O)<br>% | S+M $\div$ 2 $\times$ O<br>% values |
|----------|------------------------------|-----------------------|-----------------|-------------------------------------|
| <1       | 28.79 (131)                  | 21.05 (20)            | 13.61           | 1.83                                |
| 1        | 54.51 (248)                  | 58.95 (56)            | 74.23           | 0.76                                |
| >1       | 16.72 (76)                   | 20.00 (19)            | 12.27           | 1.49                                |
| 2        | 10.55 (48)                   | 12.63 (12)            | 10.68           | 1.08                                |
| $\geq 3$ | 4.18 (19)                    | 7.37 (7)              | 1.32            | 4.38                                |
| >3       | 2.68 (12)                    | 3.16 (3)              | 0.71            | 4.11                                |
| 4        | 2.20 (10)                    | 2.11 (2)              | 0.36            | 5.98                                |

Carbamazepine<sup>22</sup> is an illustrious example in this regard for which four polymorphs exist. Three polymorphs<sup>22a-c</sup> have  $Z' = 1$  generated from solution crystallization whereas  $Z' = 4$  polymorph is crystallized from melting.<sup>22d</sup> Generation of high  $Z'$  structures by melting and sublimation crystallization can be understood as rapid cooling of the hot liquid or vapor in the open flask or on the cold finger is a kinetic phase and the conditions under which hydrogen-bonded clusters are likely to condense in a pseudosymmetric crystalline arrangement. Aliphatic cyclic amines are also found to be notable examples to show high  $Z'$  structures on melting thus it reflect the presence of pseudosymmetry. The melt crystals of the cyclic amines, azetidine ( $C_3H_7N$ ) and hexamethyleneimine ( $C_6H_{13}N$ ) show  $Z' = 2$  structure<sup>23a</sup> for each case. Azetidine contains co-operative N–H $\cdots$ N hydrogen bonds chains propagating along  $2_1$  screw axes (Figure 4b) as observed in the hydrogen-bonded chains in aziridine<sup>23b</sup> (Figure 4a), showing the approximate  $3_1$  screw symmetry ( $Z' = 3$ ) however hexamethyleneimine (Figure 4d) contains tetrameric hydrogen-bonded rings formed about crystallographic inversion centres. The observation of crystallographically distinct molecules in the hydrogen-bonded chains of azetidine and cyclic hydrogen-bonded motifs in hexamethyleneimine is consistent with expectations derived from comparison with monoalcohols forming chains or rings by co-operative O–H $\cdots$ O hydrogen bonds and N–H $\cdots$ N hydrogen bond in benzidine.<sup>18</sup>



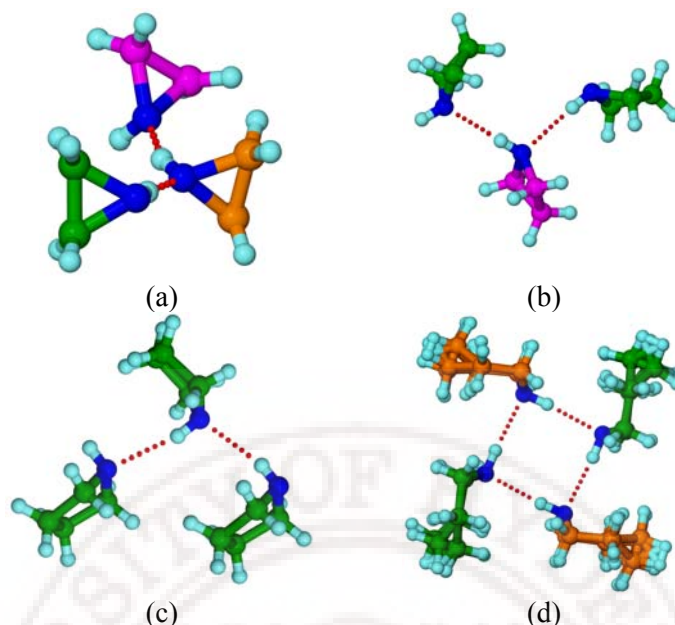


**Figure 4** (a) The hydrogen-bonded chains in Aziridine ( $Z' = 3$ ) showing the approximate  $3_1$  screw symmetry. The three crystallographically distinct molecules and their symmetry equivalents are distinguished by their color code. (b) Azetidine ( $Z' = 2$ ) along the  $c$  axis, showing one chain linked by cooperative  $N-H\cdots N$  hydrogen bonds propagating along a  $2_1$  screw axis parallel to the  $b$  axis. (c) Pyrrolidine ( $Z' = 1$ ) along the  $c$  axis, showing chains linked by cooperative  $N-H\cdots N$  hydrogen bonds propagating along  $2_1$  screw axes parallel to the  $b$  axis. (d) Hexamethyleneimine ( $Z' = 2$ ) contains tetrameric hydrogen-bonded rings formed about crystallographic inversion centres.

### 3.8 Conclusions

The structure determination depends on the degree of time and effort given, the personal interests, capabilities, and limitations of the individual investigation. Sublimation and melt crystallization have the potential to give high  $Z'$  crystal structures and guest-free forms through a green methodology. Polymorphs of 1,1-bis-(4-hydroxyphenyl)cyclohexane and isomeric hydroxybenzoic acids were generated by solvent less methods of melt and sublimation. These polymorphs show  $Z' > 1$  structures listed in Table 1. Sublimed polymorph of 1,1-bis-(4-hydroxyphenyl)cyclohexane (WETFAD01) with one strong and one weak hydrogen bond is more stable than melt phase (WETFAD) with 1.5  $O-H\cdots O$  and 0.5  $O-H\cdots\pi$  hydrogen bonds (per molecule) because the latter structure has less efficient close packing. Occurrence in  $Z'$  frequencies in organic crystals obtained under solvent-free conditions of sublimation and melt crystallization with overall data for organic crystal structures (Table 2 and 3) are



compared. There is an increase in  $Z' > 1$  frequency for solvent-free methods compared to solution crystallization however  $Z'$  is generally  $\leq 1$  in the slower nucleation process of solution crystallization. In chapter 2 it is noted that the melt phase of 1,1-bis-(4-hydroxyphenyl)cyclohexane appears upon fast cooling of liquid phase which is a kinetic process leading to  $Z' = 2$  structure.

### 3.9 References

1. C. P. Brock, *J. Res. Natl. Inst. Stand. Technol.* **1996**, *101*, 321.
2. (a) J. W. Steed, *CrystEngComm* **2003**, *5*, 169; (b) G. R. Desiraju, *CrystEngComm* **2007**, *9*, 91; (c) H. -J. Lehmler, S. Parkin, C. P. Brock, *Acta Crystallogr.* **2004**, *B60*, 325; (d) W. Clegg, G. S. Nichol, *Acta Crystallogr.* **2004**, *E60*, 1433.
3. (a) B. P. van Eijck, J. Kroon, *Acta Crystallogr.* **2000**, *B56*, 535; (b) P. van der Sluis, J. Kroon, *J. Cryst. Growth* **1989**, *97*, 645.
4. R. E. Marsh, *Acta Crystallogr.* **1999**, *B55*, 931.
5. (a) F. H. Allen, *Acta Crystallogr.* **1986**, *B42*, 515; (b) F. H. Allen, S. Bellard, M. D. Brice, B. A. Cartwright, A. Doubleday, H. Higgs, T. Hummelink, B. G. H. - Pfters, O. Kennard, W. D. S. Motherwell, J. R. Rodgers, D. G. Watson, *Acta Crystallogr.* **1979**, *35*, 2331; (c) F. H. Allen, O. Kennard, R. Taylor, *Acc. Chem. Res.* **1983**, *16*, 146; (d) CSD version 5.30, ConQuest 1.10, November 2008 release, May 2009 update.
6. (a) K. Kim, A. J. Matzger, *J. Am. Chem. Soc.* **2002**, *124*, 8772; (b) K. E. Plass, K. Kim, A. J. Matzger, *J. Am. Chem. Soc.* **2004**, *126*, 9042; (c) S. Aitipamula, A. Nangia, *Chem. Eur. J.* **2005**, *11*, 6727; (d) V. S. S. Kumar, A. Addlagatta, A. Nangia, W. T. Robinson, C. K. Broder, R. Mondal, I. R. Evans, J. A. K. Howard, F. H. Allen, *Angew. Chem. Int. Ed.* **2002**, *41*, 3848; (e) X. Hao, J. Chen, A. Cammers, S. Perkin, C. P. Brock, *Acta Crystallogr.* **2005**, *B61*, 218; (f) D. Das, R. Banerjee, R. Mondal, J. A. K. Howard, R. Boese, G. R. Desiraju, *Chem. Commun.* **2006**, 555; (g) S. Roy, R. Banerjee, A. Nangia, G. J. Kruger, *Chem. Eur. J.* **2006**, *12*, 3777; (h) K. M. Anderson, K. Afarinkia, H Yu, A. E. Goeta, J. W. Steed, *Cryst. Growth Des.* **2006**, *6*, 2109.

7. (a) A. Gavezzotti, G. Filippini, *J. Am. Chem. Soc.* **1995**, *117*, 12299; (b) A. Gavezzotti, G. Filippini, *J. Phys. Chem.* **1994**, *98*, 4831.
8. (a) N. Padmaja, S. Ramakumar, M. A. Viswamitra, *Acta Crystallogr.* **1990**, *A46*, 725; (b) A. D. Mighell, V. L. Himes, J. D. Rodgers, *Acta Crystallogr.* **1983**, *A39*, 737; (c) V. Sona, N. Gautam, *Acta Crystallogr.* **1992**, *B48*, 111; (d) A. J. C. Wilson, *Acta Crystallogr.* **1993**, *A49*, 795; (e) C. P. Brock, J. D. Dunitz, *Chem. Mater.* **1994**, *6*, 118; (f) V. K. Belsky, O. N. Zorkaya, P. M. Zorky, *Acta Crystallogr.* **1995**, *A51*, 473; (g) T. Steiner, *Acta Crystallogr.* **2000**, *B56*, 673; (h) M. Kubicki, *J. Mol. Struct.* **2005**, *743*, 209; (i) K. M. Anderson, A. E. Goeta, K. S. B. Hancock, J. W. Steed, *Chem. Commun.* **2006**, 2138. (j) R. P. Scaringe, in *Electron Crystallography of Organic Molecules*, J. R. Fryer, D. L. Dorset (Eds.), Kluwer: Dordrecht, 1991, Vol. 328, pp 85-113; (k) N. Yu. Chernikova, V. K. Bel'skii, P. M. Zorkii, *J. Struct. Chem.* **1991**, *31*, 661; (m) A. Gavezzotti, *CrystEngComm* **2008**, *10*, 389.
9. (a) G. R. Desiraju, *CrystEngComm* **2007**, *9*, 91; (b) K. M. Anderson, J. W. Steed, *CrystEngComm* **2007**, *9*, 328.
10. (a) M. Ruck, *Z. Kristallogr.* **2000**, *215*, 148; (b) B. M. Craven, *Acta Crystallogr.* **1979**, *B35*, 1123; (c) P. M. Zorky, *J. Mol. Struct.* **1996**, *374*, 9; (d) L. N. Kuleshova, M. Y. Antipin, I. V. Komkov, *J. Mol. Struct.* **2003**, *647*, 41; (e) L. Hsu, J. W. Kampf, C. E. Nordman, *Acta Crystallogr.* **2002**, *B58*, 260; (f) J. D. Wallis, J. D. Dunitz, *Acta Crystallogr.* **1988**, *C44*, 1037; (g) G. R. Desiraju, J. C. Calabrese, R. L. Harlow, *Acta Crystallogr.* **1991**, *B47*, 77; (h) D. Britton, *Acta Crystallogr.* **2000**, *B56*, 828; (i) E. Pidcock, W. D. S. Motherwell, J. C. Cole, *Acta Crystallogr.* **2003**, *B59*, 634; (j) E. Pidcock, *Acta Crystallogr.* **2006**, *B62*, 268; (k) A. Collins, *Acta Crystallogr.* **2006**, *B62*, 897.
11. (a) G. B. Deacon, E. Lawrenz, K. T. Nelson, E. R. T. Tiekink, *Main Group Met. Chem.* **1993**, *16*, 265; (b) G. de Munno, F. Lucchesini, *Acta Crystallogr.* **1992**, *C48*, 1437; (c) C. P. Brock, in *Implications of Molecular and Materials Structure for New Technologies* (Eds.) J. A. K. Howard, Kluwer, Dordrecht, 1999, p. 251; (d) C. P. Brock, R. P. Minton, *J. Am. Chem. Soc.* **1989**, *111*, 4586; (e) P. J. Langley, J. Hulliger, R. Thaimattam, G. R. Desiraju, *New J. Chem.* **1998**, *22*, 1307; (f) I. G. Voigt-Martin, Z. X. Zhang, D. H. Yan, A. Yakimanski,

- R. Matschiner, P. Kramer, C. Glania, D. Schollmeyer, R. Wortmann, N. Detzer, *Colloid Polymer Sci.* **1997**, 275, 18; (g) H. J. Lehmler, L. W. Robertson, S. Parkin, C. P. Brock, *Acta Crystallogr.* **2002**, B58, 140.
12. (a) A. B. Xia, J. P. Selegue, A. Carrillo, B. O. Patrick, S. Parkin, C. P. Brock, *Acta Crystallogr.* **2001**, B57, 507; (b) J. W. Bats, M. A. Grund, A. S. K. Hashmi, *Acta Crystallogr.* **2001**, C57, 653; (c) J. D. Dunitz, G. Fillippini, A. Gavezzotti, *Helv. Chim. Acta.* **2000**, 83, 2317.
  13. (a) C. P. Brock, L. L. Duncan, *Chem. Mater.* **1994**, 6, 1307; (b) P. D. Prince, G. S. McGrady, J. W. Steed, *New J. Chem.* **2002**, 26, 457; (c) S. E. Gibson, H. Ibrahim, J. W. Steed, *J. Am. Chem. Soc.* **2002**, 124, 5109; (d) C. P. Brock, *Acta Crystallogr.* **2002**, B58, 1025.
  14. G. S. Nichol, W. Clegg, *Cryst. Growth Des.* **2006**, 6, 451.
  15. (a) A. S. Batsanov, J. C. Collings, R. M. Ward, A. E. Goeta, L. Porre's, A. Beeby, J. A. K. Howard, J. W. Steed, T. B. Marder, *CrystEngComm* **2006**, 8, 622; (b) N. J. Babu, A. Nangia, *Cryst. Growth Des.* **2006**, 6, 1995.
  16. (a) J. Bernstein, J. D. Dunitz, A. Gavezzotti, *Cryst. Growth Des.* **2008**, 8, 2011; (b) S. K. Chandran, A. Nangia, *CrystEngComm* **2006**, 8, 581; (c) X. Hao, M. A. Siegler, S. Parkin, C. P. Brock, *Cryst. Growth Des.* **2005**, 5, 2225; (d) V. B. Gaillard, W. Paciorek, K. Schenk, G. Chapuis, *Acta Crystallogr.* **1996**, B52, 1036; (e) O. König, H.-B. Bürgi, T. Armbruster, J. Hulliger, T. Weber, *J. Am. Chem. Soc.* **1997**, 119, 10632; (f) G. S. Nichol, W. Clegg, *CrystEngComm* **2007**, 9, 959; (g) K. M. Anderson, A. E. Goeta, J. W. Steed, *Cryst. Growth Des.* **2008**, 8, 2517.
  17. (a) S. K. Chandran, N. K. Nath, S. Roy, A. Nangia, *Cryst. Growth Des.* **2008**, 8, 140; (b) S. Roy, R. Banerjee, A. Nangia, G. J. Kruger, *Chem. Eur. J.* **2006**, 12, 3777; (c) B. Sarma, S. Roy, A. Nangia, *Chem. Commun.* **2006**, 4918; (d) A. Nangia, *Acc. Chem. Res.* **2008**, 41, 595.
  18. M. Rafilovich, J. Bernstein, *J. Am. Chem. Soc.* **2006**, 128, 12185.
  19. R. Bishop, M. L. Scudder, *Cryst. Growth Des.* **2009**, 9, 2890.
  20. (a) B. Sarma, A. Nangia, *Acta Crystallogr.* **2008**, A64, C449; (b) B. Sarma, A. Nangia, manuscript under preparation.

21. (a) N. Okabe, H. Kyoyama, *Acta Crystallogr.* **2001**, 57E, o1224; (b) V. Horneffer, K. Dreisewerd, H. C. Ludemann, F. Hillenkamp, M. Lage, K. Strupat, *Int. J. Mass Spect. Ion. Proc.* **1999**, 185, 859; (c) Giacomello, *Nature (London)* **1956**, 177, 944; (d) A. Parkin, M. Adam, R. I. Cooper, D. S. Middlemiss, C. C. Wilson, *Acta Crystallogr.* **2007**, 63B, 303; (e) M. Haisa, S. Kashino, S. I. Hanada, K. Tanaka, S. Okazaki, M. Shibagaki, *Acta Crystallogr.* **1982**, 38B, 1480; (f) M. Gdaniec, M. Gilski, G. S. Denisov, *Acta Crystallogr.* **1994**, 50C, 1622; (g) L. R. MacGillivray, M. J. Zaworotko, *J. Chem. Cryst.* **1994**, 24, 703; (h) P. S. Wheatley, A. J. Lough, G. Ferguson, C. Glidewell, *Acta Crystallogr.* **1999**, C55, 1489; (i) I. Agmon, F. H. Herbstein, *Eur. Cryst. Meeting* **1982**, 7, 50.
22. (a) J. P. Reboul, B. Cristau, J. C. Soyfer, J. P. Astier, *Acta Crystallogr.* **1981**, 37B, 1844; (b) M. M. J. Lowes, M. R. Cairo, A. P. Lotter, J. G. van der Watt, *J. Pharm. Sci.* **1987**, 76, 744; (c) M. Lang, J. W. Kampf, A. J. Matzger, *J. Pharm. Sci.* **2002**, 91, 1186; (d) A. L. Grzesiak, M. Lang, K. Kim, A. J. Matzger, *J. Pharm. Sci.* **2003**, 92, 2260.
23. (a) A. D. Bond, J. E. Davies, S. Parsons, *Acta Crystallogr.* **2008**, C64, o543; (b) N. W. Mitzel, J. Riede, C. Kiener, *Angew. Chem. Int. Ed.* **1997**, 36, 2215

## POLYMORPHISM AND PHASE TRANSITION IN PHENYLBENZENESULFONAMIDES

### 4.1 Introduction

Crystal engineering has taken a vantage position in academic and industrial research. Crystal engineering not only offers design strategies for performance chemicals and characterization tools for active ingredients but also helps to provide fundamental concepts for understanding the principles behind the formation and properties of organic solids. The supramolecular diversity of a compound and more important pharmaceutical solid-state forms of the same molecule is based on the entire range of non-covalent interactions like hydrogen bonds, van der Waals interaction, electrostatic interactions,  $\pi\cdots\pi$  interactions etc. provides control of chemical stability, dissolution, solubility, bioavailability of active pharmaceutical ingredients (APIs). These interactions are expressed in molecular recognition and supramolecular assembly.<sup>1</sup> The contribution from various possible intermolecular interactions like van der Waals, ionic, hydrogen bonding etc. will be different in different solid-state forms mean that their physical and chemical properties will be different. Most important phenomenon of “polymorphism” within the crystal engineering domain has tremendous importance especially in drug development because the implication of different molecular self-assembly in the solid state relates to physical and chemical properties that affect pharmaceutical performance.<sup>2</sup> A hundred years ago polymorphism played a role in the development of azo pigments and copper phthalocyanide for the dye industry. Now polymorphism of drugs is a subject of intense interest in the post Zantac and Norvir era.<sup>3</sup> In particular the change in solubility between different polymorphs is important as it can affect drug efficacy, bioavailability and safety.

Polymorphism<sup>4</sup> is defined as the ability of a compound to crystallize in different crystalline modifications. Depending on conformation and supramolecular synthon, polymorphism can further be specified as conformational or synthon polymorphism,<sup>4c-g</sup> discussed in Chapter 1 and 2. When polymorphism exists as a result of difference in crystal packing, it is called packing polymorphism. Polymorphs have different stabilities and may spontaneously convert from a metastable form to the stable modification at a particular temperature or pressure. According to Ostwald's rule,<sup>5</sup> the system moves to equilibrium from an initial high-energy state through minimal changes in free energy. Therefore the structure that crystallizes first is one which has the lowest energy barrier (highest energy, kinetically metastable). This form would then transform to the next lower energy polymorph and so on until a thermodynamically stable state is achieved. As the nature of crystallization process is governed by thermodynamic and kinetic factors, crystallization is highly variable and difficult to control. Analysis of structures and phase relationship between different crystalline modifications of the same molecule will help us to understand more about polymorphism. The well-known incidents of Ritonavir<sup>3a,b</sup> and Ranitidine<sup>3c</sup> drugs highlight the importance and problems of polymorphism in the development of pharmaceutically active molecules. Protease inhibitor drug for human immunodeficiency virus (HIV), Ritonavir, exhibits conformational polymorphism with unique crystal lattices having significant difference in dissolution profile.<sup>3a</sup> The crystalline Form II is almost insoluble compared with Form I. Thus a thorough screening and complete characterization of all possible polymorphs is considered an essential step in pharmaceutical industry to choose the best drug formulation with desirable properties. Different condition in the crystallization process is the main reason responsible for the development of different polymorphic forms. Few of them are summarized: (i) The packing in the crystal lattice may differ with the polarity of the solvent (solvent effect), (ii) Impurities may inhibit or favor the growth of metastable form; (iii) Crystallization temperature; (iv) Flexibility in the molecule may lead to conformational polymorphs; (v) Presence of multiple functionalities can lead to hydrogen bond competition that results in formation of synthon polymorphs; (v) Concentration of the solution. Higher the concentration, the more likelihood is the formation of metastable form; (vi) Stirring, solid-state grinding, solvent drop grinding etc. can lead to a stable polymorph.



A systematic study on polymorphism gives insight into structural relationship and the mechanism of phase transition between crystalline modifications. The original antibacterial sulfonamides i.e. sulfa drugs are synthetic antimicrobial agents (sulfathiazole, sulfapyridine, sulfadiazine, sulfamerazine etc.)<sup>6</sup> that contain the sulfonamide functionality (primary or secondary). Gelbrich<sup>7</sup> recently did a comparative study of molecular packing and the nature of intermolecular interactions, hydrogen bond motifs of 133 phenylbenzenesulfonamides with *para-para* substitutions (NO<sub>2</sub>, CN, CF<sub>3</sub>, I, Br, Cl, F, H, Me, and OMe). A hierarchy for the classification of the 56 different structure types was presented. However our aim is to study the polymorphism and phase transition behavior by synthesizing a series of 13 phenylbenzenesulfonamides (with CH<sub>3</sub>, Cl, F substitution but not in *para-para* combinations, Figure 1a) with complete characterization by thermal analysis (Hot Stage Microscopy; Differential Scanning Calorimetry) and spectroscopic techniques (IR, NIR and Raman). Possible formation of different hydrogen bond patterns between sulfonamide moieties (–SO<sub>2</sub>NH–) i.e. N–H···O dimer and catemer, other weak interactions like C–H···O, C–H··· $\pi$  etc. and the torsion flexibility of the same can result different crystalline modifications (Figure 1b). The objective of this study is to draw a correlation between structures, hydrogen bond motifs and common polymorphism phenomenon in sulfonamide molecules and compare with trends in the Cambridge Structural Database (CSD).<sup>8</sup>

## 4.2 Results and Discussion

Phenylbenzenesulfonamides with methyl, chloro and fluoro substitution were synthesized through condensation of substituted aniline with substituted benzenesulfonyl chloride in basic condition (pyridine) and pure products were characterized by FT-IR and <sup>1</sup>H-NMR and then used for crystallization. Manual solid form screening was carried out for all compounds using available laboratory solvents to understand the effects of solvents on the polymorphic outcome as crystallization experiment,<sup>9a</sup> so that robust processes are identified to produce a desired crystal form. Traditionally, a variety of common methods<sup>9b</sup> for generation of new forms i.e. thermal, anti-solvent, evaporation, slurry, crystallization vessel design etc. are coupled with modern characterization methods for analysis of the solids produced. Most often, however, a combination of solvent recrystallization (cooling or evaporative, as well as slurry conversion) and

thermal analysis are employed for initial form screening. FT-IR, Raman, NIR are powerful analytical tools<sup>10</sup> for the confirmation of a new phase.

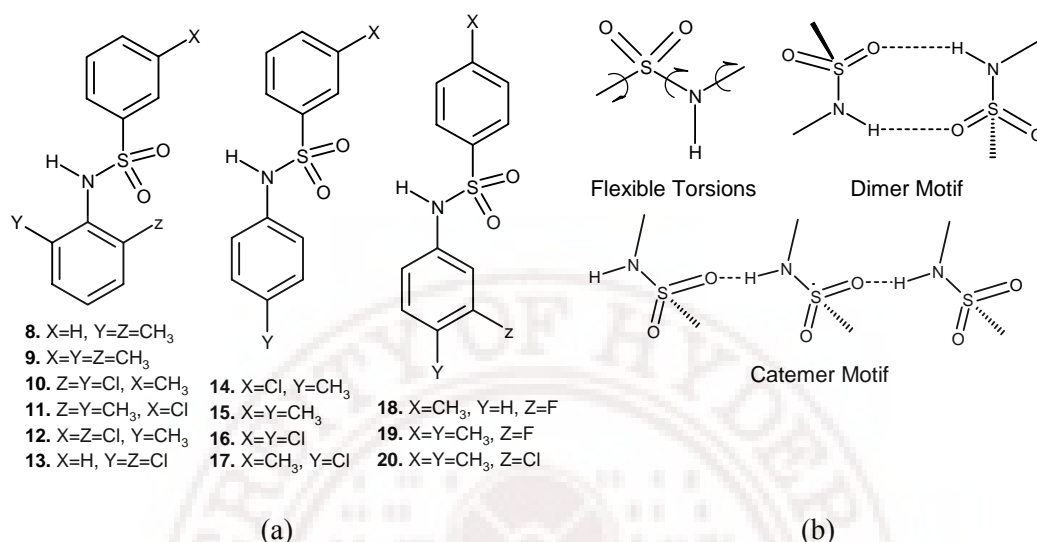


**Figure 1** (a) Phenylbenzenesulfonamides. (b) Torsion flexibility, sulfonamide N-H...O dimer or catemer hydrogen bond motifs and other weak interactions (C-H...O, C-H... $\pi$ ,  $\pi$ ... $\pi$  interactions) play a role in polymorph structures in phenylbenzenesulfonamides.

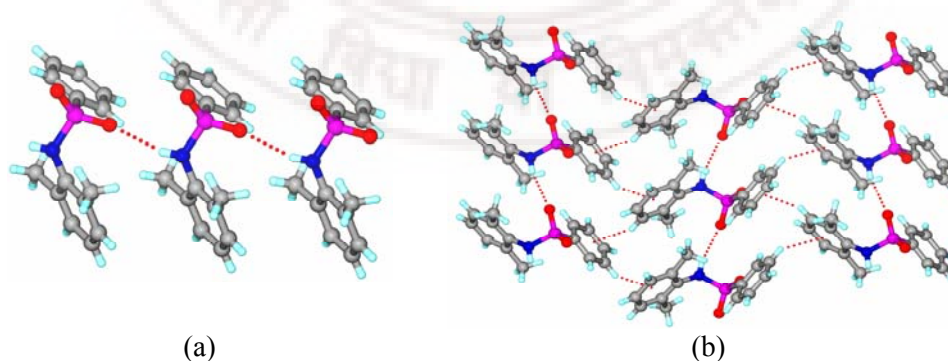
Thirteen phenylbenzenesulfonamides of three different series with Chloro-Methyl exchange are synthesized and screened for new polymorphs. Common laboratory solvents were used for crystallization. Solvent free techniques like melting and sublimation were also used to find new crystalline modifications. Sublimation was found to be not possible for these molecules. A complete list of about 20 common solvents which afforded polymorphs is summarized in Table 1. N-H...O hydrogen bond dimer and catemer between sulfonamide moieties are two common hydrogen bond motifs in their structures as they have no additional functionalities except Cl or CH<sub>3</sub> groups. Six molecules (**8**, **9**, **10**, **13**, **14**, **18**) from the set of thirteen (**8–20**) were found to be polymorphic and all are characterized by powder X-ray diffraction, single crystal X-ray diffraction, thermal analysis, hot stage microscopy, Raman, FT-IR, NIR spectroscopy, heating/grinding experiment for stability determination etc. Among them molecule **13** is trimorphic whereas others show dimorphism. Phase transition from metastable to stable polymorph was examined by HSM and DSC in two systems (molecule **8** and **18**) further confirmed by powder X-ray pattern and single crystal unit cell parameter determination.

Sulfonamide N–H···O catemer and dimer motif of sulfonamide group is seen as the main difference in molecule **8**, **10** and **13** however C–H···O, C–H··· $\pi$ , C–H···X (X = Cl or F), Cl···Cl interaction play significant role in differentiating the molecular arrangement in the crystal lattice of the remaining polymorphic pairs. Molecule **9** and **18** show N–H···O dimer in both phases, however molecule **14** show only catemeric N–H···O hydrogen bond. Solvent<sup>11</sup> is known to plays significant role in the nucleation of polymorphic crystals. Reasons for nearly equal preference for the formation of N–H···O homo dimer and catemer synthons on sulfonamides are discussed.

### 4.3 Crystal Structure Analyses

#### Molecule 8

Molecule **8** crystallized in two different phases. Form I is isolated from methanol and Form II from *p*-xylene. Form I in monoclinic space group  $P2_1/c$  with one molecule in the asymmetric unit forms 1D chain along [100] via catemeric N–H···O hydrogen bond between –SO<sub>2</sub>NH– groups (Figure 2a). The N–H···O chains are connected via C–H··· $\pi$  interactions and form a 2D sheet parallel to (001) plane (Figure 2b) and further C–H···O interaction complete the 3D packing. List of normalized N–H···O, C–H···O hydrogen bond distances are given in Table 1. Form II shows dimer motif via N–H···O hydrogen bonds (Figure 2c) which extend through weak C–H···O hydrogen bonds along [100] in a bifurcated manner (Figure 2d) that completes 3D packing. Crystal structure of Form I is recently reported by Gowda *et. al.* (HODWED).<sup>12</sup>



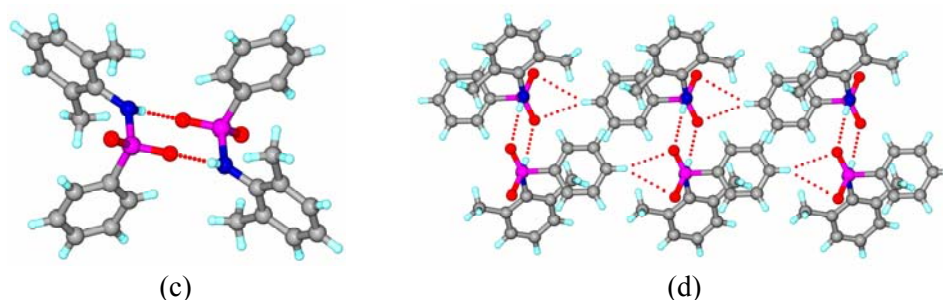


**Figure 2** (a) Catemeric N-H...O hydrogen bond along [100] in **8** Form I. (b) Herringbone like C-H... $\pi$  interactions connect tapes parallel to (001) plane in **8** Form I. (c) Dimeric N-H...O hydrogen bond in **8** Form II. (d) Dimer units are connected through C-H...O hydrogen bond along [100] axis in **8** Form II.

### Molecule 9

Two different phases were crystallized from methanol and chlorobenzene. Form I crystallizes in monoclinic space group  $P2_1/c$  whereas Form II is in triclinic space group  $P\bar{1}$ . Sulfonamide N-H...O dimer synthon is present in both polymorphs. Structural difference comes from C-H...O hydrogen bonds that leads to different 3D packing arrangement. The O atom that is not involved in the formation of N-H...O dimer in Form I acts as double acceptor for two C-H...O hydrogen bonds (Figure 3a) in a chelated manner.<sup>13</sup> However in Form II, dimer units extend through C-H...O hydrogen bonds along [001]. The N-H...O and C-H...O hydrogen bond ring motifs can be represented by  $[R_2^2(8)]$  and  $[R_2^2(16)]$  graph set notation<sup>14</sup> respectively (Figure 3b). In Form I,  $\pi\cdots\pi$  interaction (centroid to centroid distance 3.97 Å, shortest distance 3.56 Å) and weak C-H... $\pi$  interactions (to centroid 3.84 Å, 158.2°) stabilized the close packing. The C-H... $\pi$  interactions (3.50 Å, 135.8°) extends the structure parallel to (010) plane and C-H...O hydrogen bond completes the 3D molecular arrangements in Form II of molecule **9** (Table 1).

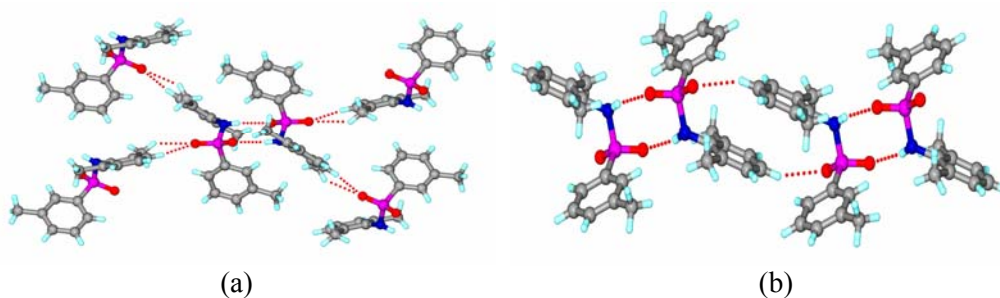


**Figure 3** (a) CH<sub>3</sub> group and ring H make chelated C–H...O hydrogen bonds that connect sulfonamide dimers along [001] direction in molecule **9** Form I. (b) Sulfonamide N–H...O dimers [graph set  $R_2^2(8)$ ] extend through C–H...O hydrogen bond [graph set  $R_2^2(16)$ ] in **9** Form II.

### Molecule 10

Polymorph I of molecule **10** crystallized in monoclinic space group  $P2_1/n$  however Form II is in  $P2_1$  with one molecule each in the asymmetric unit. Sulfonamide N–H...O hydrogen bonds form dimer [graph set  $R_2^2(8)$ , Figure 4a] in Form I and catemer (Figure 4b) in Form II. In Form I, type II, Cl...Cl interaction and C–H...O hydrogen bond arrange molecules in a 2D sheet parallel to (202) plane, however Cl...Cl interaction is absent in Form II. Catemeric chains are connected through C–H...O interaction extends into a 2D sheet running parallel to (001) in Form II (Figure 4b).

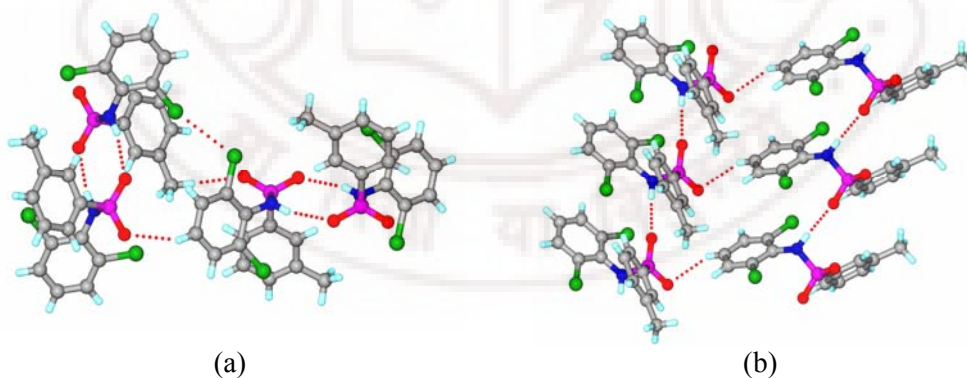


**Figure 4** (a) C–H...O and Cl...Cl type-II interaction holds two sulfonamide N–H...O dimers along [010] axis in molecule **10** Form I. (b) Catemeric N–H...O hydrogen bonds along [100] axis extend into 2D sheet through C–H...O hydrogen bond parallel to (001) plane in molecule **10** Form II.



### Molecule 13

Molecule **13** shows three different polymorphic modifications upon solution crystallization. Form I (Figure 5a) and Form II (Figure 5b) crystallized in monoclinic space group  $P2_1/n$  with one symmetry independent molecule in the asymmetric unit respectively having similar catemeric N–H $\cdots$ O chain that extend into 2D sheets via C–H $\cdots$ O interactions, however Form III shows N–H $\cdots$ O dimer motif (Figure 5c) which crystallized in monoclinic space group  $P2_1/c$ .

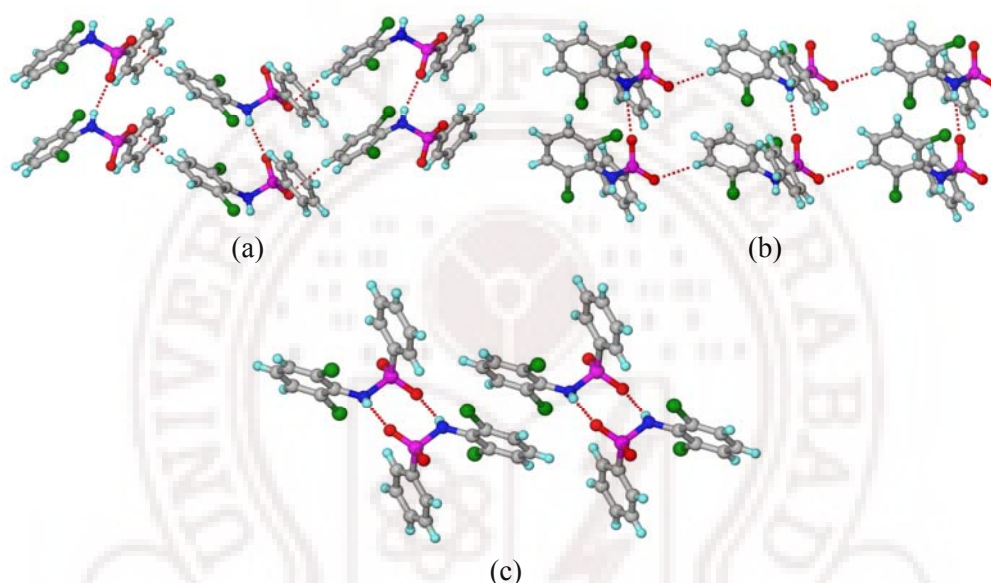


**Figure 5** Molecule **13** shows trimorphic modifications. (a) Form I and (b) II are having similar N–H $\cdots$ O catemer, however (c) Form III contains N–H $\cdots$ O dimer and additional  $\pi\cdots\pi$  stacking.

### Molecule 14

Molecule **14** also crystallized in two different crystalline modifications, Form I (Figure 6a) in  $P2_1/c$  and Form II in  $P2_1/n$  (Figure 6b) with two molecules each in the asymmetric unit. Sulfonamide N–H $\cdots$ O catemer is observed in both polymorphs. In Form I, both symmetry independent molecules are engaged in the formation of N–H $\cdots$ O helix along [010]. C–H $\cdots\pi$  interactions hold the helices in 3D (Figure 6a). In Form II one symmetry independent molecule is engaged in similar N–H $\cdots$ O catemer along [010]. The second symmetry independent molecule is N–H $\cdots$ O hydrogen bonded to catemer chain in a self host-guest like supramolecular arrangement (Figure 6b).



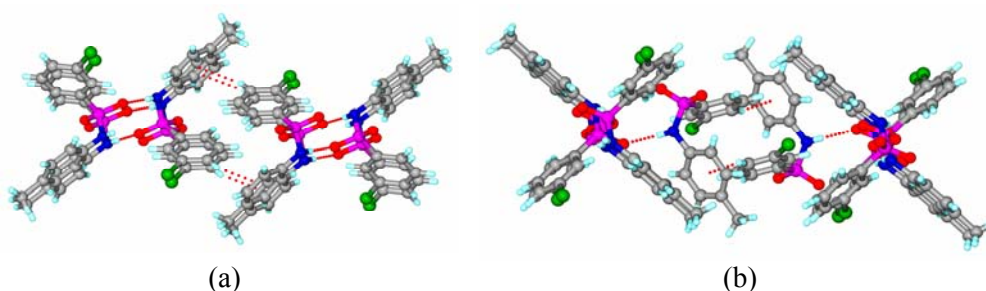


**Figure 6** (a) N-H...O helix along [010] axis in **14** Form I and C-H... $\pi$  interaction between helices completes 3D packing. (b) Catemeric N-H...O helix is formed by one asymmetry molecule along [010] in **14** Form II. Second molecule is hydrogen bonded to N-H...O catemeric chain.

### Molecule 18

Molecule **18** crystallized in two different forms. In Form I, N-H...O dimers extend in plane parallel to  $(20\bar{2})$  via C-H...O interactions. Free O of  $-\text{SO}_2-$  group in Form I acts as acceptor for C-H...O hydrogen bonds that involves phenyl ring hydrogen (Figure 7a) however this C-H...O interaction arise from the  $\text{CH}_3$  group hydrogen in Form II (Figure 7b).

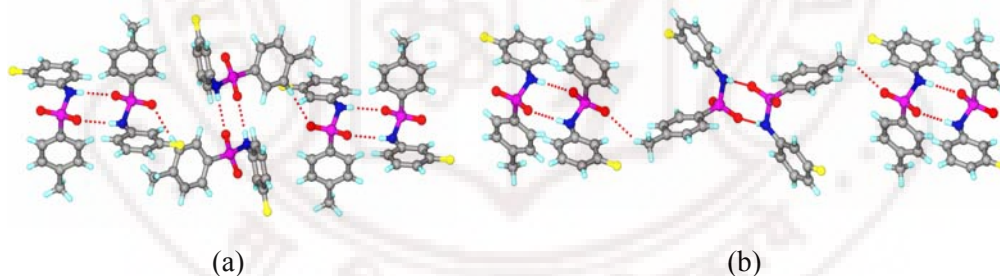


**Figure 7** (a) Sulfonamide dimer units are connected through C-H...O interaction parallel to  $(20\bar{2})$  plane in **18** Form I. (b) Methyl group is involved in the C-H...O interaction **18** Form II.

### Molecules 11, 12, 15, 16, 17, 19 and 20

Molecules **11** and **12** crystallized in monoclinic space group  $P2_1/n$  that show similar sulfonamide N-H...O dimer motif [graph set  $R_2^2(8)$ , Figure 8 and Figure 9]. C-H...O hydrogen bonds [graph set  $R_2^2(16)$ ] connect dimer units. The overall molecular packing is identical in **11** and **12**, only  $\text{CH}_3$  is replaced by Cl in **12**. Molecule **15** adopts

similar hydrogen bonding as Form II of **14** with two molecules in the asymmetric unit in  $P2_1/n$  (Figure 10). Molecule **16** in orthorhombic space group  $Pbca$  with one symmetry independent molecule shows a completely different packing arrangement. C–H $\cdots$ Cl interaction form a 1D tape like structure along [010] (Figure 11). These tapes are hydrogen bonded by N–H $\cdots$ O interactions (Figure 12) to form a 2D sheet parallel to (002) plane. In molecule **17** (Figure 13), **19** (Figure 14) and **20** (Figure 15) sulfonamide N–H $\cdots$ O catemer is absent. Dimer units are arranged by  $\pi\cdots\pi$  stacking. C–H $\cdots$ X (X = Cl, F) interaction and C–H $\cdots$ N hydrogen bonds complete the 3D packing.

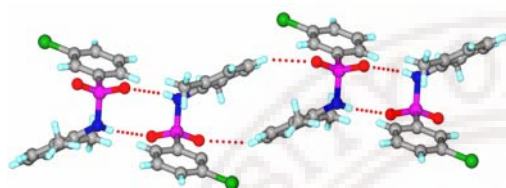


**Figure 8** Molecule **11**, N–H $\cdots$ O dimer and C–H $\cdots$ O dimer [Graph set  $R_2^2(8)$  and  $R_2^2(16)$  respectively] along [010]

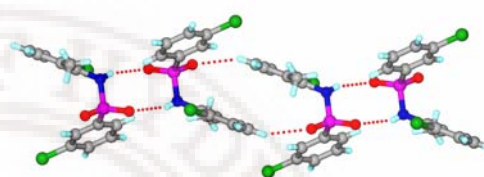


**Figure 9** N–H $\cdots$ O dimer and C–H $\cdots$ O dimer [Graph set  $R_2^2(8)$  and  $R_2^2(16)$  respectively] along [010] in **12**.

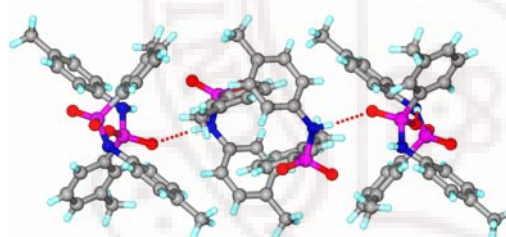


**Figure 10** Molecular arrangements in **15**, similar to **13** Form II.

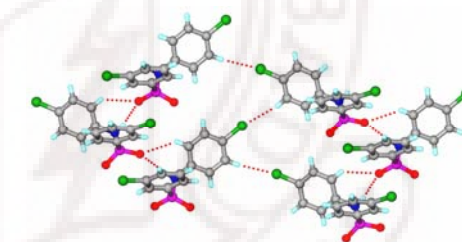


**Figure 11** C–H $\cdots$ Cl interaction along [010] in **16**

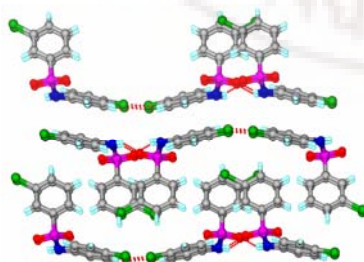


**Figure 12** Arrangement of molecules in **16**

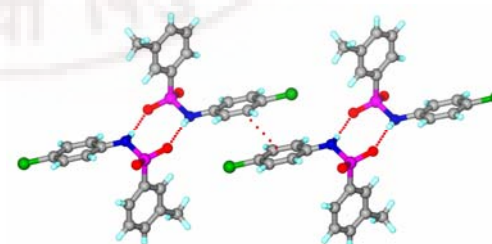


**Figure 13** Sulfonamide dimers [Graph set  $R_2^2(8)$ ] are arranged via  $\pi\cdots\pi$  stacking along [001] in **17**.

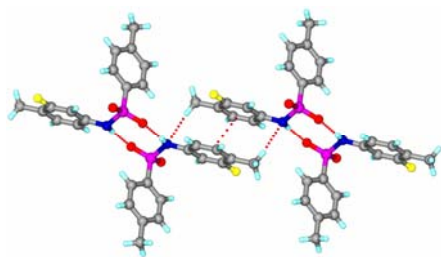


**Figure 14**  $\pi\cdots\pi$  and C-H $\cdots$ N supports the N-H $\cdots$ O dimer units in **19**

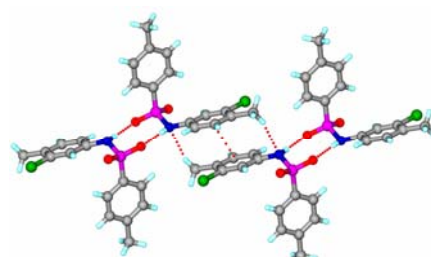


**Figure 15** Molecule **20** show similar hydrogen bonding as molecule **19**.

Conformational changes in the molecule are correlated with N-H $\cdots$ O hydrogen bonds and weak C-H $\cdots$ O interactions for the occurrences of dimer and catemer in their structures (Table 1). Normalized hydrogen bond distances are calculated in PLATON (Table 1). A very small difference in the torsion angles (–C–N–S–C–) between the polymorph structures indicate they are not conformation polymorphs (Column 2 of Table 1). Substantial torsion angle difference is observed in molecule **14** Form II between two asymmetry molecules. N-H $\cdots$ O hydrogen bond synthon (dimer and catemer) is the main difference in three polymorphic systems (**8**, **10** and **13**). Molecule **14** show only catemer however molecule **9** and **18** show dimers in their polymorphs. Weak interactions like C-H $\cdots$ O, C-H $\cdots\pi$ ,  $\pi\cdots\pi$  contribute to different molecular arrangements in these polymorphic systems.

**Table 1** Torsion angle variation in –SO<sub>2</sub>NH– functionality, formation of N-H $\cdots$ O dimer or catemer, other interactions present in 13 phenylbenzenesulfonamides and in their polymorphic structures. C-H $\cdots\pi$  and C-H $\cdots$ X (X=Cl, F) distances are calculated from heavy atom to heavy atom (D Å) using Mercury 2.2.  $\pi\cdots\pi$  distances are taken from centroid to centroid and shortest distance between the two phenyl rings.

| Sulfonamide      | -C-S-N-C-<br>torsion angle | Dimer/<br>Catemer(D/C) | N-H $\cdots$ O<br>$d$ (Å), $\angle$ (°) | C-H $\cdots$ O<br>$d$ (Å), $\angle$ (°) | C-H $\cdots\pi$ (D Å)<br>to ring<br>centroid | $\pi\cdots\pi$ centroid<br>to centroid/<br>shortest dist, Å | X $\cdots$ X (Å)<br>X=F, Cl | C-H $\cdots$ X (D Å)<br>X=F, Cl |
|------------------|----------------------------|------------------------|---|---|--|---|-----------------------------|---------------------------------|
| <b>8</b> Form I  | 78.15                      | C                      | 2.21,<br>162.5                          | 2.48,<br>126.2                          | 3.750,<br>154.8                              | -   | -                           | -                               |
| <b>8</b> Form II | 78.21                      | D                      | 2.00,<br>170.2                          | -                                       | 3.448,<br>141.9                              | -   | -                           | -                               |
| <b>9</b> Form I  | 75.33                      | D                      | 1.96,                                   | -                                       | 3.844,                                       | 3.974/  | -                           | -                               |

|                    |                |   |                |                |                 |                 |       |                 |
|--------------------|----------------|---|----------------|----------------|-----------------|-----------------|-------|-----------------|
|                    |                |   | 165.8          |                | 158.2           | 3.565           |       |                 |
| <b>9</b> Form II   | 71.26          | D | 1.95,<br>165.2 | -              | 3.502,<br>135.8 | 4.147/<br>3.493 | -     | -               |
| <b>10</b> Form I   | 77.19          | D | 1.99,<br>161.9 | 2.32,<br>157.7 | -               | 3.775/<br>3.505 | 3.440 | 3.933,<br>142.5 |
| <b>10</b> Form II  | 83.86          | C | 1.95,<br>173.3 | 2.60,<br>177.3 | 3.673,<br>129.3 | -               | 3.634 | 3.682,<br>177.5 |
| <b>11</b>          | 68.65          | D | 1.99,<br>165.2 | 2.44,<br>147.5 | 3.414,<br>108.4 | -               | -     | 3.881,<br>136.7 |
| <b>12</b>          | 70.81          | D | 2.02,<br>155.5 | 2.42,<br>144.1 | 3.508,<br>116.3 | -               | -     | 3.912,<br>165.1 |
| <b>13</b> Form I   | 82.49          | C | 2.05,<br>162.1 | 2.28,<br>149.2 | 4.018,<br>156.7 | -               | -     | 3.682,<br>168.3 |
| <b>13</b> Form II  | 80.96          | C | 2.04,<br>170.2 | 2.52,<br>100.4 | -               | -               | -     | 3.693,<br>175.1 |
|                    |                |   |                | 2.34,<br>147.3 |                 |                 |       |                 |
| <b>13</b> Form III | 78.72          | D | 1.97,<br>155.2 | 2.53,<br>100.4 | 3.997,<br>166.1 | 3.621/<br>3.600 | -     | -               |
| <b>14</b> Form I   | 66.92<br>62.09 | C | 1.92,<br>177.3 | 2.41,<br>166.9 | 3.889,<br>153.3 | -               | -     | 3.632,<br>120.9 |
|                    |                |   | 1.91,<br>176.6 | 2.56,<br>111.6 |                 |                 |       | 3.988,<br>163.2 |
| <b>14</b> Form II  | 64.42<br>54.45 | C | 2.12,<br>159.8 | 2.45,<br>145.8 | 3.616,<br>139.0 | 3.935/<br>3.346 | -     | -               |
|                    |                |   | 1.97,<br>178.9 | 2.39,<br>166.9 | 3.585,<br>140.6 |                 |       |                 |
| <b>15</b>          | 54.88<br>65.35 | C | 1.98,<br>170.0 | 2.38,<br>167.4 | 3.591,<br>163.3 | 3.941/<br>3.348 | -     | -               |
|                    |                |   | 2.07,<br>160.9 | 2.46,<br>147.1 | 3.566,<br>142.0 |                 |       |                 |
|                    |                |   |                | 2.27,<br>158.7 |                 |                 |       |                 |
| <b>16</b>          | 69.40          | C | 2.08,<br>149.2 | 2.48,<br>130.2 | -               | 3.940/<br>3.469 | -     | 3.681,<br>157.5 |
|                    |                |   |                | 2.66,<br>156.2 |                 |                 |       |                 |
| <b>17</b>          | 56.05          | D | 1.98,<br>166.8 | -              | -               | 3.725/<br>3.502 | -     | 3.845,<br>133.7 |
| <b>18</b> Form I   | 52.21          | D | 1.97,<br>173.9 | 2.44,<br>176.7 | 3.910,<br>123.4 | -               | -     | 3.539,<br>130.4 |
| <b>18</b> Form II  | 57.58          | D | 1.91,<br>173.6 | 2.44,<br>162.0 | -               | 3.655/<br>3.580 | -     | 3.611,<br>134.9 |
| <b>19</b>          | 61.26          | D | 1.90,<br>171.1 | -              | -               | 3.761/<br>3.528 | -     | 3.234,<br>129.8 |
| <b>20</b>          | 59.27          | D | 1.90,<br>175.4 | -              | 4.031,<br>165.8 | 3.801/<br>3.521 | -     | 3.458,<br>123.9 |

#### 4.4 Chloro-Methyl Exchange Rule and Isostructurality

One of the substitutions frequently employed in the crystal engineering approach is the replacement of methyl by chloro groups, especially as substituted in alkyl or aryl moieties. Kitaigorodskii and others<sup>15a-d</sup> have used the principle of close packing by interchanging substituents in such a way that each group occupies approximately the same volume. Kitaigorodskii's "close-packing model" proposed<sup>15a</sup> that the packing of molecules in a crystal structure can be predicted in such a way that the 'voids' in one are locked into the 'protrusions' of the other, volume and shape considerations hold sway rather than electronic factors. Since chloro ( $19 \text{ \AA}^3$ ) and methyl ( $24 \text{ \AA}^3$ ) groups have nearly the same volume (similarly  $-\text{CH}=\text{CH}-$  group by  $-\text{S}-$  group), they may be interchanged in a molecule without altering the crystal structure, the so-called 'chloro-methyl exchange rule'. Thus each non-polar substituent group of a certain volume can be exchanged for another non-polar group of a similar volume without any change in the crystal structure. Such isostructural behaviour is found when crystal stabilization is mainly through dispersive and repulsive interactions. The size and shape factor that controls the packing in an isosteric fashion was examined. They are equally applicable for solvent molecule present in the host. The 1:1:1 (triphenylisocyanurate).(trinitrobenzene).(benzene) solvate is isostructural to the corresponding 1:1:1 thiophene solvate confirming the benzene-thiophene exchange rule.<sup>15f</sup> Chlorobenzene/toluene solvates of tetraphenyl-anthryridine,<sup>15g</sup> substituted *gem*-alkynols<sup>15h</sup> are some of the notable examples that show solvent/substituent exchange without altering the overall packing arrangements. A recent study by Fernandes showed<sup>15i</sup> the chloro-methyl exchange between a series of 2,6-disubstituted-N-phenylformamides. Violations of this rule are also observed when directional forces or weak bonds are involved and the failure of complete chloro-methyl exchange in a substance like hexachlorobenzene, points to the importance of weakly attractive  $\text{Cl}\cdots\text{Cl}$  interactions. A classic example of the six isomeric dichlorophenols was observed by Noel to verify Schmidt's chloro rule. Only three of the compounds obeyed the rule that crystallized with higher symmetries. The remaining three structures violating Kitaigorodskii's rule did not have 4  $\text{\AA}$  axes and they adopted low-symmetry space groups. Comparing isostructural<sup>15j-n</sup> compounds is advantageous because in these structures the crystal packing is kept constant and variations in properties can be directly



correlated to the small differences present in the structures. When different molecules, usually within a family of compounds, adopt the same (similar) crystal structure, the phenomenon is termed as isostructurality. In general, isostructural compounds contain topologically similar supramolecular synthons in their crystal structures. Such isostructural compounds can form solid solutions in all proportions.<sup>15o</sup>

Kálmán<sup>16</sup> has suggested two numerical descriptors that reflect the crystallographic consequences caused either by tolerable conformational differences or by change in the chemical composition of the isostructural pairs, which quantify the extent of isostructurality between two crystal structures. They are the unit cell similarity index ( $\Pi$ ) and isostructurality index [ $I_i(n)$ ]. They can be defined as

$$\Pi = \left| \frac{a + b + c}{a' + b' + c'} \right| - 1 \cong 0$$

where  $a$ ,  $b$ ,  $c$  and  $a'$ ,  $b'$ ,  $c'$  are orthogonalized lattice parameters of the related structures. For a pair of completely isostructural crystals  $\Pi$  should be close to zero.

$$I_i(n) = \left[ 1 - \left( \frac{\sum_i \Delta R_i^2}{n} \right)^{1/2} \right] \times 100$$

The isostructurality index, [ $I_i(n)$ ] is a measure of the degree of internal isostructurality where  $n$  is the number of distance differences ( $\Delta R_i$ ) between the absolute coordinates of identical non-hydrogen atoms within the same section of asymmetric units of related structures.  $I_i(n)$  should be close to 100% for isomorphous and isostructural crystals.

Depending on the substituent exchange (Cl and CH<sub>3</sub>) molecules **8-20** are categorized into 3 different series (Figure 1a). Similarity index ( $\Pi$ ) values for closely related crystal structures of these series of phenylbenzenesulfonamides (Table 2) were calculated using *cell.cmp* software.<sup>15j</sup> Isostructurality Index ( $I_v$ ) was also calculated for similar structures using *isov* or *isov2* software.<sup>15j</sup> **8** and **13** show Cl/CH<sub>3</sub> exchange in the ortho position of aniline side. Molecule **8** is dimorphic however **13** has three polymorphs. From the cell parameters of polymorphic structures we can conclude that **8** Form I (N–H⋯O catemer) has similar cell values compared to Form I and II (N–H⋯O catemer) of molecule **13** ( $\Pi$  = 0.0041 and 0.0052 respectively). The unit cell similarity



index values are listed in Table 2.  $\Pi$  of **8** Form II does not match with any of the forms of **13** that indicate the possibility of the existence of a fourth polymorph of **13** similar to **8** Form II. There could also be the possibility of third polymorph for molecule **8** similar to **13** Form III. In the second series similar cell parameters are observed while comparing molecule **13** Form III with **10** Form I ( $\Pi = 0.0068$ ). Molecule **10** has one  $\text{CH}_3$  group at the *meta* position of sulfonyl side whereas **13** has H. Both structures have similar hydrogen bonding pattern ( $\text{N-H}\cdots\text{O}$  dimer). **10**, **11** and **12** are similar molecules interchanging their substituent Cl into  $\text{CH}_3$  and vice versa. Some sort of similar cell parameter is observed in **10** Form I when compared with **11** and **12**. However **11** and **12** are isostructural ( $I_v = 88\%$ ) as they show similar cell parameter as well the exactly similar packing of the molecules in the crystalline lattice. Molecules **14-17** are synthesized by interchanging Cl with  $\text{CH}_3$  in *meta-para* position. Only **14** shows dimorphism with Form II having similar cell parameter to **15**. So there is possibility of the existence of a second polymorph similar to **14** Form I in **15** ( $\Pi = 0.0033$ ). In the third series, **19** and **20** have almost similar cell parameter ( $\Pi = 0.0124$ ). From this observation we can conclude that although the cell parameter index show close to zero value, the packing of the molecules is quite different and they are not isostructural except **11** and **12**. The other directional forces or weak bonds like  $\text{C-H}\cdots\pi$ ,  $\text{C-H}\cdots\text{X}$  ( $\text{X}=\text{Cl}, \text{F}$ ),  $\pi\cdots\pi$  are involved in differentiating the molecular arrangement in the crystalline lattice. There is limited chloro-methyl exchange in this series of structures.

**Table 2** List for cell similarity index ( $\Pi$ ) values between the structures of **8-20** using *cell.cmp* software.

| Structures                              | $\Pi$  | $I_v$ (%) |
|---|--------|-----------|
| <b>8</b> Form I and <b>13</b> Form I    | 0.0041 | -         |
| <b>8</b> Form I and <b>13</b> Form II   | 0.0052 | -         |
| <b>10</b> Form I and <b>13</b> Form III | 0.0068 | 37.6      |
| <b>10</b> Form I and <b>11</b>          | 0.0216 | -         |
| <b>10</b> Form I and <b>12</b>          | 0.0211 | -         |
| <b>11</b> and <b>12</b>                 | 0.0004 | 88.0      |
| <b>14</b> Form II and <b>15</b>         | 0.0033 | -         |
| <b>19</b> and <b>20</b>                 | 0.0124 | 30.0      |

## 4.5 Solvent Influence on Polymorphs

The interplay between kinetics and thermodynamics of a polymorphic outcome is essentially summarized in Ostwald's Rule of Stages<sup>5</sup> which states the appearance of least stable form first and followed by more stable ones and then finally the thermodynamic modification. The nucleation and growth of metastable form occur until its solubility is reached then the nucleation of the stable form occurs and the subsequent growth of stable form is driven by the dissolution of the metastable form. On complete dissolution of metastable form, the growth of stable form continues until the solubility of the stable form is reached. This can be explained with Figure 16a).

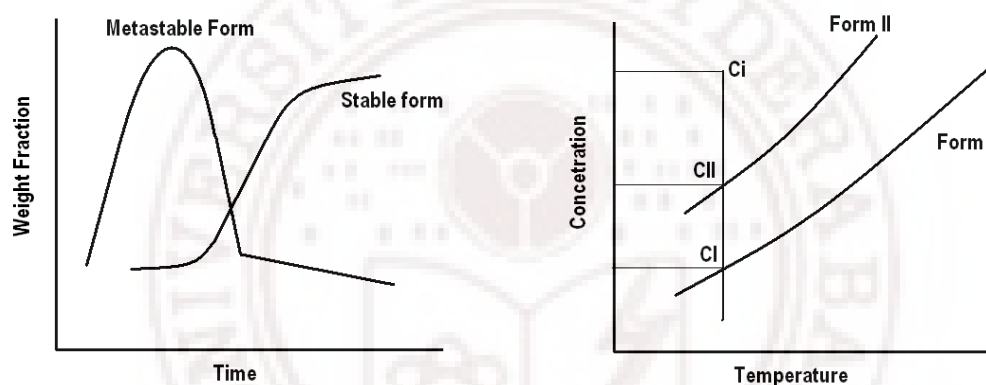


**Figure 16** (a) The kinetics of a dimorphic system. The primary nucleation stages for polymorphic transformations are involved with growth and dissolution process from a metastable to a more stable phase and finally growth of most stable or thermodynamic form. This is a solution mediated transformation process. (b) Two polymorphs system. Solution at point of spontaneous nucleation with initial supersaturation  $(C_i - C_I)/C_I$  with respect to polymorph I and supersaturation  $(C_{II} - C_I)/C_I$  of polymorph II with respect to polymorph I after Cardew and Davey simplistic description.<sup>17</sup>

It is expected that slow crystallization from dilute solution would produce the form stable at the temperature of nucleation and crystallization, whereas rapid crystallization from concentrated solution in which the kinetics could dominate would generate metastable forms. Cardew and Davey described<sup>17</sup> the nucleation and growth rate of polymorphs in a simplistic way (Figure 16b) and concluded that (a) the more stable form would crystallize preferentially at all concentrations, (b) the less stable form would crystallize preferentially only at high concentration, (c) the less stable form would crystallize preferentially only at intermediate concentrations, presumably this

intermediate concentration could be moved at least marginally towards the lower concentration region.

Depending on the polarity of the solvent the solution concentration will be different. The polarity of solvents play major role in the formation of weak or strong hydrogen bond between molecules which can direct the polymorphic outcome. In less polar or non polar solvents, the intramolecular hydrogen bonds are expected to be strong and *vice versa*. For example, Histamine H<sub>2</sub>-receptor blocker Ranitidine Hydrochloride<sup>18</sup> appears as Form I (enamine tautomer) when crystallized from anhydrous CH<sub>3</sub>OH where intramolecular hydrogen bonding is strong in the solid state. However in aqueous and/or more polar solvents the intramolecular hydrogen bonds are expected to be weakend or disrupted and thereby lead to the nitronic acid tautomer which is Form II in the solid state.

A series of easily available laboratory solvents were used to screen for the occurrences of different polymorphic phases in these molecules and summarized (Table 3). Our observation is that all the six polymorphic molecules afforded the most stable polymorph from polar solvents. Generally polar solvents result in dilute solution than the less polar or non polar solvent which could be the direct consequence of the formation of a stable modification. For example, molecule **8** stable Form I appeared from CH<sub>3</sub>OH however Form II crystallized from *p*-Xylene. Weak N–H···O hydrogen bond in Form I of **8** (Form I: 2.21 Å, 162.5°; Form II: 2.00 Å, 170.2°) is observed which crystallized from more polar solvent. Packing fraction, density and lattice energy calculation (Form I: 67.3 %, 1.318 g cm<sup>-3</sup>, –30.131 kcal mol<sup>-1</sup>; Form II: 65.4 %, 1.286 g cm<sup>-3</sup>, –30.04 kcal mol<sup>-1</sup>) suggests Form I is more stable. This observation of the solvent effect on the polymorphic outcome is consistent.

Finding a new polymorph by looking at different morphology crystals obtained from known laboratory solvents is a preliminary screen for polymorph selection. The use of solvents or solvent mixtures to promote or inhibit certain crystal motifs has been successfully applied to crystal formation. The growth of a macroscopic crystal from these nuclei will depend on the geometry of solvation process of incoming molecules and outgoing molecules.<sup>11</sup> Blagden and Davey described how different solvents can be used as templating agents for a specific motif. For an example, they used solvents with nitro groups to stabilize chain motif of 2-amino-4-nitrophenol leaving the amino group

exposed; solvents with hydroxyl groups form chains that leaves hydroxyl groups exposed; aromatic solvents promote open ring motif.<sup>19</sup> Molecular dynamics simulations<sup>19c</sup> have been used to show that relevant solvent surface interactions are not limited to hydrogen bonding, but also include electrostatic and van der Waals interaction. Role of solvent is one of the significant factors which control the nucleation of polymorphic molecules. Weissbuch and coworkers<sup>19d</sup> have investigated the growth kinetics of three polymorphs of glycine coupled with an analysis of the action of the solvent at the various crystal faces by controlling solvents. They showed why thermodynamically more stable  $\alpha$ - and  $\gamma$ -glycine polymorph do not generally precipitate in aqueous solutions even though the addition of alcohol reduces the solubility of glycine ten-fold. Kitamura *et al.* have studied<sup>19e</sup> the effect of solvent in the polymorphic crystallization of BPT propyl ester [propyl 2-(3-cyano-4-(2-methoxypropoxy)phenyl)-4-methylthiazole-5-carboxylate)]. Crystallization from CH<sub>3</sub>CN resulted in only a stable form under all conditions tried. However from EtOH and cyclohexane at high initial concentrations, a metastable form first appeared, and after that, subsequent transformation to a stable form occurred. Trifkovic *et al.* have shown<sup>19f</sup> that crystallization of ranitidine hydrochloride using a non-polar solvent, which leads to strong hydrogen bonding interactions, gave a polymorph containing the enamine tautomer (Form I). When a more polar solvent, such as water or methanol, was used, ranitidine–ranitidine hydrogen bonding interactions were disrupted and the nitronic acid tautomer (Form II) was obtained instead. More recently solvent influences on the crystallization of polymorph and hydrate forms<sup>19g</sup> of the nootropic drug piracetam (2-oxo-pyrrolidineacetamide) were investigated from water methanol, 2-propanol, isobutanol and nitromethane. Thermodynamics of solvent effect on sulfathiazole prior to nucleation has been examined theoretically.

**Table 3** Occurrences of polymorphs crystallized from various solvents

| Compound/Solvents | 8 | 9     | 10 | 13 | 14 | 18    |
|-------------------|---|-------|----|----|----|-------|
| Methanol          | I | I, II | II | II | I  | I, II |
| Propanol          | I | I     | I  | II | I  | I     |
| Acetone           | I | I     | I  | II | I  | I     |
| DCM               | I | I     | I  | II | I  | I     |

|                                 |       |    |   |       |    |    |
|---------------------------------|-------|----|---|-------|----|----|
| THF                             | I, II | II | I | II    | I  | I  |
| CH <sub>3</sub> NO <sub>2</sub> | I     | I  | I | II    | I  | I  |
| Dioxane                         | I     | I  | I | II    | I  | II |
| DMSO                            | I     | I  | I | II    | I  | I  |
| EtOAc                           | I     | I  | I | II    | I  | I  |
| MeCN                            | I     | I  | I | II    | I  | I  |
| PhCl                            | I     | II | I | II    | I  | I  |
| Benzene                         | I     | I  | I | II    | I  | I  |
| Hexane+EtOAc                    | I     | I  | I | II    | I  | I  |
| <i>p</i> -Xylene                | II    | I  | I | I, II | II | I  |
| Trifluorotoluene                | I     | I  | I | I, II | I  | I  |
| Mesitylene                      | I     | I  | I | II    | I  | I  |
| Chloroform                      | I     | I  | I | II    | I  | I  |
| Diethylether                    | I     | I  | I | II    | I  | I  |
| Toluene                         | I     | I  | I | II    | I  | I  |
| Hexane                          | -     | I  | - | III   | -  | -  |
| Cyclohexane                     | II    | -  | - | III   | -  | I  |

#### 4.6 Spectroscopic Analysis: IR, NIR and Raman

The crystallization processes for different compounds are unique and may result different polymorphic modifications. The physical and physicochemical properties of the different forms must be investigated to ensure the different bulk drug is of the same crystalline form. X-ray powder diffraction, differential scanning calorimetry (DSC), thermogravimetric analysis (TG), microcalorimetry, infrared (IR), near-infrared (NIR) and Raman spectroscopy and dissolution kinetics are the primary analytical methods for studying polymorphism in pharmaceuticals. Rantanen<sup>20a</sup> studied polymorphism of sulfathiazole by using near infrared (NIR) spectroscopy and verified by X-ray powder diffraction (XRPD) and thermal analysis. Recently Brillante showed,<sup>20b</sup> how polymorphism can be successfully recognized by using Raman spectroscopy in the region of lattice phonons, which represent the fingerprint of the individual crystal lattice. This also determines important information on phase homogeneity in crystal domains (crystal size < 1 mm). Pentacene, tetracene,  $\alpha$ -quaterthiophene,  $\alpha$ -sexithiophene are some of the typical examples of the application of Raman spectroscopy to recognize

polymorphism are reported.<sup>20c,d</sup> FT-IR, NIR, Raman spectroscopy are well-established techniques for solid-state analysis, and also for cocrystals.<sup>20e</sup>

In the spectra of solid sample, the symmetrical and asymmetrical N–H stretching vibrations absorption are observed in the ranges 3390–3323  $\text{cm}^{-1}$  and 3279–3229  $\text{cm}^{-1}$  respectively due to hydrogen bonding, however these absorptions appear at higher frequencies for dilute solutions (3520–3400  $\text{cm}^{-1}$ ).<sup>21</sup> Primary sulfonamide show strong N–H stretching bands at 3390–3330  $\text{cm}^{-1}$  in the solid state and secondary sulphonamides absorb near 3265  $\text{cm}^{-1}$ . Asymmetric and symmetric S=O stretching vibrations appear as strong absorption lines in the ranges, 1344–1317  $\text{cm}^{-1}$  and 1187–1147  $\text{cm}^{-1}$ , respectively. Sulphonamides exhibit S–N stretching vibrational absorptions in the range of 924–906  $\text{cm}^{-1}$ . All molecules synthesized are well characterized with IR spectra. Polymorphs show difference in hydrogen bonding and IR and Raman can be used to characterise them in the solid state. For example, molecule **8** show different N–H $\cdots$ O hydrogen bond strength in their polymorphs are characterized with IR (Figure 17) and Raman (Figure 18) and further confirmed with powder X-ray diffraction and single crystal X-ray diffraction. The N–H stretching at higher frequency,  $\nu$  (3304.8  $\text{cm}^{-1}$  for Form I and 3255.7  $\text{cm}^{-1}$  for Form II) indicate stronger N–H bond and weaker NH $\cdots$ O=S H bond for Form I of **8** which is confirmed by single crystal X-ray diffraction and hydrogen bond distances (Table 1). The N–H $\cdots$ O hydrogen bond distances are 2.21 Å and 2.00 Å for Form I and Form II respectively. Similarly Raman spectroscopy of the two polymorphs of molecule **8** show higher stretching frequency,  $\nu$  of N–H for Form I (red curve) that suggests stronger N–H and as a consequence weaker NH $\cdots$ O hydrogen bond. Form II at lower  $\nu$  indicates stronger NH $\cdots$ O hydrogen bonds. IR and Raman are found to be useful spectroscopic tools for characterising polymorphs. Spectral parameters for N–H stretching ( $\text{cm}^{-1}$ ), N–H bending ( $\text{cm}^{-1}$ ) and S=O symmetric/ asymmetric ( $\text{cm}^{-1}$ ) stretching for all polymorphs are summarized in Table 4 (IR stretching) and Table 5 (Raman shift).



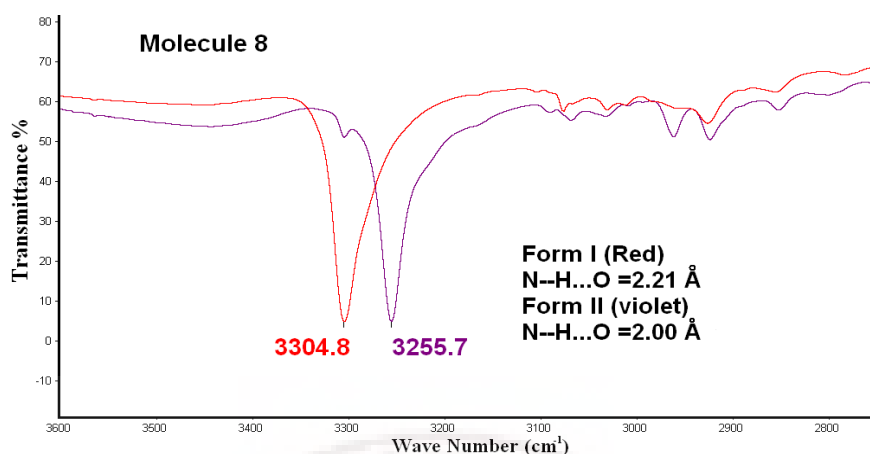


**Figure 17** IR spectra of two polymorphs of molecule **8**. Higher stretching frequency for Form I (red curve) of molecule **8** suggests stronger N–H and as a consequence weaker N–H $\cdots$ O hydrogen bond distance (2.21 Å). Form II (violet curve) at lower frequency does indicate stronger N–H $\cdots$ O hydrogen bond (2.00 Å).

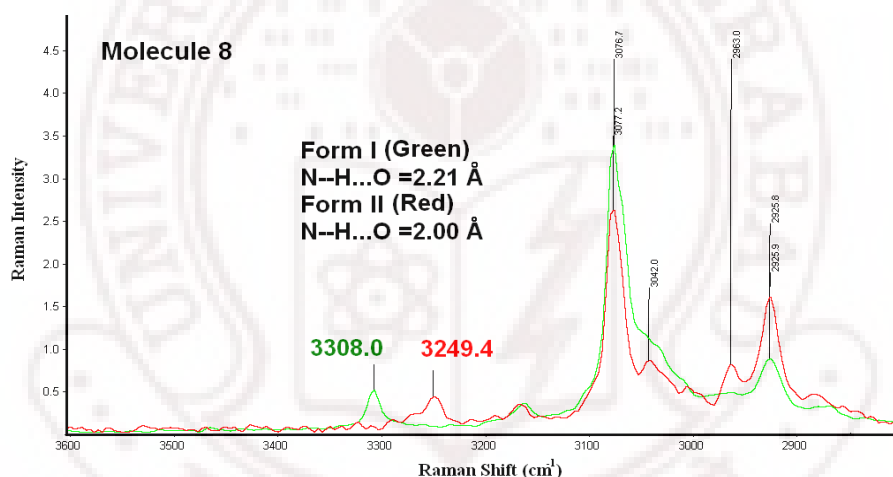


**Figure 18** Raman spectra of two polymorphs of molecule **8**. Higher N–H stretching frequency for Form I (green curve) and lower for Form II (red curve) indicate weaker N–H $\cdots$ O hydrogen bond (2.21 Å) for Form I and stronger for Form II (2.00 Å) in similar to IR.

**Table 4** Comparison of N–H stretching and bending, S=O symmetric/asymmetric IR stretching frequencies of six polymorphic systems of phenylbenzenesulfonamide

| Molecule        | N–H stretching (cm <sup>-1</sup> ) | N–H bending (cm <sup>-1</sup> ) | S=O Symmetric/Asymmetric (cm <sup>-1</sup> ) |
|-----------------|------------------------------------|---------------------------------|--|
| <b>8</b> Form I | 3304.8                             | 1472.0                          | 1327.6/1161.5                                |

|                    |        |        |               |
|--------------------|--------|--------|---------------|
| <b>8</b> Form II   | 3255.7 | 1473.0 | 1329.6/1162.0 |
| <b>9</b> Form I    | 3261.1 | 1473.8 | 1331.2/1158.6 |
| <b>9</b> Form II   | 3261.2 | 1473.8 | 1331.0/1158.1 |
| <b>10</b> Form I   | 3249.1 | 1478.5 | 1340.8/1157.4 |
| <b>10</b> Form II  | 3251.5 | 1477.8 | 1339.6/1157.5 |
| <b>13</b> Form I   | 3271.1 | 1445.6 | 1336.8/1168.5 |
| <b>13</b> Form II  | 3259.4 | 1447.9 | 1341.0/1168.7 |
| <b>13</b> Form III | -      | -      | -             |
| <b>14</b> Form I   | 3215.5 | 1463.7 | 1334.7/1157.7 |
| <b>14</b> Form II  | 3215.7 | 1463.5 | 1341.9/1157.7 |
| <b>18</b> Form I   | 3243.3 | 1498.0 | 1333.2/1163.8 |
| <b>18</b> Form II  | 3245.2 | 1497.7 | 1328.8/1162.9 |

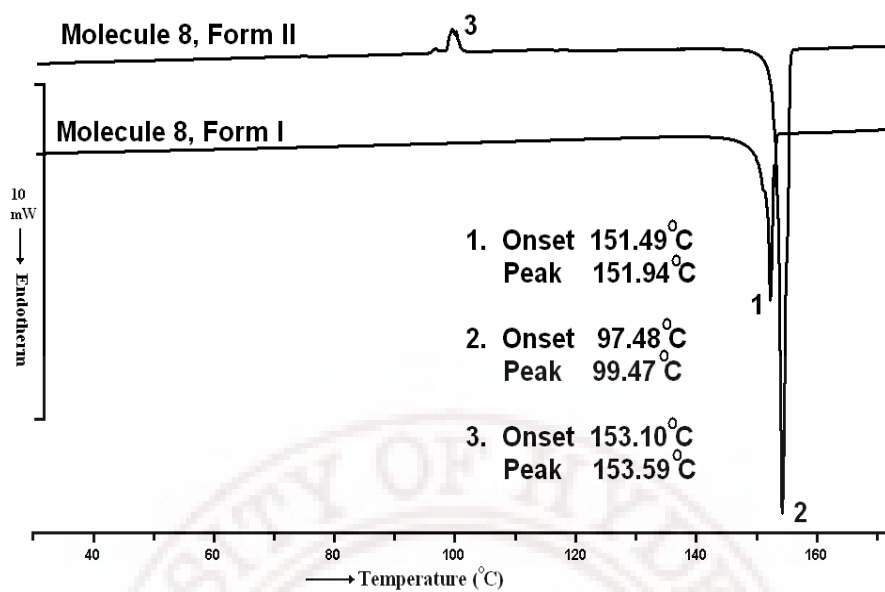
**Table 5** Comparison of Raman stretching frequencies of N–H and S=O functionalities of six polymorphic systems of phenylbenzenesulfonamide.

| Molecule           | N–H stretching<br>(cm <sup>-1</sup> ) | N–H bending<br>(cm <sup>-1</sup> ) | S=O Symmetric/<br>Assymmetric (cm <sup>-1</sup> ) |
|--------------------|---------------------------------------|------------------------------------|---|
| <b>8</b> Form I    | 3308.0                                | 1584.7                             | 1325.5/1160.8                                     |
| <b>8</b> Form II   | 3249.4                                | 1587.0                             | 1325.3/1150.7                                     |
| <b>9</b> Form I    | 3257.4                                | 1593.4                             | 1321.5/1145.4                                     |
| <b>9</b> Form II   | 3252.2                                | 1597.4                             | 1326.4/1145.1                                     |
| <b>10</b> Form I   | 3249.0                                | 1575.4                             | 1333.2/1165.2                                     |
| <b>10</b> Form II  | 3249.8                                | 1575.2                             | 1334.0/1154.5                                     |
| <b>13</b> Form I   | 3271.9                                | 1583.3                             | 1336.7/1164.6                                     |
| <b>13</b> Form II  | 3278.9                                | 1580.5                             | 1336.7/1163.3                                     |
| <b>13</b> Form III | -                                     | -                                  | -   |
| <b>14</b> Form I   | 3220.3                                | 1580.8                             | 1336.5/1157.1                                     |
| <b>14</b> Form II  | 3214.6                                | 1581.5                             | 1336.3/1157.2                                     |
| <b>18</b> Form I   | 3239.8                                | 1597.5                             | 1332.4/1154.4                                     |
| <b>18</b> Form II  | 3237.9                                | 1597.4                             | 1331.8/1154.2                                     |

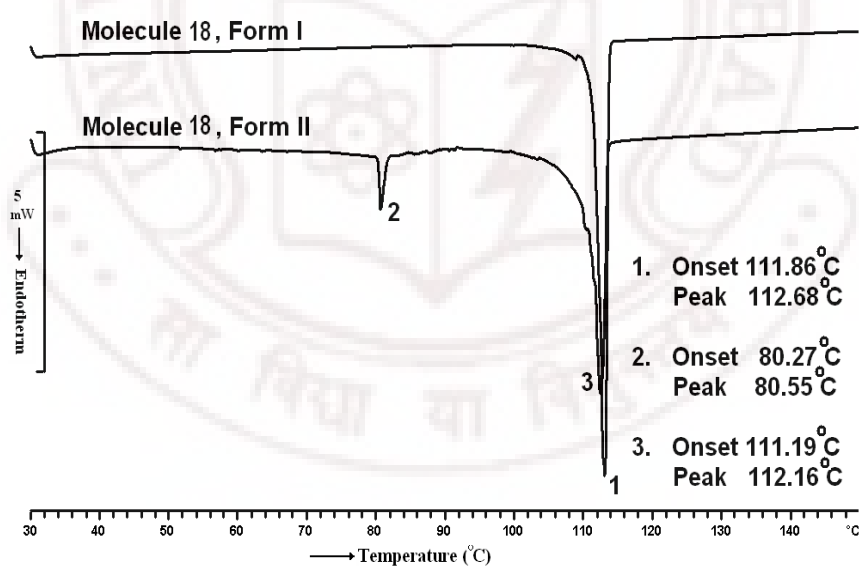
## 4.7 Thermal Analysis and Phase Transition

Phase transition is a natural physical process in a material when a given structure transforms to a new structure. Polymorphism exists in the solid state and phase transition between polymorphs is common. The relative stability and interconversion of polymorphs are important to study during preformulation of a drug, because an incorrect choice of polymorph may cause adverse effect on the issue of physical stability and pharmaco-kinetic profile. The stability relationship of polymorphs of a molecule can be established by measuring their enantiotropic or monotropic relationship.<sup>2c</sup> An enantiotropic relationship in a dimorphic system implies that each form has a range of temperature over which it is stable with respect to the other and a transition point at which the forms are equistable and in principle interconvertible. Above the transition temperature the thermodynamic tendency is for the formation of stable form at higher temperature and below the transition temperature the low temperature form is stable one with respect to the other. Thus two polymorphic modifications are said to be enantiotropic when the transition point between the two phases is found at a temperature below the melting point of either of them. However in case of monotropic relationship one form is metastable with respect to another at all temperatures having no transition temperature. Aripiprazole, tolbutamide, ulfathiazole, sulfamerazine, piracetam, premarloxacin etc. are some of the notable drug examples<sup>22</sup> that show phase transition. Five pure modifications of the antipsychotic drug aripiprazole were recently reported,<sup>22a</sup> of which six pairs of the ten polymorphic pairs are enantiotropically related and two monotropically related as confirmed by thermal analysis, spectroscopy and X-ray diffraction. A detailed discussion with typical examples of monotropic and enantiotropic related polymorphs are presented in Chapter 1. Heating, grinding, slurry method<sup>23</sup> are common operations on such systems. The presence of solvent can speed up interconversion by lowering transition barrier. Trace moisture, acid or alkali on vessels<sup>23c</sup> can be similarly effective in interconverting polymorphs. Polymorphism and phase behavior have significant importance and finding out a stable phase of active pharmaceutical ingredients is being extended with a non-carboxylic acid nonsteroidal anti-inflammatory drug (NSAID) and COX-2 inhibitor, widely used in solid oral formulations, Nimesulide,<sup>24</sup> that shows concomitant conformational polymorphism.

For enantiotropic system, plot of the free energy against temperature shows a crossing point before the various melting points, and it may be possible to convert reversibly between the two polymorphs on heating and cooling. Differential scanning calorimetry was carried out to investigate the thermal behavior of all the six polymorphic systems. Molecule **8** (Figure 19a) and **18** (Figure 19b) shows phase transition<sup>4,25</sup> from metastable phase to stable form. In both cases Form II is kinetic and converts into Form I, the thermodynamic stable form when temperature rises. Molecule **9**, **10**, **13**, and **14** do not show phase transition. Form II of molecule **8** show one small exotherm at the onset temperature of 97.5 °C and then melts at 153.1 °C which shows a sharp melting temperature of Form I (Onset 151.5 °C, Peak 152 °C). Structurally we can explain the transition from Form II to Form I which is favorable in terms of hydrogen bonds. Breaking of one N–H···O bond of Form II –SO<sub>2</sub>NH– dimer and rearrangement of molecules will afford the structural arrangement of Form I (Figure 20) with the formation of additional C–H···O hydrogen bond and C–H··· $\pi$  interaction that stabilize the structure. At about 97-98 °C there is transition on Form II visualized as plate shaped crystals becoming black then melts at around 152 °C. The melting temperature is same as Form I. The transition of Form II to Form I is confirmed by single crystal cell parameter determination and powder X-ray diffraction pattern. A similar behavior is shown by molecule **18** (Figure 21). Transition of (melting and then brightening) Form II crystal to Form I at around 80 °C is observed as a small endotherm in DSC thermogram. This transformation from Form II to Form I is confirmed by visual inspection on HSM snapshot (or video) (Figure 22), cell parameter determination and powder X-ray diffraction pattern. This phase conversion from metastable to stable polymorph was further confirmed by solvent drop grinding and slurry methods. A list of melting onset and peak temperature from the DSC endotherm are summarized for all the polymorphic systems in Table 6. Packing fractions of all the polymorphs are also calculated to measure the stability between them. Since the conformational difference is found negligible between polymorphs of each molecule only lattice energy was calculated to confirm the stability. Lattice energies are calculated in Cerius<sup>2</sup> (B3LYP basis set, Dreiding 2.2.1 force field) and listed in Table 6.

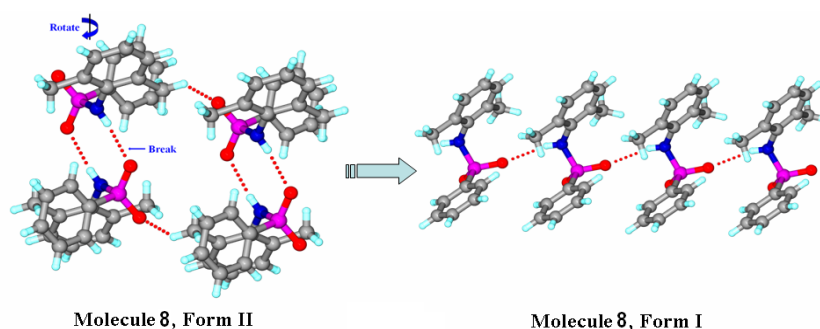


(a)

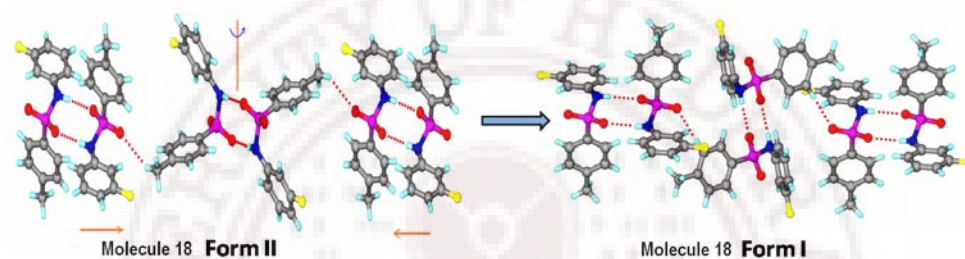


(b)

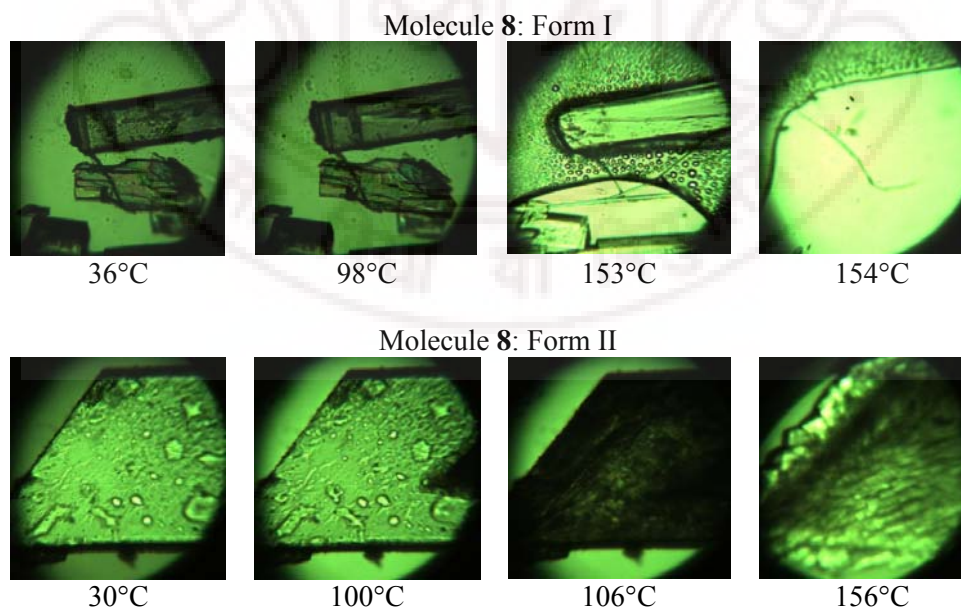
**Figure 19** Differential scanning calorimetry (DSC) confirms phase transition from metastable to thermodynamic stable polymorph in molecule **8** (a) and molecule **18** (b).



**Figure 20** Breaking of one N–H···O hydrogen bond of sulfonamide dimer unit and then rotation of the molecule will give the molecular arrangement (catemer N–H···O hydrogen bond) for thermodynamic stable Form I in **8**.



**Figure 21** Conversion of polymorph II of molecule **18** to polymorph I is mere rotation of the middle dimer unit so that phenyl H can participate in Form I C–H···O hydrogen bond. CH<sub>3</sub> group is involved in Form II C–H···O hydrogen bond.





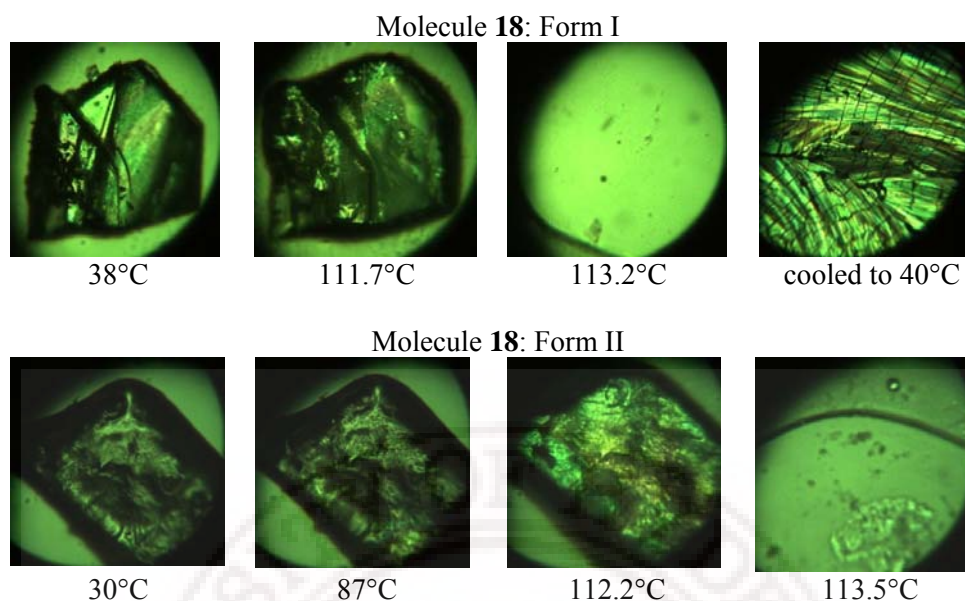


**Figure 22** HSM snapshots for molecule **8** and **18** represent phase transition. Darkening of crystals at around 100°C for molecule **8** (top two rows) indicate change in phase from Form II to Form I. The brightening of crystal at around 87 °C for molecule **18** (last two rows) confirms a phase transition. Crystal morphology does not change during phase transition.

**Table 6** Melting onset and peak temperature for the six polymorphic systems taken from DSC endotherm data.

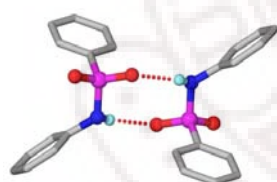
| Polymorphs         | Differential Scanning Calorimetry |                                | Packing Fraction (%) /Density (g cm <sup>-3</sup> ) (in PLATON) | Lattice Energy (kcal mol <sup>-1</sup> ) (in Cerius <sup>2</sup> DREIDING 2.21) |
|--------------------|-----------------------------------|--------------------------------|---|---|
|                    | Transition Temperature (°C)       | Melting Point Onset/ Peak (°C) |   |   |
| <b>8</b> Form I    | -                                 | 151.49/151.94                  | 67.3/1.318  | -30.131   |
| <b>8</b> Form II   | 97.48/99.47                       | 153.10/153.59                  | 65.4/1.286  | -30.040   |
| <b>9</b> Form I    | -                                 | 120.87/123.86                  | 65.1/1.259  | -30.973   |
| <b>9</b> Form II   | -                                 | 124.34/126.74                  | 64.5/1.243  | -30.583   |
| <b>10</b> Form I   | -                                 | 168.22/168.95                  | 66.8/1.496  | -30.696   |
| <b>10</b> Form II  | -                                 | 167.25/168.50                  | 67.2/1.507  | -30.583   |
| <b>13</b> Form I   | -                                 | 155.31/156.70                  | 66.0/1.517  | -30.535   |
| <b>13</b> Form II  | -                                 | 156.51/157.08                  | 67.3/1.548  | -31.693   |
| <b>13</b> Form III | -                                 | -                              | 65.0/1.513  | -30.403   |

|                   |             |               |            |         |
|-------------------|-------------|---------------|------------|---------|
| <b>14</b> Form I  | -           | 93.63/94.38   | 64.4/1.371 | -30.745 |
| <b>14</b> Form II | -           | 91.62/93.31   | 66.5/1.415 | -31.119 |
| <b>18</b> Form I  | -           | 111.86/112.68 | 64.7/1.355 | -29.243 |
| <b>18</b> Form II | 80.27/80.55 | 111.19/112.16 | 65.7/1.376 | -29.186 |

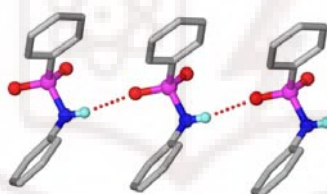
#### 4.8 Cambridge Structural Database (CSD)

A CSD study (CSD version 5.30, conquest 1.11, May 2009 update) was carried out to draw a comparison of frequency of polymorphism in secondary and primary sulfonamides. 3D coordinates determined, R factor  $\leq 0.10$ , Not disordered, No errors, No polymeric and only Organic crystal structures were retrieved for the search. Duplicate refcodes were removed retaining the less R factor structure and crystal structures were visualized in Mercury 2.2. Presence of the second oxygen in the  $\text{SO}_2\text{NH}-$  group provide an equal probability to form  $\text{N}-\text{H}\cdots\text{O}$  catemer (Figure 23b) or dimer (Figure 23a) synthon (19.6% catemer and 19.2% dimer probabilities are observed) and the trends in our subset of structures are comparable with the statistics (Figure 23). More favorable anti ( $\text{N}-\text{H}$  to  $\text{C}=\text{O}$ ) conformation of secondary carboxamide leads to the formation of only  $\text{N}-\text{H}\cdots\text{O}$  catemer motif (Figure 23d, e) because of steric hindrance whereas for primary carboxamide both catemer and dimer are equally well-disposed. Over 70% carboxamide structures show  $\text{N}-\text{H}\cdots\text{O}$  catemer hydrogen bond motif. A few cyclic secondary carboxamide structures show  $\text{N}-\text{H}\cdots\text{O}$  dimer (Figure 23d). The reason is that steric hinderance of two bulky groups in both sides of the  $-\text{CONH}-$  functionality preferably allows catemeric synthon. The tautomer, where the amide H is located in the conjugated position of  $-\text{NH}$  group of sulfonamide moiety is seen in several polymorphic systems (BEWKUJ, HORTAJ, SEFMEV, SUTHAZ, UJIRIO etc.). A detailed list of the number of hits of secondary and primary sulfonamides are listed in the Table 7 and the list of refcode for the 17 polymorphic systems for secondary sulfonamide is given in Table 8. The monoclinic  $P2_1/n$  (Form vi, BEWKUJ14) undergoes a phase transition to polymorph III ( $C2/c$ , Form iii, BEWKUJ04) after several days that is isostructural with polymorph I of sulfathiazole.<sup>26a-c</sup> Both the tautomeric forms are trapped in the sixth polymorph of sulfathiazole (BEWKUJ14). Sulfamethoxazole (SLFNMB01, SLFNMB02, SLFNMB05, SLFNMB06)<sup>26f,g</sup> and sulfathiazole (SUTHAZ04, SUTHAZ05, SUTHAZ07, SUTHAZ09, SUTHAZ11)<sup>26e</sup> are tetramorphic and

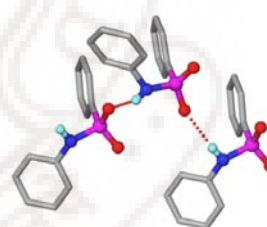
pentamorphic respectively. N,N'-Bis-(benzenesulfonyl)-*p*-phenylenediamine (FIBKUW01 and FIBKUW02)<sup>26h</sup> and sulfanilamide (SULAMD07, SULAMD08 and SULAMD09)<sup>26i</sup> are the only pair of secondary and primary sulfonamide with basic difference in structure is sulfonamide N–H···O catemer vs dimer synthon. From the set of 13 molecules studied here, three molecules (molecule **8**, **10** and **13**) show N–H···O catemer and dimer synthon in their polymorphs. Molecule **9** and **18** show only N–H···O dimer however molecule **14** shows catemeric motif. Trends in formation of dimer and catemer N–H···O hydrogen bond motif in this set of 13 molecules including polymorph structures is consistent with the overall CSD trend. Two S=O groups are available adjacent to N–H of –SO<sub>2</sub>NH– functionality, so the probability in occurrence of the formation dimer and catemer is about equal. Anti N–H···O catemeric (Figure 23b) synthon prefers over syn N–H···O catemer (Figure 23c, 69.1% anti and 30.9% syn). Six structures from the set of 20 gives anti catemeric N–H···O hydrogen bond and three structures show syn catemeric N–H···O motif (Table 9). Remaining 12 structures contain N–H···O dimer motif. In **14**.Form II, one symmetry independent molecule shows anti N–H···O catemer whereas second symmetry independent molecule has syn N–H···O catemer.



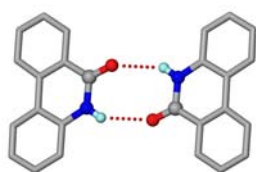
(a) Secondary sulfonamide N–H···O dimer, [graph set  $R_2^2(8)$ ]



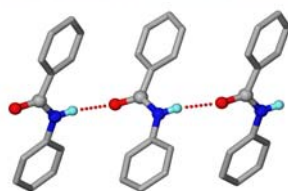
(b) Secondary sulfonamide N–H···O catemer (Anti)



(c) Secondary sulfonamide N–H···O catemer (Syn)



(d) Secondary carboxamide N–H···O dimer, [graph set  $R_2^2(8)$ ]



(e) Secondary carboxamide N–H···O catemer (Anti)



(f) Secondary carboxamide N–H···O catemer (Syn)

**Figure 23** Secondary Sulfonamides show (a) N–H···O dimer (19.6% occurrence probability) and (b) catemeric (19.2% occurrence probability) hydrogen bond that are compared with the secondary carboxamide (d) N–H···O dimer and (e) catemer motifs. All H, substituents and functional groups are removed for clarity. N–H···O catemer in secondary carboxamide are common, however dimer motif (d) is rare and found in few cyclic secondary carboxamide structures (CSD refcodes: ABEBIT, ABEBOZ, ABEBUF, FUSZEY, IDOSAW, ISOHAZ, LIWVAP, TAFCUY, XIKMEK, QOFGIC). Carboxamide N–H···O syn catemer (f) is found in two structures (CSD refcodes: PHENDO, ISOHIH) however syn and anti catemer hydrogen bond motifs are equally disposed in primary carboxamide structures.

**Table 7** List of sulfonamides extracted from CSD show equal preferences of formation of N–H···O dimer and catemer found rare combination in polymorphic pairs.

|   |   |
|---|---|
| Number of secondary sulfonamides (Total)                              | 958 hits  |
| Number of primary sulfonamides (Total)                                | 171 hits  |
| Primary sulfonamide polymorphs  | 4 hits [ATDZSA 01/02, FOGVIG 04/05, SULAMD 02/07, FURSEM 01/02] |
| Secondary sulfonamide polymorphs                                      | 17 molecules  |
| Primary sulfonamides polymorphs containing N–H···O catemer and dimer  | 1 molecule [SULAMD 02/07]                                       |
| Secondary sulfonamide polymorphs containing N–H···O dimer and catemer | 1 molecule [FIBKUW01/02]  |
| Secondary sulfonamide with N–H···O dimer                              | 184 hits (19.2%)  |
| Secondary sulfonamide with N–H···O catemer                            | 188 hits (19.6%)  |
| Primary sulfonamide with N–H···O dimer                                | 29 hits (16.9%)   |
| Primary sulfonamide with N–H···O catemer                              | 45 hits (26.3%)   |
| N–H···O catemer in secondary sulfonamides as Syn conformer            | 30.9%   |
| N–H···O catemer in secondary sulfonamides as Anti conformer           | 69.1%   |

**Table 8** List of the refcodes of secondary sulfonamide polymorphs

|  |  |
|--|--|
| BEDMIG, BEDMIG01, BEDMIG02, BEDMIG03, BEDMIG04   | BEWKUJ04, BEWKUJ05, BEWKUJ11, BEWKUJ13, BEWKUJ14 |
| SUTHAZ04, SUTHAZ05, SUTHAZ07, SUTHAZ09, SUTHAZ11 | SLFNMB01, SLFNMB02, SLFNMB05, SLFNMB06           |
| SLFNMA01, SLFNMA02, SLFNMA03                     | SAMPYM, SAMPYM01, SAMPYM03                       |

|                            |                    |
|----------------------------|--------------------|
| MILHOF, MILHOF01, MILHOF02 | FIBKUW01, FIBKUW02 |
| TORSEM02, TORSEM03         | TOHBUN01, TOHBUN02 |
| JAWXEK, JAWXEK01           | UJIRIO03, UJIRIO04 |
| HCSBTZ03, HCSBTZ04         | QIJZOY, QIJZOY01   |
| HORTAJ, HORTAJ01           | ACIROT, ACIRUZ     |
| SEFMEV, SEFMEV01           |                    |

**Table 9** Formation of N–H···O dimer and catemeric motifs in syn/anti fashion in set of 13 phenylbenzenesulfonamides is compared with CSD trend.

| Structures        | N–H···O Catemer (Syn/Anti) or Dimer | Structures         | N–H···O Catemer (Syn/Anti) or Dimer |
|-------------------|-------------------------------------|--------------------|-------------------------------------|
| <b>8</b> Form I   | Catemer (Anti)                      | <b>13</b> Form III | Dimer                               |
| <b>8</b> Form II  | Dimer                               | <b>14</b> Form I   | Catemer (Syn)                       |
| <b>9</b> Form I   | Dimer                               | <b>14</b> Form II  | Catemer (Anti and Syn)              |
| <b>9</b> Form II  | Dimer                               | <b>15</b>          | Catemer (Anti)                      |
| <b>10</b> Form I  | Dimer                               | <b>16</b>          | Catemer (Syn)                       |
| <b>10</b> Form II | Catemer (Anti)                      | <b>17</b>          | Dimer                               |
| <b>11</b>         | Dimer                               | <b>18</b> Form I   | Dimer                               |
| <b>12</b>         | Dimer                               | <b>18</b> Form II  | Dimer                               |
| <b>13</b> Form I  | Catemer (Anti)                      | <b>19</b>          | Dimer                               |
| <b>13</b> Form II | Catemer (Anti)                      | <b>20</b>          | Dimer                               |

## 4.9 Summary and Conclusions

Catemer and dimer motifs of sulfonamide group (–SO<sub>2</sub>NH–, Synthon polymorphs),<sup>4c,d</sup> variation in torsions (conformational polymorphs),<sup>4e-g</sup> role of weak interactions like C–H···O, C–H··· $\pi$ ,  $\pi$ ··· $\pi$ , halogen–halogen and molecular arrangements (packing polymorphs) were analyzed. This set of 13 phenylbenzenesulfonamides are mainly elaborated from two connectivity motifs, N–H···O hydrogen bond dimer and catemer. Other weak interactions like C–H···O, C–H··· $\pi$ ,  $\pi$ ··· $\pi$ , halogen-halogen etc. are observed in these structures and they influence in differentiating the packing of molecules in the crystal. These polymorphic systems are more of synthon polymorphs and packing polymorphs rather conformational although the possibility of varying conformations cannot be ignored. Three polymorphic systems (molecule **8**, **13** and **18**)

are found to be catemeric and dimeric N–H...O hydrogen bond motifs of –SO<sub>2</sub>NH– group as their main difference. Only one molecule having N–H...O hydrogen bond dimer and catemer motifs is reported [FIBKUW01, FIBKUW02] in literature. Out of twenty structures (Total 13 molecules) 12 are found to be dimeric N–H...O hydrogen bond motif whereas remaining structures show N–H...O catemeric motif. All polymorphs were characterized by single crystal X-ray diffraction, powder X-ray diffraction (PXRD), Hot Stage Microscopy (HSM), Differential Scanning Calorimetry (DSC) and spectroscopy (Raman, NIR, IR). The presence of a second oxygen on S atom of –SO<sub>2</sub>NH– group provides equal preferences to the formation of N–H...O homo dimer and catemer as compared in the Cambridge Structural Database (CSD). The effect of solvents on polymorphic outcome is discussed. Polar solvents normally give a dilute solution compared to less polar or non polar solvents for a given compound. An outcome of Ostwald's Rules of Stages is that the more stable form will be the desired polymorph in dilute solution, as we observed in the six polymorphic systems.

In pharmaceutical development an appropriate choice of polymorph can enhance the rate of absorption of a drug, improve the stability of the drug delivery system or ease processing in the manufacture of pharmaceuticals. The need to be able to crystallize pure batches of a desired polymorphic form is therefore important.<sup>28</sup> The influence of solvent for crystallization is important in polymorphism. There is no method that can provide absolute confidence that the most stable polymorph of a compound has been obtained. New forms may appear as a result of change in manufacturing processes. The appearance of a new polymorphic form of an API is a major concern for drug industries and hence a high throughput search of possible polymorphs, then complete characterization with the help of thermal measurement and spectroscopy is advisable. Phase transformation, a physical phenomenon from metastable to stable polymorph is established by thermal analysis, cell parameter determination, powder X-ray diffraction, grinding experiments and spectroscopic methods in at least two systems, **8** and **18**.

#### 4.10 Experimental Section

Phenylbenzenesulfonamide (secondary sulfonamide) of three different series given in Figure 1a were synthesized by condensation of substituted aniline with substituted sulfonylchloride in presence of base, pyridine in 1:1 molar ratios. All starting



materials were purchased from Aldrich and/ or Lancaster. Molecules **8** to **20** were purified through crystallization using solvents. All products were characterized and determined by  $^1\text{H}$ -NMR integration (chemical shift  $\delta$ ,  $J$  Hz) and their structures were confirmed by FT-IR and single crystal X-ray diffraction. Extensive solvent crystallization and melting were used to find new crystalline modification of these molecules (Table 3). All the polymorphic structures are confirmed by FT-IR (KBr and ATR mode), NIR, and Raman, DSC, Powder X-ray diffraction and single crystal X-ray diffraction. Melting point, IR stretching frequencies,  $^1\text{H}$ -NMR integration values are summarized for molecules **8-20**.

Molecule **8**: Melting point: 151-153 °C, Yield: 78 %

IR (KBr,  $\text{cm}^{-1}$ ): 3306, 2928, 1586, 1471, 1451, 1393, 1327, 1194, 1161, 1090, 899, 825, 777, 762, 742, 719, 688.

$^1\text{H}$ -NMR ( $\text{CDCl}_3$ ):  $\delta$  7.60 (2H, d,  $J=8$ ), 7.44 (2H, t,  $J=8$ ), 7.34 (1H, t,  $J=8$ ), 6.95 (1H, t,  $J=8$ ), 6.88 (2H, d,  $J=8$ ), 5.94 (1H, s), 1.89 (6H, s).

Molecule **9**: Melting point: 127-129 °C, Yield: 76%

IR (KBr,  $\text{cm}^{-1}$ ): 3262, 3059, 2926, 1474, 1398, 1381, 1333, 1157, 1097, 910, 829, 791.

$^1\text{H}$ -NMR ( $\text{CDCl}_3$ ):  $\delta$  7.51-7.49 (2H, m), 7.38-7.32 (2H, m), 7.08 (1H, t,  $J=8$ ), 6.99 (2H, d,  $J=8$ ), 5.88 (1H, s), 2.35 (3H, s), 2.03 (6H, s).

Molecule **10**: Melting point: 167-168 °C, Yield: 65%

IR (KBr,  $\text{cm}^{-1}$ ): 3252, 2928, 1586, 1468, 1450, 1408, 1392, 1327, 1273, 1161, 1140, 1090, 897, 866, 826, 777, 761, 742, 717, 688.

$^1\text{H}$ -NMR ( $\text{CDCl}_3$ ):  $\delta$  7.65 (2H, d,  $J=12$ ), 7.40 (1H, t,  $J=8$ ), 7.36-7.32 (3H, m), 7.18 (1H, t,  $J=8$ ), 6.32 (1H, s), 2.40 (3H, s).

Molecule **11**: Melting point: 140-142 °C, Yield: 75%

IR (KBr,  $\text{cm}^{-1}$ ): 3270, 3084, 2917, 1460, 1373, 1331, 1161, 1080, 907, 837, 789, 772.

$^1\text{H}$ -NMR ( $\text{CDCl}_3$ ):  $\delta$  7.67 (1H, s), 7.52 (1H, d,  $J=8$ ), 7.47 (1H, d,  $J=8$ ), 7.35 (1H, t,  $J=8$ ), 7.03 (1H, t,  $J=8$ ), 6.95 (2H, d,  $J=8$ ), 6.00 (1H, s), 1.99 (6H, s).

Molecule **12**: Melting point: 102-104 °C, Yield: 56%

IR (KBr,  $\text{cm}^{-1}$ ): 3260, 2961, 1456, 1383, 1339, 1261, 1167, 1080, 907, 872, 793, 773.

$^1\text{H}$ -NMR ( $\text{CDCl}_3$ ):  $\delta$  7.60 (1H, s), 7.49-7.46 (2H, m), 7.32 (1H, t,  $J=8$ ), 7.16 (1H, d,  $J=3$ ), 7.09-7.03 (2H, m), 6.21 (1H, s), 2.48 (3H, s).

Molecule **13**: Melting point 153-156 °C, Yield: 39%

IR (KBr, cm<sup>-1</sup>): 3259, 1567, 1448, 1341, 1167, 1088, 779, 753.

<sup>1</sup>H-NMR (CDCl<sub>3</sub>): δ 7.85 (2H, d, *J*=8), 7.62 (2H, t, *J*=8), 7.52 (2H, t, *J*=8), 7.28 (2H, d, *J*=8), 7.21 (1H, t, *J*=8), 6.45 (1H, s).

Molecule **14**: Melting point: 91-93 °C, Yield: 70%

IR (KBr, cm<sup>-1</sup>): 3217, 3040, 2917, 2861, 1464, 1397, 1337, 1298, 1159, 997, 914, 828.

<sup>1</sup>H-NMR (CDCl<sub>3</sub>): δ 10.20 (1H, s), 8.31 (1H, s), 7.72-7.68 (2H, m), 7.62 (1H, t, *J*=8), 7.06 (2H, d, *J*=8), 6.97 (2H, d, *J*=8), 2.19 (3H, s).

Molecule **15**: Melting point: 98-100 °C, Yield: 74%

IR (KBr, cm<sup>-1</sup>): 3270, 2922, 2856, 1456, 1338, 1298, 1219, 1153, 914, 818, 687.

<sup>1</sup>H-NMR (CDCl<sub>3</sub>): δ 7.44 (1H, s), 7.40 (2H, d, *J*=8), 7.18-7.12 (2H, m), 6.90 (2H, d, *J*=8), 6.82 (2H, d, *J*=8), 2.21 (3H, s), 2.14 (3H, s).

Molecule **16**: Melting point: 92-94 °C, Yield: 65%

IR (KBr, cm<sup>-1</sup>): 3283, 3088, 1489, 1447, 1410, 1389, 1335, 1294, 1219, 1163, 1125, 1107, 1076, 1011, 941, 908, 883, 847, 785, 717, 675.

<sup>1</sup>H-NMR (CDCl<sub>3</sub>): δ 7.70 (1H, s), 7.53 (1H, d, *J*=8), 7.47 (1H, d, *J*=8), 7.34 (1H, t, *J*=8), 7.17 (2H, d, *J*=8), 6.95 (2H, d, *J*=8), 6.40 (1H, s).

Molecule **17**: Melting point: 82-84 °C, Yield: 87%

IR (KBr, cm<sup>-1</sup>): 3256, 2916, 2849, 1491, 1452, 1385, 1329, 1223, 1153, 1082, 1013, 910.

<sup>1</sup>H-NMR (CDCl<sub>3</sub>): δ 7.59 (1H, s), 7.56 (1H, d, *J*=7), 7.36-7.30 (2H, m), 7.21 (2H, d, *J*=8), 7.02 (2H, d, *J*=8), 6.84 (1H, s), 2.37 (3H, s).

Molecule **18**: Melting point: 108-111 °C, Yield: 80%

IR (KBr, cm<sup>-1</sup>): 3250, 2897, 1497, 1408, 1329, 1273, 1163, 1140, 1090, 917, 897, 818.

<sup>1</sup>H-NMR (CDCl<sub>3</sub>): δ 7.68 (2H, d, *J*=8), 7.23 (2H, d, *J*=8), 7.15 (1H, s), 6.86-6.72 (3H, m), 2.36 (3H, s).

Molecule **19**: Melting point: 156-158 °C, Yield: 82%

IR (KBr, cm<sup>-1</sup>): 3235, 2924, 1609, 1495, 1458, 1389, 1329, 1287, 1260, 1227, 1161, 1088, 1049, 931, 889, 812, 702, 683.

<sup>1</sup>H-NMR (CDCl<sub>3</sub>): δ 9.17 (1H, s), 7.01 (2H, d, *J*=8), 6.58 (2H, d, *J*=8), 6.32 (2H, d, *J*=8), 6.19-6.13 (2H, m), 2.35 (3H, s), 1.98 (3H, s).

Molecule **20**: Melting point: 141-144 °C, Yield: 74%

IR (KBr,  $\text{cm}^{-1}$ ): 3235, 2928, 2868, 1597, 1510, 1474, 1406, 1333, 1271, 1167, 1116, 1090, 966, 901, 810, 679.

$^1\text{H-NMR}$  ( $\text{CDCl}_3$ ):  $\delta$  7.67 (2H, d,  $J=8$ ), 7.26 (2H, d,  $J=8$ ), 7.08 (1H, s), 6.89 (1H, d,  $J=4$ ), 6.71 (1H, d,  $J=4$ ), 2.39 (3H, s), 2.28 (3H, s).

#### 4.11 References

- (a) M. C. Etter, J. C. Macdonald, J. Bernstein, *Acta Crystallogr.* **1990**, *B46*, 256; (b) M. C. Etter, S. M. Reutzel, *J. Am. Chem. Soc.* **1991**, *113*, 2586; (c) G. R. Desiraju, *Angew. Chem. Int. Ed. Engl.* **1995**, *34*, 2311; (d) G. R. Desiraju, Eds., *The Crystal as a Supramolecular Entity; Perspectives in Supramolecular Chemistry*, Wiley: Chichester, 1996, Vol. 2; (e) A. Nangia, G. R. Desiraju, *Top. Curr. Chem.* **1998**, *198*, 57; (f) J. W. Steed, J. L. Atwood, *Supramolecular Chemistry*, Wiley, Chichester, 2000; (g) G. R. Desiraju, *Curr. Sci.* **2001**, *81*, 1038; (h) G. R. Desiraju, *Nature* **2001**, *412*, 397; (i) B. Moulton, M. J. Zaworotko, *Chem. Rev.* **2001**, *101*, 1629; (j) E. R. T. Tiekink, J. J. Vittal (Eds.), *Frontiers in Crystal Engineering*, Wiley, 2006.
- (a) H. G. Brittan, *Polymorphism in Pharmaceutical Solids*, Marcel Dekker, New York, 1999; (b) S. R. Byrn, R. R. Pfeiffer, G. Stephenson, D. J. W. Grant, W. B. Gleason, *Solid State Chemistry of Drugs*, SSCI, West Lafayette, IN, 1999; (c) J. Bernstein, *Polymorphism in Molecular Crystals*; Oxford University Press: New York, 2002.
- (a) S. R. Chemburkar, J. Bauer, K. Deming, H. Spiwek, K. Patel, J. Morris, R. Henry, S. Spanton, W. Dziki, W. Porter, J. Quick, P. Bauer, J. Donaubauer, B. A. Narayanan, M. Soldani, D. Riley, K. McFarland, *Org. Process Res. Dev.* **2000**, *4*, 413; (b) J. Bauer, S. Spanton, R. Henry, R. Quick, W. Dziki, W. Porter, J. Morris, *Pharm. Res.* **2001**, *18*, 859; (c) K. Knapman, *Mod. Drug. Disc.* **2000**, *3*, 53; (d) S. Datta, D. J. W. Grant, *Nat. Rev. Drug. Disc.* **2004**, *3*, 42; (e) Glaxo Inc. V. Novapharm Ltd. *52F3d 1043*, *34 U. S. P. Q. 2d* (BNA), 1565 (fed. Cir. 1995).

4. (a) W. C. McCrone, *Physics and Chemistry of the Organic Solid State* (Eds.), D. Fox, M. M. Labes, A. Weissberger, 1965, Vol. 2, pp. 725-767, New York: Interscience; (b) J. Bernstein, *Polymorphism in Molecular Crystals*, Clarendon Press, Oxford, 2002; (c) N. J. Babu, L. S. Reddy, S. Aitipamula, A. Nangia, *Chem Asian J.* **2008**, 3, 1122; (d) B. Sarma, A. Nangia, *Acta Crystallogr.* **2008**, A64, C449; (e) A. Nangia, *Acc. Chem. Res.* **2008**, 41, 595; (f) B. Sarma, S. Roy, A. Nangia, *Chem Commun.* **2006**, 4918; (g) B. Sarma, A. Nangia (unpublished results).
5. W. F. Ostwald, *Z. Phys. Chem.* **1897**, 22, 289.
6. (a) G. J. Kruger, G. Gafner, *Acta Crystallogr.* **1971**, B27, 326; (b) T. Gelbrich, D. S. Hughes, M. B. Hursthouse, T. L. Threlfall, *CrystEngComm.* **2008**, 10, 1328; (c) C. H. Koo, Y. J. Lee, *Arch. Pharm. Res.* **1979**, 2, 99; (d) I. Bar, J. Bernstein, *Eur. Cryst. Meeting* **1982**, 7, 182; (e) A. K. Basak, S. Chaudhuri, S. K. Mazumdar, *Acta Crystallogr.* **1984**, C40, 1848; (f) J. Bernstein, *Acta Crystallogr.* **1988**, C44, 900; (g) I. Bar, J. Bernstein, *J. Pharm. Sci.* **1985**, 74, 255; (h) P. A. Ajibade, G. A. Kolawole, P. Ó'Brien, M. Helliwell, J. Raftery, *Inorg. Chim. Acta.* **2006**, 359, 3111.
7. T. Gelbrich, M. B. Hursthouse, T. L. Threlfall, *Acta Crystallogr.* **2007**, B63, 621.
8. Cambridge Structural Database, version 5.30, ConQuest 1.11, May 2009 update.
9. (a) M. M. Parmar, O. Khan, L. Seton, J. L. Ford, *Cryst. Growth Des.* **2007**, 7, 1635; (b) S. L. Morissette, Ö. Almarsson, M. L. Peterson, J. F. Remenar, M. J. Read, A. V. Lemmo, S. Ellis, M. J. Cima, C. R. Gardner, *Adv. Drug Deliv. Rev.* **2004**, 56, 275.
10. (a) R.K. Gilpin, W. Zhou, *Vibrational Spectroscopy* **2005**, 37, 53; (b) G. Reich, *Adv. Drug Deliv. Rev.* **2005**, 57, 1109; (c) J. Aaltonen, J. Rantanen, S. Siirila, M. Karjalainen, A. Jørgensen, N. Laitinen, M. Savolainen, P. Seitavuopio, M. L. -Kultanen, J. Yliruusi, *Anal. Chem.* **2003**, 75, 5267; (d) A. Brillante, I. Bilotti, R. G. D. Valle, E. Venutia, A. Girlando, *CrystEngComm* **2008**, 10, 937; (e) A. M. Tudor, S. J. Church, P. J. Hendra, M. C. Davies, C. D. Melia, *Pharm. Res.* **1993**, 10, 1772; (f) U. Griesser, A. Burger, K. Mereiter, *J. Pharm. Res.* **1997**, 86, 352.
11. (a) S. Khoshkhoo, J. Anwar, *J. Phys. D. Appl. Phys.* **1993**, 26, B90; (b) T. Threlfall, *Org. Proc. Res. Dev.* **2000**, 4, 384; (c) N. Blagden, *Powder Technol.*

- 2001**, 121, 46; (d) N. Blagden, R. J. Davey, H. F. Lieberman, L. Williams, R. Payne, R. Roberts, R. Rowe, R. J. Docherty, *Chem. Soc., Faraday Trans.* **1998**, 94, 1035; (e) M. M. Parmar, O. Khan, L. Seton, J. L. Ford, *Cryst. Growth Des.* **2007**, 7, 1635; (f) C. -H. Gu, V. Young Jr. D. J. W. Grant, *J. Pharm. Sci.* **2001**, 90, 1878; (i) E. Smakula, A. Gori, H. H. Wotiz, *Spectrochim. Acta.* **1957**, 9, 346.
12. B. T. Gowda, S. Foro, K. S. Babitha, H. Fuess, *Acta Crystallogr.* **2008**, E64, o1691.
13. G. A. Jeffrey, *An Introduction to Hydrogen Bonding*, Oxford University Press, New York, 1997.
14. J. Bernstein, R. E. Davis, L. Shimon, N. L. Chang, *Angew. Chem., Int. Ed. Engl.* **1995**, 34, 1555.
15. (a) A. I. Kitaigorodskii in *Molecular Crystals and Molecules*, Academic Press, London, 1973; (b) M. D. Cohen, G. M. J. Schmidt, *J. Chem. Soc.* **1964**, 1996; (c) G. M. J. Schmidt in *Reactivity of the Photoexcited Organic Molecules*, Interscience, New York, 1967; (d) L. Addadi, M. Lahav, *Pure Appl. Chem.* **1979**, 51, 1269; (e) G. R. Desiraju, J. A. R. P. Sarma, *Proc. Indian Acad. Sci (Chem. Sci.)* **1986**, 96, 599; (f) P. K. Thallapally, K. Chakraborty, H. L. Carrell, S. Kotha, G. R. Desiraju, *Tetrahedron*, **2000**, 56, 6721; (g) N. N. Laxmi Madhavi, A. K. Katz, H. L. Carrell, A. Nangia, G. R. Desiraju, *Chem. Commun.* **1997**, 1953; (h) R. Banerjee, R. Mondal, J. A. K. Howard, G. R. Desiraju, *Cryst. Growth Des.* **2006**, 6, 999; (i) B. Omondi, M. A. Fernandes, M. Layh, D. C. Levendis, J. L. Look, T. S. P. Mkwizu, *CrystEngComm* **2005**, 7, 690; (j) L. Fábíán and A. Kálmán, *Acta Crystallogr.*, **1999**, B55, 1099; (k) A. Kálmán, L. Párkányi, G. Argay, *Acta Crystallogr.* **1993**, B49, 1039; (m) A. Kálmán, L. Párkányi, *Adv. Mol. Struct. Res.* **1997**, 3, 189; (n) N. K. Nath, B. K. Saha, A. Nangia, *New J. Chem.* **2008**, 32, 1693; (o) C. R. Theocharis, G. R. Desiraju, W. Jones, *J. Am. Chem. Soc.* **1984**, 106, 3606.
16. (a) A. Kálmán, G. Argay, D. Scharfenberg-Pfeiffer, E. Höhne, B. Ribár, *Acta Crystallogr.* **1991**, B47, 68; (b) A. Anthony, M. Jaskoński, A. Nangia, **2000**, B56, 512.

17. (a) P. T. Cardew, R. J. Davey, *Tailoring of Crystal Growth; Institution of Chemical Engineers*: Rugby, England, 1982, ISBN 0-9066-3623-X; (b) T. Threlfall, *Org. Proc. Res. Dev.* **2000**, *4*, 384.
18. (a) M. Trifkovic, S. Rohani, *Org. Proc. Res. Dev.* **2007**, *11*, 138.
19. (a) N. Blagden, R. J. Davey, *Cryst. Growth Des.* **2003**, *3*, 873; (b) N. Blagden, W. I. Cross, R. J. Davey, M. Broderick, R. G. Pritchard, R. J. Roberts, R. C. Rowe, *Phys. Chem. Chem. Phys.* **2001**, *3*, 3819; (c) C. Stoica, P. Verwer, H. Meekes, P. J. C. M. van Hoof, F. M. Kaspersen, E. Vlieg, *Cryst. Growth Des.* **2004**, *4*, 765; (d) I. Weissbuch, V. Y. Torbeev, L. Leiserowitz, M. Lahav, *Angew. Chem. Int. Ed. Engl.* **2005**, *44*, 3226; (e) Kitamura, M. et al. *Cryst. Growth Des.* **2006**, *6*, 1945; (f) M. Trifkovic, S. Rohani, M. Mirmehrabi, *Org. Proc. Res. Dev.* **2007**, *11*, 138; (g) L. L. Dematos, A. C. Williams, S. W. Booth, C. R. Petts, D. J. Taylor, N. Blagden, *J. Pharm. Sci.* **2006**, *96*, 1069.
20. (a) J. Raltonen, J. Rantanen, S. Siiria, M. Karjalainen, A. Jørgensen, N. Laitinen, M. Savolainen, P. Seitavuopio, M. L. -Kultanen, J. Yliruusi, *Anal. Chem.* **2003**, *75*, 5267; (b) A. Brillante, I. Bilotti, R. G. D. Valle, E. Venutia, A. Girlandob, *CrystEngComm* **2008**, *10*, 937; (c) A. Brillante, R. G. Della Valle, L. Farina, A. Girlando, M. Masino and E. Venuti, *Chem. Phys. Lett.* **2002**, *357*, 32; (d) T. Siegrist, C. Besnard, S. Haas, M. Schiltz, P. Pattison, D. Chernyshov, B. Batlogg, C. Kloc, *Adv. Mater.* **2007**, *19*, 2079; (e) M. Allesø, S. Velaga, A. Alhalaweh, C. Cornett, M. A. Rasmussen, F. van den Berg, H. L. Diego, J. Rantanen, *Anal. Chem.* **2008**, *80*, 7755.
21. R. M. Silverstein, G. C. Bassler, T. C. Morrill, *Spectrometric Identification of Organic Compounds*, John Wiley & Sons, Inc.
22. (a) D. E. Braun, T. Gelbrich, V. Kahlenberg, R. Tessadri, J. Wieser, U. J. Griesser, *J. Pharm. Sci.* **2009**, *98*, 2010; (b) W. C. Schinzer, M. S. Bergren, D. S. Aldrich, R. S. Chao, M. J. Dunn, A. Jeganathan, L. M. Madden, *J. Pharm. Sci.* **1997**, *86*, 1426; (c) K. Kimura, F. Hirayama, K. Uekama, *J. Pharm. Sci.* **1999**, *88*, 385; (d) C. -H. Gu, V. Young Jr., D. J. W. Grant, *J. Pharm. Sci.* **2001**, *90*, 1878; (e) G. G. Z. Zhang, C. Gu, M. T. Zell, R. T. Burkhardt, E. J. Munson; *J. Pharm. Sci.* **2002**, *91*, 1089; (f) Y. Gong, B. M. Collman, S. M. Mehrens, E. Lu, J. M. Miller, A. Blackburn, D. J. W. Grant, *J. Pharm. Sci.* **2008**, *97*, 2130.



23. (a) D. J. Good, N. Rodríguez-Hornedo, *Cryst. Growth Des.* **2009**, *9*, 2252; (b) A. Jayasankar, L. S. Reddy, S. J. Bethune, N. Rodríguez-Hornedo *Cryst. Growth Des.* **2009**, *9*, 889; (c) A. Burger, R. Ramberger, *Mikrochim. Acta*, **1979**, *II*, 271; (d) A. V. Trask, W. D. S. Motherwell, W. Jones, *Chem. Commun.* **2004**, 890; (e) A. V. Trask, N. Shan, W. D. S. Motherwell, W. Jones, S. Feng, R. B. H. Tan, K. J. Carpenter, *Chem. Commun.* **2005**, 880; (f) A. V. Trask, J. van de Streek, W. D. S. Motherwell, W. Jones, *Cryst. Growth Des.* **2005**, *5*, 2233; (g) T. Friččić, W. Jones, *Cryst. Growth Des.* **2009**, *9*, 1621; (h) S. Aitipamula, P. S. Chow, R. B. H. Tan, *CrystEngComm* **2009**, *11*, 889; (i) S. Karki, T. Friččić, W. Jones, *CrystEngComm* **2009**, *11*, 470;
24. (a) B. Pirotte, B. Maserrel, J. Delarge, *Acta Crystallogr.* **1995**, *C51*, 507.
25. (a) B. Sarma, S. Roy, A. Nangia, *Chem. Commun.* **2006**, 4918; (b) ) S. Roy, R. Banerjee, A. Nangia, G. J. Kruger, *Chem. Eur. J.* **2006**, *12*, 3777; (c) S. Long, S. Parkin, M. A. Siegler, A. Cammers, T. Li, *Cryst. Growth Des.* **2008**, *8*, 4006; (d) J. R. Cox, L. A. Ferris, V. R. Thalladi, *Angew. Chem., Int. Ed. Engl.* **2007**, *46*, 4333.
26. (a) A. K. Basak, S. Chaudhuri, S. K. Mazumdar, *Acta Crystallogr.* **1984**, *C40*, 1848 [BEWKUJ04]; (b) I. Bar, J. Bernstein, *J. Pharm. Sci.* **1985**, *74*, 255 [BEWKUJ11, BEWKUJ13]; (c) T. Gelbrich, T. L. Threlfall, A. L. Bingham, M. B. Hursthouse, *Acta Crystallogr.* **2007**, *C63*, o323 [BEWKUJ14]; (d) D. S. Hughes, M. B. Hursthouse, T. Threlfall, S. Tavener, *Acta Crystallogr.* **1999**, *C55*, 1831 [SUTHAZ]; (e) T. Gelbrich, D. S. Hughes, M. B. Hursthouse, T. L. Threlfall, *CrystEngComm* **2008**, *10*, 1328 [SUTHAZ05]; (f) G. P. Bettinetti, F. Giordano, A. L. Manna, G. Giuseppetti, C. Tadini, *Cryst. Struct. Commun.* **1982**, *11*, 821 [SLFNMB01 and SLFNMB02]; (g) C. P. Price, A. L. Grzesiak, A. J. Matzger, *J. Am. Chem. Soc.* **2005**, *127*, 5512 [SLFNMB05 and SLFNMB06]; (h) N. Nagel, H. Bock, P. Eller, *Acta Crystallogr.* **2000**, *B56*, 234 [FIBKUW01 and FIBKUW02]; (i) M. B. Hursthouse, T. L. Threlfall, S. J. Coles, S. C. Ward, University of Southampton, *Crystal Structure Report Archive*, 1999 [SULAMD07, SULAMD08 and SULAMD09].
27. (a) I. Halebian, W. McCrone, *J. Pharm. Sci.* **1969**, *58*, 8911; (b) W. Cabri, P. Ghetti, G. Pozzi, M. Alpegiani, *Org. Process Res. Dev.* **2007** *11*, 64; (c) B. R. –

Spong, C. P. Price, A. Jayasankar, A. J. Matzger, N. Rodríguez-Hornedo, *Adv. Drug Deliv. Rev.* **2004**, 56, 241; (d) A. Llinas, J. M. Goodman, *Drug Disc. Today* **2008**, 13, 198.



---

## TETRAHEDRAL AND H-SHAPED HOST TECTONS

---

### 5.1 Introduction

Porous solids<sup>1</sup> based on organic building blocks are an important class of materials that have been studied extensively for several decades because they have the potential for rational construction by employing crystal engineering principles.<sup>2</sup> Design, synthesis and characterization of porous materials is an active topic in chemistry, biology and materials science. Properties of these materials, such as high surface area and pore size (less than 2 nm for micropores, 2-50 nm for mesopores and above 50 nm are macropores) comparable in size to small molecules, have attracted attention because of applications in chemical separation, catalysis, and gas storage.<sup>3</sup> Zeolites and activated carbons are two widely used microporous materials in catalysis, chemical separation, and small molecule adsorption. Porosity is described as the fraction of void space in the material, where the void may contain guest molecules, for example, solvents, air or water. Another possibility to fill the void space is the interpenetration of host molecules through hydrogen bond or other intermolecular interactions. Construction of porous material in organic system is more difficult as hydrogen bonds are weaker and less directional than metal–heteroatom and metal–ligand bonds which means that the geometry of organic structures is not as clearly definable as that at metal centers in microporous metal-organic frameworks (MOFs).<sup>4</sup> Weber proposed<sup>5</sup> rules for the design of host framework after extensive studies of aromatic molecules: (i) bulky and awkward shape; (ii) rigid framework which can survive upon guest loss; (iii) high affinity functional groups for strong and directional synthon and (iv) an overall balanced shape to achieve close- packing in the host–guest crystal after an extensive study on a series of aromatic molecules. The guest molecules can be incorporated in the adjustable cavities upon crystallization because of more frequently observed channels and cavities formed

by inclusion host compounds. Helical molecules can form channel along its axis, however macrocycles can be stacked without off-set to form cylinder and cavities. The organic channel structures are more attractive than the cage framework due to its fascinating applications and functions of tubular structure in biological systems, e.g. construction of carbon nanotubes<sup>6a</sup>. Cyclic oligosaccharides,<sup>6b</sup> cyclic peptides,<sup>6c</sup> bile acids,<sup>6d</sup> helical tubular diols,<sup>6e</sup> cyclodextrins,<sup>6f</sup> urea, thiourea,<sup>6g</sup> perhydrotriphenylene,<sup>6h</sup> tri-o-thymotide,<sup>6i</sup> triphenylphosphazene,<sup>6j</sup> dianin's compounds,<sup>6k</sup> etc. are some of the well known organic host materials reported in recent years. Nangia *et. al.* showed<sup>1a,b</sup> the construction of open molecular frameworks which offer the promise of specific structures, functions and properties via hydrogen bond synthon approach for functionalized organic molecules in inclusion complexes. Wheel-axle topology through carboxylic acid dimer of 4-tritylbenzoic acid<sup>7a</sup> crystallizes as microporous framework leaving space for guest inclusion in their crystal structure, 4-halo and nitrophenoxy triazines [2,4,6-Tris(4-chlorophenoxy)-1,3,5-triazine; 2,4,6-Tris(4-nitrophenoxy)-1,3,5-triazine]<sup>7b,c,d</sup> self assembled as hexagonal channel hosts and 4,4'-bis(4'-biphenyl)cyclohexa-2,5-dienone<sup>7e</sup> behave as clay mimic organic host. Host-guest chemistry of T-shaped<sup>7f</sup> and H-shaped<sup>8</sup> organic molecules were discussed and the hydrogen bonded networks present in their structures were analyzed systematically. Polymorphism in solvent free methods of the popular host 1,1-bis-(4-hydroxyphenyl) cyclohexane<sup>9</sup> and isomeric dihydroxybenzoic acids were discussed<sup>9a</sup> in chapter 2. Shimizu *et. al.* have reported<sup>6m</sup> crystal structure of macro cyclic bis-urea which self-assemble via N-H...O H-bonding to form nano tube and functions as zeolite showing reversible guest uptake. The self-complementarity strategy for designing rigid crystal structures of bis(resorcinol) and mono(resorcinol) derivatives of anthracene was extensively studied by Aoyama and co-workers<sup>10</sup> to develop crystal engineering approaches. These molecules show organic zeolite like properties. Guest exchange properties and host-guest chemistry of the fascinating molecule calix[4]arene<sup>11</sup> and its various derivatives were widely studied. The large and unoccupied voids in their crystal lattice are stabilized by van der Waals forces. Volatile guest molecules like methane, freons etc. are entrapped in the voids. In biology, transmembrane ion channels are believed to be responsible for chemical information and internal surfaces of protein tubes

enhance the enzyme activity through functional group complementarity and chemical catalysis, protein folding and protein degradation enzymes.

Hydrated structures have attracted considerable attention from structural chemists to biologists because of their different topologies in the structure, conformation and function of nucleotides and peptides as well as in protein–DNA binding and in the pharmaceuticals. If water clusters are trapped in the cavity of organic or metal–organic host framework are known as hydrated clathrates that show significant variation in their nature. The included water molecules can form discrete and extended motifs, e.g. finite and infinite chains, ring motifs and different topologies. In biological systems water channels have been found and water topology is widely studied because of its application in water and ion transport.<sup>12</sup> In red blood cells and the renal tubules water can rapidly and selectively cross the plasma membrane. Thus water release from the interface, in general, is favored entropically but enthalpically unfavorable. Infantes and co-workers<sup>13a-d</sup> reported that 6.6% of organic compounds are hydrated and this value increases to 75% for bioactive pharmaceutical compounds. They categorized and ranked different functional groups which promote hydration. Though water molecules always prefer to form the pattern of two donor (OH) and one acceptor (O) hydrogen bonds,<sup>13c</sup> one may think that small ratio of donor/acceptor would result hydrates to balance the ratio. In fact, this ratio does not have any significant effect on the frequency of hydrate formation showed by Infantes<sup>13c</sup> after analyzing organic crystal hydrates extracted from CSD. Molecules containing charged or strong H-bonding functional groups favor hydration or entrapment of waters. One-dimensional water chain structures constitute a potentially important form of water. Many fundamental biological processes depend on water chains.<sup>14</sup> Ordered water chain motif is involved in proton transport in Gramicidin-A.<sup>14f,g,h</sup> 1D chain is generally stabilized by strong H-bonding between neighboring waters along the chain and functional groups along the channel wall. Buchanan<sup>14i</sup> *et. al.* have trapped water chains in the crystal structures of 4,4'-methylene-bis(2,5-dimethylimidazole) and 1-methylimidazole-4-carboxaldehyde and showed that these water chains in the small molecular lattice channel can serve as a model for biological proton wires. Ripmeester<sup>14j</sup> and his research group showed that the water chain included in the channel of hydrophobic molecule tris(5-acetyl-3-thienyl)methane crystal is capable of water transport.

Tetrakis(4-sulfophenyl)methane<sup>14a</sup> (**21**, Figure 1a), hereafter TPM-SO<sub>3</sub>H, was synthesized to study their thermal analysis and structural chemistry. The structural and thermal behavior of sulfonic acid at the tetrahedral periphery has not been explored in detail. Porous architectures and network solids have important applications. H-shaped molecule 1,4-di[bis(4'-hydroxyphenyl)methyl]benzene (**22**) and its octamethyl derivative (**23**) were synthesized (Figure 5) and crystallized in solvated and guest-free forms to analyze the occurrence of specific network architectures. Selective and reversible water uptake by TPM-SO<sub>3</sub>H, (**21**) an organic host and the rare hydrogen bonded network topologies present in H shaped molecules (**22**, **23**) are analyzed and discussed.

## 5.2 Results and Discussion

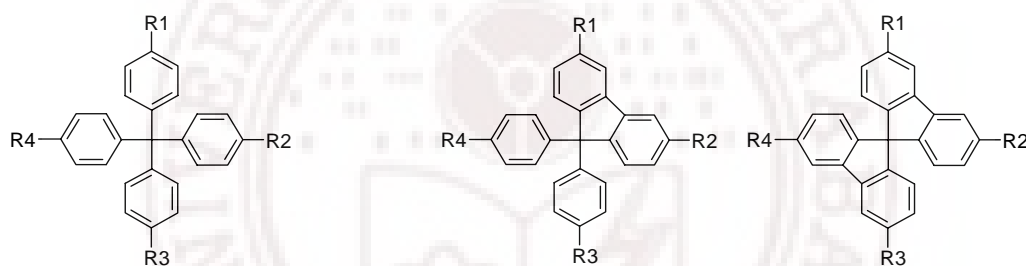
### A. Tetrakis(4-sulfophenyl)methane - An Organic Host Hydrate

#### (i) Tetrahedral Tecton

Supramolecular architectures can be built from molecular tectonics<sup>15a</sup> defined by Wuest as the supramolecular construction using tectonic subunits (molecules with sticky functional groups). The word “tecton” is taken from Greek for “builder”. Wuest has popularized<sup>15</sup> the concept of molecular tectonics. Tetrahedral molecular scaffolds are versatile building blocks that can be used for the construction of interpenetrated networks.<sup>16a,b</sup> Host–guest chemistry<sup>16c-f</sup> has been carried out on tetrahedral building blocks using many functional groups but chemistry of sulfonic acid at the tetrahedral periphery is sparse. Sulfonated calixarenes<sup>16g-i</sup> are well known in host-guest inclusion and supramolecular chemistry. Tetrahedral molecules like tetraphenylmethanes have always offered opportunities for the study of predictable tetrahedral molecular packing<sup>17</sup> and its solid-state properties. Kitaigorodskii<sup>18</sup> first recognized that molecules of tetrahedral type Ph<sub>4</sub>X (X = C, Si, Ge, Pb, Sn) form isomorphous series in tetragonal crystal symmetry. In addition to C at the tetrahedral core e.g. as in tetraphenylmethanes, Si and adamantane group<sup>16f,19</sup> with *para*-substituted phenyl rings are also reported. Crystal structures of symmetrical molecules are extensively studied having strong H bonding functional groups, halogens, ethynyl, and various heterocycles at the periphery (4 identical R groups) but there are a few examples of unsymmetrical molecules as well (different R groups) in crystal engineering<sup>20</sup>. Most of the reported structures are covered and summarized in Scheme 1. Metal ions e.g. of Ag, Ba etc. coordinated to sulfonate



with adamantane based tetrahedral tectons are studied.<sup>21a,b</sup> Tetrafunctional adamantane-based ligands particularly afford rigid framework which typically direct the diamondoid assemblies. However Ba sulfonates exclusively form layer structure. It is common that tetraphenyl methanes crystallize in a columnar architecture usually in tetragonal or monoclinic space groups, e.g.  $I4_1/a$ ,  $I\bar{4}$ ,  $C2/c$ , etc. In general they organize in diamondoid, rhombohedral or columnar type assembly directed by the molecular node and supramolecular synthon of tetrahedron symmetry. This is because the tetrahedrally oriented arms fit into the voids created by the molecular core of the same symmetry. Tetraphenyl methanes and silanes with boronic acid group include guest species to the extent of 60-65% in inter-connected channels (Figure 1c)<sup>19c</sup>. However, structural chemistry of sulfonic acid group has not been studied in tetrahedral molecules particularly in tetraphenylmethanes.



1. R1=R2=R3=R4= CN; NH<sub>2</sub>; N=C=S; NHCOOR; I; Br; NHCONH<sub>2</sub>; NHCONHR; C<sub>6</sub>(Ph)<sub>5</sub>; N(2'-Pyridone)<sub>2</sub>; OH; COOH; C\*\*\*CH; H; CH<sub>2</sub>Cl; NO<sub>2</sub>; NHCOMe; C\*\*\*CPh; CH=CHPh; C\*\*\*C-C\*\*\*C-C(Me<sub>2</sub>)(OH); C\*\*\*CBr; I(OCOMe)<sub>2</sub>

R1, R2, R3, R4 are functional groups such as OH; NO(t-Bu); CH<sub>2</sub>OH; COOH; H; CN; NHCOMe; CHO; CH=C(CN)<sub>2</sub>; Br; NH<sub>2</sub>; t-Bu; NO<sub>2</sub>

2. R1=R2=R3= C<sub>6</sub>H<sub>2</sub>(2'-OH-3'-t-Bu-5'-Me), R4= H
  3. R1=R2=R3=H, R4= CONH<sub>2</sub>
  4. R1=R2= NO<sub>2</sub>, R3=R4= H
  5. R1=R2=R3= H, R4= OH
  6. R1=R2=R3= CH<sub>3</sub>, R4= H
  7. R1=R2=R3= COOH, R4= H
  8. R1=R2= C\*\*\*CH, R3=R4= Br
  9. R1=R2=R3 = C\*\*\*CH, R4 = Br
  10. R1=R2=R3 = H, R4= OH
  11. R1=R2= NO<sub>2</sub>, R3=R4 = I
- where \*\*\* = triple bond

**Scheme 1** List of tetrahedral tectons having the tetraphenylmethane aromatic core and diverse R groups reported in literature.

## (ii) Synthesis and Structural Analysis

TPM-SO<sub>3</sub>H (**21**, Figure 1a) was synthesized<sup>21d</sup> by the *para*-sulfonation of tetraphenylmethane with chlorosulfonic acid in 93% yield. The compound is highly soluble in water and alcoholic solvents. Needle shaped X-ray diffraction quality single crystals were prepared by recrystallization from MeOH at room temperature. Single crystal data was collected on Bruker SMART APEX CCD diffractometer with graphite-monochromator Mo-K $\alpha$  radiation ( $\lambda$  = 0.71073 Å) at 100K. Structure solution and refinement showed the asymmetric unit contains  $\frac{1}{4}$  TPM-SO<sub>3</sub>H molecule and 3 water molecules in *I*4<sub>1</sub>/*a* space group (Figure 1b), giving a host: guest ratio of 1:12. One SO<sub>3</sub> oxygen is disordered over two positions (s.o.f. O1A 0.30, O1B 0.70; O2 and O3 are fully ordered) otherwise the aromatic hydrocarbon core is ordered in the crystal structure. S – O bond distances indicate that S–O1 is a single bond [S – O1A, 1.546(4) Å; S – O1B, 1.48(7) Å] whereas S = O2 and S = O3 are double bonds [1.426(4) Å, 1.446(4) Å] in the sulfonic acid group.

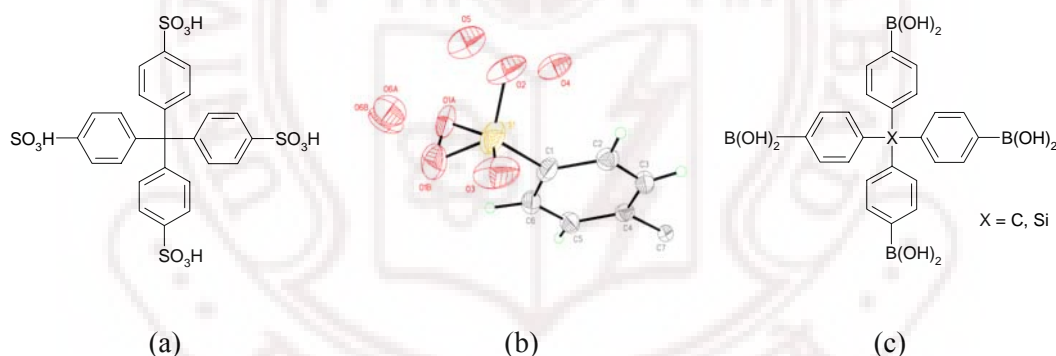
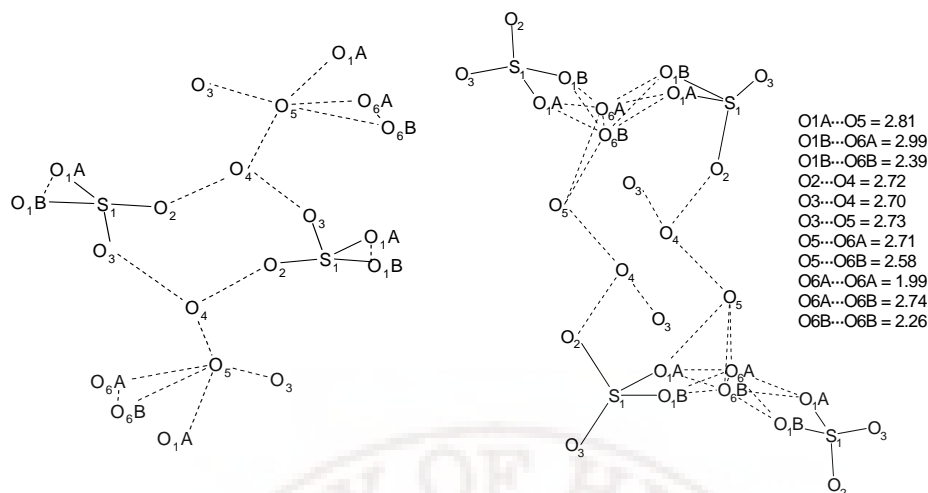


**Figure 1** (a) Tetrakis(4-sulfophenyl)methane (TPM-SO<sub>3</sub>H), (b) ORTEP of TPM-SO<sub>3</sub>H ( $\frac{1}{4}$  molecule) and water (3 molecules). (c) Reported tetraphenyl methanes and silanes with boronic acid group include guest species to the extent of 60-65% in inter-connected channels. Of the three water molecules, two O atoms have full occupancy (O4, O5) while the third water is distributed over two positions (O6A, O6B, s.o.f. 0.25 each). Hydrogen atoms of neither the SO<sub>3</sub>H group nor water molecules could be located in difference electron density map. There are no direct SO<sub>3</sub>H $\cdots$ SO<sub>3</sub>H hydrogen bonds in the crystal structure. The inclusion of three symmetry-independent water molecules and strong SO<sub>3</sub>H group produce an extended network of O–H $\cdots$ O hydrogen bonds shown in Scheme 2. O $\cdots$ O distances are in the typical range (2.4-3.0 Å) for strong, cooperative H bonds. The list of O $\cdots$ O and C–H $\cdots$ O distances are given in Table 1 and Table 2 respectively.



**Scheme 2** Hydrogen bond networks of SO<sub>3</sub>H group and H<sub>2</sub>O molecules. O...O distances are given in Å.

**Table 1** O...O and O...H distances in H bonds calculated using PLATON.

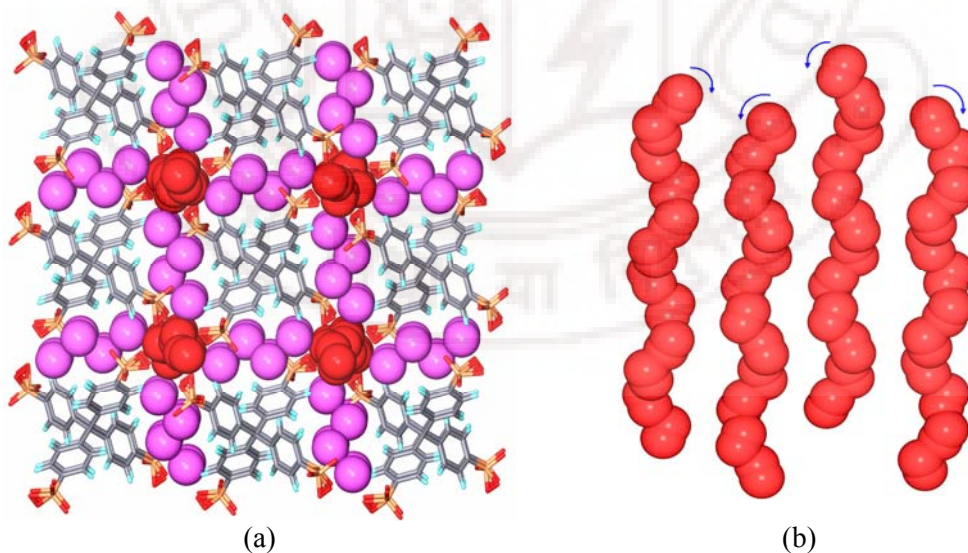
| Interaction | Distance /Å            |           |
|-------------|------------------------|-----------|
|             | < $\Sigma$ vdW = 3.0 Å | 3.0-4.0 Å |
| O1A...O5    | 2.810(12)              | -         |
| O1A...H6    | 2.48(4)                | -         |
| O1B...O5    | -                      | 3.842(8)  |
| O1B...O6B   | 2.39(3)                | -         |
| O1B...O2    | -                      | 3.838(8)  |
| O1B...O5    | -                      | 3.306(9)  |
| O1B...O6B   | -                      | 3.40(3)   |
| O1B...H6    | -                      | 3.39(4)   |
| O1B...O6A   | 2.60(2)                | -         |
| O1B...O6B   | 2.89(2)                | -         |
| O2...O5     | -                      | 3.468(6)  |
| O2...H6     | 2.60(4)                | -         |
| O2...O4     | 2.716(6)               | -         |
| O3...O4     | 2.697(6)               | -         |
| O3...O5     | 2.729(6)               | -         |
| O3...O6A    | -                      | 3.66(2)   |
| O3...O6B    | -                      | 3.81(3)   |
| O3...H3     | 2.67(4)                | -         |
| O6A...O5    | 2.71(2)                | -         |
| O6A...H6    | -                      | 3.37(5)   |
| O6A...O6B   | 2.74(4)                | -         |
| O6B...O2    | -                      | 3.74(2)   |
| O6B...O5    | 2.58(2)                | -         |
| O6B...O6A   | 2.74(4)                | -         |

|           |   |         |
|-----------|---|---------|
| O6B...O6A | - | 3.34(4) |
| O6B...H6  | - | 3.11(5) |

**Table 2** C–H...O distances (neutron-normalized C–H = 1.083 Å).

| Interaction | H...O/Å | C...O/ Å | ∠C–H...O/° |
|-------------|---------|----------|------------|
| C3–H3...O3  | 2.50    | 3.467(6) | 147        |
| C5–H 5...O5 | 2.70    | 3.460(6) | 126        |
| C5–H5...O4  | 2.94    | 3.669(6) | 124        |
| C6–H6...O2  | 2.54    | 3.342(6) | 129        |

Disordered S–O1 groups make square channels of 3.5 Å on each side that includes O6 water molecules which are arranged in a helix down [001]. The four helices at the corners of TPM-SO<sub>3</sub>H host (O6 water) have opposite handedness<sup>14a,b,d</sup> (Figure 2). O4 and O5 waters are present in irregular-shaped but inter-connected channels (Figure 2b) surrounded by SO1A/B and SO2 polar groups and hydrophobic phenyl CH walls. A difference between O4, O5 and O6 water molecules is that the cooperative network of H bonds to ordered O4 and O5 waters is more extended compared to that of disordered O6 water. Whereas O6 form 1D helical chains,<sup>14d,k</sup> O4 and O5 are engaged in 2D H bond networks.



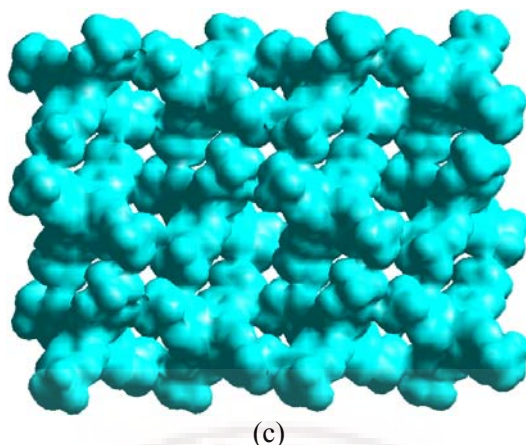


**Figure 2** (a) TPM-SO<sub>3</sub>H host layer shows two types of channels, square channels accommodate O6 water helices (red) and irregular-shaped channels contain H-bonded water molecules O4 and O5 (magenta). (b) Water helices down [001] at the four vertices have opposite handedness. O6 of partial occupancy at both sites are shown. (c) Porosity of the host molecule is shown as space filling model having 3.5 Å square channels at the vertices and irregular, interconnected channels along the sides.

### (iii) Cambridge Crystallographic Database Analysis

Free volume in the host molecule for solvent inclusion and solvent occupied volume in the crystal structure were calculated in PLATON (Table 3). Only organic crystal structures having no disorder, no errors, not polymeric, and 3D coordinates determined were retrieved. The Cambridge Structural Database (version 5.30, ConQuest 1.11, Feb 2009 update) was searched to obtain results reported. All the crystal structures were visualized in Mercury 2.0. TPM-SO<sub>3</sub>H (Refcode HIGMUG, highlighted in bold in Table 3) has a favorable position in the list as the refcodes are arranged in decreasing order of free volume for solvent inclusion. The total available free volume in the crystal is 46.5% of which guest water molecules occupy 19.1%. This value compares well with water occupancy (by volume) in recently reported hydrates.<sup>13</sup>

A separate CSD search was carried out for dodecahydrate crystal structures and a list of 32 refcodes was extracted for organic crystal structures and listed in Table 4. The search was done by keeping the 'All Text phrase' 'dodecahydrate' and having *R*-factor < 0.10, no disorder, no error, not polymeric, and having 3D coordinates. The lower *R*-factor structure was retained for duplicate refcodes. There are 16 ordered structures and remaining 16 structures are disordered. Only in 6 structures all hydrogen atoms including those of water hydrogens were located. Three crystal structures of refcode EBIFIE,

NIQHOK and YENQOX have hydrated sulfonic acid dimer motif similar to that shown in Scheme 2 (first one).<sup>22</sup>

**Table 3** Percentage of free volume for solvent inclusion and solvent occupied volume in dodecahydrate structures (only organic structures).

| Refcode       | Free vol. for solvent inclusion | Solvent occupied volume | Refcode | Free vol. for solvent inclusion | Solvent occupied volume |
|---------------|---------------------------------|-------------------------|---------|---------------------------------|-------------------------|
| XUVBEV        | 65.94                           | -                       | DEKTOC  | 43.26                           | 14.66                   |
| XUVBAR        | 63.75                           | -                       | QOWDIP  | 42.35                           | 13.74                   |
| VOJFEF        | 61.88                           | 29.71                   | UJOFEF  | 41.43                           | 15.34                   |
| QOWDAH        | 57.49                           | 27.17                   | XOGJEI  | 40.91                           | 12.18                   |
| LASVEH        | 55.96                           | 24.46                   | KAPGAK  | 40.88                           | 9.20                    |
| EVEMOH        | 54.61                           | 27.17                   | NUJKIM  | 40.06                           | 10.38                   |
| EGILAH        | 53.17                           | 11.54                   | OGENUJ  | 39.81                           | 11.21                   |
| OMADOV        | 51.67                           | 23.52                   | XECWOS  | 39.06                           | 4.32                    |
| LOJRAD        | 49.90                           | 18.44                   | DAHHAU  | 38.48                           | 3.58                    |
| XOVLID        | 48.98                           | 22.20                   | LOJQUW  | 37.98                           | 9.54                    |
| ZADROL        | 48.87                           | -                       | QOVZUW  | 37.78                           | 10.38                   |
| BONBEL        | 48.50                           | 22.50                   | NAWSOU  | 37.06                           | 10.43                   |
| TAHHAL        | 47.75                           | 20.16                   | DEKTUI  | 36.97                           | 4.91                    |
| XOVLAV        | 47.61                           | 19.90                   | RARRIM  | 36.88                           | 9.51                    |
| NUJKEI        | 47.38                           | 17.04                   | QOLMOT  | 36.78                           | 6.04                    |
| XEBTIH        | 47.23                           | 17.31                   | EVEBAI  | 36.62                           | 8.51                    |
| EVEMUN        | 46.90                           | 13.14                   | QOWBAF  | 36.19                           | 7.93                    |
| <b>HIGMUG</b> | <b>46.50</b>                    | <b>19.10</b>            | LONDUT  | 35.77                           | 4.94                    |
| BEQFIN        | 46.30                           | 12.30                   | ABUCUV  | 35.40                           | 7.97                    |
| XOGJAE        | 46.05                           | 13.72                   | QOWBEJ  | 34.22                           | 10.43                   |
| HEXXAJ        | 45.69                           | 17.48                   | FEWDOB  | 33.49                           | 10.08                   |
| WANGAU        | 45.14                           | 18.01                   | QOWCOU  | 32.22                           | 4.22                    |
| FOMKUO        | 44.89                           | 15.14                   | QOWCIO  | 31.04                           | 4.24                    |
| BAGBAM        | 43.50                           | 14.01                   |         |                                 |                         |

**Table 4** List of CSD refcodes of dodecahydrate crystal structures

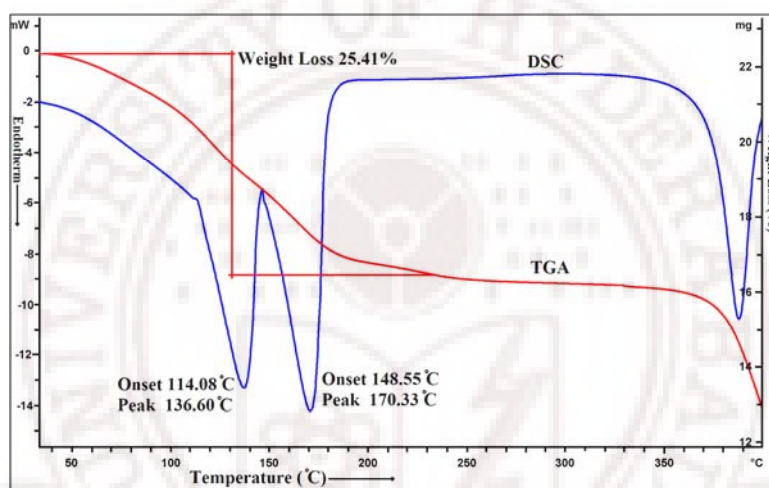
|          |        |        |          |        |          |
|----------|--------|--------|----------|--------|----------|
| ACTDGUI0 | AGAZOX | ARACEB | BCDEXD10 | EDOJOW | GOSQOU   |
| HIFKEM   | IJOLUO | IQOZIX | JOSTOA   | KAFPEN | KUTKOZ   |
| LEDRUH   | LOZMUI | LOZNAP | LOZNET   | LOZNIX | LOZNOD   |
| LOZNUJ   | MORSAN | NOJPAD | NUKFII   | OGIZIN | PAANTD01 |
| PEZNAJ   | POXKIW | REGRIE | SAFJEO10 | XIVWAA | XUSBOC   |
| ZUWQEN   | QENTIN |        |          |        |          |



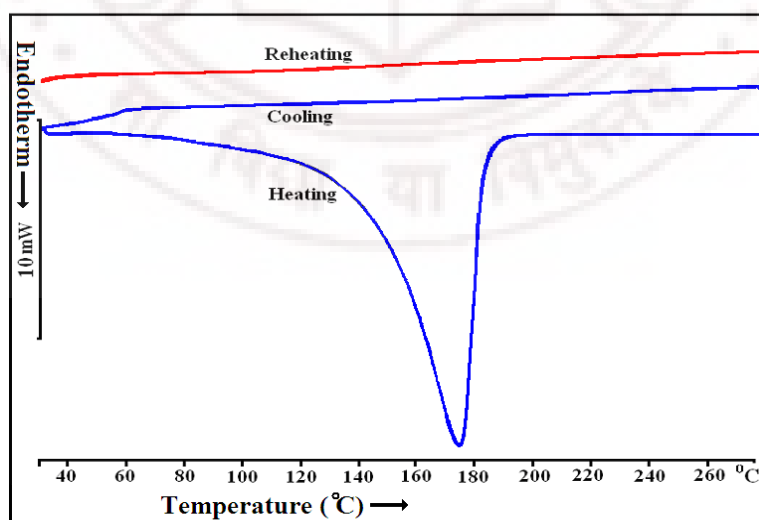
#### (iv) Differential Scanning Calorimetry, Thermo Gravimetry and XRPD

Differential scanning calorimetry (DSC) was used to observe the structural and H bonding differences between guest molecules (water). Two endothermic steps in DSC thermogram (Figure 3a) – one at 120-150 °C ( $T_{\text{peak}}$  140 °C) and second at 150-185 °C ( $T_{\text{peak}}$  165 °C) indicate two kinds of distinct water molecules that are manifested during water release. First endotherm represents release of one water molecule however second endotherm is responsible for two molecules further proved by weight loss in thermogravimetry. The total weight loss between 100-200 °C (Figure 3a) is consistent with 1:12 host: guest stoichiometry from the X-ray crystal structure (obs. 25.41%, calc. 25.23%). A similar example by Chakravarty<sup>14d</sup> showed 1D helical chains of hydrogen bonded water molecules, showing both handedness and bonded onto a helical supramolecular host formed from the self assembly of a dicopper(II) complex containing a pentadentate Schiff base and *p*-hydroxycinnamate in 1·2H<sub>2</sub>O. Two endotherms due to loss of water molecules at 61.5 and 88.5 °C in the differential scanning calorimetry were observed. The loss of O6 water helix occurs first from the parallel channels at the vertices followed by the loss of strongly bonded O4 and O5 waters from the inter-connected channels along the sides of the host molecule. Heat-cool-heat cycle in DSC showed that water is completely lost below 200 °C (Figure 3b). The sample does not absorb moisture within the DSC sample chamber, and there is no weight loss in the second heating cycle up to 280 °C. Simultaneous TG experiments were carried out for the sample completely dried at higher temperature (~200 °C) in several cycles to see the hydration-dehydration behavior (Figure 3c). Immediate TG experiment of the dried material showed negligible weight loss (Cycle I, 1.52%) however the same material showed 24.1% weight loss (Cycle I) after keeping it open to atmosphere for re-uptake of water. This rehydration upto 100% is reproducible for several cycles; three cycles are shown in Figure 3c. Decomposition of the organic host material occurs beyond 350 °C. Aluminium ethylene diphosphonate,<sup>23a</sup> Mobile Crystalline Material (MCM),<sup>23b</sup> hydroxylated poly(*N*-isopropylacrylamide),<sup>23c</sup> coordination polymers<sup>23d</sup> etc. show reversible solvent re-uptake particularly for water. The loss and uptake of water<sup>23</sup> is quantitative in three successive cycles (Figure 3c) for TPM-SO<sub>3</sub>H. Powder X-ray diffraction pattern of the solid after heating under vacuum matched with the original dodecahydrate. This suggests that the material absorbs moisture during handling and data collection time (Figure 4). PXRD

patterns **c**, **d**, **e** in Figure 4 are for the material dried at 100, 200 and 250 °C at 0.5 Torr are consistent with the PXRD pattern **a** (simulated from the crystal structure) and **b** which is for the crude TPM-SO<sub>3</sub>H. Beginning of moisture absorption is almost immediate and takes about 1.5 hrs at 60-70% humidity for 100% reuptake. The dehydrated solid was immediately coated with wax and powder XRD recorded. PXRD pattern **f** (Figure 4) showed a different crystalline phase. The single crystal of this anhydrous apohost could not be isolated and hence a complete structural and thermal characterization of this new apohost material after drying has to be done by structure determination from powder data (SDPD).



(a)



(b)

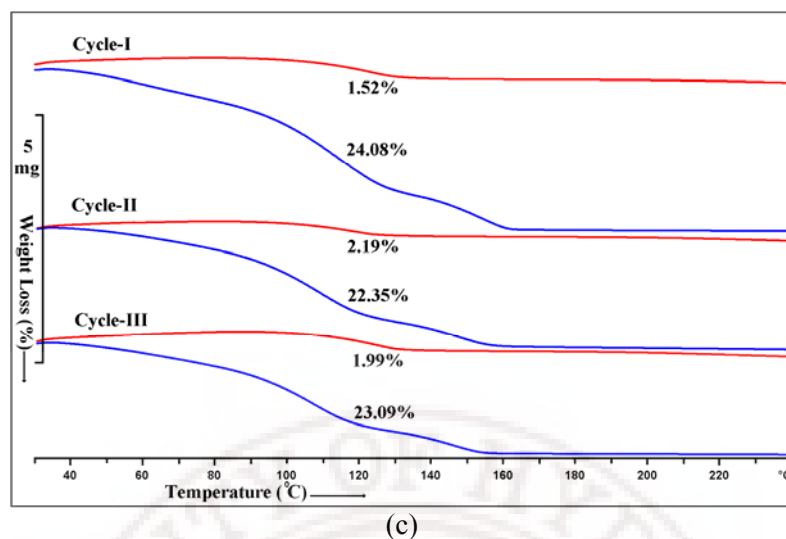


**Figure 3** (a) DSC shows weight loss in two steps corresponding to O6 and O4 + O5 water molecules in TG. (b) Differential scanning calorimetry. A heat-cool-heat cycle of  $\text{TPM-SO}_3\text{H} \cdot (\text{H}_2\text{O})_{12}$  (sample dried at 150 °C/ 0.5 Torr) shows complete loss of water below 200 °C and no weight loss in the second heating cycle. (c) TGA exhibits complete water uptake after dehydration and release in three successive heat-cool-heat cycles.

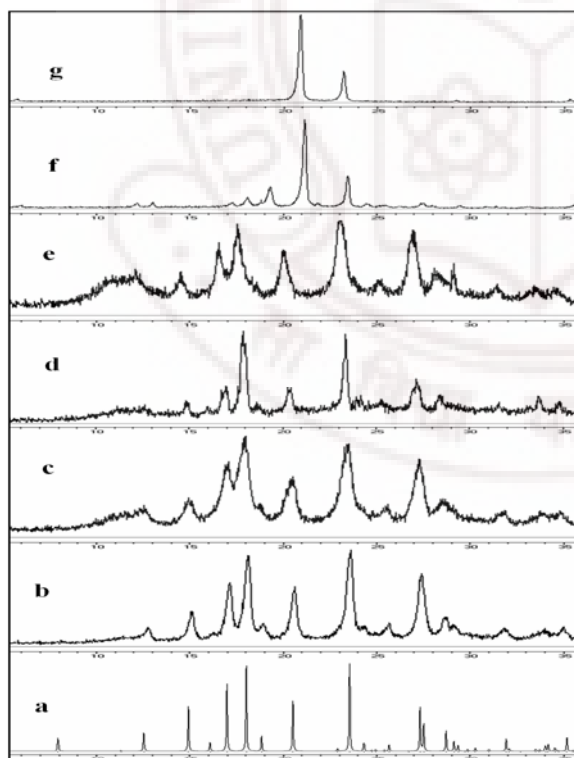


**Figure 4** Powder X-ray diffraction pattern of  $\text{TPM-SO}_3\text{H} \cdot (\text{H}_2\text{O})_{12}$  under different dehydration conditions. (a)  $\text{TPM-SO}_3\text{H} \cdot (\text{H}_2\text{O})_{12}$ . Simulated from the X-ray crystal structure. (b) Dodecahydrate host material. (c-e) Dried sample at 100, 200, 250 °C/ 0.5 Torr. There is little change in the powder lines due to immediate re-absorption of water by the apohost during sample handling and data collection. The amorphous content varies after heat-cool cycles. (f) The solid was immediately coated with wax after heating at 200 °C/ 0.5 Torr. (g) Reference wax. The powder diffraction lines in profiles (b-e) are similar. The new crystalline phase in (f) is possibly the anhydrous form.

## (v) Summary

Tetrakis(4-sulfophenyl)methane, an organic host hydrate was synthesized and its interesting structural and thermal chemistry was analyzed. Hydrogen bonding of opposite handedness water helices and clusters in TPM-SO<sub>3</sub>H host channels are described. TPM-SO<sub>3</sub>H can absorb water from atmosphere quickly and selectively. TPM-SO<sub>3</sub>H does not include alcoholic co-solvents. Water release from the interconnected channels of the host is quantitative and reversible. These properties have potential application in organic zeolites and/or as dehydrating reagents.

## B. H-Shaped Aromatic Phenol Host

### (i) Introduction

Network solids have potential properties as functional materials<sup>24</sup> in host–guest chemistry,<sup>24b,c</sup> ion exchange, catalysis,<sup>24d</sup> and the development of optical,<sup>24e</sup> magnetic<sup>24f</sup> and electronic devices<sup>24g</sup> etc. Basic concepts of the fascinating architectures and topologies within the realm of supramolecular chemistry, the crystal engineering of coordination polymers<sup>25</sup> were proposed in the early nineties by Robson and coworkers.<sup>26</sup> Carlucci, Ciani and Proserpio reviewed<sup>27</sup> crystal structures of a number of entangled polymeric networks and proposed a topological classification as polycatenation, polythreading, polyknotting, interweaving of 1D chain, unexpected borromean links of the different interlocked and interweaved species reported in the recent years by many groups. When the entanglement involves no change in dimensionality of the original 2D or 3D nets are called interpenetration and increase in dimensionality from 1D→2D or 2D→3D or to a higher level is known as catenation.<sup>27c,d</sup> Interpenetrating structures, are characterized by the presence of infinite structurally regular motifs that must contain rings “through which independent components are inextricably entangled” and that “can be disentangled only by breaking internal connections”. Basic difference is that each interpenetrated individual motif is interlaced with all others whereas each motif is not threaded through all others in a polycatenated array. Classification of networks in organic systems is a recent and less common trend.<sup>25e</sup> Despite hydrogen bonds are weaker and less directional than metal–heteroatom and metal–ligand bonds, very recently organic crystal structures have been topologically classified in a similar way to inorganic and coordination network structures.<sup>25e,g</sup> New examples of rare 2D pentagonal

network modulated by the guest species and its interpenetration/ catenation modes in organic supramolecular architectures built from an H-shaped Tecton is discussed here.

## (ii) 1,4-Di[bis(4'-hydroxyphenyl)methyl]benzene and Octamethyl Derivative

The compound 1,4-di[bis(4'-hydroxyphenyl)methyl]benzene (**22**) and its octamethyl derivatives (**23**) were synthesized (Figure 5). by the acid catalyzed condensation of terephthalaldehyde with the appropriate phenol and 2,6-dimethylphenol (4 equiv)<sup>8</sup> respectively and characterized by NMR and IR spectra. These molecules may be viewed as having a *p*-substituted phenyl linker that connects bis(hydroxyphenyl)methyl groups on the two sides for directed self-assembly (Figure 6a). The peripheral O atoms of phenolic OH that engage in hydrogen bonding and their connectivity to the carbon core via tetrahedral C atoms is considered to define the H-shape of these molecules. The mean plane of the phenol O and the *p*-phenyl linker C atoms (marked \* in Figure 6a) are nearly coplanar (Figures 6b, deviation from the mean plane < 1 Å) and make an idealized H-shape.

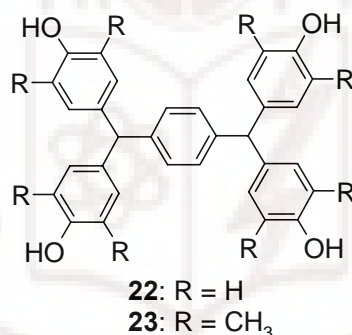


**Figure 5** 1,4-di[bis(4'-hydroxyphenyl)methyl]benzene (**22**) and its octamethyl derivatives (**23**) were synthesized to analyze the occurrence of specific network architectures.

Aoyama and coworkers<sup>28</sup> emphasized the importance of tetraphenol hosts as a new class of organic zeolites in inclusion structures of **22a** and its derivatives. H-shaped organic molecular tectons are rare. There are examples of Y- and T-shaped organic tectons,<sup>25e,g,29a,b</sup> and L-shaped<sup>29c</sup> molecules, and V-shaped<sup>29d-f</sup> molecular tweezers. H-shaped organic pentiptycene scaffold<sup>30a</sup> and Mo-Au phosphinidene complex<sup>30b</sup> are reported but not in host-guest category. H shaped tetraphenol molecule **22 & 23** are as such a new tecton in organic nets.<sup>8</sup>

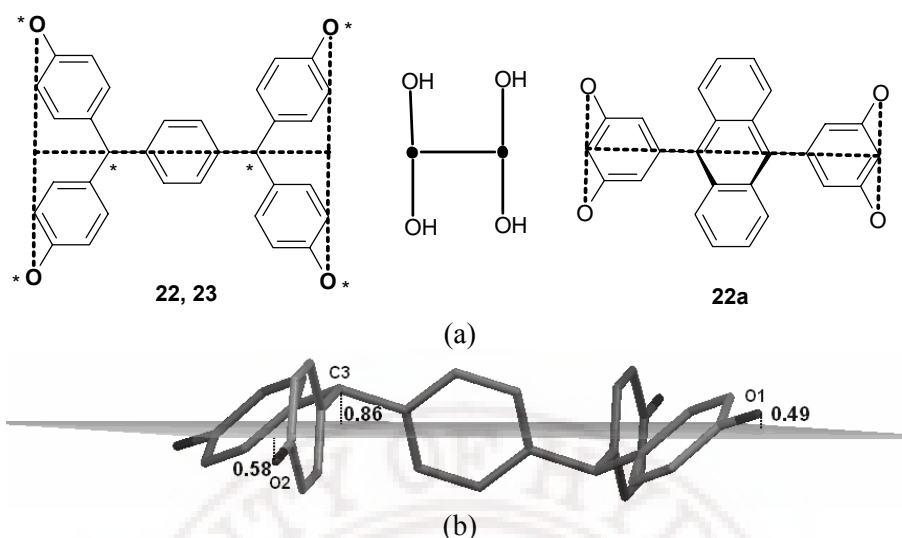


**Figure 6** (a) The phenol OH groups are oriented outward to make hydrogen bond networks. (b) The H-shape of molecular core of **22** is realized by connecting the phenol O atoms and the central *p*-phenyl linker C atoms. (c) The \* atoms that make up the H-shape are nearly coplanar, deviating from the mean plane by 0.49, 0.58 and 0.86 Å. Molecule **22** is extracted from its MeOH solvate structure (ref. 8a).

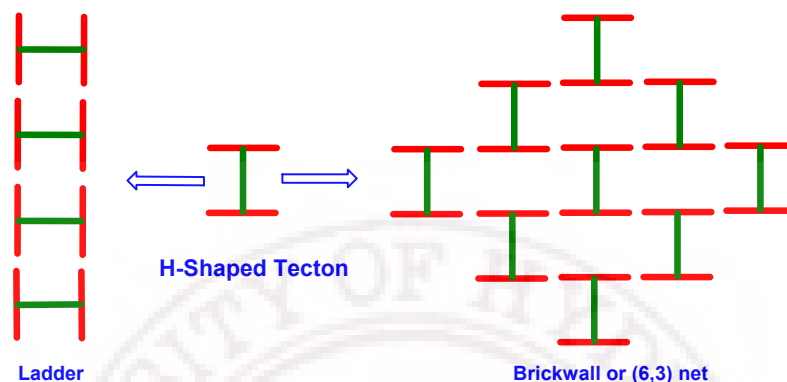
### (iii) Construction of Rare Pentagonal Net

Construction of network is the periodic system of connecting points to simplify crystal structures<sup>25a</sup>. The Platonic and Plane nets ( $n$ ,  $p$ ) may be regarded as way of connecting points so that each is connected to the same number of others to form systems in which all the short circuits are  $n$ -gons. In 3D networks the points repeat regularly in space and have the property of the shortest circuit. Starting from any point and including any two of the links meeting at the points is an  $n$ -gon and may be describe as Uniform net which is further classified as follows,

|                            |             |  |
|----------------------------|-------------|--|
| Uniform ( $n$ , $p$ ) nets | 1. Platonic | all shortest circuits $n$ -gons<br>all points $p$ -connected               |
|                            | 2. Catalan  | all shortest circuits $n$ -gons<br>points $p$ -, $q$ - and so on connected |
|                            | Archimedean | shortest circuits of more than one kind<br>all points $p$ -connected       |



The H-shaped tecton can propagate to a 1D ladder or 2D brick wall topologically identical to the hexagonal or (6,3) network depending on the hydrogen bonding patterns or the arrangement of the molecules (Scheme 3). 1D extension requires that the OH group is oriented inwards whereas a 2D grid results when the OH groups are divergent.



**Scheme 3** Ladder, brickwall or (6,3) net constructed from H-shaped tecton

The (6,3) hexagonal net is easily accessible among the 2D net category. However, 5-membered nets are rare. There are only two examples of self-assembled molecular pentagons prepared using combinations of metal, ligands, and counterions.<sup>31</sup> Furthermore, there are two examples of metal-organic coordination solids that contain pentagonal cavities in extended domains.<sup>32</sup> In  $[\text{Cu}(4,4'\text{-bipyridine})_{1.5}(\text{PPh}_3)]\text{BF}_4 \cdot (\text{THF})_{1.33}(\text{CHCl}_3)_{0.33}$  five Cu atoms (corners) and five bipy ligands (sides) assemble into a nearly regular pentagonal cavity which contains solvated  $\text{CHCl}_3$  and THF molecules and noncoordinated counterions. The 1D tapes formed by 5-membered rings are connected through 8-membered rings in this Archimedean solid.<sup>32a</sup> The dual coordination mode of hexamethylenetetraamine (HMTA) as a 3- and 4-connected tetrahedral node was exploited in  $(\text{HMTA})_3(\text{Cu}_2(\mu\text{-O}_2\text{CCH}_2\text{CH}_3)_4)_5$  to construct congruent pentagonal cavities which are filled by the ethyl groups and found that the structure is the only example of exclusive 5-membered rings in a Catalan net.<sup>32b</sup> Platonic (6,3) and Catalan  $(5, \frac{3}{4})$  nets under the broader category of uniform network topology. Catalan  $(5, \frac{3}{4})$  net is of pentagon tiling with 3 and 4 connected nodes. There are

total 14 different pentagon tiling patterns, of which five  $(5,3)$  nets, eight  $(5,4)$  nets and one  $(5,6)$  net (Figure 7).

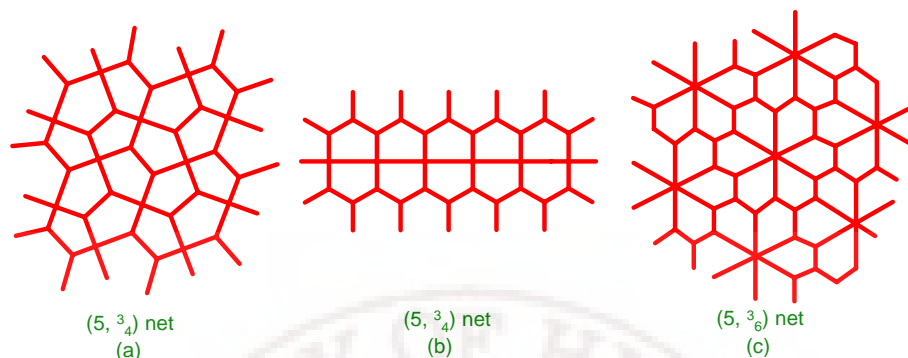
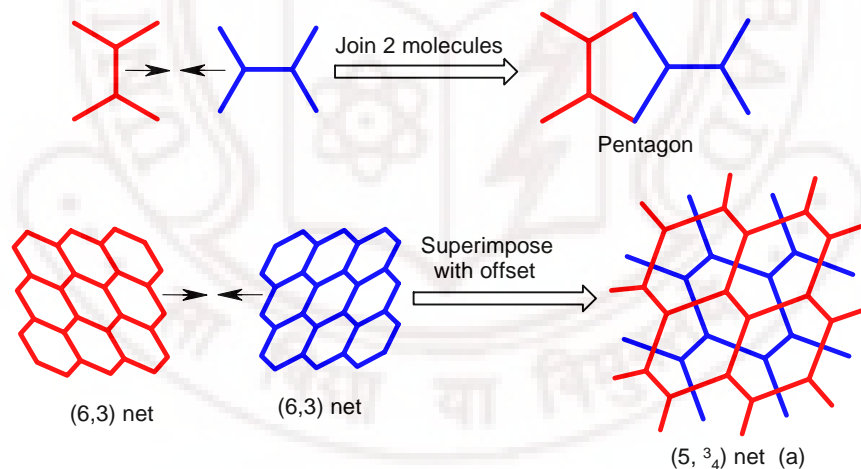


**Figure 7** Three different congruent pentagon tiling patterns, the  $(5,4)$  (type a and b) and  $(5,6)$  nets (c), are shown.

Catalan  $(5,4)$  net, type-(a) can be constructed in two ways – (i) from the union of two H shaped molecules or (ii) by the offset superposition of two  $(6,3)$  nets are shown in Scheme 4.



**Scheme 4** Construction of  $(5,4)$  net (a) in two ways – from the union of two H shaped molecules or by the offset superposition of two  $(6,3)$  nets.

#### (iv) Solvate Polymorphism, Interpenetration, Catenation and Rare $(5,4)$ Net

The common hexagonal network obtained in H-shaped host molecules could be modulated via appropriate choice of guest species to the rare pentagonal 2D sheet

pattern. Crystallization of **22** from  $\text{CH}_3\text{NO}_2$  with a trace amount of  $\text{CF}_3\text{CH}_2\text{OH}$  added ( $\text{CH}_3\text{NO}_2$ :  $\text{CF}_3\text{CH}_2\text{OH}$   $\sim 50:1$ ) afforded the solvate  $(\mathbf{22})_{0.5} \bullet \text{CH}_3\text{NO}_2$  as plate-shaped crystals in the space group *Pbca*. Four molecules of **22** are connected via solvent molecules to form an idealized (6,3) net of  $12 \times 18.7$  Å cavities (after removing the van der Waals radius of benzene rings on opposite faces). Polycatenation of 2D hexagonal sheets completes the 3D crystal structure (Figure 8). This  $\text{CH}_3\text{NO}_2$  solvate of **22** is identical to its MeOH and EtOH solvates<sup>8a</sup> in terms of stoichiometry, space group, lattice parameters, interpenetration mode, and the role of solvent as bridges between the host molecules. This structure is an example of  $2\text{D} \rightarrow 3\text{D}$  polycatenation with degree of catenation<sup>27</sup> ( $\text{DOC} = 2/2$ ), which means that two layers are catenated with one hexagonal ring and vice versa.

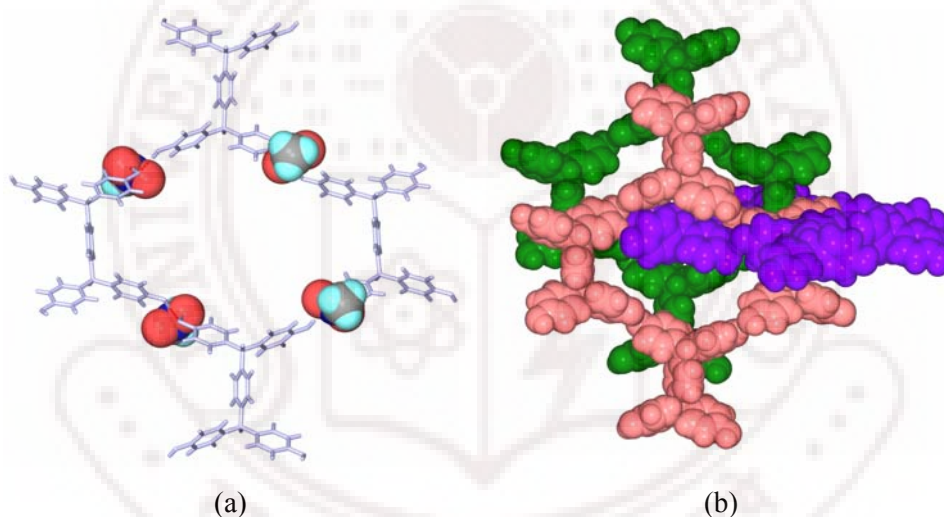
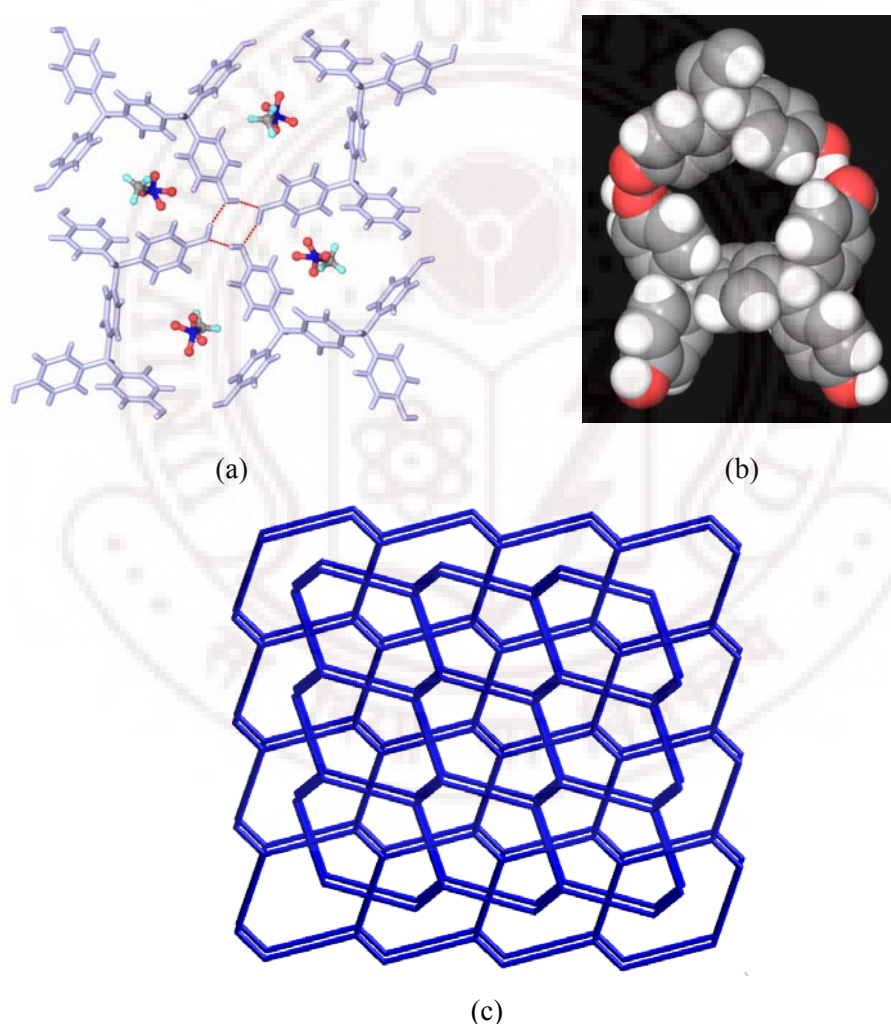


Figure 8 (a)  $\text{CH}_3\text{NO}_2$  molecules act as bridges in the supramolecular hexagon of four H-shaped molecules in  $(\mathbf{22})_{0.5} \bullet (\text{CH}_3\text{NO}_2)$  *Pbca* form. (b)  $2\text{D} \rightarrow 3\text{D}$  polycatenation with degree of catenation ( $\text{DOC} = 2/2$ ) of the  $12 \times 18.7$  Å cavities completes the molecular packing and space filling.

The use of  $\text{CH}_3\text{NO}_2$  as the minor component in the solvent mixture ( $\text{CH}_3\text{NO}_2$ :  $\text{CF}_3\text{CH}_2\text{OH}$   $\sim 1:6$ ) gave a solvated polymorph of  $(\mathbf{22})_{0.5} \bullet \text{CH}_3\text{NO}_2$  in the space group *P2<sub>1</sub>/c*. The asymmetric unit contains 0.5 host and 1 guest molecule in both crystal structures (Cell parameters are tabulated in Appendix). In this latter monoclinic form, two host molecules hydrogen bond in the shape of a pentagonal cavity of  $4.7 \times 5.7$  Å

dimensions (after subtracting the van der Waals radius of benzene rings on opposite faces) which includes the guest species (Figure 9). The 4 and 3 connected nodes of the pentagonal 2D sheet are in a 1:2 ratio as shown for the  $(5,3_4)$  net (a) of Figure 7a. The tetrahedral carbon centers form the 3-connected trigonal nodes and O–H $\cdots$ O hydrogen bonds act as the 4-connected square nodes. Helices of O2–H2A $\cdots$ O1 H bonds (1.86, 158.7°) create channels along [100] and O1–H1 $\cdots$ O2 (1.79, 163.1°) extend the molecules into 2D sheet in the *bc*-plane. Disordered nitromethane solvent molecules occupy the channel host lattice. Hydrogen bond parameters are given in Table 5.



**Figure 9** (a) Pentagonal cavities of  $4.7 \times 5.7$  Å dimensions are filled with  $\text{CH}_3\text{NO}_2$  guest species in the  $P2_1/c$  form of  $(\mathbf{22})_{0.5} \bullet (\text{CH}_3\text{NO}_2)$ . (b) The channel host framework. Guest molecules are omitted for clarity. (c) Idealized pentagonal tiling.

**Table 5** Hydrogen bond parameter (neutron normalized)

|   | Interaction   | $d / (\text{\AA})$ | $D / (\text{\AA})$ | $\theta / (^\circ)$ |
|---|---------------|--------------------|--------------------|---------------------|
| <b>22</b> •pure   | O1–H1A...O3   | 1.76               | 2.729(4)           | 167.9               |
|   | O2–H2A...O1   | 1.82               | 2.789(4)           | 166.8               |
|   | O3–H3A...O4   | 1.72               | 2.683(5)           | 165.4               |
|   | C16–H16...O2  | 2.45               | 3.512(5)           | 167.4               |
|   | C22–H22...O2  | 2.46               | 3.389(5)           | 143.4               |
| (22) <sub>0.5</sub> •(CH <sub>3</sub> NO <sub>2</sub> )<br><i>P2<sub>1</sub>/c</i> form | O1–H1...O2    | 1.79               | 2.749(3)           | 163.1               |
|   | O2–H2A...O1   | 1.86               | 2.804(3)           | 158.7               |
| (22) <sub>0.5</sub> •(CH <sub>3</sub> NO <sub>2</sub> )<br><i>Pbca</i> form             | O2–H1A...O3   | 1.88               | 2.855(3)           | 171.0               |
|   | O1–H2A...O2   | 1.82               | 2.795(4)           | 173.3               |
|   | C17–H17A...O2 | 2.43               | 3.514(4)           | 175.7               |
| (23) <sub>0.5</sub> •CHCl <sub>3</sub>  | O1–H1...O2    | 1.93               | 2.797(3)           | 145.6               |
|   | O2–H2...O1    | 1.94               | 2.850(4)           | 153.7               |
| (1b) <sub>0.5</sub> •CH <sub>3</sub> NO <sub>2</sub>                                    | O1–H1...O2    | 1.93               | 2.830(4)           | 150.2               |
|   | O2–H2...O2    | 2.16               | 2.958(4)           | 137.2               |
|   | C19–H19C...O1 | 2.48               | 3.392(4)           | 140.8               |
|   | C21–H21B...O4 | 2.49               | 3.453(5)           | 147.9               |

The crystal structures of orthorhombic and monoclinic polymorphs of CH<sub>3</sub>NO<sub>2</sub> solvate of **22** are very different host–guest arrangements of (6,3) and (5,<sub>4</sub><sup>3</sup>) network topology. The former is polycatenated with degree of catenation, DOC = 2/2, hydrogen-bonded solvate whereas the latter is a lattice inclusion host–guest structure with rare network topology of catalan (5,<sub>4</sub><sup>3</sup>). Literature show only one nitromethane solvate polymorphic pair<sup>33a</sup> but polymorphic host–guest structures are not uncommon.<sup>33b-g</sup>

A guest-free form of **22** was obtained upon crystallization from CH<sub>3</sub>NO<sub>2</sub> in space group *P* $\bar{1}$  with two half molecules in the asymmetric unit. 1D ladder networks sustained by O–H...O hydrogen bonds (O1–H1A...O3, 1.76 Å, 167.9°; O2–H2A...O1, 1.82 Å, 166.8°; O3–H3A...O4, 1.72 Å, 165.4°) run along [010], and two such networks are inclined at an angle of 73.6° and catenated via Hopf link such that the *p*-phenyl connectors of the second ladder weave through the rectangular rungs of the first ladder (Figure 10). Trifluoroethanol co-solvent plays a role because when pure CH<sub>3</sub>NO<sub>2</sub> was used, a guest free form of **22** crystallized in space group *P* $\bar{1}$ . CF<sub>3</sub>CH<sub>2</sub>OH solubilizes the host molecule to promote inclusion of CH<sub>3</sub>NO<sub>2</sub>. When CH<sub>3</sub>NO<sub>2</sub> is in excess it becomes a part of the hydrogen bonded framework in the orthorhombic solvate whereas when this

solvent is deficient it is included within the host channels. The pseudotrigonal symmetry and size of the guest molecule appear to be crucial in giving the  $(5, \frac{3}{4})$  net.

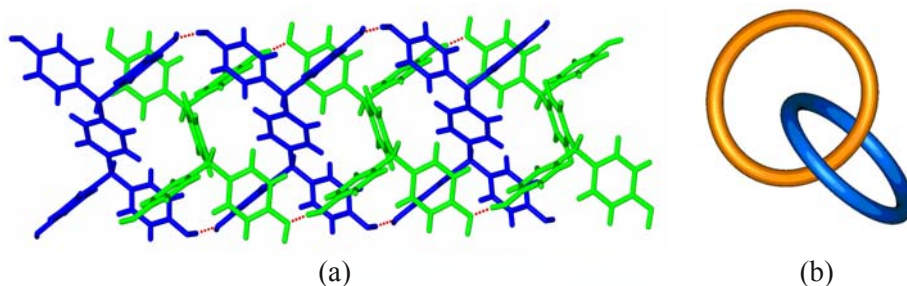


**Figure 10** (a) Double interpenetration of inclined ladders in guest-free form of **22**. Symmetry-independent molecules are colored differently. (b) Hopf link.

Crystallization of the octamethyl derivative **23** from  $\text{CHCl}_3$  gave a crystalline solvate  $(\mathbf{23})_{0.5} \cdot \text{CHCl}_3$  in the space group  $P2_1/n$ . Pentagonal cavities of  $5.2 \times 5.4 \text{ \AA}$  (after removing the van der Waals radius of benzene) include the guest species. The OH donors point out of the phenyl ring plane because of the flanking *ortho*-Me groups in **23** compared to the coplanar orientation of OH groups in **22**. The 2D layer of pentagons in the  $(5, \frac{3}{4})$  tiling pattern (Figure 11) is a flat sheet parallel to the (202) plane constructed by  $\text{O}-\text{H} \cdots \text{O}$  hydrogen bonds ( $\text{O1}-\text{H1} \cdots \text{O2}$  1.93,  $145.6^\circ$ ;  $\text{O2}-\text{H2} \cdots \text{O1}$  1.94,  $153.7^\circ$ ). Stacking of adjacent molecular sheets by close packing gives channels down [101] for solvent incorporation.

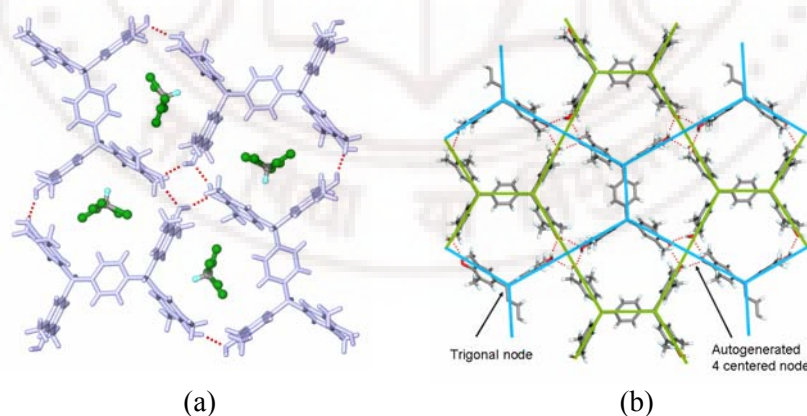


**Figure 11** (a) Hydrogen-bonded sheet of **23** molecules having the  $(5, \frac{3}{4})$  net in  $(\mathbf{23})_{0.5} \cdot \text{CHCl}_3$ . Disordered  $\text{CHCl}_3$  guests occupy the channels down [101]. (b) The side-on hydrogen bonding of H-shaped molecules via  $\text{O}-\text{H} \cdots \text{O}$  tetramer form a 2D pentagonal (202) sheet. Connection of the trigonal carbon centers (3- connected) auto-generates the 4-connected node ( $\text{O}-\text{H} \cdots \text{O}$  tetramer).



The use of  $\text{CH}_3\text{NO}_2$  solvent gave the more common ladder network of H-shaped tecton<sup>29a</sup> in  $(\mathbf{23})_{0.5} \cdot \text{CH}_3\text{NO}_2$  which extend into 2D sheet through  $\text{O}-\text{H} \cdots \text{O}$  hydrogen bonds (Figure 12a).  $\text{CH}_3\text{NO}_2$  solvent molecules are present as a dimer pair in the ladder inclusion structure. Nitromethane solvate of **23** with a pentagonal cavity similar to **23** could not be crystallized. However crystallization from  $\text{CH}_2\text{Cl}_2$  afforded a guest-free form of **23**, but its close-packed structure cannot be classified as a net. The crystal structure of **22** with 4,4'-bipyridine<sup>8a</sup>  $(\mathbf{22})_{0.5} \cdot (4,4'\text{-Bipy})$  makes a perfect 1D ladder network (Figure 12b).

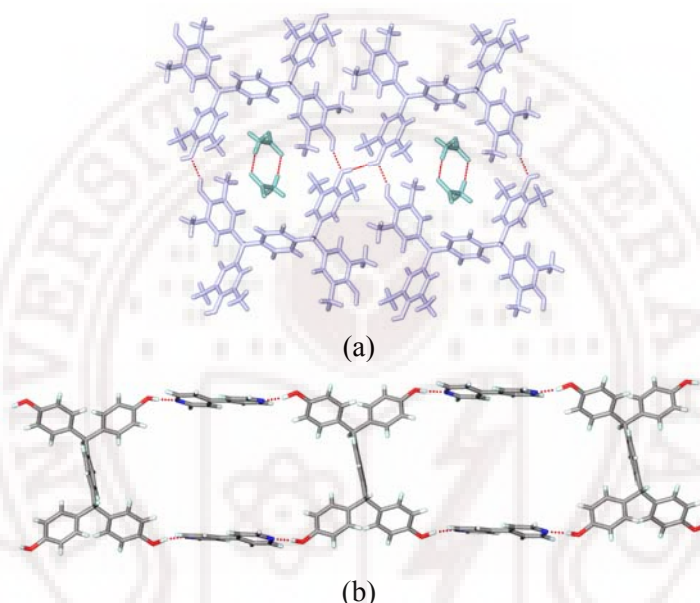


**Figure 12** (a) 1D hydrogen bonded ladder of **23** molecules in  $(\mathbf{23})_{0.5} \cdot \text{CH}_3\text{NO}_2$ . Two guest molecules are present in the  $7.4 \times 8.7 \text{ \AA}$  rectangular cavities. (b) Hydrogen-bonded ladders in  $(\mathbf{22})_{0.5} \cdot (4,4'\text{-Bipy})^{8a}$  with rectangular rungs of  $16.7 \times 6.9 \text{ \AA}$  dimensions. No solvent is included in the crystal lattice. Close packing is achieved by the offset stacking of ladders

The  $(5,3_4)$  Catalan net (Figure 7a) is specifically accessible via the H-shaped molecule in competition to other pentagonal nets because the 5-membered ring may be viewed as arising from two H-shaped molecules approaching such that three sides of the pentagon come from one molecule and two sides from the other. The phenol OH groups serve to create the 4-connected square node via H bonds while the tetrahedral covalent centers are the 3-connected planar nodes. The size of guest is crucial in giving the pentagonal assembly of host molecules. However brick wall, parquet, ladder and bilayer

patterns are common architectures for T-shaped molecules. The unsolvated form of **22** and **23** shows very different crystal structure from the nitromethane and chloroform solvated adducts means that crystallization of H-shaped host **22** and **23** are highly guest-induced. This observation validates our hypothesis that the host molecule will serve as a template for the synthesis of uncommon pentagonal sheets by the selection of guest species. T and H shaped molecules give common structures such as 1D ladder, brick wall, parquet grid, bilayer, and 3D nets.<sup>8,25,29a</sup> Whereas tiling of uniform pentagons in a plane is not possible, the tetrahedral centers of the organic H tecton behave as 3-connected nodes in the cyclopentanoid sheet. The O–H⋯O hydrogen bonds serve as 4-connected supramolecular nodes. There is only one example of a  $(5,^3_4)$  net (a) in a coordination polymer<sup>32a</sup> but no pure organic examples are known till date.

#### (v) Summary

In summary, rare  $(5,^3_4)$  net was realized using a crystal engineering strategy from an easily available H building block for the first time in organic molecules. The construction of  $(5,^3_4)$  net as the superposition of two  $(6,3)$  nets or self assembly of two H shaped molecules in a side on manner was explained schematically. The angle at the corners of a regular pentagon ( $108^\circ$ ) is close to the tetrahedron angle and any tetrahedral center can serve as either 3-connected trigonal or 4-connected square node. The larger volume of  $\text{CHCl}_3$  compared to  $\text{CH}_3\text{NO}_2$  means that the latter is present as a dimer whereas the former solvent has one molecule in the cavity of **23**. Small sized solvent molecules, such as MeOH and EtOH, generally form hexagonal sheet structures through hydrogen bonding with the solvent. Since the hexagonal ring size is large close packing is achieved through catenation or interpenetration.

### 5.3 Conclusions

Tetrakis(4-sulfophenyl)methane was synthesized and studied structural and thermal behavior as structural chemistry of sulfonic acid group has not been explored in tetrahedral molecules. DSC/TGA and X-ray crystal structure are consistent with dodecahydrate structure. TPM- $\text{SO}_3\text{H}$  can reversibly uptake water from atmosphere. This loss/re-uptake of water is quantitative and selective in successive cycles (Figure 3d).

Compounds having properties of reversible, quantitative and selective uptake of water/solvent can have potential applications in dehydrating agents and organic zeolites. Structural part including water helices, interconnected channels, hydrogen bonding pattern on TPM-SO<sub>3</sub>H are analyzed.

Rare network topologies catalan ( $5, \frac{3}{4}$ ) and interpenetration, catenation were built and analyzed in H-shaped aromatic phenol host tecton by using crystal engineering approach. Aoyama's group<sup>28</sup> illustrated organic zeolites constructed from tetraphenol (**22a**) systems.

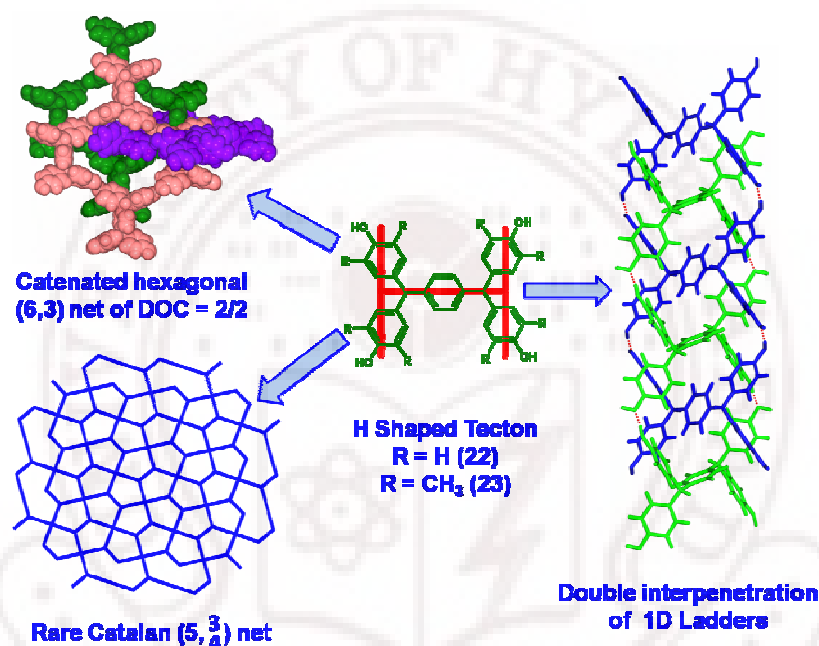


**Figure 13** Rare 2D Catalan ( $5, \frac{3}{4}$ ) net, catenation of hexagonal (6,3) net and double interpenetration in an H-shaped organic host molecule modulated by the guest species.

Zeolites are a class of porous materials capable of sorbing guest molecules in pores or cavities. The guest molecules reside in internal cavities, which may be constructed by using intermolecular interactions such as hydrogen bonds and metal-coordination bonds. Pentagonal and hexagonal channels and cavities can easily include a variety of solvent molecules. Thermo-gravimetric analysis showed the solvent molecule is released at its boiling point or slightly higher temperature. The host is stable up to ~260°C. The network diversity constructed from H shaped host **22** and **23** is summarized in Figure 13.

## 5.4 Experimental section

### Synthesis of Tetrakis(4-sulfophenyl)methane (21)

Tetraphenylmethane<sup>21d</sup> 640 mg (2.0 mmol) was dissolved in 25-30 mL of dry CH<sub>2</sub>Cl<sub>2</sub> under inert N<sub>2</sub> atmosphere. Freshly distilled chlorosulfonic acid (660  $\mu$ L, 10.0 mmol) dissolved in 12 mL of dry CH<sub>2</sub>Cl<sub>2</sub> was added dropwise over 1 h to the stirred reaction mixture at 5-10 °C. The reaction was continued for another 3 h. The precipitate was filtered and washed thoroughly using CH<sub>2</sub>Cl<sub>2</sub> in which it is practically insoluble. The product was recrystallized from MeOH. <sup>1</sup>H NMR ( $\delta$ , D<sub>2</sub>O): 7.38 (d, *J* = 8 Hz, 2 H); 7.12 (d, *J* = 8 Hz, 2 H). <sup>13</sup>C NMR (D<sub>2</sub>O): 148.70, 140.66, 131.28 (x2), 125.18 (x2), 64.78. IR (KBr): 3650-3000 (br, O-H), 1685, 1487, 1367 (SO<sub>3</sub>H), 1285 (SO<sub>3</sub>H), 1192 (hydrated SO<sub>3</sub>H), 1006, 873 cm<sup>-1</sup>. TPM-SO<sub>3</sub>H is readily soluble in alcoholic solvents and water. Colorless needle-shaped crystals suitable for X-ray diffraction were crystallized after evaporation of solvent over a few days.

### Synthesis of 1,4-Di[bis(4'-hydroxyphenyl)methyl]benzene (22) and its Octamethyl Derivative (23)

A mixture of terephthalaldehyde (500mg, 3.7 mmol) and phenol (1.8 mL, 14.9 mmol, 4 equiv) in glacial acetic acid (10 mL) was treated dropwise with concentrated HCl (10 mL). The reaction mixture was stirred at room temperature for 24 h, poured onto crushed ice, the precipitate was filtered, and washed with cold water. The dried compound **1a** was purified by column chromatography using EtOAc-n-hexane (1:4) to yield 884 mg (50%) of the pure product. Octamethyl derivative was prepared by a similar method using 2,6-dimethylphenol as starting material. Compounds **22** and **23** were purified and characterized by IR and NMR spectroscopy. NMR spectra were recorded on Bruker Avance spectrometer at 400 MHz and FT-IR spectra were recorded on Jasco 5300 spectrophotometer. NMR chemical shifts on the  $\delta$  scale (ppm) and *J* coupling (Hz) are reported. Melting points were recorded on Fisher-Johns apparatus and confirmed by endotherm peak in DSC.

**1,4-Di[bis(4'-hydroxyphenyl)methyl]benzene (22):** IR (KBr, cm<sup>-1</sup>): 3366, 1599, 1446, 1371, 1224, 760, 636; <sup>1</sup>H NMR ( $\delta$ , DMSO-d<sub>6</sub>): 5.28 (2H, s, methine CH), 6.64 (8H, d, *J*=8, Ph CH), 6.85 (8H, d, *J*=8, Ph CH), 6.97 (4H, s, Ar CH), 9.22 (4H, s, OH). mp 275-278 °C. Yield 50%.

**1,4-Di[bis(4'-hydroxy 3',5'-dimethylphenyl)methyl]benzene (23):** IR (KBr,  $\text{cm}^{-1}$ ): 3586, 2918, 1670, 1302, 1147, 760, 694;  $^1\text{H}$  NMR ( $\delta$ ,  $\text{CDCl}_3$ ): 2.17 (24H, s,  $\text{CH}_3$ ), 4.48 (4H, s, OH), 5.25 (2H, s, methine CH), 6.70 (8H, s, Ph CH), 6.99 (4H, s, Ar CH). 261-264°C. Yield 60%.

## 5.5 References

1. (a) A. Nangia, *Nanoporous Materials: Science and Engineering*, (Eds.) G. Q. Lu, X. S. Zhao, Imperial College Press, London, 2004, pp. 165; (b) A. Nangia, *Curr. Opin. Solid State Mater. Sci.* **2001**, 5, 115; (c) L. R. MacGillivray, J. L. Atwood, *Angew. Chem. Int. Ed.* **1999**, 38, 1018; (d) P. J. Langley, J. Hulliger, *Chem. Soc. Rev.* **1999**, 28, 279; (e) Y. Aoyama, *Top. Curr. Chem.* **1998**, 198, 131; (f) M. D. Hollingsworth, *Science* **2002**, 295, 2410.
2. G. R. Desiraju, *Angew. Chem. Int. Ed.* **1995**, 34, 2311.
3. (a) M. E. Davis, *Nature* **2002**, 417, 813; (b) R. E. Morris, P. S. Wheatley, *Angew. Chem. Int. Ed.* **2008**, 47, 4966; (c) K. E. Maly, *J. Mater. Chem.* **2009**, 19, 1781.
4. (a) O. M. Yaghi, H. L. Li, C. Davis, D. Richardson, T. L. Groy, *Acc. Chem. Res.* **1998**, 31, 474; (b) M. Eddaoudi, D. B. Moler, H. L. Li, B. L. Chen, T. M. Reineke, M. O'Keeffe, O. M. Yaghi, *Acc. Chem. Res.* **2001**, 34, 319.
5. E. Weber, in *Comprehensive Supramolecular Chemistry*, (Eds.) D. D. MacNicol, F. Toda, R. Bishop, Pergamon, Oxford, 1996, vol. 6.
6. (a) G. Hummer, J. C. Rasaiah, J. P. Noworyta, *Nature* **2001**, 414, 188; (b) P. R. Ashton, S. J. Cantrill, G. Gattuso, S. Menzer, S. A. Nepogodiev, A. N. Shipway, J. F. Stoddart, D. J. Williams, *Chem. Eur. J.* **1997**, 3, 1299; (c) T. D. Clark, M. R. Ghadiri, *J. Am. Chem. Soc.* **1995**, 117, 12364; (d) M. Miyata, K. Sada, *Comprehensive Supramolecular Chemistry*, (Eds.) D. D. MacNicol, F. Toda, R. Bishop, Pergamon Press: Oxford, 1996, 6, 147; (e) A. T. Ung, D. Gizachew, R. Bishop, M. L. Scudder, I. G. Dance, D. C. Craig, *J. Am. Chem. Soc.* **1995**, 117, 8745; (f) D. Mentzafos, I. M. Mavridis, G. Le Bas, G. Tsoucaris, *Acta Crystallogr.* **1990**, B46, 746; (g) K. D. M. Harris, *Chem. Soc. Rev.* **1997**, 26, 279; (h) M. Farina, *Inclusion Compounds*, (Eds.) J. L. Atwood, J. E. D. Davies, D. D. MacNicol, Academic Press: London, 1984, 2, 69; (i) R. Gerdil, *Topics in*

- Current Chemistry*, (Eds.) E. Weber, Springer: Berlin, 1986, 140, 71; (j) P. Sozzani, S. Bracco, A. Comotti, L. Ferretti, R. Simonutti, *Angew. Chem. Int. Ed.* **2005**, 44, 1816; (k) R. M. Barrer, V. H. Shanson, *J. Chem. Soc., Chem. Commun.* **1976**, 333; (m) L. S. Shimizu, M. D. Smith, A. D. Hughes, K. D. Shimizu, *Chem. Commun.* **2001**, 1592.
7. (a) R. K. R. Jetti, F. Xue, T. C. W. Mak, A. Nangia, *J. Chem. Soc. Perkin Trans.2* **2000**, 6, 1223; (b) B. K. Saha, R. K. R. Jetti, L. S. Reddy, S. Aitipamula, A. Nangia, *Cryst. Growth Des.* **2005**, 5, 887; (c) R. K. R. Jetti, P. K. Thallapally, A. Nangia, C. -K. Lam, T. C. W. Mak, *Chem. Commun.* **2000**, 952; (d) R. K. R. Jetti, A. Nangia, F. Xue, T. C. W. Mak, *Chem. Commun.* **2001**, 919; (e) V. S. S. Kumar, A. Nangia, *Chem. Commun.* **2001**, 2392; (f) S. Aitipamula, A. Nangia, *Chem. Eur. J.* **2005**, 11, 6727.
  8. (a) S. Aitipamula, A. Nangia, *Supramol. Chem.* **2005**, 17, 17; (b) R. Thakuria, B. Sarma, A. Nangia, *Cryst. Growth Des.* **2008**, 8, 1471; (c) R. Thakuria, B. Sarma, A. Nangia, *New J. Chem.* **2009** (in press).
  9. (a) B. Sarma, S. Roy, A. Nangia, *Chem. Commun.* **2006**, 4918; (b) F. Toda, K. Tanaka, T. Fujiwara, *Angew. Chem. Int. Ed. Engl.* **1990**, 29, 662; (c) M. R. Caira, A. Horne, L. R. Nassimbeni, F. Toda, *J. Mater. Chem.* **1998**, 8, 1481; (d) Z. -Lipkowska, K. Yoshizawa, S. Toyota, F. Toda, *CrystEngComm* **2003**, 5, 114.
  10. (a) Y. Aoyama, K. Endo, K. Kobayashi, H. Masuda, *Supramol. Chem.* **1995**, 4, 229; (b) K. Endo, T. Sawaki, M. Koyanagi, K. Kobayashi, H. Masuda, Y. Aoyama, *J. Am. Chem. Soc.* **1995**, 117, 8341; (c) Y. Aoyama, K. Endo, T. Anzai, Y. Yamaguchi, T. Sawaki, K. Kobayashi, N. Kanehisa, H. Hashimoto, Y. Kai, H. Masuda, *J. Am. Chem. Soc.* **1996**, 118, 5562; (d) K. Endo, T. Koike, T. Sawaki, O. Hayashida, H. Masuda, Y. Aoyama, *J. Am. Chem. Soc.* **1997**, 119, 4117; (e) K. Endo, T. Ezuhara, M. Koyanagi, H. Masuda, Y. Aoyama, *J. Am. Chem. Soc.* **1997**, 119, 499; (f) T. Tanaka, T. Tasaki, Y. Aoyama, *J. Am. Chem. Soc.* **2002**, 124, 12453.
  11. (a) P. Timmerman, R. H. Vreekamp, R. Hulst, W. Verboom, D. N. Reinhoudt, K. Rissanen, K. A. Udachin, J. Ripmeester, *Chem. Eur. J.* **1997**, 3, 1823; (b) G. S. Ananchenko, K. A. Udachin, M. Pojarova, S. Jebors, A. W. Coleman, J. A. Ripmeester, *Chem. Commun.* **2007**, 707; (c) A. Shivanyuk, *J. Am. Chem. Soc.*



- 2007**, 129, 14196; (d) M. A. Ziganshin, L. S. Yakimova, K. R. Khayarov, V. V. Gorbachuk, M. O. Vysotsky, V. Böhmer, *Chem. Commun.* **2006**, 3897.
12. (a) R. Custelcean, C. Afloroaei, M. Vlassa, M. Polverejan, *Angew. Chem. Int. Ed.* **2000**, 39, 3094; (b) J. N. Moorthy, R. Natarajan, P. Venugopalan, *Angew. Chem. Int. Ed.* **2002**, 41, 3417; (c) R. Ludwig, *Angew. Chem. Int. Ed.* **2001**, 40, 1808; (d) R. Ludwig, *Angew. Chem. Int. Ed.* **2003**, 42, 258.
13. (a) L. Infantes, J. Chisholm, S. Motherwell, *CrystEngComm* **2003**, 5, 480; (b) L. Infantes, W. D. S. Motherwell, *CrystEngComm* **2004**, 4, 454; (c) L. Infantes, L. Fabian, W. D. S. Motherwell, *CrystEngComm* **2007**, 9, 65; (d) L. Infantes, S. Motherwell, *CrystEngComm* **2002**, 4, 454; (e) A. L. Gillon, N. Feeder, R. J. Davey, R. Storey, *Cryst. Growth Des.* **2003**, 3, 663.
14. (a) B. Sarma, A. Nangia, *CrystEngComm* **2007**, 9, 65; (b) B. K. Saha, A. Nangia, *Chem. Commun.* **2005**, 3024; (c) A. Nangia, *Encyclopedia of Supramolecular Chemistry*, DOI: 10.1081/E-ESMC-120023838, Taylor & Francis, New York, 2007; (d) A. Mukherjee, M. K. Saha, M. Nethaji, A. R. Chakravarty, *Chem. Commun.* **2004**, 716; (e) B. Sreenivasulu, J. J. Vittal, *Angew. Chem. Int. Ed.* **2004**, 43, 5769; (f) F. Kovacs, J. Quine, T. A. Cross, *Proc. Natl. Acad. Sci. USA* **1999**, 96, 7910; (g) R. Pomes, B. Roux, *Biophys. J.* **1996**, 71, 19; (h) J. F. Nagale, H. J. Morowitz, *Proc. Natl. Acad. Sci. USA* **1978**, 75, 298; (i) L. E. Cheruzel, M. S. Pometun, M. R. Cecil, M. S. Mashuta, R. J. Wittebort, R. M. Buchanan, *Angew. Chem. Int. Ed.* **2003**, 42, 5452; (j) P. S. Sidhu, K. A. Udachin, J. A. Ripmeester, *Chem. Commun.* **2004**, 1358; (k) A. Wakahara, T. Ishida, *Chem. Lett.* **2004**, 33, 354.
15. (a) N. Malek, T. Maris, M. -Ève. Perron, J. D. Wuest, *Angew. Chem. Int. Ed.* **2005**, 44, 4021; (b) M. Simard, D. Su, J. D. Wuest, *J. Am. Chem. Soc.* **1991**, 113, 4696; (c) X. Wang, M. Simard, J. D. Wuest, *J. Am. Chem. Soc.* **1994**, 116, 12119; (d) P. Brunet, M. Simard, J. D. Wuest, *J. Am. Chem. Soc.* **1997**, 119, 2737; (e) J. D. Wuest, *Chem. Commun.* **2005**, 5830; (f) D. Laliberte, T. Maris, E. Demers, F. Helzy, M. Arseneault, J. D. Wuest, *Cryst. Growth Des.* **2005**, 5, 1451; (g) E. Demers, T. Maris, J. D. Wuest, *Cryst. Growth Des.* **2005**, 5, 1227; (h) J. H. Fournier, T. Maris, M. Simard, J. D. Wuest, *Cryst. Growth Des.* **2003**, 3, 535; (i) D. Laliberte, T. Maris, J. D. Wuest, *Can. J. Chem.* **2004**, 82, 386.

16. (a) D. S. Reddy, T. Dewa, K. Endo, Y. Aoyama, *Angew. Chem. Int. Ed.* **2000**, 39, 4266; (b) D. S. Reddy, D. C. Craig, G. R. Desiraju, *J. Am. Chem. Soc.* **1996**, 118, 4090; (c) R. Thaimattam, F. Xue, J. A. R. P. Sarma, T. C. W. Mak, G. R. Desiraju, *J. Am. Chem. Soc.* **2001**, 123, 4432; (d) R. Thaimattam, D. S. Reddy, F. Xue, T. C. W. Mak, A. Nangia, G. R. Desiraju, *New J. Chem.* **1998**, 22, 143; (e) A. Anthony, G. R. Desiraju, R. K. R. Jetti, S. S. Kuduva, N. N. L. Madhavi, A. Nangia, R. Thaimattam, V. R. Thalladi, *Cryst. Eng.* **1998**, 1, 1; (f) E. Galloppini, R. Gilardi, *Chem. Commun.* **1999**, 173; (g) F. G. Gulino, R. Lauceri, L. Frish, T. Evan-Salem, Y. Cohen, R. De Zorzi, S. Geremia, L. Di Costanzo, L. Randaccio, D. Sciotto, R. Purrello, *Chem. Eur. J.* **2006**, 12, 2722; (h) J. L. Atwood, T. Ness, P. J. Nichols, C. L. Raston, *Cryst. Growth Des.* **2002**, 2, 171; (i) D. S. Guo, H. Y. Zhang, C. J. Li, Y. Liu, *Chem. Commun.* **2006**, 2592.
17. (a) I. Dance, M. Scudder, *Chem. Eur. J.* **1996**, 2, 481; (b) M. A. Lloyd, C. P. Brock, *Acta Crystallogr.* **1997**, B53, 780; (c) C. P. Brock, J. D. Dunitz, *Chem. Mater.* **1994**, 6, 1118.
18. A. I. Kitaigorodskii, *Molecular Crystals and Molecules*; Academic Press: New York, 1973; pp 67-71.
19. (a) O. Ermer, *J. Am. Chem. Soc.* **1988**, 110, 3141; (b) K. M. E. Jones, A. H. Mahmoudkhani, B. D. Chandler, G. K. H. Shimizu, *CrystEngComm* **2006**, 8, 303; (c) J. H. Fournier, T. Maris, J. D. Wuest, W. Guo, E. Galoppini, *J. Am. Chem. Soc.* **2003**, 125, 1002.
20. (a) M. Czugler, J. J. Stezowski, E. Weber, *Chem. Commun.* **1983**, 154; (b) W. Guo, E. Galoppini, R. Gilardi, G. I. Rydja, Y. H. Chen, *Cryst. Growth Des.* **2001**, 1, 231; (c) S. Apel, S. Nitsche, K. Beketov, W. Seichter, J. Seidel, E. Weber, *J. Chem. Soc. Perkin Trans.2* **2001**, 1212.
21. (a) D. J. Hoffart, A. P. Cote, G. K. H. Shimizu, *Inorg. Chem.* **2003**, 42, 8603; (b) D. J. Hoffart, S. A. Dalrymple, G. K. H. Shimizu, *Inorg. Chem.* **2005**, 44, 8868; (c) A. Bacchi, E. Bosetti, M. Carcelli, *CrystEngComm* **2007**, 9, 313; (d) D. Su, F. M. Menger, *Tetrahedron Lett.* **1997**, 38, 1485.
22. (a) Y. Ishii, K. Matsunaka, S. Sakaguchi, *J. Am. Chem. Soc.* **2000**, 122, 7390; (b) A. F. Benedetto, P. J. Squattrito, F. Adani, E. Montoneri, *Inorg. Chim. Acta.*

- 1997**, 260, 207; (c) T. Ness, P. J. Nichols, C. L. Raston, *Eur. J. Inorg. Chem.* **2001**, 1993.
23. (a) R. N. Devi, P. Wormald, P. A. Cox, P. A. Wright, *Chem. Mater.* **2004**, *16*, 2229; (b) X. S. Zhao, F. Audsley, G. Q. Lu, *J. Phys. Chem. B* **1998**, *102*, 4143; (c) T. Maeda, K. Yamamoto, T. Aoyagi, *J. Coll. Int. Sci.* **2006**, *302*, 467; (d) A. Michaelides, S. Skoulika, *Cryst. Growth Des.* **2005**, *2*, 529; (e) A. Michaelides, S. Skoulika, E. G. Bakalbassis, J. Mrozinski, *Cryst. Growth Des.* **2003**, *3*, 487; (f) T. E. Alcacio, A. Sistla, T. Hsieh, T. J. Thamann, *Mol. Cryst. Liq. Cryst.* **2006**, *456*, 117; (g) H. Kim, M. P. Suh, *Inorg. Chem.* **2005**, *4*, 44; (h) D. Braga, M. Gandolfi, M. Lusi, M. Polito, K. Rubini, F. Grepioni, *Cryst. Growth Des.* **2007**, *7*, 919.
24. (a) C. Janiak, *Dalton Trans.* **2003**, 2781; (b) O.M. Yaghi, G. Li, H. Li, *Nature* **1995**, *378*, 703; (c) O.M. Yaghi, H. Li, C. Davis, D. Richardson, T. L. Groy, *Acc. Chem. Res.* **1998**, *31*, 474; (d) M. Fujita, Y.J. Kwon, S. Washizu, K. Ogura, *J. Am. Chem. Soc.* **1994**, *116*, 1151; (e) O.R. Evans, W. Lin, *Acc. Chem. Res.* **2002**, *35*, 511; (f) O. Kahn, *Acc. Chem. Res.* **2000**, *33*, 647; (g) A. Aumuller, P. Erk, G. Klebe, S. Hunig, J. U. von Schutz, H. -P. Werner, *Angew. Chem. Int. Ed. Engl.* **1986**, *25*, 740.
25. (a) A. F. Wells, *Three-Dimensional Nets and Polyhedra*, Wiley, New York, 1977; (b) M. O'Keeffe, B. G. Hyde, *Phil. Trans. R. Soc. (London), Ser. A* **1980**, *295*, 553; (c) S. R. Batten, R. Robson, *Angew. Chem. Int. Ed.* **1998**, *37*, 1460; *Angew. Chem.* **1998**, *110*, 1558; (d) G. R. Desiraju, *Chem. Commun.* **1997**, 1475; (e) B. Moulton, M. J. Zaworotko, *Chem. Rev.* **2001**, *101*, 16298; (f) K. Biradha, M. Sarkar, L. Rajput, *Chem. Commun.* **2006**, 4169; (g) I. A. Baburin, V. A. Blatov, L. Carlucci, G. Ciani, D. M. Proserpio, *Cryst. Growth Des.* **2008**, *8*, 519.
26. B. F. Hoskins, R. Robson, *J. Am. Chem. Soc.* **1990**, *112*, 1546.
27. (a) L. Carlucci, G. Ciani, D. M. Proserpio, *Coord. Chem. Rev.* **2003**, *246*, 247; (b) L. Carlucci, G. Ciani, D. M. Proserpio, *CrystEngComm* **2003**, *5*, 269; (c) L. Carlucci, G. Ciani, D. M. Proserpio, *Chem. Commun.* **2004**, 380; (d) L. Carlucci, G. Ciani, S. Maggini, D. M. Proserpio, *Cryst. Growth Des.* **2008**, *8*, 162.
28. (a) K. Endo, T. Sawaki, M. Koyanagi, K. Kobayashi, H. Masuda, Y. Aoyama, *J. Am. Chem. Soc.* **1995**, *117*, 8341; (b) T. Tanaka, T. Tasaki, Y. Aoyama, *J. Am.*

- Chem. Soc.* **2002**, *124*, 12453; (c) K. Endo, T. Koike, T. Sawaki, O. Hayashida, H. Masuda, Y. Aoyama, *J. Am. Chem. Soc.* **1997**, *119*, 4117; (d) Y. Aoyama, K. Endo, T. Anzai, Y. Yamaguchi, T. Sawaki, K. Kobayashi, N. Kanehisa, H. Hashimoto, Y. Kai, H. Masuda, *J. Am. Chem. Soc.* **1996**, *118*, 5562; (e) K. Tanaka, K. Endo, Y. Aoyama, *Chem. Lett.* **1999**, 887; (f) Y. Aoyama, K. Endo, K. Kobayashi, H. Masuda, *Supramol. Chem.* **1995**, *4*, 229.
29. (a) V. S. S. Kumar, A. Nangia, M. T. Kirchner, R. Boese, *New J. Chem.* **2003**, *27*, 224; (b) G. R. Swiegers, T. J. Malefetse, *Chem. Rev.* **2000**, *100*, 3483; (c) P. Grosshans, A. Jouaiti, N. Kardouh, M. W. Hosseini, N. Kyritsakas, *New J. Chem.* **2003**, *27*, 1806; (d) F. G. Klärner, B. Kahlert, *Acc. Chem. Res.* **2003**, *36*, 919; (e) M. Harmata, *Acc. Chem. Res.* **2004**, *37*, 862; (f) A. Sygula, F. R. Fronczek, R. Sygula, P. W. Rabideau, M. M. Olmstead, *J. Am. Chem. Soc.* **2007**, *129*, 3842.
30. (a) J. -S. Yang, J. -L. Yanb, *Chem. Commun.* **2008**, 1501; (b) M. A. Alvarez, I. Amor, M. E. Garci, M. A. Ruiz, *Inorg. Chem.* **2008**, *47*, 7963.
31. (a) B. Hasenknopf, J. -M. Lehn, B. O. Kneisel, G. Baum, D. Fenske, *Angew. Chem. Int. Ed. Engl.* **1996**, *35*, 1838; (b) C. S. C. -Fernández, R. Clérac, J. M. Koomen, D. H. Russell, K. R. Dunbar, *J. Am. Chem. Soc.* **2001**, *123*, 773.
32. (a) S. W. Keller, S. Lopez, *J. Am. Chem. Soc.* **1999**, *121*, 6306; (b) B. Moulton, J. Lu, M. J. Zaworotko, *J. Am. Chem. Soc.* **2001**, *123*, 9224.
33. (a) J. H. Burns, J. C. Bryan, M. C. Davis, R. A. Sachleben, *J. Incl. Phenomenon* **1996**, *26*, 197; (b) P. S. Sidhu, G. D. Enright, K. A. Udachin, J. A. Ripmeester, *Cryst. Growth Des.* **2004**, *4*, 1249; (c) S. Ahn, B. M. Kariuki, K. D. M. Harris, *Cryst. Growth Des.* **2001**, *1*, 107; (d) A. Jayaraman, V. Balasubramaniam, S. Valiyaveetil, *Cryst. Growth Des.* **2004**, *4*, 1403; (e) K. Nakano, M. Katsuta, K. Sada, M. Miyata, *CrystEngComm* **2001**, *11*, 44; (f) B. Ibragimov, K. Beketov, K. Makhkamov, E. Weber, *Perkin Trans.* **1997**, *2*, 1349; (g) A. V. Trask, J. van de Streek, W. D. S. Motherwell, W. Jones, *Cryst. Growth Des.* **2005**, *5*, 2233.

## SYNTHON COMPETITION AND COOPERATION IN COCRYSTALS AND SALTS

### 6.1 Introduction

The identification of supramolecular synthons<sup>1</sup> between common functional groups is the first step toward crystal engineering. Self-assembly of supramolecular architectures can be designed from hydrogen bond synthons in crystals generated from multifunctional molecules. A retrosynthetic pathway for the design of supramolecular assemblies is the use of intermolecular interactions between molecular functionalities. To prepare a desired crystal structure of interest, one must first identify molecular functionalities that will generate predictable intermolecular interactions or synthons<sup>2</sup>. Competition between hydrogen bonds among different functional groups makes the situation more complicated. In this context one has to establish which synthon is favoured over competing motifs to design a novel structure in a tailored fashion. Favoured synthons or hydrogen bonds in protein-ligand complexes can be engineered by the involvement of functional group replacement or altering a molecular framework to enhance the properties in a well planned manner. Etter's<sup>3</sup> hydrogen bond rules (1990) state that, (1) *all acidic hydrogens available in a molecule will be used in hydrogen bonding in the crystal structure of that compound.* (2) *All good proton acceptors will be used in hydrogen bonding when there are available hydrogen-bond donors.* (3) *The best hydrogen-bond donor and the best hydrogen acceptor will preferentially form hydrogen bonds to one another.* Hydrogen bonding and competition in organic crystals offer information about preferred connectivity patterns, hydrogen bond competition and its stereo electronic properties for a particular functional group or sets of functional groups. Mainly hydrogen bond preferences are based on functional group competitions in homomeric crystals or heteromeric cocrystals. Competition arises when one donor is

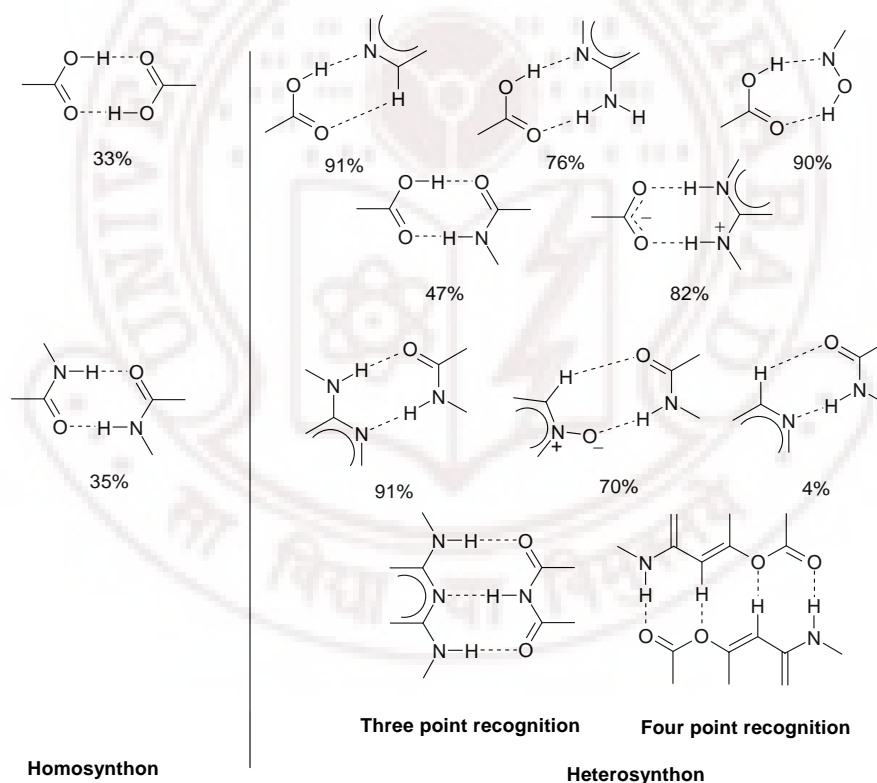
selected by a number of acceptors or *vice versa* during crystallization. Strong and directional O–H $\cdots$ O, O–H $\cdots$ N, and N–H $\cdots$ O are frequently used hydrogen bonds<sup>4a,b</sup> to construct supramolecular architectures<sup>5</sup>. Weak hydrogen bonds C–H $\cdots$ O, C–H $\cdots$ N<sup>6</sup>, weak halogen-halogen and heteroatom interactions<sup>7</sup> also have the potential to steer the supramolecular assembly. The studies on hydrogen bond and its cooperation and competition will move forward our understanding to construct target architectures and functional materials.

The Cambridge Structural Database (CSD)<sup>8a</sup> of nearly 4,80,000 crystal structures compared to a mere 2000 entries in 1965 provides an excellent tool for accessing the efficiency and reproducibility of a particular supramolecular synthon. This storehouse of structural and molecular motifs acts as a guide to build up information about molecular dimensions, molecular conformation and intermolecular interactions.<sup>8b-e</sup> i.e. the probability of formation of X–H $\cdots$ A hydrogen bonds (where X is donor, A is acceptor) can be accessed among the number of such kind of hydrogen bonds that could be formed between functionalities in various crystal structures that are available in the CSD. Those hydrogen bond synthons that have reasonably high probability of formation are preferred for rational crystal design. Molecular shapes, substituent groups, competition of intermolecular interactions and solvents have potential effect on the formation of a desired synthon.

Allen's systematic analysis<sup>9a</sup> on the probabilities of formation of bimolecular hydrogen-bonded ring motifs constructed from O–H $\cdots$ O, O–H $\cdots$ N, N–H $\cdots$ O and N–H $\cdots$ N hydrogen bonds in organic crystal structures extracted from Cambridge Crystallographic Database comprising  $\leq 20$  atoms provides insights into the relative robustness of supramolecular synthons. The global probabilities of formation of 75 bimolecular hydrogen-bonded ring motifs in organic crystal structures were determined. In 2000, Steiner<sup>9b</sup> carried out a database study on the competition of 34 different hydrogen bond acceptors (O, N, S, halogen and  $\pi$ -acceptors) for the strong carboxyl donor. Carboxylic groups are among the best investigated hydrogen bond functionalities possess a hydrogen bond donor as well as an acceptor site that can readily form cyclic dimers (85%) or open arrays or catemer (15%). However the probability drops to 33% for dimer and 2.8% for catemer in presence of other functional groups. In a parallel study Zaworotko and coworkers<sup>9c</sup> showed 84% probability for amide dimers and 14% for catemers in the



absence of competing hydrogen bond donors/acceptors. Again the probability of formation of amide dimer and catemer comes down to 35% and 18% respectively when there are competing groups such as carboxylic acid, secondary amide, aminopyridine, pyridine, water, alcohol, amines etc. For example, presence of pyridyl-N as a competitor makes the probability of formation of acid–pyridine heterosynthon 91% than a carboxylic acid dimer or catemer and is known as the highly robust synthon that can be utilized for crystal design. Zaworotko<sup>9d</sup> sub-classified synthons as homosynthons and heterosynthons based on the interacting functional groups. For example acid–pyridine,<sup>10</sup> phenol–pyridine,<sup>11</sup> phenol–amine,<sup>12</sup> acid–amide,<sup>13</sup> aminopyridine–acid and amide–pyridine-*N*-oxide<sup>14</sup> are robust heterosynthons well exploited in crystal engineering summarized in Scheme 1.



**Scheme 1** Some examples of supramolecular synthons with their probabilities calculated from CSD statistical study.

Exploiting the differences in acidity and basicity of different hydrogen bond acceptors and donors Aakeröy and coworkers have prepared<sup>15</sup> variety of cocrystals in a well-planned manner. Very recently they have examined the hydrogen bond competition and hierarchy<sup>15b,d</sup> of hydrogen bonding in a family of amide derivatives with carboxylic acids. Nangia *et. al.* showed<sup>13a</sup> that hydrogen bonding in 1:2 cocrystals of aliphatic dicarboxylic acid and isonicotinamide obeys hierarchy rules whereas in 1:1 cocrystals the hydrogen bonding does not follow the best donor–best acceptor order. For better understanding of the hydrogen bond motifs present in a supramolecular system having more than two functionalities we have chosen four functional groups that are simultaneously present in the same supramolecular system. They are carboxylic acid, pyridine, amine, and hydroxyl group.<sup>16</sup> Easily available isomeric hydroxybenzoic acids and aminopyridines were selected for cocrystallization experiments (Figure 1). Strong and specific recognition of the popular and robust acid-pyridine<sup>10</sup> and amine-phenol<sup>12</sup> heterosynthons are well studied. Their hydrogen bond donor and acceptor groups are complementary and well matched for specific hydrogen bonding (Figure 2). The acidic COOH donor will bond to the basic pyridine acceptor in acid-pyridine systems and O–H···N + N–H···O bond combinations satisfy donors and acceptors in amino-phenols. The presence of these four functionalities: carboxylic acid, phenol OH, NH<sub>2</sub>, and pyridine-N in the same supramolecular system were investigated. The first surprising finding was that the presence of above four functional groups resulted in proton transfer throughout the series of 11 crystal structures (Figure 1) analyzed by X-ray diffraction and characterized by FT-IR and <sup>1</sup>H-NMR spectroscopy. A synthon analysis study of carboxylate, pyridinium, amine, and hydroxyl functional groups and water included in four structures was carried out. However, hydrogen bond recognition and pairing when all these four functional groups are present in the same crystal structure are relatively less studied<sup>17</sup> and cocrystal hits were extracted from the Cambridge Structural Database<sup>18</sup> (CSD version 5.29, ConQuest 1.10, November 2007 release, January 2008 update). The amino pyridines used here (4-Aminopyridine and 3-Aminopyridine) for cocrystallization are bioactive and exist in neutral/ ionic form at physiological pH (*pKa* 6-9).<sup>19</sup> Antioxidants are molecules capable of preventing the oxidation of other molecules by terminating the chain reactions by removing free radical intermediates, and inhibit other oxidation reactions by being oxidized themselves. Antioxidants are often reducing agents

such as thiols, ascorbic acid, gallic acid, polyphenols etc. Hydroxy-benzoic acids are known to be good antioxidants and cause apoptosis or cell death characterized by DNA fragmentation.<sup>20</sup>

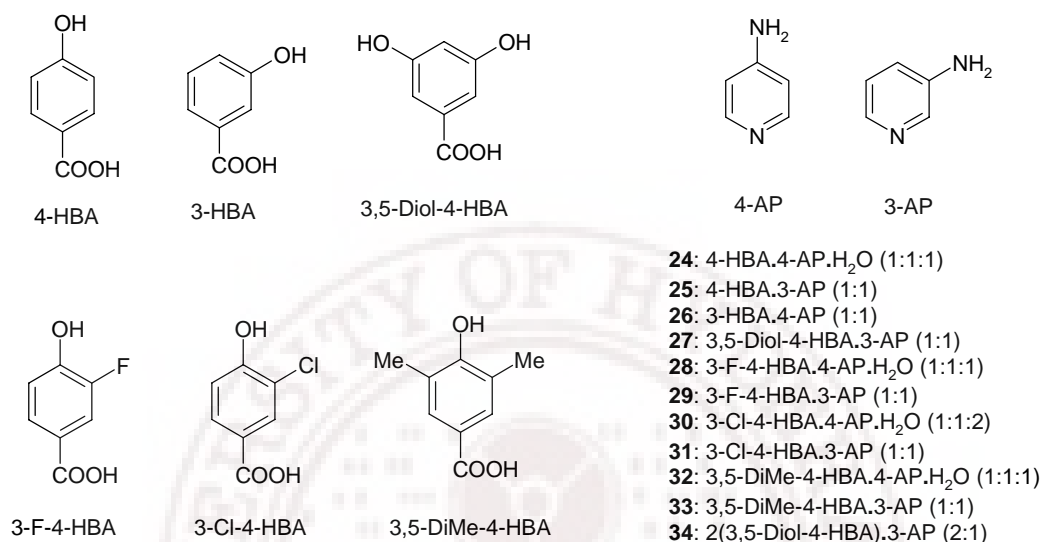


**Figure 1** Hydroxybenzoic acids (HBA) cocrystallized with aminopyridines (AP) and the resulting cocrystal compositions. Four from eleven structures are cocrystal hydrates (**24**, **28**, **30**, and **32**).

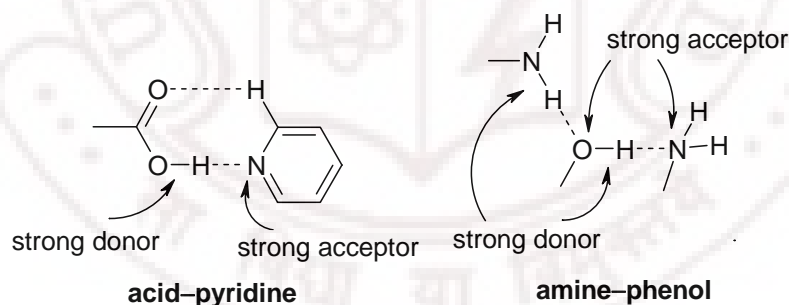


**Figure 2** Acid-pyridine and amine-phenol robust synthons are stabilized by strong hydrogen bond pairing.

## 6.2 Results and Discussion

Positional isomers of hydroxybenzoic acid (3-HBA, 4-HBA) and its F, Cl, Me, OH substituents, positional isomers of aminopyridine (3-AP, 4-AP) were selected for this study of synthon competition and cooperation. All cocrystallization experiments were carried out in MeOH solvent to obtain diffraction quality single crystals of 11 molecular

salts (**24** to **34**) listed in Figure 1. During crystallization four hydrates were obtained (**24**, **28**, **30** and **32**) and analyzed as part of the same structural family.

The robust acid-pyridine heterosynthon ( $\text{PyNH}\cdots\text{HOOC}$  or  $\text{PyNH}^+\cdots\text{OOC}^-$ ) can exist in four variants.<sup>10</sup> They are (i) neutral, two-point; (ii) neutral, single-point; (iii) ionic, two point; and (iv) ionic, single-point (Figure 3). The carboxylic acid OH donor is localized on the acid group and pyridine N is the acceptor in neutral synthons. There is auxiliary support from (pyridine)  $\text{C-H}\cdots\text{O}$  (carbonyl) interaction to the two-point cyclic motif (i) in the coplanar arrangement of interacting functional groups. The acid-pyridine neutral two point synthon has energy of  $9.9\text{--}10.0\text{ kcal mol}^{-1}$  and occurrence probability of 91% when competing functional groups are absent.<sup>10i,13a</sup> Twisting of the acid and pyridine groups across the  $\text{O-H}\cdots\text{N}$  hydrogen bond gives motif (ii). When there is a sufficient  $\text{pK}_a$  difference between the  $\text{COOH}$  and pyridyl groups proton transfer will occur to give an ionic hydrogen bond  $\text{N}^+\text{--H}\cdots\text{O}^-$ , which too can exist as two-point or single interaction, (iii) and (iv). Motifs (iii) and (iv) are observed in the crystal structures of this study (molecular salt **24–34**).

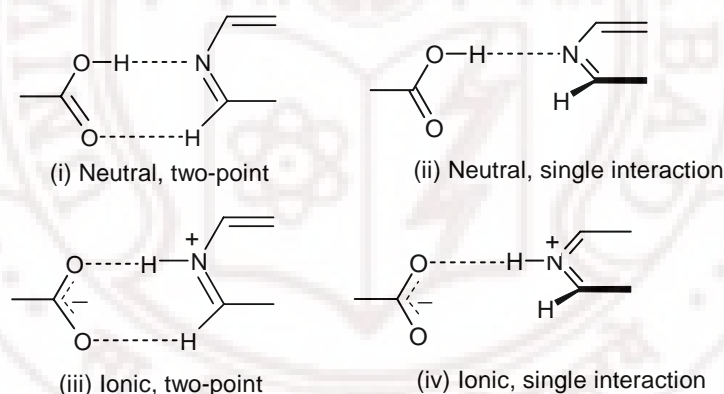


**Figure 3** Four variants of acid–pyridine H bonding in crystal structures. The two point synthon i, iii is present when the groups are coplanar but single interaction in ii, iv when the pyridyl ring is twisted out of the  $\text{COO}$  plane.

There has been a long standing and lively debate on the nomenclature issues in crystal engineering, starting from what is a cocrystal, or cocrystal/salt, to the definition of pseudopolymorph, solvate, host–guest compounds etc. Cocrystal<sup>21</sup> can be defined as multiple-component crystal structure in which two or more compounds coexist through hydrogen bonds or non-covalent interactions. If the reactants are solids at ambient

conditions, the multi-component crystalline materials are cocrystals and those composed of one or more solids and a liquid are known solvates or pseudopolymorphs. However the multi-component system is known as molecular salt/ salt if proton is transferred from acid to base in the ionic state. Thus salts and cocrystals are multicomponent crystals that can be distinguished by the location of the proton between an acid and a base. An advantage of neutral cocrystals or ionic salts is that existing properties of solids can be improved. The transfer from neutral to ionic hydrogen bond can be as a continuum of intermediate  $N\cdots H\cdots O$  bond state.<sup>22,23</sup> The extent of proton transfer in the solid state is not predictable in the continuum between the two extremes. The  $\Delta pK_a$  value ( $pK_a$  of base –  $pK_a$  of acid) in solution and the crystalline environment determines the extent of proton transfer. The issue of whether the acid-pyridine synthon is neutral or ionic is more difficult unless we have 3D coordinates of the complex or neutron diffraction to locate the hydrogen position accurately.

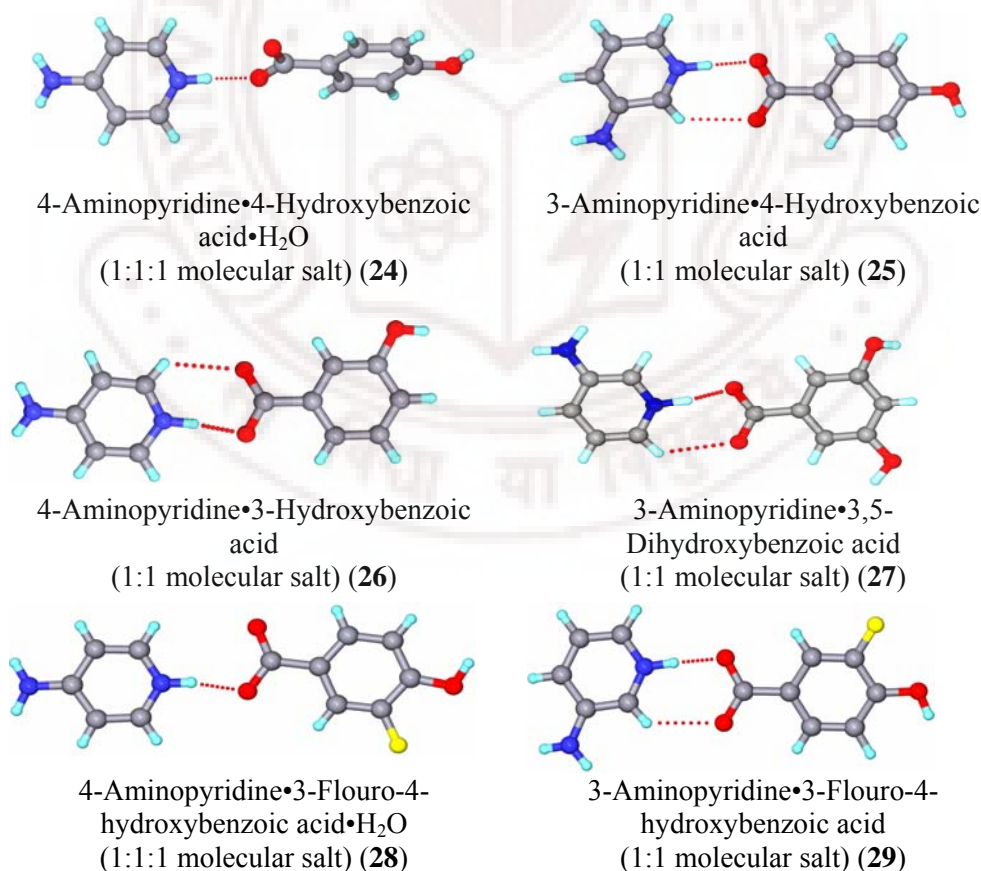
The term “molecular salt” is used where both anion and cation are derived from acidic and basic molecules, or electron acceptor and donor species. Molecular salts have been referred to in the context of organic nonlinear optical materials,<sup>24a</sup> pharmaceutical solids,<sup>24b</sup> and structural chemistry<sup>24c</sup>. When both ionic components are neutral organic molecules prior to proton or electron transfer they may be referred to as “molecular salt” after proton transfer. When one or both components are simple counterions (say  $Cl^-$  or  $Na^+$ ) then the common word salt is correct; for example, ranitidine hydrochloride, sodium diclofenac, and sodium chloride are all salts. Multiple hydrogen bond synthon combinations can be possible in molecular salts because of multiple functional groups on both cation and anion species compared to salts in which hydrogen bonding modes with the counterion are simpler and well-defined.

Some examples of  $COOH/COO^-$ , pyridine/ $PyNH^+$ , aniline, and phenol fragments in the same multicomponent crystal structures are extracted from CSD listed<sup>17</sup> in Table 1. There is a mix of neutral  $O-H\cdots N$  and ionic  $N^+-H\cdots O^-$  acid-pyridine synthons in these crystal structures. Hydrogen bond recognition and pairing studies when many functional groups ( $COOH/COO^-$ ,  $Py/PyNH^+$ ,  $OH$ , and  $NH_2$ ) are present in the same crystal structure are relatively few, and this was a reason for carrying out the present work.

**Table 1** Cocrystal/molecular salt structures wherein COOH/COO<sup>−</sup>, pyridine/PyNH<sup>+</sup>, NH<sub>2</sub>, and phenol OH functional groups are all present are listed in (a) and structure pairs of 3-AP and 4-AP with the carboxylic acid having no phenol OH groups show neutral synthon is listed in (b).

|     |          |        |        |        |        |
|-----|----------|--------|--------|--------|--------|
| (a) | AJECX    | EYIWIS | GIMSIF | GIMSOL | KEFZAX |
|     | KERFUJ   | LEWRUA | MIPRIM | MIPROS | RIGWUA |
|     | SLCADB10 | TEZXIG |        |        |        |
| (b) | BAXZAC   | OMIHIB | RALDUD | RALFAL |        |

The ionic (Py)N<sup>+</sup>–H<sup>+</sup>···O<sup>−</sup> (carboxylate) synthon is common in 10 crystal structures from **24–33**, whereas crystal structure **34** is sustained by (Py)N<sup>+</sup>–H<sup>+</sup>···O (acid) hydrogen bond. Acid-pyridine ionic synthon N<sup>+</sup>–H<sup>+</sup>···O<sup>−</sup> hydrogen bond and auxiliary C–H<sup>+</sup>···O interaction in the crystal structures **24–34** are shown in Figure 4. In all cases proton is transferred from COOH to PyN. The two-point ionic synthon (iii) is present in six structures (**25, 26, 27, 29, 30, 31**), and a single point ionic hydrogen bond (iv) is present in four structures (**24, 28, 32, 33**).





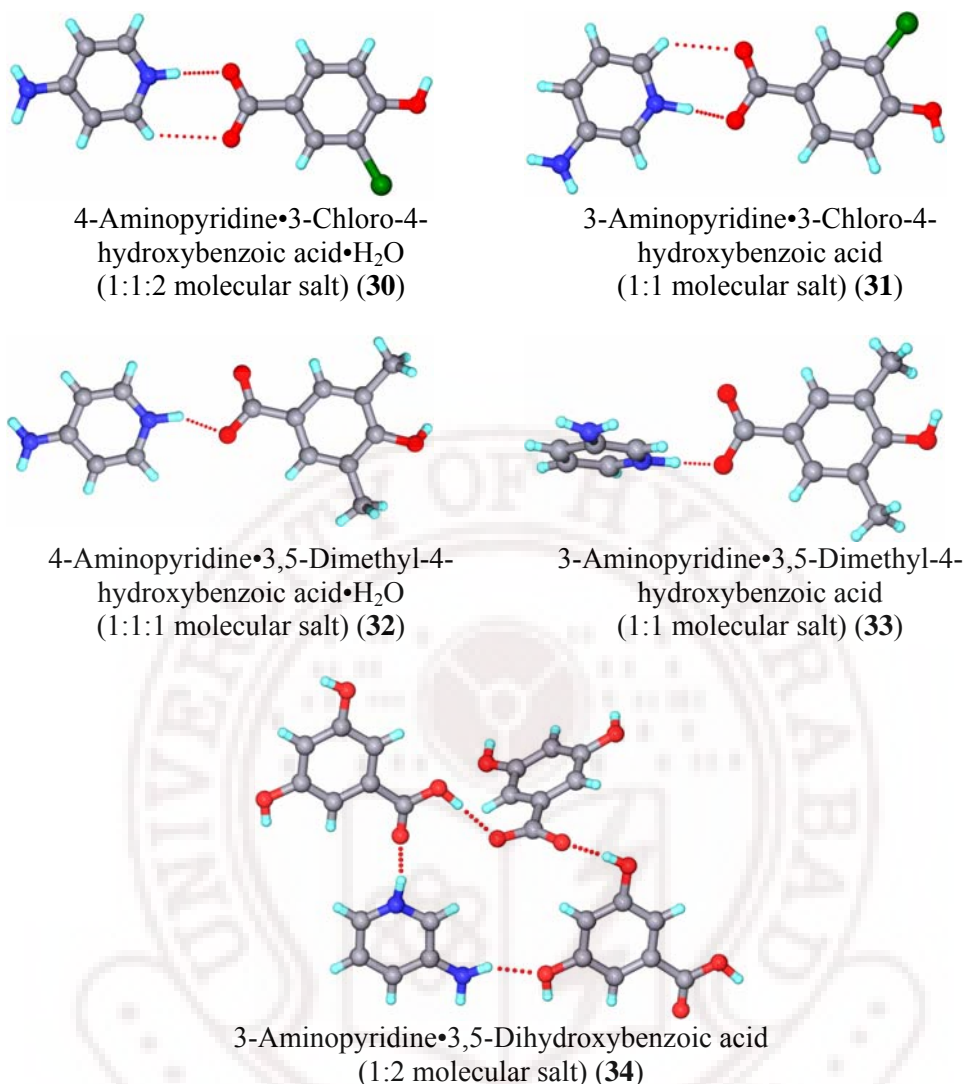


**Figure 4** Acid-pyridine ionic synthon  $N^+-H\cdots O^-$  hydrogen bond and auxiliary  $C-H\cdots O$  interaction in crystal structures **24-33** except for **34** the acceptor is neutral  $O=C$  from  $COOH$  group.

The spectroscopic properties and structure analysis of strongly hydrogen-bonded molecular salts can unveil whether the  $COOH$  and pyridine groups are neutral or ionized. The  $C-O$ ,  $C=O$  bond distances and  $C-N-C$ ,  $C-N^+-C$  angles also ascertain whether it is neutral cocrystal or ionic salt. For example, bond distances of 1.30, 1.20 Å and angles of 117-118° indicate a neutral synthon, whereas an intermediate distance of 1.25 Å and a slightly obtuse angle of 120-121° mean an ionized pyridinium state.<sup>22,25</sup> The  $C-O$  distance parameter is restated as  $\Delta r < 0.03$  Å for ionic  $COO^-$  and  $\Delta r > 0.08$  Å for neutral

COOH.<sup>23</sup> Similarly, C–O···N–C torsion angles upto 15° may be considered coplanar and two-point synthon, whereas greater twist implies a single hydrogen bond. However, in **28**, **32** the groups are coplanar but oriented away to a single-point hydrogen bond. As a preliminary confirmation of cocrystal or salt, carbonyl stretch frequencies<sup>26</sup> for complexes **24** to **34** are summarized in the Table 2. The monomeric C=O stretching band of a carboxylic acid, when on an aromatic ring, appears at around 1760 cm<sup>-1</sup>, while the acid dimeric C=O stretching mode absorbs at a lower frequency in the region of 1720-1706 cm<sup>-1</sup>. The carboxylate ion displays a strong asymmetrical stretching band around 1650-1550 cm<sup>-1</sup> and a weaker symmetric stretch ~1400 cm<sup>-1</sup>. The results directly correlate with the proton transfer from acid to pyridine nitrogen. Furthermore structure **34** shows a strong peak at 1748 cm<sup>-1</sup> indicates the presence of carboxylic acid group. No peak was found in the region of 1720-1706 cm<sup>-1</sup> suggesting carboxylic acid dimer is absent in all the structures. N<sup>+</sup>–H···O<sup>-</sup> and C–H···O hydrogen bond distances for all molecular salts and C–O, C=O bond distances and C–N–C, C–N<sup>+</sup>–C angles for ionic pyridinium···carboxylate synthon are listed in Table 3.

**Table 2** FT-IR stretching frequencies for molecular salts **24–34**.

| Molecular salt  | <b>24</b>     | <b>25</b>     | <b>26</b>     | <b>27</b>     | <b>28</b>     | <b>29</b>     |
|---|---------------|---------------|---------------|---------------|---------------|---------------|
| Carboxylate<br>C–O <sub>as</sub> , $\nu_s$ (cm <sup>-1</sup> )    | 1644,<br>1379 | 1611,<br>1377 | 1636,<br>1372 | 1617,<br>1372 | 1655,<br>1375 | 1616,<br>1493 |
| Carboxylic acid<br>C=O <sub>as</sub> (cm <sup>-1</sup> )          | ---           | ---           | ---           | ---           | ---           | ---           |
| Molecular salt  | <b>30</b>     | <b>31</b>     | <b>32</b>     | <b>33</b>     | <b>34</b>     |               |
| Carboxylate<br>C–O <sub>as</sub> , $\nu_s$<br>(cm <sup>-1</sup> ) | 1628,<br>1367 | 1634,<br>1380 | 1626,<br>1365 | 1618,<br>1381 | 1601,<br>1375 |               |
| Carboxylic acid<br>C=O <sub>as</sub> (cm <sup>-1</sup> )          | ---           | ---           | ---           | ---           | 1748          |               |

**Table 3**  $\text{N}^+-\text{H}\cdots\text{O}^-$ ,  $\text{C}-\text{H}\cdots\text{O}$  bond parameters (neutron normalized),  $\text{C}-\text{O}$  bond distances for  $\text{COO}^-$  group  $\text{C}-\text{N}^+-\text{C}$  angle for pyridine and  $\text{C}-\text{O}\cdots\text{N}-\text{C}$  torsion angles in molecular salts **24–34**.

| Molecular Salt | $\text{N}^+-\text{H}\cdots\text{O}^-$<br>$d$ (Å), $\theta$ (°) | $\text{C}-\text{H}\cdots\text{O}$<br>$d$ (Å), $\theta$ (°) | $\text{C}-\text{O}$<br>$r_1, r_2$ (Å) | $\text{C}-\text{N}^+-\text{C}$<br>$\angle$ (°) | $\text{C}-\text{O}\cdots\text{N}-\text{C}$<br>$\tau$ (°) |
|----------------|--|--|---------------------------------------|--|--|
| <b>24</b>      | 1.66, 168.4  |  | 1.264(2), 1.245(2);                   | 119.6(2),                                      | 54.7   |
|                | 1.67, 170.1  | ---  | 1.228(2), 1.270(2)                    | 119.9(2)                                       | 49.5   |
| <b>25</b>      | 1.61, 179.6  | 2.44, 123.6  | 1.261(1), 1.268(1)                    | 122.7(1)                                       | 13.6   |
| <b>26</b>      | 1.66, 173.8  | 2.55, 121.3  | 1.252(1), 1.272(1)                    | 120.0(1)                                       | 5.2  |
| <b>27</b>      | 1.68, 173.1  | 2.50, 139.0  | 1.274(3), 1.259(3)                    | 122.1(3)                                       | 16.5   |
| <b>28</b>      | 1.67, 167.5  | ---  | 1.248(3), 1.257(3)                    | 120.0(2)                                       | 4.5  |
| <b>29</b>      | 1.63, 177.0  | 2.40, 126.6  | 1.258(2), 1.260(2)                    | 122.4(2)                                       | 9.6  |
| <b>30</b>      | 1.75, 174.7  | 2.66, 125.5  | 1.261(6), 1.241(6)                    | 120.8(5)                                       | 6.8  |
| <b>31</b>      | 1.61, 175.8  | 2.51, 128.3  | 1.292(3), 1.235(3)                    | 123.0(3)                                       | 5.5  |
| <b>32</b>      | 1.81, 151.0  | ---  | 1.250(2), 1.260(2)                    | 120.0(2)                                       | 17.0   |
| <b>33</b>      | 1.57, 171.7  | ---  | 1.261(2), 1.246(2)                    | 122.4(2)                                       | 59.0   |
| <b>34</b>      | 1.67, 170.2  | ---  | 1.267(3), 1.249(3);                   | 125.1(4)                                       | 12.5   |
|                | ( $\text{N}^+-\text{H}\cdots\text{O}$ )                        |  | 1.193(5), 1.300(4)                    |  |  |

For structure **34** the acceptor is neutral  $\text{C}=\text{O}$  instead of ionic  $\text{COO}^-$  ( $\text{N}^+-\text{H}\cdots\text{O}=\text{C}$ , Table 3). Additional hydrogen bond parameters calculated in PLATON for structures **24–34** are summarized in Table 4. All distances are neutron normalized.

**Table 4** Hydrogen bond parameters in molecular salts **24–34** calculated in PLATON.  $\text{O}-\text{H}$ ,  $\text{N}-\text{H}$ ,  $\text{C}-\text{H}$  distances are neutron-normalized.

| Molecular salt | Hydrogen bond                         | $\text{H}\cdots\text{A}/\text{Å}$ | $\text{D}\cdots\text{A}/\text{Å}$ | $\angle\text{D}-\text{H}\cdots\text{A}/^\circ$ |
|----------------|---------------------------------------|-----------------------------------|-----------------------------------|--|
| <b>24</b>      | $\text{N1}-\text{H1A}\cdots\text{O2}$ | 1.90                              | 2.887(2)                          | 164.9  |
|                | $\text{N1}-\text{H1B}\cdots\text{O6}$ | 2.01                              | 3.011(2)                          | 172.0  |
|                | $\text{N2}-\text{H2}\cdots\text{O5}$  | 1.67                              | 2.668(2)                          | 170.1  |
|                | $\text{N3}-\text{H3A}\cdots\text{O3}$ | 1.98                              | 2.972(2)                          | 166.4  |
|                | $\text{N3}-\text{H3B}\cdots\text{O4}$ | 1.89                              | 2.871(2)                          | 163.2  |
|                | $\text{O3}-\text{H3C}\cdots\text{O7}$ | 1.70                              | 2.641(2)                          | 158.9  |
|                | $\text{N4}-\text{H4A}\cdots\text{O1}$ | 1.66                              | 2.652(2)                          | 168.4  |
|                | $\text{O6}-\text{H6A}\cdots\text{O8}$ | 1.62                              | 2.587(2)                          | 165.8  |
|                | $\text{O7}-\text{H7A}\cdots\text{O5}$ | 1.74                              | 2.703(2)                          | 165.9  |

|    |              |      |          |       |
|----|--------------|------|----------|-------|
| 25 | O8–H8A···O1  | 1.78 | 2.750(2) | 168.8 |
|    | O8–H8B···O2  | 1.82 | 2.793(2) | 169.3 |
|    | N1–H1···O2   | 1.61 | 2.622(1) | 179.6 |
|    | N2–H2A···O2  | 1.90 | 2.877(1) | 162.8 |
|    | N2–H2B···O1  | 1.90 | 2.895(2) | 168.8 |
|    | O3–H3···O1   | 1.65 | 2.635(1) | 175.0 |
|    | C7–H7···O3   | 2.47 | 3.438(1) | 147.8 |
|    | C8–H8···O1   | 2.44 | 3.172(2) | 123.6 |
| 26 | C10–H9···O3  | 2.43 | 3.504(2) | 171.6 |
|    | N1–H1A···O2  | 1.83 | 2.843(1) | 177.5 |
|    | N1–H1B···O3  | 1.95 | 2.943(1) | 168.0 |
|    | N2–H2A···O1  | 1.66 | 2.664(1) | 173.8 |
|    | N2–H2A···O2  | 2.47 | 3.148(1) | 123.8 |
|    | O3–H3A···O2  | 1.67 | 2.651(1) | 173.2 |
|    | C9–H9···O1   | 2.37 | 3.185(2) | 130.5 |
|    | C8–H8···O2   | 2.55 | 3.242(1) | 121.3 |
| 27 | N1–H1···O1   | 1.68 | 2.688(3) | 173.1 |
|    | N1–H1···O2   | 2.46 | 3.157(3) | 125.3 |
|    | N2–H2A···O2  | 2.08 | 3.031(3) | 156.7 |
|    | N2–H2B···O3  | 1.97 | 2.970(4) | 173.0 |
|    | O3–H3A···O1  | 1.67 | 2.649(2) | 172.0 |
|    | O4–H4···O2   | 1.81 | 2.746(2) | 158.8 |
|    | C8–H8···O2   | 2.22 | 3.126(3) | 140.0 |
|    | C12–H12···O4 | 2.50 | 3.388(3) | 139.0 |
| 28 | N1–H1···O2   | 1.67 | 2.668(2) | 167.5 |
|    | N2–H2A···F1  | 2.34 | 2.975(2) | 119.6 |
|    | N2–H2A···O3  | 2.18 | 3.173(3) | 168.4 |
|    | N2–H2B···O1  | 2.10 | 3.069(3) | 161.6 |
|    | O3–H3A···O4  | 1.67 | 2.616(3) | 160.5 |
|    | O4–H4A···O2  | 1.82 | 2.785(2) | 167.8 |
|    | O4–H4B···O1  | 1.84 | 2.807(3) | 168.8 |
|    | C7–H7···F1   | 2.31 | 3.086(2) | 126.9 |
| 29 | C9–H9···O1   | 2.45 | 3.341(3) | 138.8 |
|    | N1–H1···O2   | 1.63 | 2.643(2) | 177.0 |
|    | N2–H2A···O2  | 1.94 | 2.916(3) | 162.7 |
|    | N2–H2B···O1  | 1.94 | 2.934(3) | 167.5 |
|    | O3–H3A···O1  | 1.65 | 2.630(2) | 172.7 |
|    | C8–H8···O1   | 2.40 | 3.167(3) | 126.6 |
|    | C11–H11···F1 | 2.46 | 3.198(2) | 124.6 |
|    | N1–H1···O1   | 1.75 | 2.752(6) | 174.7 |
| 30 | N2–H2A···O3  | 2.02 | 2.992(6) | 160.8 |
|    | N2–H2B···O5  | 1.85 | 2.853(7) | 171.8 |
|    | O3–H3A···O4  | 1.63 | 2.605(5) | 170.5 |
|    | O4–H4A···O1  | 1.88 | 2.798(6) | 153.7 |
|    | O4–H4B···O2  | 1.77 | 2.753(7) | 174.9 |
|    | O5–H5A···O2  | 1.77 | 2.743(7) | 172.0 |
|    | O5–H5B···O1  | 1.77 | 2.747(7) | 169.6 |

|    |              |      |          |       |
|----|--------------|------|----------|-------|
| 31 | C8–H8...O2   | 2.66 | 3.408(7) | 125.5 |
|    | N1–H1...O1   | 1.61 | 2.617(3) | 175.8 |
|    | N2–H2A...O3  | 2.18 | 3.171(3) | 166.4 |
|    | N2–H2B...O2  | 1.89 | 2.887(4) | 171.2 |
|    | O3–H3A...O1  | 1.64 | 2.611(3) | 167.0 |
|    | C7–H7...Cl1  | 2.70 | 3.329(3) | 116.6 |
| 32 | C12–H12...O2 | 2.51 | 3.292(3) | 128.3 |
|    | N1–H1...O1   | 1.81 | 2.737(2) | 151.0 |
|    | N2–H2A...O4  | 1.85 | 2.852(3) | 171.3 |
|    | N2–H2B...O3  | 1.97 | 2.933(2) | 158.3 |
|    | O3–H3A...O2  | 1.69 | 2.663(2) | 172.7 |
|    | O4–H4A...O2  | 1.78 | 2.757(2) | 176.3 |
| 33 | O4–H4B...O1  | 1.78 | 2.753(2) | 170.9 |
|    | C8–H8A...O2  | 2.51 | 3.275(3) | 126.5 |
|    | N1–H1...O1   | 1.57 | 2.570(2) | 171.7 |
|    | N2–H2A...O2  | 1.97 | 2.972(2) | 171.6 |
|    | N2–H2B...O3  | 2.45 | 3.364(2) | 151.0 |
|    | O3–H3A...O2  | 1.75 | 2.722(2) | 171.4 |
| 34 | C9–H9B...O2  | 2.37 | 3.233(3) | 135.5 |
|    | C10–H10...O3 | 2.46 | 3.398(2) | 144.3 |
|    | C14–H14...O1 | 2.28 | 3.295(2) | 154.8 |
|    | O4–H1...O1   | 1.59 | 2.567(3) | 171.8 |
|    | N1–H1A...O5  | 1.67 | 2.671(5) | 170.2 |
|    | O3–H2...O2   | 1.76 | 2.738(3) | 175.2 |
|    | N2–H2A...O3  | 2.00 | 2.995(5) | 166.8 |
|    | N2–H2B...O8  | 1.97 | 2.939(5) | 161.1 |
|    | O8–H4...O4   | 1.73 | 2.693(3) | 164.5 |
|    | O6–H6A...O1  | 1.74 | 2.707(3) | 165.4 |
|    | O7–H7A...O2  | 1.75 | 2.729(3) | 173.1 |
|    | C5–H5...O1   | 2.49 | 3.221(4) | 124.0 |
|    | C10–H10...O7 | 2.36 | 3.324(5) | 147.1 |

### 6.3 Structural Analysis

#### Molecular Salt 24: 4-Aminopyridinium 4-Hydroxybenzoate Hydrate (1:1:1)

Upon slow evaporation of MeOH solvent at ambient temperature from the crystallization batch of 4-HBA and 4-AP afforded single crystals of molecular salt **24** which is solved and refined in triclinic space group  $P\bar{1}$  containing two 4-hydroxybenzoate (4-HBA<sup>−</sup>), two 4-aminopyridinium (4-APH<sup>+</sup>), and two water molecules in its asymmetric unit. The carboxylic acid proton is transferred to the pyridine nitrogen. Symmetry-independent 4-HBA<sup>−</sup> ions are connected via O–H...O<sup>−</sup> hydrogen bonds to form a staircase like network in the (102) plane. Aminopyridinium ions link staircase networks of 4-HBA<sup>−</sup> and water via N–H...O, N<sup>+</sup>–H...O<sup>−</sup>, N–H...O hydrogen bonds

(Figure 5). There are  $\text{H}_2\text{O}\cdots\text{OOC}$  tetramers and  $4\text{-APH}^+\cdots\text{phenol}$  hydrogen bonds in the structure. The cell parameters of molecular salts **24-34** are tabulated in appendix.

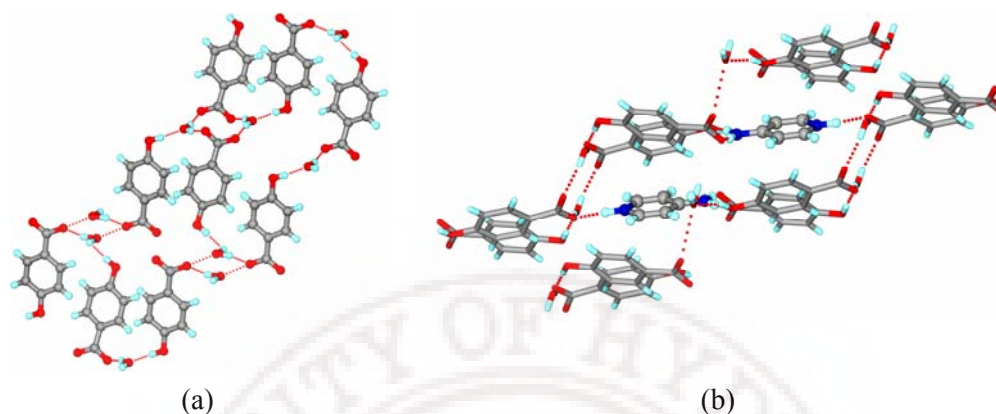


**Figure 5** (a) Staircase like network of  $4\text{-HBA}^-$  connected via water-carboxylate  $\text{O-H}\cdots\text{O}$  tetramer synthon along  $[010]$  and (b)  $\text{N-H}\cdots\text{O}$  bond with  $4\text{-APH}^+$  molecules connect staircase networks of molecular salt **24**.

#### Molecular Salt 25: 3-Aminopyridinium 4-Hydroxybenzoate (1:1).

The asymmetric unit of molecular salt **25** in monoclinic space group  $P2_1/c$  contains  $4\text{-HBA}^-$  and  $3\text{-APH}^+$  ions that make the acid-pyridine  $\text{N}^+\text{-H}\cdots\text{O}^-$  synthon. Helices along  $[010]$  connect the OH group to  $\text{COO}^-$  (Figure 6). The amino groups connect helices of hydroxybenzoate ions via  $\text{N-H}\cdots\text{O}^-$  hydrogen bonds.

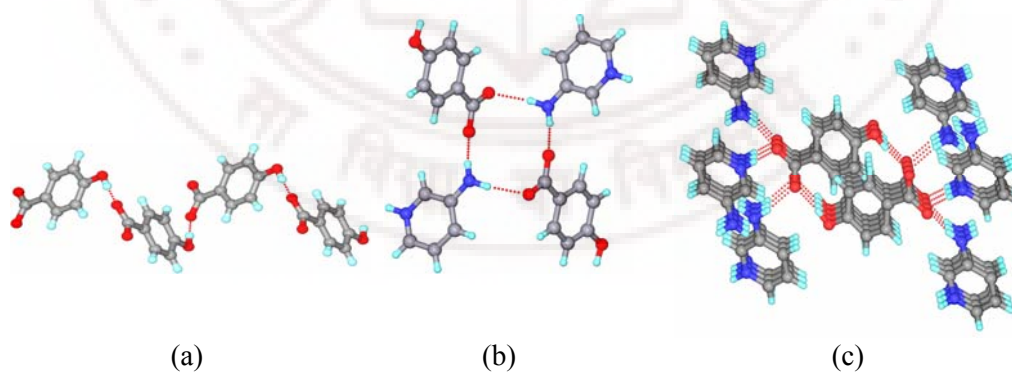


**Figure 6** (a) Helices of  $4\text{-HBA}^-$  along  $[010]$  in **25**. There are no direct hydrogen bonds between the helices. (b) Amine-carboxylate tetramer synthon between  $3\text{-APH}^+$  and  $4\text{-HBA}^-$  molecules in molecular salt **25** and the 3D packing (c) mediated via  $\text{O-H}\cdots\text{O}$  helices and  $\text{N-H}\cdots\text{O}$  tetramer synthon.



### Molecular Salt 26: 4-Aminopyridinium 3-Hydroxybenzoate (1:1).

The hydroxyl group of 3-HBA<sup>-</sup> is bonded to COO<sup>-</sup> oxygen in a 1D zigzag tape along [010] in structure **26**. The tapes are connected through NH<sub>2</sub> group of 4-APH<sup>+</sup> to make a sheet-like structure (Figure 7) in the (200) plane.

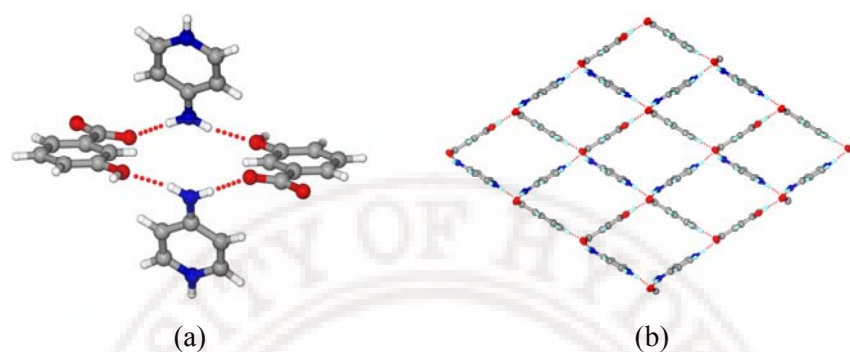


**Figure 7** (a) Tetramer of amino...carboxylate hydrogen bonded molecules 3-APH<sup>+</sup> and 4-HBA<sup>-</sup> in **26**, (b) Square network constructed by H bonds at the nodes and phenyl ring spacers as the molecular connectors. The four H bonds at each node are (pyridinium)N<sup>+</sup>–H...O<sup>-</sup>(carboxylate), (aniline)N–H...O<sup>-</sup>(carboxylate), (phenol)O–H...O<sup>-</sup>(carboxylate), and (aniline)N–H...O(phenol).

### Molecular Salts 27-33

Occurrences of the major synthons in molecular salts **27-33** (Figures 8 – 11) show the similarities in this family of crystal structures. Common PyNH<sup>+</sup>...<sup>-</sup>OOC synthon from molecular salt **24** to **33** is replaced by a neutral C=O acceptor in **34** (Figure 12). 3,5-DiHBA, its conjugate base 3,5-DiHBA<sup>-</sup>, and one 3-APH<sup>+</sup> are the unit cell components.

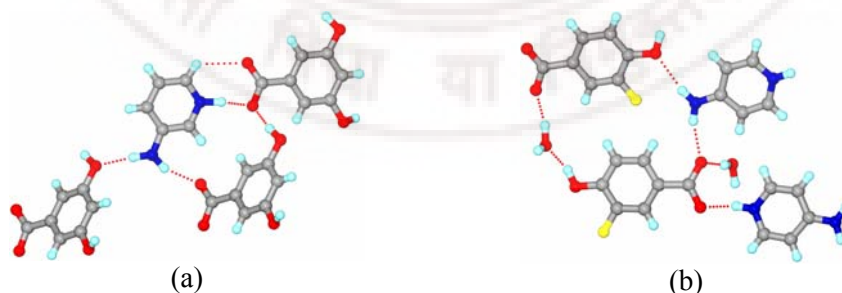


**Figure 8** (a) Major synthons in molecular salt **27** are pyridinium...carboxylate, amine...carboxylate, amine...hydroxyl and hydroxyl...carboxylate hydrogen bonds. (b) Major synthons in 3-F-4-HBA<sup>-</sup>•4-APH<sup>+</sup>•H<sub>2</sub>O molecular salt **28** are pyridinium...carboxylate, amine...carboxylate, amine...hydroxyl, water...carboxylate and hydroxyl...water.

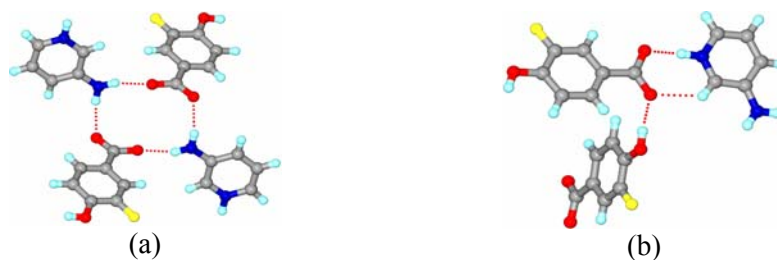


**Figure 9** Major synthons in 3-F-4-HBA<sup>−</sup>•3-APH<sup>+</sup> (molecular salt **29**) are amine...carboxylate tetramer in (a), and pyridinium...carboxylate and hydroxyl...carboxylate hydrogen bonds shown in (b).

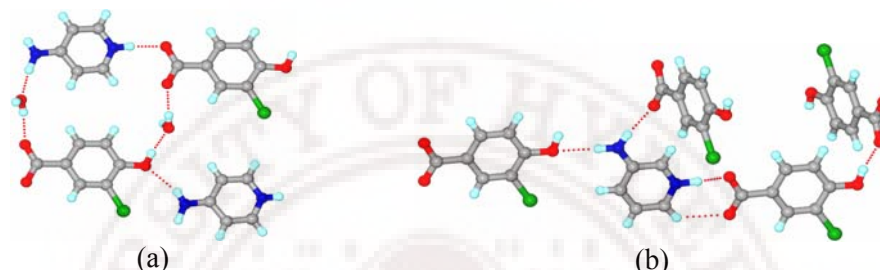


**Figure 10** (a) Major synthons in 3-Cl-4-HBA<sup>−</sup>•4-APH<sup>+</sup>•2H<sub>2</sub>O (molecular salt **30**) are pyridinium...carboxylate, amine...hydroxyl, water...carboxylate, hydroxyl...water, and amine...water. (b) Major synthons in 3-Cl-4-HBA<sup>−</sup>•3-APH<sup>+</sup> (molecular salt **31**) are pyridinium...carboxylate, amine...carboxylate, amine...hydroxyl, and hydroxyl...carboxylate.

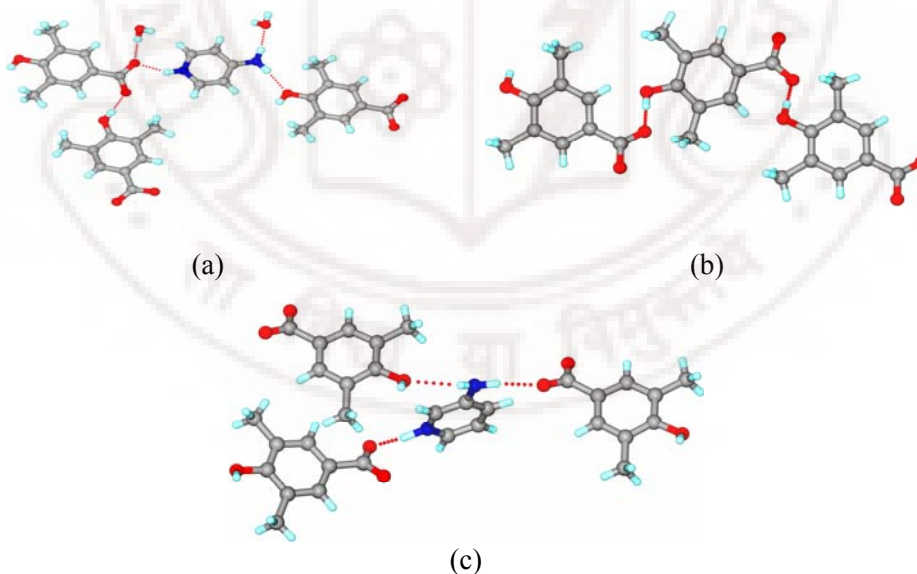


**Figure 11** (a) Major synthons in 3,5-DiMe-4-HBA<sup>−</sup>•4-APH<sup>+</sup>•H<sub>2</sub>O (molecular salt **32**) are pyridinium...carboxylate, amine...hydroxyl, hydroxyl...carboxylate, water...carboxylate, and amine...water. (b) Major synthons in 3,5-DiMe-4-HBA<sup>−</sup>•3-APH<sup>+</sup> (molecular salt **33**) are pyridinium...carboxylate, amine...carboxylate, amine...hydroxyl, hydroxyl...carboxylate hydrogen bonds (c).

**Molecular Salt 34: (3-Aminopyridinium 3,5-Hydroxybenzoate 3,5-Hydroxybenzoic acid (1:1:1))**

Slow solvent evaporation inside refrigerator ( $\sim 5^{\circ}\text{C}$ ) gave needle shaped brown crystals of molecular salt **34**, crystallized in orthorhombic space group *Pccn* with one neutral 3,5-dihydroxybenzoic acid, one 3-aminopyridinium and a 3,5-dihydroxybenzoate molecules in the asymmetric unit. Hydrogen bond synthons in the crystal structure is shown in Figure 12a. Neutral acid molecule and amino pyridine forms zig-zag tape along [010] direction via  $\text{N}^+-\text{H}\cdots\text{O}$  and  $\text{N}-\text{H}\cdots\text{O}^-$  hydrogen bond which further extends to a layer structure forming distorted hexagonal like channels along [001] direction. The carboxylate molecule sits in channels forming a 1D tape like structure via  $\text{O}-\text{H}\cdots\text{O}$  hydrogen bond (Figure 12b). Hydrogen parameters are summarized in Table 4.

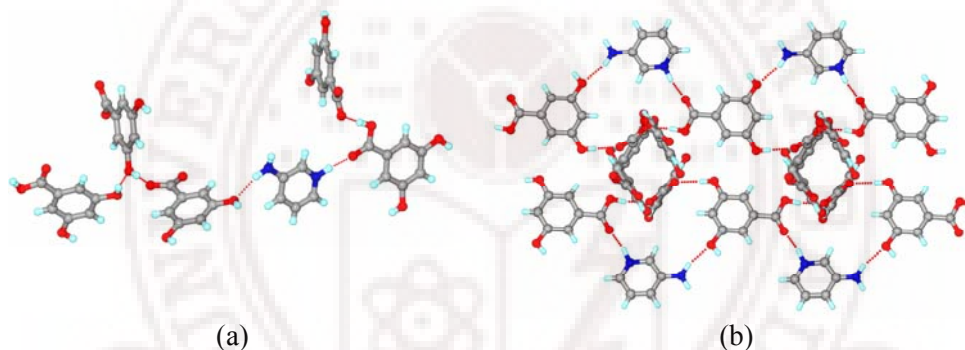


**Figure 12** (a) Major synthons in 3,5-DiHBA•3,5-DiHBA<sup>-</sup>•3-APH<sup>+</sup> (molecular salt **34**) amine $\cdots$ hydroxyl, hydroxyl $\cdots$ carboxylate, carboxyl $\cdots$ carboxylate and hydroxyl $\cdots$ hydroxyl are depicted in two views of the crystal structure. (b) Pyridinium–carboxyl molecular tapes along [010] are connected via second carboxylate molecules, which reside in channels created by the binary components.

The para/para combination of hydroxybenzoic acid and amino pyridine (4-HBA<sup>-</sup> and 4-APH<sup>+</sup>) results in hydrated structures. Water content in crystal structures **24**, **28**, **30**, **32** (color code blue in Table 5) was further confirmed by thermogravimetry (TG) and from the melting onset of endotherm in Differential Scanning Calorimetry (DSC) (Table 5). However meta/para combination gave non-hydrated structures. Clear difference in the melting onset temperature from the starting material indicates the formation of these multicomponent systems.

**Table 5** DSC and TG analysis for molecular salts **24-34**.

| Molecular salt | Differential Scanning Calorimetry (DSC) |                                   | Thermogravimetry (TG) |            |
|----------------|---|-----------------------------------|-----------------------|------------|
|                | Water release (°C)                      | Melting Point (°C)<br>Onset/ Peak | Experimental          | Calculated |
| <b>24</b>      | 110.26, 114.0                           | 186.60, 187.84                    | 7.11                  | 7.19       |
| <b>25</b>      | ---                                     | 184.14, 185.70                    |                       |            |
| <b>26</b>      | ---                                     | 209.26, 210.53                    |                       |            |
| <b>27</b>      | ---                                     | 184.05, 185.83                    |                       |            |
| <b>28</b>      | 104.86, 111.13                          | 179.51, 180.80                    | 6.71                  | 6.71       |
| <b>29</b>      | ---                                     | 173.86, 174.48                    |                       |            |
| <b>30</b>      | 111.87, 113.71                          | 165.05, 167.69                    | 11.89                 | 11.90      |
| <b>31</b>      | ---                                     | 150.59, 152.24                    |                       |            |
| <b>32</b>      | 115.60, 117.42                          | 170.93, 171.96                    | 6.52                  | 6.47       |
| <b>33</b>      | ---                                     | 164.13, 167.81                    |                       |            |
| <b>34</b>      | ---                                     | 204.14, 205.77                    |                       |            |

Occurrences for a particular synthon were analyzed (Table 6) in molecular salts **24 - 34**. In all four hydrate structures **24, 28, 30, 32** water is hydrogen bonded to ionic carboxylate via  $\text{O-H}\cdots\text{O}^-$  hydrogen bonds in  $R_4^4(12)$  motif (Figure 13a). The corresponding amine-carboxylate  $\text{N-H}\cdots\text{O}^-$  of the same graph set notation<sup>27a</sup> is present in structures **25** and **29**. Graph set approach is nothing but to analyze the molecular connectivity of hydrogen-bond patterns. There are four motifs, each specified by a designator: chains (**C**), rings (**R**), intramolecular hydrogen-bonded patterns (**S**), and finite patterns (**D**). Specification of a pattern is augmented by a subscript designating the number of hydrogen-bond donors **d** and a superscript giving the number of hydrogen-bond acceptors **a**. In addition, the number of atoms **n** in the pattern is called the degree of the pattern and is specified in parentheses. The graph set descriptor is then given as  $\mathbf{G}_d^a(\mathbf{n})$ , where **G** represents one of the four possible designators. The  $R_4^2(8)$  motif of  $\text{N-H}\cdots\text{O}^-$  bonds<sup>27b,c</sup> which is observed frequently in cocrystals/salts having  $\text{COOH}/\text{COO}^-$  is not found in this set of structures.  $\text{OH}\cdots\text{OOC}$  synthon is absent in **24, 28, 30** and  $\text{NH}_2\cdots\text{OH}$  hydrogen bond is not present in structures **25, 29**.  $\text{COOH}\cdots\text{OOC}$ ,  $\text{OH}\cdots\text{OH}$  hydrogen bonding is present only in **34**. The phenol group in **32** does not bond with

water. The amine group interacts with water in structures **30**, **32**. Structures **27**, **34** are made up of 3-AP and 3,5-DiHBA in 1:1 (ionic) and 1:1:1 (ionic and neutral) stoichiometry. Naturally, they contain different hydrogen bond synthons; for example, **34** has neutral COOH and ionic COO<sup>-</sup>, PyNH<sup>+</sup> species, whereas the usual PyNH<sup>+</sup>...<sup>-</sup>OOC synthon is present in **27** but apparently their stoichiometry of 3-aminopyridine and 3,5-dihydroxybenzoic acid is 1:1 and 1:2 respectively. A series of cocrystals of variable stoichiometry of phloroglucinol and phenazine (cocrystals of 1:1.5, 1:1.75 and 1:2 phloroglucinol:phenazine stoichiometry)<sup>28</sup> was studied by us. A list of all reported examples of multiple stoichiometry cocrystals was tabulated at that time. The outcome of the analysis of synthon cooperation and competition between four functional groups, COO<sup>-</sup>, PyNH<sup>+</sup>, OH and NH<sub>2</sub> and H<sub>2</sub>O, is summarized in Table 6.

#### 6.4 Proton Transfer: Cocrystal or Salt

Proton transfer phenomenon is important because of its widespread occurrence as elementary step in many reactions of chemistry and biology. When  $\Delta pK_a$  is sufficiently large ( $>4$ ) salt formation is very likely.<sup>29</sup> Johnson and Rumon studied<sup>29a</sup> the type of hydrogen bonding interaction as a function of  $\Delta pK_a$ , where  $\Delta pK_a$  refers to the difference in  $pK_a$  of pyridinium ion (BH<sup>+</sup>) and the benzoic acid (AH) in water via infrared spectra of solid state complexes of benzoic acid and substituted benzoic acids with pyridine and substituted pyridines. Continuum between two extremes, B...HA and BH<sup>+</sup>...<sup>-</sup>A, where B represents the pyridine base and HA represents the carboxylic acid in interaction were considered. The issue of proton transfer in carboxylic acid...pyridine synthon to give PyNH<sup>+</sup>...<sup>-</sup>OOC (O-H...N → N<sup>+</sup>-H...O<sup>-</sup>) as a function of  $pK_a$  is still a problem.

**Table 6** Hydrogen bonding in molecular salts **24–34** (donor⋯acceptor). The number of occurrences for a particular synthon (green cell) decrease from left to right. Hydrate salts are numbered in blue color font.

| Molecular Salt | Pyridinium⋯<br>Carboxylate | Amine⋯<br>Hydroxyl | Amine⋯<br>Carboxylate | Hydroxyl⋯<br>Carboxylate | Water⋯<br>Carboxylate | Hydroxyl⋯<br>Water | Amine⋯<br>Water |
|----------------|----------------------------|--------------------|-----------------------|--------------------------|-----------------------|--------------------|-----------------|
| <b>24</b>      |                            |                    |                       |                          |                       |                    |                 |
| <b>25</b>      |                            |                    |                       |                          |                       |                    |                 |
| <b>26</b>      |                            |                    |                       |                          |                       |                    |                 |
| <b>27</b>      |                            |                    |                       |                          |                       |                    |                 |
| <b>28</b>      |                            |                    |                       |                          |                       |                    |                 |
| <b>29</b>      |                            |                    |                       |                          |                       |                    |                 |
| <b>30</b>      |                            |                    |                       |                          |                       |                    |                 |
| <b>31</b>      |                            |                    |                       |                          |                       |                    |                 |
| <b>32</b>      |                            |                    |                       |                          |                       |                    |                 |
| <b>33</b>      |                            |                    |                       |                          |                       |                    |                 |
| <b>34</b>      |                            |                    |                       |                          |                       |                    |                 |

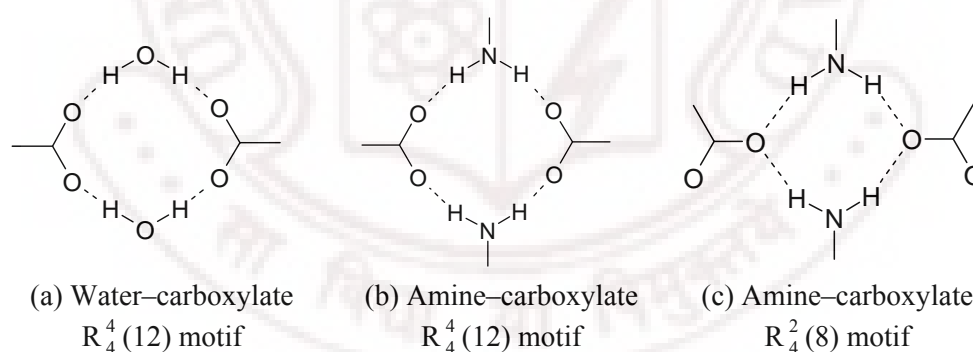


**Figure 13** Water-carboxylate synthon of  $\text{O}-\text{H}\cdots\text{O}^-$  hydrogen bonds (a) in hydrates **24**, **28**, **30**, **32** and amine-carboxylate  $\text{N}-\text{H}\cdots\text{O}^-$  synthon (b) in molecular salts **25**, **29** have  $R_4^4(12)$  motif. The smaller  $R_4^2(8)$  motif (c) typical of amine-carboxylate groups is absent in these structures.

A study by Wilson<sup>22f</sup> on the position of proton in the complexes of pentachlorophenol with a series of dimethylpyridines (lutidines) showed competition for the hydrogen atom in the strong hydrogen bonds by the  $\text{p}K_a$ -matched molecules lead to a



variable degree of hydrogen transfer from pentachlorophenol towards lutidines, depending on the  $\Delta pK_a$  value in that particular complex. Neutron diffraction and new advances in X-ray can accurately predict the exact location<sup>25</sup> of the proton in a strong hydrogen bond which has got immense importance particularly in pharmaceutical industry.<sup>22,23</sup> A rule of thumb is that proton transfer will occur from acid to base when the difference in  $pK_a$  between the conjugate acid of the base and the carboxylic acid is  $>3.75$ , and neutral complex will form when  $\Delta pK_a < 3.75$ , the so-called “rule of 3”<sup>29a</sup> is discussed in chapter 1. With additional structural data on acid...pyridine cocrystals and salts the crucial  $pK_a$  range of  $-2.5$  to  $+2.5$ , in which many organic acids and pyridine/amine complexes lie, was subdivided into three categories. The O–H...N interaction of a COOH...Py system will be neutral when  $\Delta pK_a < 0$ , it will have an intermediate hydrogen bond character of O–H...N and/or  $N^+–H...O^-$  when  $0 < \Delta pK_a < 3.75$ , and it will be ionic  $N^+–H...O^-$  when  $\Delta pK_a > 3.75$ .<sup>10b</sup> Black and coworkers performed a screening of 17 molecular salts of a model pharmaceutical base (1R,2S)-2-methylamino-1-phenylpropan-1-ol or more commonly ephedrine [1R,2S-(–)-ephedrine] on the basis of most important molecular properties for the design of a salt screen i.e. the acid and base dissociation constants ( $pK_a$  value). This illustrates the oft-quoted “rule of 2”; that is, for salt formation or proton transfer, the difference between the acid and base dissociation constants ( $\Delta pK_a$ ) must be  $>2$ .<sup>24b</sup> A very recent study by Tocher *et. al.* on two component crystals formed from pyridine or 4-dimethylaminopyridine with maleic, fumaric, phthalic, isophthalic or terephthalic acids showed the multicomponent systems involving pyridine results both salts and cocrystals, while 4-dimethylaminopyridine crystallized exclusively as a salt which is in agreement with differences in  $pK_a$  values.

Even as bioavailability of a drug is intimately related to its formulation, neutral cocrystal or ionic salt, there is no easy way to know the answer before structure determination. Until we do not have a single crystal data or even better a neutron diffraction data it is difficult to predict accurately the location of the hydrogen atom in the solid-state from acid/base strength or  $pK_a$  differences. In general  $pK_a$  of a compound defines only the ability of the proton to be transferred from acid to base. Also  $pK_a$  values are specific to solvent and thus have limited predictive ability about the location of the hydrogen atom in the crystal structure. Dissociation constants can differ by up to 4-5 orders of magnitude by change from water to MeOH medium,<sup>30</sup> for example, AcOH  $pK_a$

is 4.76 in water and 9.63 in MeOH. In effect, salt formation is certain with an organic base (e.g., ephedrine  $pK_a$  is 9.74 in water and 8.69 in MeOH) when crystallized in aqueous medium but not in MeOH.<sup>24c</sup> The nature of the crystalline solid which precipitates from an equilibrium mixture of hydrogen bonded aggregates in solution will depend on many factors such as pH, solvent polarity, temperature, concentration, rate of cooling, supersaturation, crystal nucleation, growth morphology, etc. The crystallized solid is the species at supersaturation from among many others present in solution under the given conditions. Ionic species are generally less soluble in organic solvents and hence more likely to precipitate compared to neutral aggregates, even though they are present only in a minor amount.

Multifunctional molecules are capable of making different supramolecular synthons in different crystal structures, or synthon polymorphs and the hydrogen bond competition between the functional groups having comparable strength can be illustrated by the four polymorphs [I (BIXGIY), II (BIXGIY04), III (BIXGIY02), IV (BIXGIY03)] of clonixin [(2- (2-methyl-3-chloroanilino)nicotinic acid)],<sup>31a</sup> those were respectively obtained from ethyl acetate, methanol, ethanol, and acetone solutions. Clonixin (Figure 14) has COOH, pyridyl, and NH functional groups which engage in neutral O–H $\cdots$ N synthon in form I, ionic N<sup>+</sup>–H $\cdots$ O<sup>–</sup> bond in form II, and O–H $\cdots$ O dimer in forms III and IV (Figure 14a). Nonsteroidal anti-inflammatory drug tolfenamic acid exists as pentamorphs contain only –COOH group. The only hydrogen bond functionality leads to the occurrence of same carboxylic acid homo dimer synthon in all polymorphic structures.<sup>31b</sup> They are mainly conformational polymorphs.<sup>32</sup> The occurrence of synthon polymorphism<sup>33</sup> in clonixin means that hydrogen bonding is important during crystallization. In general, one may say that the stronger the hydrogen bonds the greater is the role of kinetic factors during crystallization.<sup>34</sup> However, the structurally related drug niflumic acid [2-(3-(trifluoromethyl)anilino)nicotinic acid] has only one crystal structure (Figure 14b, right) with carboxylic acid dimer,<sup>35</sup> implying that any general conclusions about proton transfer in acid-base systems are difficult to validate.

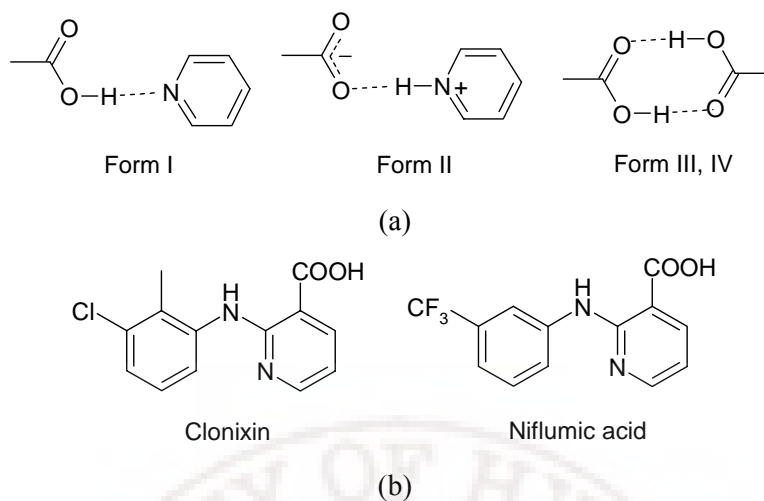


**Figure 14** (a) Synthon variation in the tetramorphic clonixin (Form I, II, III, and IV) molecule. (b) Molecular structure of clonixin (left) and niflumic acid (right)

## 6.5 SPARC $pK_a$ Calculator

SPARC<sup>36</sup> is an online  $pK_a$  calculator developed by S. W. Karickhoff; L. A. Carreira and S. H. Hilal. SPARC Performs Automated Reasoning in Chemistry. It uses computational algorithms based on fundamental chemical structure theory to estimate a variety of reactivity parameters. SPARC does not do "first principles" computation; rather, it analyzes chemical structure relative to a specific reactivity query much as an expert chemist might. SPARC execution involves the classification of molecular structure and the selection and execution of appropriate mechanistic models to quantify reactivity. It can estimate numerous physical processes such as vapor pressure, boiling point, solubility, distribution coefficients, Henry's constant and GC/LC retention times for a large number of molecular structures. For chemical reactivity SPARC estimates  $pK_a$ 's in almost any solvent and in the gas phase, zwitterionic/hydration constants, tautomeric equilibrium, carboxylic acid ester hydrolysis rate constants, chemical reduction potential and electron affinity.

The  $pK_a$  of all the starting material (hydroxybenzoic acids and aminopyridines) used in the preparation of the molecular salts **24-34** were calculated using the SPARC program in different media (gas phase, water and MeOH) is listed in Table 7. The  $pK_a$  of the starting materials in gas phase are comparable with the values from water however methanol gave a much higher values for COOH group. Their difference in  $pK_a$  ( $\Delta pK_a$  =

baseH<sup>+</sup> – acid, Table 8) is < 2 for cocrystals with 3-AP but > 4 for cocrystals of 4-AP in the gas phase as well as in aqueous medium. As the crystallization experiments were carried out in MeOH, the difference in pK<sub>a</sub> is calculated in MeOH. A negative ΔpK<sub>a</sub> observed in MeOH means that the base is not strong enough to abstract the proton from the acid, and so a neutral hydrogen bond will result. Thus, about half the complexes were expected to be molecular salts and the balance cocrystals using difference in ionization constants in the gas phase and water as a guide (Table 8). In all systems (**24-34**) proton transfer was observed and all these crystallization were carried out in MeOH which now found completely inconsistent with the oft-quoted ΔpK<sub>a</sub> rules<sup>10b, 16a, 23,24c</sup> in that a neutral hydrogen bond is expected but the ionic state is observed throughout the hydroxybenzoic acids-amino-pyridines series. pK<sub>a</sub> constants in MeOH and water cover the experimental conditions used since MeOH often picks up atmospheric moisture during crystallization. The ΔpK<sub>a</sub> rule for predicting neutral or ionic O-H...N/N<sup>+</sup>-H...O<sup>-</sup> hydrogen bonds is found to be inadequate in the present system.

**Table 7** pK<sub>a</sub> values calculated<sup>36</sup> in SPARC in different medium for acids and bases used in this study.

| Molecule       | pK <sub>a</sub> (gas phase) | pK <sub>a</sub> (water) | pK <sub>a</sub> (MeOH)   |
|----------------|-----------------------------|-------------------------|--------------------------|
| 4-HBA          | 4.17 (COOH)                 | 4.19 (COOH)             | 9.34 (COOH)              |
|                | 7.91 (OH)                   | 7.94 (OH)               | 12.40 (OH)               |
| 3-HBA          | 3.94 (COOH)                 | 3.96 (COOH)             | 9.16 (COOH)              |
|                | 9.30 (OH)                   | 9.34 (OH)               | 14.35 (OH)               |
| 3,5-DiHBA      | 3.85 (COOH)                 | 3.87 (COOH)             | 8.83 (COOH)              |
|                | 9.13 (OH)                   | 9.17 (OH)               | 13.77, 11.37 (OH)        |
| 3-F-4-HBA      | 3.82 (COOH)                 | 3.83 (COOH)             | 8.56 (COOH)              |
|                | 6.59 (OH)                   | 6.62 (OH)               | 9.60 (OH)                |
| 3-Cl-4-HBA     | 3.75 (COOH)                 | 3.77 (COOH)             | 8.33 (COOH)              |
|                | 6.36 (OH)                   | 6.39 (OH)               | 9.09 (OH)                |
| 3,5-DiMe-4-HBA | 4.31 (COOH)                 | 4.33 (COOH)             | 9.13 (COOH)              |
|                | 8.70 (OH)                   | 8.74 (OH)               | 12.91 (OH)               |
| 4-AP           | 8.55 (Ar N)                 | 8.59 (Ar N)             | 7.26 (Ar N)              |
|                | 1.98 (NH <sub>2</sub> )     | 1.99 (NH <sub>2</sub> ) | -1.13 (NH <sub>2</sub> ) |
| 3-AP           | 5.61 (Ar N)                 | 5.64 (Ar N)             | 3.48 (Ar N)              |
|                | 2.90 (NH <sub>2</sub> )     | 2.91 (NH <sub>2</sub> ) | -0.04 (NH <sub>2</sub> ) |

**Table 8**  $\Delta pK_a$  for molecular salts **24–34** in gas phase, water and methanol media.

| Cocrystal/ Molecular Salt                          | $\Delta pK_a$<br>(gas phase) | $\Delta pK_a$<br>(water) | $\Delta pK_a$<br>(methanol) |
|--|------------------------------|--------------------------|-----------------------------|
| 4-HBA•4-AP•H <sub>2</sub> O ( <b>24</b> )          | 4.38                         | 4.40                     | −2.08                       |
| 4-HBA•3-AP ( <b>25</b> )                           | 1.44                         | 1.45                     | −5.86                       |
| 3-HBA•4-AP ( <b>26</b> )                           | 4.61                         | 4.63                     | −1.90                       |
| 3,5-DiHBA•3-AP ( <b>27</b> )                       | 1.76                         | 1.77                     | −5.35                       |
| 3-F-4-HBA•4-AP•H <sub>2</sub> O ( <b>28</b> )      | 4.73                         | 4.76                     | −1.30                       |
| 3-F-4-HBA•3-AP ( <b>29</b> )                       | 1.79                         | 1.81                     | −5.08                       |
| 3-Cl-4-HBA•4-AP•H <sub>2</sub> O ( <b>30</b> )     | 4.80                         | 4.82                     | −1.07                       |
| 3-Cl-4-HBA•3-AP ( <b>31</b> )                      | 1.86                         | 1.87                     | −4.85                       |
| 3,5-DiMe-4-HBA•4-AP ( <b>32</b> )                  | 4.24                         | 4.26                     | −1.87                       |
| 3,5-DiMe-4-HBA•3-AP•H <sub>2</sub> O ( <b>33</b> ) | 1.30                         | 1.31                     | −5.65                       |
| 2(3,5-DiHBA)•3-AP ( <b>34</b> )                    | 1.76                         | 1.77                     | −5.35                       |

## 6.6 Cambridge Crystallographic Database Search

Hydrogen bond synthons in this study are compared with statistics extracted from the Cambridge Structural Database to summarize trends and predict the hydrogen bonding in new cocrystal and salt structures and found that hydrogen bonding functional groups such as OH and NH<sub>2</sub> promote persistent formation of ionic PyNH<sup>+</sup>⋯OOC synthon in the same supramolecular system. The CSD<sup>8</sup> was used to search for organic molecules containing COOH/ COO<sup>−</sup> and pyridyl/PyNH<sup>+</sup> fragments in multicomponent systems. The nature of acid⋯pyridine synthon was inferred manually by checking C–O bond distances and N protonation to ascertain whether it is neutral (O–H⋯N), ionic (N<sup>+</sup>–H⋯O<sup>−</sup>), or an intermediate bond (O⋯H⋯N) in the crystal structures. Data are summarized in Table 9. The number of hits showing neutral and ionic synthons for acid⋯pyridine bonding is comparable (326 and 352 hits, respectively). Intermediate proton transfer situation of neutral donor/ acceptor atoms but long (O–H) and short (H⋯N) bonds are relatively few (42 hits) and are classified in the neutral category. The presence of phenol OH gives neutral and ionic synthon structures to a similar extent (21 and 26 hits). However, phenol pyridine fragment gave ionic hits only (30 and 0). The aniline NH group favors ionic synthon (91 compared to 24, 96, vs 35). *The main*

*structural discrimination occurs when OH and NH functional groups are simultaneously present.* There are no crystal structures with both COOH and pyridine together with phenol OH and NH groups in the neutral category, but there are 12 ionic structures when all four functional groups are present. Of these, 9 structures contain the  $\text{PyNH}^+\cdots\text{OOC}^-$  synthon. Their CSD refcodes are AJECEX, KEFZAX, KERFUJ, LEWRUA, MIPRIM, MIPROS, RIGWUA, SLCADB10, TEZXIG. Refcodes EYIWIS, GIMSIF, GIMSOL have both COOH and  $\text{SO}_3\text{H}$  present. Thus the proton is usually abstracted from the stronger sulfonic acid by the PyN. Structural trends in the CSD offer an explanation that presence of a OH group in the benzoic acid component and  $\text{NH}_2$  in pyridine ring promote proton transfer to give a  $\text{PyNH}^+\cdots\text{OOC}^-$  ionic synthon although the numbers of hits in this subsets is not statistically significant. The competition between the  $\text{COOH}\cdots\text{N}_{\text{arom}}$  and the  $\text{OH}\cdots\text{N}_{\text{arom}}$  supramolecular heterosynthons were recently analyzed by Zaworotko<sup>37</sup> for the structures that are composed of cocrystal formers which contain a permutation of  $-\text{COOH}$ ,  $-\text{OH}$  and  $\text{N}_{\text{arom}}$  functional groups and observed  $\text{COOH}\cdots\text{NPy}$  synthon with a 78% occurrence probability in the presence of phenol OH based on an analysis of 30 cocrystals structures, of which only two are salts and the balance neutral cocrystals. However our results show the presence of phenol OH and  $\text{NH}_2$  groups modify the  $\text{COOH}\cdots\text{NPy}$  neutral synthon to give proton transfer or ionic synthon.

**Table 9** Distribution of neutral and ionic variants of acid $\cdots$ pyridine synthon. The in-between bonding situation is listed under neutral hits. Numbers indicate structure hits in each category.

|   | Neutral O–H $\cdots$ N bond                     | Ionic N <sup>+</sup> –H $\cdots$ O <sup>–</sup> bond |
|---|---|--|
| Acid $\cdots$ pyridine synthon (total)                          | 326   | 352  |
| Subset having partial proton transfer (O $\cdots$ H $\cdots$ N) | 42  | ---  |
| Subset containing aromatic OH                                   | 21  | 26   |
| Subset containing hydroxy-pyridine                              | 0   | 30   |
| Subset containing amino-pyridine                                | 35  | 96   |
| Subset containing aromatic NH                                   | 16 (primary $\text{NH}_2$ )<br>8 (secondary NH) | 57 (primary $\text{NH}_2$ )<br>34 (secondary NH)     |
| Subset contain aromatic OH and NH                               | 0   | 12   |



## 6.7 Conclusions

Over the last two decades, the number of research publications outlining the advances in design strategies, crystal growing techniques and characterization of cocrystals/salts has continued to increase significantly and more recently these ideas have got their place in pharmaceutical sciences. Making a neutral cocrystal or an ionic salt can modify the existing properties of solids by altering hydrogen bonding. Solubility, dissolution rates, stability etc. are a few problems with API that can be solved through making salts or cocrystals. Approximately half of all drug molecules used in medicine are administered as salts. In addition to this, salt formation also influences many other properties like melting point, hygroscopicity, chemical stability, dissolution rate, solution pH, crystal form, and mechanical properties. It is easier to select a salt forming agent by knowing the  $pK_a$  value of each ionisable group present in API. Inorganic acids (e.g., hydrochloride, sulphate, or phosphate), a sulphonic acid (mesylate or isethionate), a carboxylic acid (acetate, maleate or fumarate etc.), a hydroxyacid (citrate or tartrate), or possibly an amino acid (arginine or lysine) are most preferred counterpart for salt selection of a basic drug. Hydrochloride salts is the first choice among all.

Depending on acidity and basicity of different hydrogen bond donors and acceptors the position of hydrogen between the two heavy atoms will vary as acidic protons are responsible for hydrogen bonding. The well known  $\Delta pK_a$  rule was re-examined. The predictions about neutral or ionic states are found to be less reliable and inadequate for organic acids and amines/ pyridines combinations in the  $0 < \Delta pK_a < 4$  range. Presence of strong hydrogen bonding functional groups such as OH and  $NH_2$  promotes persistent formation of ionic  $PyNH^+ \cdots ^-OOC$  synthon further confirmed with the consistent trend of the occurrence of molecular salts with CSD analysis. CSD shows the presence of both OH and  $NH_2$  functional groups leads to proton transfer only but no neutral cocrystals. A hierarchy of hydrogen bonds when COOH, pyridine, OH and  $NH_2$  groups are in competition and cooperation is extracted and tabulated for  $N^+ - H \cdots O^-$ ,  $N - H \cdots O$ ,  $O - H \cdots O^-$  and  $O - H \cdots O$  motifs. The common motif pyridinium $\cdots$ carboxylate  $N^+ - H \cdots O^-$  synthon (Figure 15) persists in 10 molecular salts (in molecular salt **24** to **33**) including 4 hydrate structures of hydroxy-benzoic acids and amino-pyridines however molecular salt **34** shows  $N^+ - H \cdots O = C$  synthon.

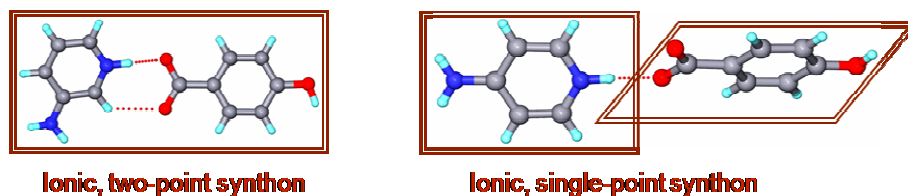


**Figure 15** The single point and two point ionic pyridinium $\cdots$ carboxylate  $N^+-H\cdots O^-$  synthon.

Detailed molecular packing, competition/cooperation and occurrences of hydrogen bonds or synthons like  $O-H\cdots N$ , or  $N^+-H\cdots O^-$ ,  $NH_2\cdots OOC$ ,  $NH_2\cdots OH$ ,  $OH\cdots Py$ ,  $OH\cdots OOC$ , etc. are known only after crystal structure determination and spectroscopic analysis. Given the immense potential of salt selection in pharmaceuticals<sup>10n,29b,38</sup> and the bioavailability that is intimately related to whether the drug is present in neutral or ionized form to know the best solid dosage form of drugs. Proton transfer phenomenon from acid to base using  $\Delta pK_a$  rule of 3 is discussed and evaluated.

## 6.8 Experimental Section

**Cocrystallization:** Hydroxybenzoic acids and aminopyridines (Figure 1) were purchased from Aldrich and/ or Lancaster and directly used for cocrystallization. Molecular salts **24-34** were obtained upon cocrystallization of the appropriate hydroxybenzoic acid (HBA) and aminopyridine (AP) in a 1:1 molar ratio in MeOH at ambient temperature by slow evaporation of solvent. Crystals of **34** appeared when the experiment was carried out at low temperature (inside a refrigerator). Melting points of all salt products were determined from DSC endotherms that show melting points significantly different from the neutral starting materials (Table 5). The product stoichiometry was determined by  $^1H$ -NMR integration ( $\delta$  ppm,  $J$  Hz) and structures confirmed by FT-IR spectroscopy (Table 2) and finally by single crystal X-ray diffraction (cell parameters are given in appendix). Water loss in hydrates was measured by TGA.

**CSD Search:** CSD version 5.29, ConQuest 1.10, November 2007 release, January 2008 update was used in all searches and crystal structures were visualized in Mercury 2.0. Only organic crystal structures with  $R < 0.10$ , no error and no polymeric were retrieved

from the database. The lower *R*-factor structure was retained for duplicate refcodes. Structures for intermediate proton transfer were retrieved from the neutral acid-pyridine cocrystal set by examining the O–H and N–H distances defined as O–H > 1.1 Å in O⋯H⋯N hydrogen bond.

**Molecular salt 24 (4-APH<sup>+</sup> • 4-HBA<sup>−</sup> • H<sub>2</sub>O, 1:1:1)**

M.p. 186–188 °C. Water release at 110–114 °C.

IR (KBr): 3356, 3123, 2078, 1676, 1644, 1520, 1379, 981 cm<sup>−1</sup>.

<sup>1</sup>H NMR (DMSO-*d*<sub>6</sub>): δ 8.01 (d, *J*=4, 2H), 7.80 (d, *J*=8, 2H), 6.83 (d, *J*=8, 2H), 6.52 (d, *J*=4, 2H), 6.29 (s, 1H), 5.60 (br s, 2H).

**Molecular salt 25 (3-APH<sup>+</sup> • 4-HBA<sup>−</sup>, 1:1)**

M.p. 184–186 °C.

IR (KBr): 3339, 3202, 2363, 1657, 1611, 1489, 1377, 1283, 1254, 974, 682, 607 cm<sup>−1</sup>.

<sup>1</sup>H NMR (DMSO-*d*<sub>6</sub>): δ 10.39 (br s, 1H), 7.93 (s, 1H), 7.80 (d, *J*=8, 2H), 7.73 (d, *J*=8, 1H), 7.02 (dd, *J*<sub>1</sub>=8, *J*<sub>2</sub>=4, 1H), 6.91 (d, *J*=8, 1H), 6.84 (d, *J*=8, 2H), 5.28 (br s, 2H).

**Molecular salt 26 (4-APH<sup>+</sup> • 3-HBA<sup>−</sup>, 1:1)**

M.p. 209–211 °C.

IR (KBr): 3380, 3154, 1665, 1636, 1593, 1530, 1372, 1246, 1161, 833 cm<sup>−1</sup>.

<sup>1</sup>H NMR (DMSO-*d*<sub>6</sub>): δ 8.03 (s, 1H), 7.38 (d, *J*=8, 2H), 7.22–7.26 (m, 2H), 6.95 (d, *J*=8, 1H), 6.55 (d, *J*=8, 2H), 6.46 (s, 1H), 5.94 (br s, 2H).

**Molecular salt 27 (3-APH<sup>+</sup> • 3,5-Di-HBA<sup>−</sup>, 1:1)**

M.p. 184–186 °C.

IR (KBr): 3417, 3340, 3236, 3091, 3068, 2639, 2161, 1644, 1617, 1572, 1508, 1468, 1372, 1288, 1158, 1006, 996, 804, 767, 684 cm<sup>−1</sup>.

<sup>1</sup>H NMR (DMSO-*d*<sub>6</sub>): δ 9.52 (br s, 2H), 7.91 (s, 1H), 7.71 (d, *J*=4, 1H), 7.00 (t, *J*=4, 1H), 6.88 (d, *J*=8, 1H), 6.78 (s, 2H), 6.39 (s, 1H), 5.22 (br s, 2H).

**Molecular salt 28 (4-APH<sup>+</sup> • 3-F-4-HBA<sup>−</sup> • H<sub>2</sub>O, 1:1:1)**

M.p. 179–181 °C. Water release at 107–110 °C.

IR (KBr): 3418, 3341, 3227, 2069, 1655, 1529, 1375, 1288, 1196, 831, 777, 636 cm<sup>−1</sup>.

<sup>1</sup>H NMR (DMSO-*d*<sub>6</sub>): δ 8.04 (d, *J*=8, 2H), 7.65 (d, *J*=4, 1H), 7.63 (s, 1H), 6.90 (d, *J*=4, 1H), 6.85 (d, *J*=8, 2H), 4.88 (br s, 2H).

**Molecular salt 29 (3-APH<sup>+</sup> • 3-F-4-HBA<sup>−</sup>, 1:1)**

M.p. 173–175 °C.

IR (KBr): 3356, 3219, 2162, 1659, 1616, 1572, 1493, 1240, 1132, 983, 771, 642  $\text{cm}^{-1}$ .

$^1\text{H}$  NMR ( $\text{DMSO}-d_6$ ):  $\delta$  8.06 (s, 1H), 7.81 (s, 1H), 7.80 (s, 1H), 7.64–7.68 (m, 2H), 7.21 (dd,  $J_1=8$ ,  $J_2=6$ , 1H), 6.99–7.03 (m, 2H), 4.86 (br, s, 2H).

**Molecular salt 30 (4-APH<sup>+</sup> • 3-Cl-4-HBA<sup>-</sup> • H<sub>2</sub>O, 1:1:2)**

M.p. 165–168 °C. Water release at 111–114 °C.

IR (KBr): 3370, 3200, 2932, 2789, 1894, 1822, 1659, 1628, 1587, 1531, 1367, 1294, 1197, 833, 794, 710, 634  $\text{cm}^{-1}$ .

$^1\text{H}$  NMR ( $\text{DMSO}-d_6$ ):  $\delta$  8.21 (br, 1H), 8.03 (d,  $J=4$ , 2H), 7.93 (d,  $J=8$ , 1H), 7.23 (d,  $J=8$ , 1H), 6.72 (d,  $J=4$ , 2H), 6.53 (s, 1H), 6.29 (br, s, 2H).

**Molecular salt 31 (3-APH<sup>+</sup> • 3-Cl-4-HBA<sup>-</sup>, 1:1)**

M.p. 150–152 °C.

IR (KBr): 3478, 3318, 3200, 3076, 2154, 1633, 1576, 1336, 1294, 1047, 989, 802, 777, 707, 638, 613  $\text{cm}^{-1}$ .

$^1\text{H}$  NMR ( $\text{DMSO}-d_6$ ):  $\delta$  7.92 (br, s, 1H), 7.83 (s, 1H), 7.72–7.74 (m, 2H), 6.99–7.04 (m, 3H), 6.89 (d,  $J=8$ , 1H), 5.24 (br s, 2H).

**Molecular salt 32 (4-APH<sup>+</sup> • 3,5-DiMe-4-HBA<sup>-</sup> • H<sub>2</sub>O, 1:1:1)**

M.p. 170–172 °C. Water release at 115–118 °C.

IR (KBr): 3372, 3159, 2662, 1674, 1626, 1523, 1365, 1222, 1113, 821, 723  $\text{cm}^{-1}$ .

$^1\text{H}$  NMR ( $\text{DMSO}-d_6$ ):  $\delta$  8.04 (d,  $J=8$ , 2H), 7.60 (s, 2H), 6.81 (d,  $J=8$ , 2H), 2.24 (s, 6H).

**Molecular salt 33 (3-APH<sup>+</sup> • 3,5-DiMe-4-HBA<sup>-</sup>, 1:1)**

M.p. 164–168 °C.

IR (KBr): 3441, 3324, 3196, 3090, 2964, 2941, 2917, 2709, 1644, 1618, 1600, 1489, 1381, 1221, 1122, 1043, 837, 812, 797  $\text{cm}^{-1}$ .

$^1\text{H}$  NMR ( $\text{DMSO}-d_6$ ):  $\delta$  9.00 (br s, 1H), 7.91 (s, 1H), 7.70 (d,  $J=4$ , 1H), 7.52 (s, 2H), 6.96 (dd,  $J=4,4$ , 1H), 6.88 (dd,  $J=8,1$ , 1H), 5.23 (br s, 2H), 2.17 (s, 6H).

**Molecular salt 34 (3-APH<sup>+</sup> • 3,5-DiHBA<sup>-</sup> • 3,5-DiHBA, 1:1:1)**

M.p. 204–206 °C.

IR (KBr): 3445, 3364, 3094, 3057, 1868, 1884, 1748, 1683, 1600, 1565, 1375, 1242, 1167, 1010, 780  $\text{cm}^{-1}$ .

$^1\text{H}$  NMR ( $\text{DMSO}-d_6$ ):  $\delta$  12.48 (br s, 1H), 9.78 (br s, 4H), 7.93 (br s, 1H), 7.72 (br s, 1H), 7.00 (br, s, 1H), 6.87 (br s, 1H), 6.78 (s, 4H), 6.57 (s, 2H), 5.23 (br, s, 2H).

## 6.9 References

1. G. R. Desiraju, *Angew. Chem. Int. Ed. Engl.* **1995**, *34*, 2311.
2. (a) G. M. Whitesides, E. E. Simanek, J. P. Mathias, C. T. Seto, D. N. Chin, M. Mammen, D. M. Gordon, *Acc. Chem. Res.* **1995**, *28*, 37; (b) M. C. T. Fyfe, J. F. Stoddart, *Acc. Chem. Res.* **1997**, *30*, 393; (c) L. J. Prins, D. N. Reinhoudt, P. Timmerman, *Angew. Chem. Int. Ed.* **2001**, *40*, 2382; (d) A. Nangia, *Curr. Opin. Solid State Mater. Sci.* **2001**, *5*, 115.
3. (a) M. C. Etter, *J. Am. Chem. Soc.* **1982**, *104*, 1095; (b) M. C. Etter, *Acc. Chem. Res.* **1990**, *23*, 120; (c) M. C. Etter, *J. Phys. Chem.* **1991**, *95*, 4601.
4. (a) G. A. Jeffrey, W. Saenger, *Hydrogen Bonding in Biological Structures*; Springer-Verlag: Berlin, 1991; (b) G. A. Jeffrey, *An Introduction to Hydrogen Bonding*; Oxford University Press: New York, 1997.
5. (a) J. A. Zerkowski, G. M. Whitesides, *J. Am. Chem. Soc.* **1994**, *116*, 4298; (b) K. Endo, T. Sawaki, M. Koyanagi, K. Kobayashi, H. Masuda, Y. Aoyama, *J. Am. Chem. Soc.* **1995**, *117*, 8341; (c) L. R. MacGillivray, J. L. Atwood, *J. Am. Chem. Soc.* **1997**, *119*, 6931; (d) P. R. Ashton, A. N. Collins, M. C. T. Fyfe, S. Menzer, J. F. Stoddart, D. J. Williams, *Angew. Chem. Int. Ed. Engl.* **1997**, *36*, 735; (e) E. A. Simanek, A. Tsoi, C. C. C. Wang, G. M. Whitesides, M. T. McBride, G. T. R. Palmore, *Chem. Mater.* **1997**, *9*, 1954; (f) K. Biradha, D. Dennis, V. A. MacKinnon, C. V. K. Sharma, M. J. Zaworotko, *J. Am. Chem. Soc.* **1998**, *120*, 11894; (g) D. Ranganathan, C. Lakshmi, I. L. Karle, *J. Am. Chem. Soc.* **1999**, *121*, 6103; (h) S. Hanessian, R. Saladino, R. Margarita, M. Simard, *Chem. Eur. J.* **1999**, *5*, 2169; (i) W. Yue, R. Bishop, D. C. Craig, M. L. Scudder, *Tetrahedron* **2000**, *56*, 6667; (j) T. C. W. Mak, F. Xue, *J. Am. Chem. Soc.* **2000**, *122*, 9860; (k) R. K. R. Jetti, F. Xue, T. C. W. Mak, A. Nangia, *J. Chem. Soc. Perkin Trans.2* **2000**, 1223; (m) K. T. Holman, S. M. Martin, D. P. Parker, M. D. Ward, *J. Am. Chem. Soc.* **2001**, *123*, 4421; (n) M. B. Zaman, M. Tomura, Y. Yamashita, *J. Org. Chem.* **2001**, *66*, 5987.
6. G. R. Desiraju, T. Steiner, *The Weak Hydrogen Bond in Structural Chemistry and Biology*; Oxford University Press: Oxford, 1999.
7. (a) G. R. Desiraju, R. Parthasarthy, *J. Am. Chem. Soc.* **1989**, *111*, 8725; (b) O. Navon, J. Bernstein, V. Khodorkovsky, *Angew. Chem. Int. Ed. Engl.* **1997**, *36*,

- 601; (c) J. M. A. Robinson, D. Philp, K. D. M. Harris, B. M. Kariuki, *New J. Chem.* **2000**, 24, 799; (d) Q. Chu, Z. Wang, Q. Huang, C. Yan, S. Zhu, *J. Am. Chem. Soc.* **2001**, 123, 11069.
8. (a) Cambridge Structural Database, CSD, version 5.29, ConQuest 1.10, November 2007 release, January update; (b) F. H. Allen, *Acta. Crystallogr.* **2002**, B58, 380; (c) A. Nangia, *CrystEngComm* **2002**, 4, 93; (d) F. H. Allen, R. Taylor, *Chem. Soc. Rev.* **2004**, 33, 463; (e) F. H. Allen, W. D. S. Motherwell, *Acta. Crystallogr.* **2002**, B58, 407.
  9. (a) F. H. Allen, W. D. S. Motherwell, P. R. Raithby, G. P. Shields, R. Taylor, *New J. Chem.* **1999**, 25; (b) T. Steiner, *Acta. Crystallogr.* **2001**, B57, 103; (c) J. A. McMahon, J. A. Bis, P. Vishweshwar, T. R. Shattock, O. L. McLaughlin, M. J. Zaworotko, *Z. Kristallogr.* **2005**, 220, 340; (d) R. D. B. Walsh, M. W. Bradner, S. Fleishman, L. A. Morales, B. Moulton, N. Rodríguez-Hornedo, M. J. Zaworotko, *Chem. Commun.* **2003**, 186.
  10. (a) C. B. Aakeröy, D. J. Salmon, *CrystEngComm* **2005**, 7, 439; (b) B. R. Bhogala, S. Basavoju, A. Nangia, *CrystEngComm* **2005**, 7, 551; (c) B. R. Bhogala, S. Basavoju, A. Nangia, *Cryst. Growth Des.* **2005**, 5, 1683; (d) A. V. Trask, W. D. S. Motherwell, W. Jones, *Cryst. Growth Des.* **2005**, 5, 1013; (e) X. Gao, T. T. Frišćić, L. R. MacGillivray, *Angew. Chem. Int. Ed.* **2004**, 43, 232; (f) B. R. Bhogala, A. Nangia, *Cryst. Growth Des.* **2003**, 3, 547; (g) C. B. Aakeröy, A. M. Beatty, B. A. Helfrich, *Angew. Chem. Int. Ed.* **2001**, 40, 3240; (h) B. R. Bhogala, A. Nangia, *New J. Chem.* **2008**, 32, 800; (i) P. Vishweshwar, A. Nangia, V. M. Lynch, *J. Org. Chem.* **2002**, 67, 556; (j) B. R. Bhogala, P. Vishweshwar, A. Nangia, *Cryst. Growth Des.* **2002**, 2, 325; (k) N. Shan, A. D. Bond, W. Jones, *New J. Chem.* **2003**, 27, 365; (m) B. R. Bhogala, A. Nangia, *Cryst. Growth Des.* **2002**, 2, 325; (n) Ö, Almarsson, M. J. Zaworotko, *Chem. Commun.* **2004**, 1889; (o) C. V. K. Sharma, G. A. Broker, G. J. Szulczewski, R. D. Rogers, *Chem. Commun.* **2000**, 1023; (p) M. Tomura, Y. Yamashita, *Chem. Lett.* **2001**, 532; (q) N. Shan, E. Batchelor, W. Jones, *Tetrahedron Lett.* **2002**, 43, 8721; (r) B. Olenik, T. Smolka, R. Boese, R. Sustmann, *Cryst. Growth Des.* **2003**, 3, 183; (s) A. D. Bond, *Chem. Commun.* **2003**, 250; (t) S. Varughese, V. R. Pedireddi, *Chem. Eur. J.* **2006**, 12, 1597; (u) M. Du, Z. H. Zhang, X. J. Zhao,

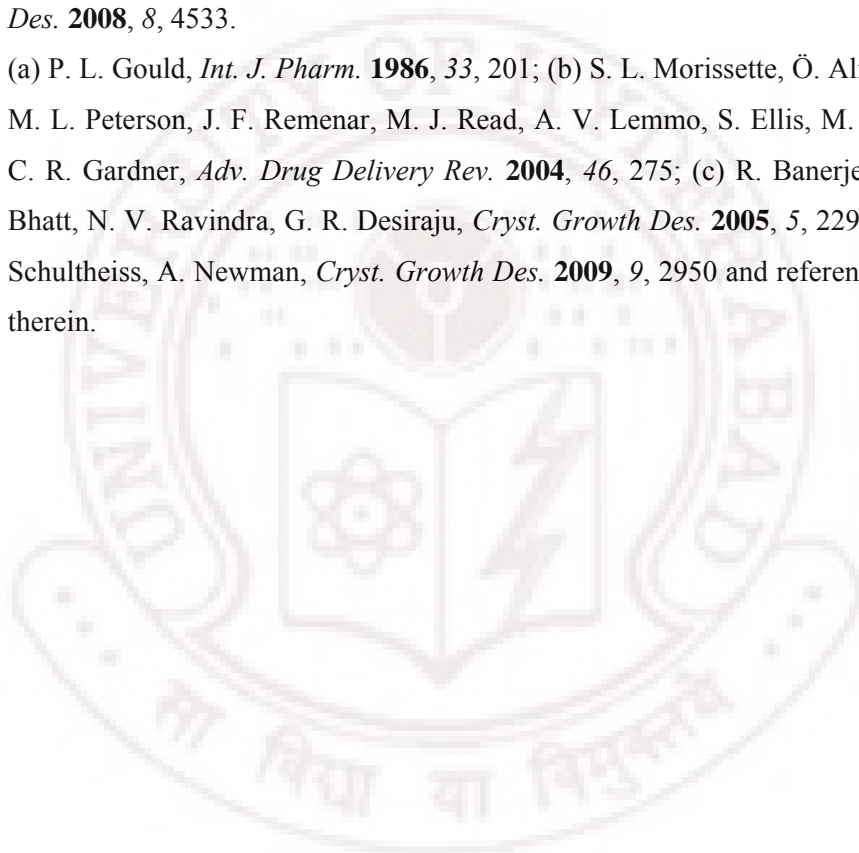


- H. Cai, *Cryst. Growth Des.* **2006**, 6, 114; (v) C. M. Grossel, A. N. Dwyer, M. B. Hursthouse, J. B. Orton, *CrystEngComm* **2006**, 8, 123; (w) B. R. Bhogala, A. Nangia, *New J. Chem.* **2008**, 32, 800; (x) R. Santra, N. Ghosh, K. Biradha, *New J. Chem.* **2008**, 32, 1673.
11. (a) P. Vishweshwar, A. Nangia, V. M. Lynch, *CrystEngComm* **2003**, 5, 164; (b) K. Biradha, M. J. Zaworotko, *J. Am. Chem. Soc.* **1998**, 120, 6431; (c) J. A. Bis, O. L. McLaughlin, P. Vishweshwar, M. J. Zaworotko, *Cryst. Growth Des.* **2006**, 6, 2648.
12. (a) V. R. Vangala, R. Mondal, C. K. Broder, J. A. K. Howard, G. R. Desiraju, *Cryst. Growth Des.* **2005**, 5, 99; (b) O. Ermer, A. Eling, *J. Chem. Soc. Perkin Trans. 2* **1994**, 925; (c) S. Hanessian, M. Simard, S. Roelens, *J. Am. Chem. Soc.* **1995**, 117, 7630; (d) F. H. Allen, V. J. Hoy, J. A. K. Howard, V. R. Thalladi, G. R. Desiraju, C. C. Wilson, G. J. McIntyre, *J. Am. Chem. Soc.* **1997**, 119, 3477; (e) V. R. Vangala, B. R. Bhogala, A. Dey, G. R. Desiraju, C. K. Broder, P. S. Smith, R. Mondal, J. A. K. Howard, C. C. Wilson, *J. Am. Chem. Soc.* **2003**, 125, 14495; (f) S. Hanessian, R. Saladino, R. Margarita, M. Simard, *Chem. Eur. J.* **1999**, 5, 2169; (g) A. Dey, G. R. Desiraju, R. Mondal, J. A. K. Howard, *Chem. Commun.* **2004**, 2528.
13. (a) P. Vishweshwar, A. Nangia, V. M. Lynch, *Cryst. Growth Des.* **2003**, 3, 783; (b) L. S. Reddy, P. M. Bhatt, R. Banerjee, A. Nangia, G. J. Kruger, *Chem. Asian J.* **2007**, 2, 505; (c) J. A. Bis, M. J. Zaworotko, *Cryst. Growth Des.* **2005**, 5, 1169.
14. (a) L. S. Reddy, N. J. Babu, A. Nangia, *Chem. Commun.* **2006**, 1369; (b) N. J. Babu, L. S. Reddy, A. Nangia, *Mol. Pharma.* **2007**, 4, 417.
15. (a) C. B. Aakeröy, J. Desper, J. F. Urbina, *Chem. Commun.* **2005**, 2820; (b) C. B. Aakeröy, J. Desper, J. F. Urbina, *Chem. Commun.* **2006**, 1445; (c) C. B. Aakeröy, A. M. Beatty, B. A. Helfrich, M. Nieuwenhuyzen, *Cryst. Growth Des.* **2003**, 3, 159; (d) C. B. Aakeröy, A. M. Beatty, B. A. Helfrich, *Angew. Chem. Int. Ed.* **2001**, 40, 3240.
16. B. Sarma, N. K. Nath, B. R. Bhogala, A. Nangia, *Cryst. Growth Des.* **2009**, 9, 1545.

17. (a) G. Smith, U. D. Wermuth, P. C. Healy, J. M. White, *Aust. J. Chem.* **2003**, *56*, 707 [AJECEX]; (b) G. Smith, U. D. Wermuth, J. M. White, *Acta Crystallogr.* **2004**, *C60*, o575 [EYIWIS]; (c) X. -G. Meng, C. -S. Zhao, L. Wang, C. -L. Liu, *Acta Crystallogr.* **2007**, *C63*, o667 [GIMSIF, GIMSOL]; (d) S. -L. Li, J. -F. Ma, G. -J. Ping, *Acta Crystallogr.* **2006**, *C62*, o1173 [KEFZAX]; (e) D. -J. Yang, S. -H. Qu, *Acta Crystallogr.* **2006**, *C62*, o5127 [KERFUJ]; (f) D. E. Lynch, D. Smith, D. Freney, K. A. Byriel, C. H. L. Kennard, *Aust. J. Chem.* **1994**, *47*, 1097 [LEWRUA]; (g) G. Smith, U. D. Wermuth, R. C. Bott, J. M. White, A. C. Willis, *Aust. J. Chem.* **2001**, *54*, 165 [MIPRIM, MIPROS]; (h) M. A. Braverman, R. L. LaDuca, *Acta Crystallogr.* **2007**, *E63*, o3167 [RIGWUA]; (i) R. W. Gellert, I. -N. Hsu, *Acta Crystallogr.* **1988**, *C44*, 311 [SLCADB10]; (j) Z. -L. Wang, J. -G. Xie, L. -H. Wei, *Acta Crystallogr.* **2007**, *E63*, o1579 [TEZXIG]; (k) N. Kobayashi, T. Naito, T. Inabe, *Bull. Chem. Soc. Jpn.* **2003**, *76*, 1351 [BAXZAC]; (m) I. Karle, R. D. Gilardi, C. C. Rao, K. M. Muraleedharan, S. Ranganathan, *J. Chem. Cryst.* **2003**, *33*, 727 [OMIHIB]; (n) V. Bertolasi, P. Gilli, V. Ferretti, G. Gilli, *Acta Crystallogr.* **2001**, *B57*, 591 [RALDUD, RALFAL].
18. (a) F. H. Allen, *Acta Crystallogr.* **2002**, *B58*, 380; (b) Cambridge Structural Database, version 5.29, ConQuest 1.10, November 2007 release, January 2008 update, [www.ccdc.cam.ac.uk](http://www.ccdc.cam.ac.uk).
19. N. A. Caballero, F. J. Melendez, C. Muñoz-Caro, A. Niño, *Biophys. Chem.* **2006**, *124*, 155, and references cited therein.
20. M. Kawase, N. Motohashi, T. Kurihara, M. Inagaki, K. Satoh, H. Sakagami, *Anticancer Res.* **1998**, *18*, 1069, and references therein.
21. (a) G. R. Desiraju, *CrystEngComm* **2003**, *5*, 466; (b) J. D. Dunitz, *CrystEngComm* **2003**, *5*, 506; (c) A. D. Bond, *CrystEngComm* **2007**, *9*, 833; (d) J. Z. Schpector, E. R. T. Tiekink, *Z. Kristallogr.* **2008**, *223*, 233.
22. (a) D. Boenigk, D. Mootz, *J. Am. Chem. Soc.* **1988**, *110*, 2135; (b) J. A. Cowan, J. A. K. Howard, G. J. McIntyre, S. M. -F. Lo, I. D. Williams, *Acta Crystallogr.* **2003**, *B59*, 794; (c) T. Steiner, I. Majerz, C. C. Wilson, *Angew. Chem. Int. Ed.* **2001**, *40*, 2651; (d) A. Parkin, S. M. Harte, A. E. Goeta, C. C. Wilson, *New. J. Chem.* **2004**, *28*, 718; (e) C. B. Aakeröy, I. Hussain, J. Desper, *Cryst. Growth*

- Des.* **2006**, *6*, 474; (f) M. Schmidtman, C. C. Wilson, *CrystEngComm* **2008**, *10*, 177.
23. (a) S. L. Childs, K. I. Hardcastle, *Cryst. Growth Des.* **2007**, *7*, 1291; (b) S. L. Childs, G. P. Stahly, A. Park, *Mol. Pharmaceutics* **2007**, *4*, 323.
  24. (a) B. J. Coe, J. A. Harris, B. S. Brunschwig, J. Garin, J. Orduna, *J. Am. Chem. Soc.* **2005**, *127*, 3284; (b) S. N. Black, E. A. Collier, R. J. Davey, R. J. Roberts, *J. Pharma Sci.* **2007**, *96*, 1053; (c) S. E. McKay, K. A. Wheeler, S. C. Blackstock, *CrystEngComm* **2006**, *8*, 129.
  25. P. Vishweshwar, N. Jagadeesh Babu, A. Nangia, S. A. Mason, H. Puschmann, R. Mondal, J. A. K. Howard, *J. Phys. Chem. A* **2004**, *108*, 9406.
  26. (a) R. M. Silverstein, F. X. Webster, *Spectrometric Identification of Organic Compounds*, 6th ed. John Wiley & Sons: Singapore, 2004.
  27. (a) J. Bernstein, R. E. Davis, L. Shimoni, N. L. Chang, *Angew. Chem. Int. Ed. Engl.* **1995**, *34*, 1555; (b) M. Rafilovich, J. Bernstein, M. B. Hickey, M. Tauber, *Cryst. Growth Des.* **2007**, *7*, 1777; (c) M. Wenger, J. Bernstein, *Cryst. Growth Des.* **2008**, *8*, 1595.
  28. B. Sarma, L. S. Reddy, A. Nangia, *Cryst. Growth Des.* **2008**, *8*, 4546, and references cited therein (Special Issue on Cocrystals).
  29. (a) S. L. Johnson, K. A. Rumon, *J. Phys. Chem.* **1965**, *69*, 74; (b) W. Q. Tong, G. Whitesell, *Pharm. Dev. Technol.* **1998**, *3*, 215; (c) M. J. Bowker, *A Procedure for Salt Selection and Optimization. In Handbook of Pharmaceutical Salts*; P. H. Stahl, C. G. Wermuth, (Eds.); VHCA and Wiley-VCH: New York, 2002.
  30. F. Rived, M. Rose's, E. Bosch, *Anal. Chim. Acta* **1998**, *374*, 309.
  31. (a) M. Takasuka, H. Nakai, M. Shiro, *J. Chem. Soc., Perkin Trans.* **1982**, *2*, 1061; [BIXGIY, BIXGIY02, BIXGIY03, BIXGIY04]; (b) V. L. -Mejías, J. W. Kampf, A. J. Matzger, *J. Am. Chem. Soc.* **2009**, *131*, 4554.
  32. (a) A. Nangia, *Acc. Chem. Res.* **2008**, *41*, 595; (b) B. Sarma, S. Roy, A. Nangia, *Chem. Commun.* **2006**, 4918.
  33. (a) N. J. Babu, L. S. Reddy, S. Aitipamula, A. Nangia, *Chem Asian J.* **2008**, *3*, 1122; (b) B. Sarma, A. Nangia, *Acta Crystallogr.* **2008**, *A64*, C449; (c) B. Sarma, A. Nangia (unpublished results).
  34. G. R. Desiraju, *Angew. Chem. Int. Ed.* **2007**, *46*, 8342.

35. H. M. Krishna Murthy, M. Vijayan, *Acta Crystallogr.* **1979**, B35, 262.
36. (a) S. H. Hilal, S. W. Karickhoff, L. A. Carreira, *Quant. Struc. Act. Rel.* **1995**, 14, 348; (b) F. Z. Erdemgil, S. S. Sanli, N. S. Sanli, G. Ozkan, J. Barbosa, J. Guiteras, J. L. Beltran, *Talanta*, **2007**, 72, 489; (c) S. H. Hilal, L. A. Carreira, S. W. Karickhoff, *Talanta*, **1996**, 43, 607; (d) S. H. Hilal, L. A. Carreira, C. Melton, G. Baughman, S. W. Karickhoff, *J. Phys. Org. Chem.*, **1994**, 7, 122; (e) Single point calculation in SPARC pK<sub>a</sub> calculator, [ibmlc2.chem.uga.edu/sparc/](http://ibmlc2.chem.uga.edu/sparc/)
37. T. R. Shattock, K. K. Arora, P. Vishweshwar, M. J. Zaworotko, *Cryst. Growth Des.* **2008**, 8, 4533.
38. (a) P. L. Gould, *Int. J. Pharm.* **1986**, 33, 201; (b) S. L. Morissette, Ö. Almarsson, M. L. Peterson, J. F. Remenar, M. J. Read, A. V. Lemmo, S. Ellis, M. J. Cima, C. R. Gardner, *Adv. Drug Delivery Rev.* **2004**, 46, 275; (c) R. Banerjee, P. M. Bhatt, N. V. Ravindra, G. R. Desiraju, *Cryst. Growth Des.* **2005**, 5, 2299; (d) N. Schultheiss, A. Newman, *Cryst. Growth Des.* **2009**, 9, 2950 and references cited therein.



---

## CONCLUSIONS AND FUTURE PROSPECTS

---

### 7.1 Guest Free Host Structures by Solvent Less Methods

Charged species, awkward shape and/or size, sticky functional moieties (like OH, NH<sub>2</sub>, SO<sub>3</sub>H etc) on the organic molecules especially for APIs (Active Pharmaceutical Ingredients) induce solvent inclusion.<sup>1</sup> Solvates are not recommended in drug industries because of their toxic nature and volatility although hydrates have importance but are limited due to stability and solubility reasons. Therefore synthesis and characterization of guest-free crystalline forms of the host molecules has great importance. But it is generally difficult because they do not crystallize in the absence of a second component, usually a solvent and/or water molecule, which acts as a crystallization aid or filler in the voids. Various methods have been used to obtain guest free structures of lattice inclusion host compounds by growing single crystals of organic compounds that commonly includes temperature lowering, isothermal evaporation, and isothermal diffusion crystallization techniques, etc. Misfit size/shape of guest molecules, unfavourable electrostatic interactions with guest molecules, leaching methods, solvent-anti solvent techniques, sonication etc. are common methods used to isolate guest free structure of lattice inclusion host. Two high temperature solvent less methods of green methodology to generate guest free structures of 1,1-bis-(4-hydroxyphenyl)cyclohexane<sup>2</sup> (**1**, Figure 1) were discussed in Chapter 2. The idea of employing high temperature solvent free crystallization techniques is further illustrated with isomeric dihydroxybenzoic acids (**2**, **3** and **4**; Figure 1) and successfully isolating guest free forms and new polymorphic modifications in many cases. Two polymorphs of molecule **1** and **2** each, a new polymorph of **3** and a guest free form of **4** were isolated using solvent less methods. We explored melting and sublimation, two solvent free high temperature techniques to afford guest free host structures and these methods may particularly be

employed to generate new polymorphs in good probability of compounds that are prone to give guest included crystals on solvent crystallization.

## 7.2 Polymorphism and Phase Transition

Polymorphism<sup>3</sup> in crystalline solids is defined as materials with the same chemical composition but different lattice structures. Polymorphism is a major challenge in the fundamental understanding of crystallization and received practical importance in pharmaceuticals.<sup>4</sup> The implication of different molecular self-assembly in the solid state relates to physical and chemical properties that affect pharmaceutical performance. These effects are well documented in literature that include different physiochemical properties such as stability, solubility, dissolution rate, oral absorption, bioavailability, melting point, optical and mechanical properties, vapour pressure, etc. Depending on packing of molecules, conformational change and hydrogen bond synthon in polymorphic structures, they can be defined as packing, conformational and synthon polymorphs, respectively. Similarly multi-component molecular solids,<sup>3b</sup> i.e. cocrystal, salt, solvate etc. can also show polymorphism like single molecular entity. In this context several polymorphic structures were generated by high temperature solvent less methods of melt and sublimation and by solution crystallization. These solvent less methods have potential to generate new polymorphic modifications. Two conformational polymorphs of 1,1-bis-(4-hydroxyphenyl)cyclohexane (**1**) generated by sublimation and melt were discussed in Chapter 2.. Further two polymorphs of 3,5-dihydroxybenzoic acid (**2**), a new polymorph of 2,3-dihydroxybenzoic acid (**3**) and a guest free structure of pure host 3,4-dihydroxybenzoic acid (**4**) were isolated<sup>5</sup> using the same methods. A new hydrate polymorph was also isolated while crystallizing 3,4-dihydroxybenzoic acid from water in refrigerator at 0-5°C. These polymorphs are synthon polymorphs. This new hydrate polymorph of 3,4-dihydroxybenzoic acid along with tetrahydrofuran, acetylacetone and dioxane solvates of 3,5-dihydroxybenzoic acid (**2**•THF, **2**•Acac and **2**•Diox) were crystallized to confirm that these molecules are good host compounds. A systematic study on polymorphism gives insight into structural relationship and the mechanism of phase transition between crystalline modifications. Manual solid form screening was carried out using available laboratory solvents to understand the effects of solvents<sup>6</sup> on the polymorphic outcome as crystallization experiments on phenylbenzenesulfonamides.



Five molecules (**8**, **9**, **10**, **14**, **18**; in Figure 1) are found to be dimorphic and molecule **13** is trimorphic as discussed in Chapter 4. Among the various analytical methods used for the characterization of polymorphs, thermal analysis (i.e. differential scanning calorimetry, thermogravimetry, hot stage microscopy), spectroscopy (FT-IR, NIR, Raman), in-situ variable temperature powder X-ray diffraction and finally single crystal X-ray diffraction that received considerable attention and used for the analysis of various solid-state forms. Two nitromethane solvate polymorphs and a guest free form were isolated for the molecule 1,4-di[bis(4'-hydroxyphenyl)methyl]benzene (**22**) using variable amount of  $\text{CF}_3\text{CH}_2\text{OH}$  with  $\text{CH}_3\text{NO}_2$  and the effect of the additive  $\text{CF}_3\text{CH}_2\text{OH}$  on polymorph production was discussed in Chapter 5.

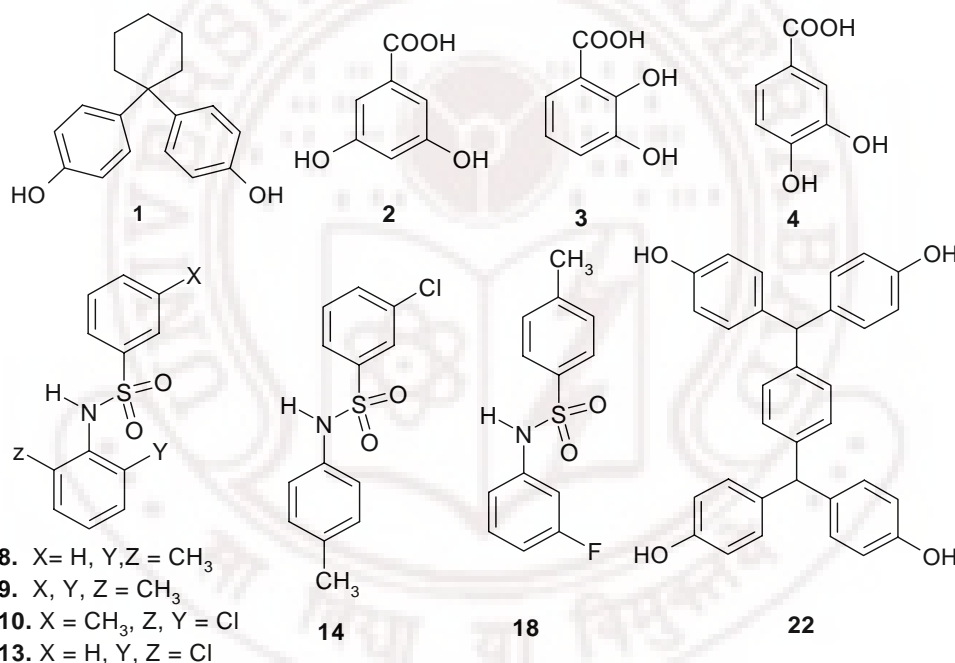


**Figure 1** Host 1,1-bis-(4-hydroxyphenyl)cyclohexane (**1**) afforded guest free form and conformational polymorphs on melting and sublimation and using the same solvent less methods on isomeric dihydroxybenzoic acid molecules (**2**, **3**, **4**), successfully isolated two polymorphs of **2**, a new polymorph of **3** and a guest free structure of **4**. Common solution crystallization afforded five dimorphic (**8**, **9**, **10**, **14** and **18**) and one trimorphic (**13**) phenylbenzenesulfonamides. Two nitromethane solvate polymorphs of **22** and a new hydrate polymorph of **4** were isolated by solution crystallization.

The search and control of solid state forms has motivated the development of new crystallization methods from liquid solutions, supercritical fluids, and solids via solvent free methods. Production of a new and selective crystalline modification, understanding polymorphism, phase transformations between polymorphs have received immense importance in academic research and in pharmaceutical industries because of limiting factors like stability, solubility, bioavailability etc. affecting the efficacy of drugs. Hence it is essential to control polymorph formation by screening out all possible modifications of a compound and choose the right candidate preferably the most stable polymorph because polymorphs can convert spontaneously from less stable to more stable state. Since different intra- and intermolecular interactions such as hydrogen bonds, halogen interactions,  $\pi$ -stacking and van der Waals interactions are present in different crystal structures, different crystalline materials will have different free energies and therefore dissimilar stability. Polymorph interconversion<sup>3</sup> upon heating, grinding, slurry method is common and this physical phenomenon is observed in molecules **1**, **8** and **18**. Phase transition from metastable to stable polymorph, monotropic and enantiotropic relationship between polymorphs was explained for compound **1** by differential scanning calorimetry (DSC), hot stage microscopy (HSM) and hydrogen bonding changes. In succession, molecules **8** and **18** that showed phase transitions are confirmed with thermal analysis, spectroscopic tools, powder and single crystal X-ray diffraction. Our understanding of polymorphism is being extended to a non-carboxylic acid nonsteroidal anti-inflammatory drug (NSAID) Nimesulide, widely used in solid oral formulations.<sup>7</sup>

### 7.3 Reasons for High $Z'$ Structures: Solvent Less Methods

Crystallographers or crystal chemists have been curious for what reasons compounds crystallize with high  $Z'$  ( $Z' > 1$ )<sup>8a</sup> structures. Crystal structures with multiple  $Z'$  are now being intensely studied to understand the factors leading to high  $Z'$  crystal structures although occurrence of high  $Z'$  structures<sup>8b,c</sup> are still not properly understood. Our observation<sup>2</sup> is the frequent occurrence of high  $Z'$  structures in high temperature solvent less methods of melt and sublimation. The formation of crystals under non-equilibrium conditions is viewed as a fossil relic of the fastest growing crystal nucleus rather than a thermodynamic minimum structure. A Cambridge Structural Database

(CSD) study was carried out on structures crystallized using solvent free methods, melt and sublimation. It is found that solvent-free crystallization methods show a much higher probability of multiple  $Z'$  structures (~18%) compared to overall CSD trends on  $Z'$  frequencies (<12%).<sup>2</sup> Generation of high  $Z'$  structures by melting and sublimation crystallization can be understood<sup>8b</sup> as rapid cooling of the hot liquid or vapor in the open flask or on the cold finger is a kinetic phase and the conditions under which hydrogen-bonded clusters are likely to condense in a pseudo-symmetric crystalline arrangement. Presence of pseudosymmetry, awkward shape, formation of molecular helices via hydrogen bond or other interactions, strong hydrogen bonds, chirality, kinetic or temperature effect are the various reasons of affording high  $Z'$  structures as discussed in Chapter 3. Popular host 1,1-bis-(4-hydroxyphenyl)cyclohexane is found to be a remarkable example to illustrate the occurrence of high  $Z'$  structure in metastable polymorph by melting. The phase transition shows how close packing conflicts in a metastable  $Z' = 2$  structure are resolved in the thermodynamic  $Z' = 1$  polymorph. Solvent less methods when used to generate guest free host structures of isomeric dihydroxybenzoic acids,  $Z' > 1$  structure is observed commonly, as discussed in Chapter 2 and 3. Carbamazepine<sup>9</sup> is another exciting example for which  $Z' = 1$  from solution crystallization (3 polymorphs) whereas  $Z' = 4$  when it is crystallized by melting.

## 7.4 A Host Hydrate: Organic Zeolite

Reproducibility in the construction of novel open-framework<sup>1,10</sup> organic solids reflects their many possible uses such as chemical separation, drying agents, reactions and catalysis in a microcavity and for electro optic, nonlinear, magnetic materials to drug delivery. Hydration of molecules in the crystal structure is a common phenomenon, especially in pharmaceuticals that show effective advantages over solvates or sometime neutral APIs. It is more difficult to construct porous material in organic system as hydrogen bonds are weaker and less directional compared to metal–heteroatom and metal–ligand bonds in metal organic frameworks (MOFs). Aoyama and co-workers<sup>11</sup> reported organic zeolites by designing rigid crystal structures of bis(resorcinol) and mono(resorcinol) derivatives of anthracene using strong hydrogen bond functionality. We successfully utilized this idea by synthesizing tetrasulfonic acid in a tetrahedral scaffold (Tetraphenylmethane tetrasulfonic; TPM-SO<sub>3</sub>H, refcode HIGMUG) that are

known to versatile building blocks for host guest and interpenetrated networks. This molecule shows reversible and selective uptake<sup>12</sup> of water molecules into its crystalline lattice. The loss and reuptake of water is quantitative and is consistent up to several successive cycles (Figure 2). Decomposition temperature of TPM-SO<sub>3</sub>H is > 390 °C. Structural and thermal analysis of TPM-SO<sub>3</sub>H that includes water helices, interconnected channels, hydrogen bonding pattern were discussed in Chapter 5. The high thermal stability and its properties discussed can have potential applications in dehydrating agents and organic zeolites.

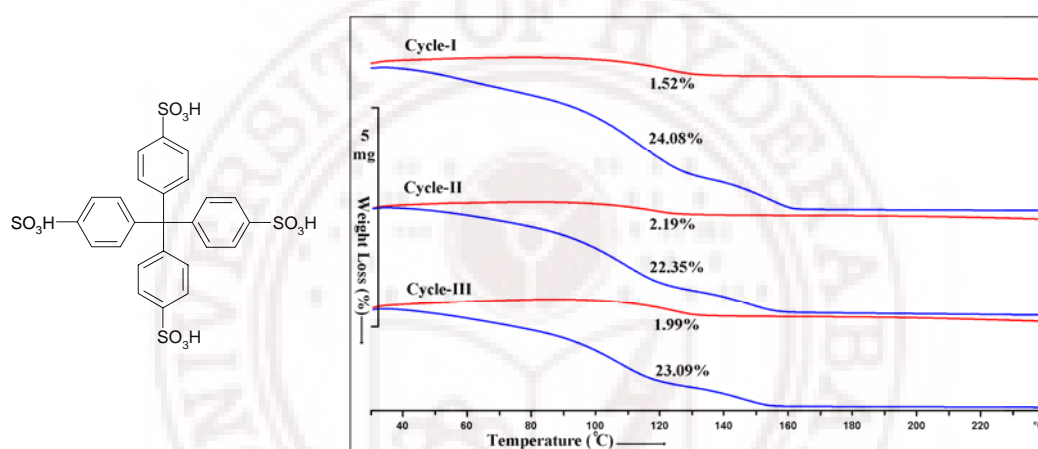


**Figure 2** (a) Tetrakis(4-sulfophenyl)methane (**21**). (b) Water loss and uptake is reversible up to 3 successive cycles in thermogravimetry (TG).

## 7.5 Rare Hydrogen Bond Networks: Pentagonal tiling

The subject of crystal design and crystal engineering<sup>13</sup> have developed rapidly in recent years after the advent of Single-crystal X-ray diffractometer and now being an active area of research. Design and synthesis of porous architectures and network solids offer clear potential advantages for efficient, cost-effective alternatives to current methods of enantiomeric separations, new materials for separation of gases, liquids, and solutes, new industrial heterogeneous catalysts, new drug delivery matrixes, a new generation of chemical sensors, and new storage matrixes for gases such as methane.<sup>10</sup> Recent results indicate that synthetic metal-organic polymers can offer high levels of thermal stability and can supersede zeolites in terms of surface area and capacity for

small guest molecules. In this context an organic system with H-shaped building block 1,4-di[bis(4'-hydroxyphenyl)methyl]benzene (**22**) and its octamethyl derivative (**23**) were synthesized to analyze the occurrence of specific hydrogen bonded network architectures.<sup>14</sup> Crystallization of **22** (Figure 1) from CH<sub>3</sub>NO<sub>2</sub> with varying amount of CF<sub>3</sub>CH<sub>2</sub>OH afforded two CH<sub>3</sub>NO<sub>2</sub> solvate polymorphs as plate-shaped crystals in space group *Pbca* and block crystals in space group *P2<sub>1</sub>/c* having different network topologies respectively (Figure 3). Our study showed pentagonal (5, <sup>3</sup>/<sub>4</sub>) tiling<sup>15</sup> of hydrogen bonded net in **22**·CH<sub>3</sub>NO<sub>2</sub>, *P2<sub>1</sub>/c* form and **23**·CHCl<sub>3</sub> for the first time (Figure 3) in organic structures using the crystal engineering strategy. Solvent dependent diversity of hydrogen bonded networks and its structural features in the H shaped phenol host were discussed in Chapter 5.

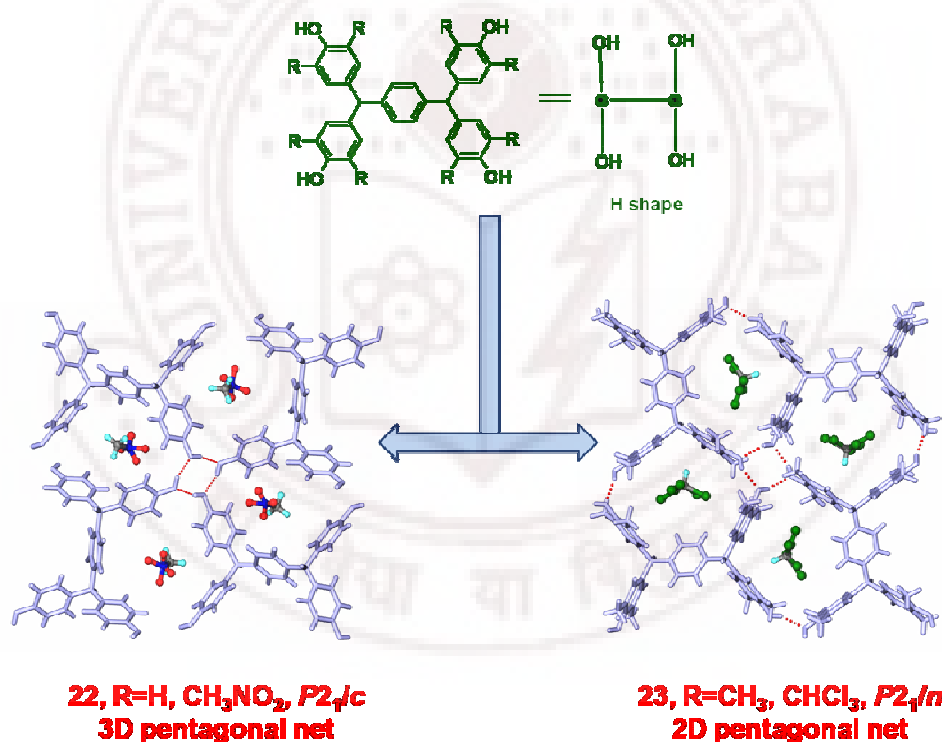


**Figure 3** Simple H-shaped molecule and octamethyl derivative (**22** and **23**) are synthesized and crystallized in solvated and guest free form. **22**• CH<sub>3</sub>NO<sub>2</sub> and **23**• CHCl<sub>3</sub> show rare pentagonal (5, <sup>3</sup>/<sub>4</sub>) net.

## 7.6 Synthron Competition and Cooperation in Cocrystals and Salts

The study of supramolecular synthons between functional groups is a key step in crystal engineering. Competition between hydrogen bonds among different functional groups makes the situation more complicated. In this context it is necessary to establish which synthon is favoured over competing motifs to design a novel structure. Cocrystals, pharmaceutical cocrystals, salts, hydrates have substantial importance in pharmaceutical industry<sup>4</sup> as they modify the properties of drugs. Rational cocrystal design and engineering on the basis of heterosynthon approach in model compounds, APIs and GRAS (Generally Regarded as Safe) molecules, the reliable guidelines that influence the formation of neutral cocrystal or ionic salt based on pK<sub>a</sub> differences between acid and base is still illusive. Our study<sup>16</sup> reflects these circumstances that show hydrogen bond synthon competition and cooperation when four functionalities: carboxylic acid, pyridine, amine, and hydroxyl are simultaneously present in the supramolecular system by taking isomeric and substituted hydroxybenzoic acids and isomeric aminopyridines. 11 cocrystals (Figure 4) are prepared from methanol solvent and their structures were characterized by FT-IR and <sup>1</sup>H-NMR spectroscopy and single crystal X-ray diffraction.

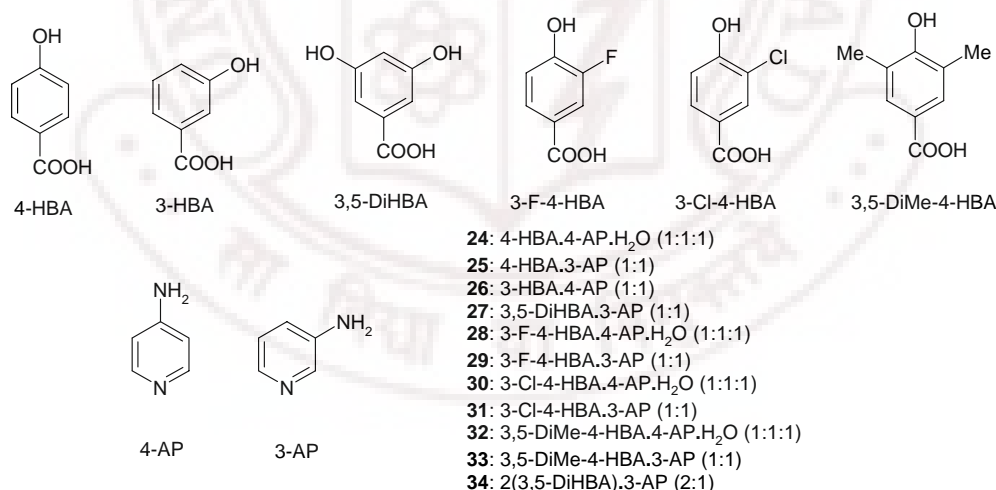


**Figure 4** Hydroxybenzoic acids (HBA) cocrystallized with aminopyridines (AP) and the resulting organic salt composition (24-34). Four are hydrate (24, 28, 30, 32) structures.



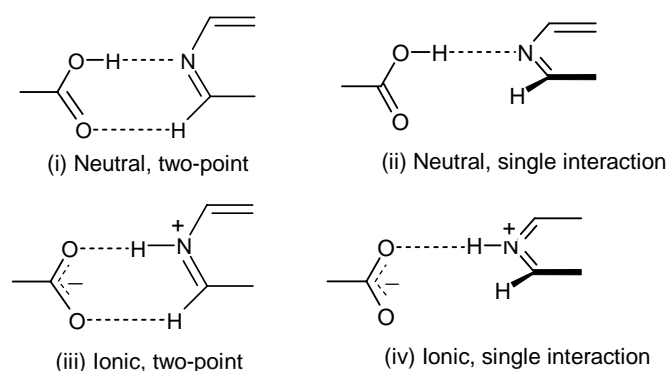


**Figure 5** Observed four variants of acid–pyridine H bonding in crystal structures. The two point synthon i, iii is present when the groups are coplanar but single interaction in ii, iv when the pyridyl ring is twisted out of the COO plane.

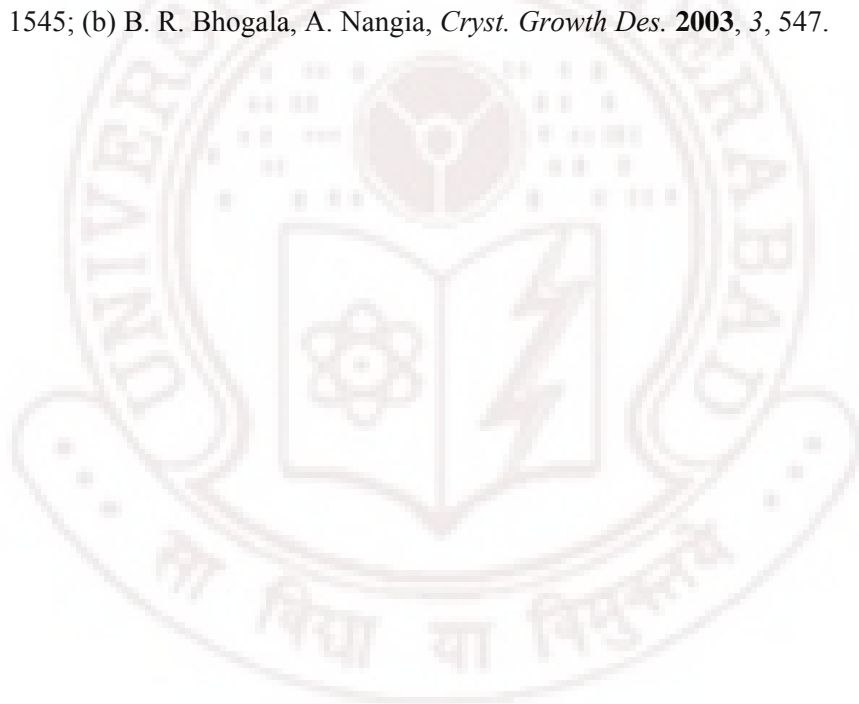
All 11 molecular salts (**24–34**) show proton transfer from COOH to pyridyl N acceptor (PyN) leading to a  $\text{PyNH}^+\cdots\text{OOC}^-$  ionic synthon (Figure 5) in 10 structures (**24–33**) and  $\text{PyNH}^+\cdots\text{O}=\text{C}$  hydrogen bond in **34** where acceptor is neutral. The observed hydrogen bonds were analyzed between  $\text{COO}^-$ , OH,  $\text{NH}_2$ ,  $\text{PyNH}^+$ , and  $\text{H}_2\text{O}$  functional groups in these 11 structures, of which 4 are hydrates (**24, 28, 30, 32**) (Chapter 6). Synthons in this study are compared with statistics extracted from the Cambridge Structural Database to summarize trends and predict hydrogen bonding in new cocrystal and salt structures. It is observed that hydrogen bonding functional groups such as OH and  $\text{NH}_2$  promote persistent formation of ionic  $\text{PyNH}^+\cdots\text{OOC}^-$  synthon in the same supramolecular system, however the  $\Delta\text{pK}_a$  rule for predicting neutral or ionic  $\text{O}-\text{H}\cdots\text{N}/\text{N}^+-\text{H}\cdots\text{O}^-$  hydrogen bonds is found to be inadequate in these systems. Bioavailability of drugs is intimately related to its formulation whether it is a neutral cocrystal or ionic salt.

Polymorphs, salts and cocrystals have the potential to be much more useful in pharmaceutical products than solvates or hydrates because the number of pharmaceutically acceptable solvents is very small, and moreover solvents tend to undergo dehydration/desolvation in the solid dosage forms. The interdisciplinary subject of crystal engineering has overlap with organic chemistry, inorganic chemistry, supramolecular chemistry, X-ray crystallography, materials research, computational chemistry and pharmaceutical chemistry and in current times it is moving from structure design to function fabrication.

## 7.7 References

1. (a) M. Farina, *Inclusion Compounds* (Eds.), J. L. Atwood, J. E. D. Davies, D. D. MacNicol, Academic Press: London, 1984, 2, 69; (b) A. Nangia, *Nanoporous Materials: Science and Engineering* (Eds.), G. Q. Lu, X. S. Zhao, Imperial College Press, London, 2004, pp. 165; (c) L. Infantes, S. Motherwell, *CrystEngComm* **2002**, 4, 454.
2. B. Sarma, S. Roy, A. Nangia, *Chem. Commun.* **2006**, 4918.
3. (a) J. Bernstein, *Polymorphism in Molecular Crystals*, Clarendon Press, Oxford, 2002; (b) N. J. Babu, L. S. Reddy, S. Aitipamula, A. Nangia, *Chem Asian J.* **2008**, 3, 1122; (c) A. Nangia, *Acc. Chem. Res.* **2008**, 41, 595;
4. (a) R. Hilfiker, *Polymorphism in the Pharmaceutical Industry*, Wiley-VCH, Weinheim, Weinheim, 2006; (b) H. G. Brittan, *Polymorphism in Pharmaceutical Solids*, Marcel Dekker, New York, 1999; (c) S. R. Byrn, R. R. Pfeiffer, G. Stephenson, D. J. W. Grant, W. B. Gleason, *Solid State Chemistry of Drugs*, SSCI, West Lafayette, IN, 1999.
5. (a) B. Sarma, A. Nangia, *Acta Crystallogr.* **2008**, A64, C449; (b) B. Sarma, A. Nangia, (manuscript in preparation).
6. (a) T. Gelbrich, M. B. Hursthouse, T. L. Threlfall, *Acta Crystallogr.* **2007**, B63, 621; (b) B. Sarma, A. Nangia (manuscript in preparation); (c) N. Blagden, R. J. Davey, *Cryst. Growth Des.* **2003**, 3, 873; (d) N. Blagden, *Powder Technol.* **2001**, 121, 46.
7. B. Pirotte, B. Maserrel, J. Delarge, *Acta Crystallogr.* **1995**, C51, 507..
8. (a) C. P. Brock, *J. Res. Natl. Inst. Stand. Technol.* **1996**, 101, 321; (b) J. W. Steed, *CrystEngComm*, **2003**, 5, 169; (c) G. R. Desiraju, *CrystEngComm* **2007**, 9, 91.
9. A. L. Grzesiak, M. Lang, K. Kim, A. J. Matzger, *J. Pharm. Sci.* **2003**, 92, 2260.
10. (a) M. E. Davis, *Nature* **2002**, 417, 813; (b) R. E. Morris, P. S. Wheatley, *Angew. Chem. Int. Ed.* **2008**, 47, 4966.
11. (a) T. Tanaka, T. Tasaki, Y. Aoyama, *J. Am. Chem. Soc.* **2002**, 124, 12453; (b) Y. Aoyama, K. Endo, T. Anzai, Y. Yamaguchi, T. Sawaki, K. Kobayashi, N. Kanehisa, H. Hashimoto, Y. Kai, H. Masuda, *J. Am. Chem. Soc.* **1996**, 118,

- 5562; (c) Y. Aoyama, K. Endo, K. Kobayashi, H. Masuda, *Supramol. Chem.* **1995**, *4*, 229.
12. B. Sarma, A. Nangia, *CrystEngComm* **2007**, *9*, 65.
13. (a) G. R. Desiraju, *Crystal Engineering: The Design of Organic Solids*, Elsevier, Amsterdam, 1989; (b) E. R. T. Tiekink, J. J. Vittal (Eds.), *Frontiers in Crystal Engineering*, Wiley, 2006.
14. (a) R. Thakuria, B. Sarma, A. Nangia, *Cryst. Growth Des.* **2008**, *8*, 1471; (c) R. Thakuria, B. Sarma, A. Nangia, *New J. Chem.* **2009**. (In press).
15. (a) S. W. Keller, S. Lopez, *J. Am. Chem. Soc.* **1999**, *121*, 6306; (b) B. Moulton, J. Lu, M. J. Zaworotko, *J. Am. Chem. Soc.* **2001**, *123*, 9224.
16. (a) B. Sarma, N. K. Nath, B. R. Bhogala, A. Nangia, *Cryst. Growth Des.* **2009**, *9*, 1545; (b) B. R. Bhogala, A. Nangia, *Cryst. Growth Des.* **2003**, *3*, 547.





## APPENDIX

Crystallographic data for the structures discussed in this thesis.

| Crystal Data                            | 1s   | 1m   | 2•Acac  |
|---|--|--|---|
| Emp. Formula                            | C <sub>18</sub> H <sub>20</sub> O <sub>2</sub> | C <sub>18</sub> H <sub>20</sub> O <sub>2</sub> | C <sub>33</sub> H <sub>39</sub> O <sub>22</sub> |
| Formula wt.                             | 268.34   | 268.34   | 787.64  |
| Crystal system                          | Triclinic                                      | Orthorhombic                                   | Monoclinic                                      |
| Space group                             | $P\bar{1}$                                     | $Pbca$   | $Cc$  |
| T [K]                                   | 100  | 100  | 298   |
| a [Å]                                   | 6.2275(6)                                      | 9.6278(5)                                      | 9.3556(11)                                      |
| b [Å]                                   | 10.8480(10)                                    | 20.9561(11)                                    | 30.024(3)                                       |
| c [Å]                                   | 11.3359(11)                                    | 28.0324(14)                                    | 13.4635(15)                                     |
| $\alpha$ [°]                            | 101.611(2)                                     | 90   | 90  |
| $\beta$ [°]                             | 103.424(10)                                    | 90   | 104.955(2)                                      |
| $\gamma$ [°]                            | 103.117(2)                                     | 90   | 90  |
| Z                                       | 2  | 16   | 4   |
| Volume [Å <sup>3</sup> ]                | 698.90(12)                                     | 5655.8(5)                                      | 3653.7(7)                                       |
| $D_{\text{calc}}$ [g cm <sup>-3</sup> ] | 1.275  | 1.261  | 1.432   |
| $\mu$ /mm <sup>-1</sup>                 | 0.081  | 0.080  | 0.122   |
| Reflns. collected                       | 7287   | 51362  | 11443   |
| Unique reflns.                          | 2753   | 4984   | 3745  |
| $R_1$ [ $I > 2\sigma(I)$ ], $wR_2$      | 0.0424, 0.1189                                 | 0.0570, 0.1253                                 | 0.0472, 0.1179                                  |
| GOF                                     | 1.046  | 1.115  | 1.011   |

| 2•Diox  | 2•THF   | 2m   | 2s   |
|---|---|--|--|
| C <sub>9</sub> H <sub>10</sub> O <sub>5</sub> | C <sub>32</sub> H <sub>40</sub> O <sub>21</sub> | C <sub>7</sub> H <sub>6</sub> O <sub>4</sub> | C <sub>7</sub> H <sub>6</sub> O <sub>4</sub> |
| 198.17  | 760.64  | 154.12                                       | 154.12                                       |
| Monoclinic                                    | Monoclinic                                      | Monoclinic                                   | Monoclinic                                   |
| $P2_1/c$                                      | $Cc$  | $C2/c$                                       | $C2/c$                                       |
| 100   | 298   | 298  | 298  |
| 14.878(6)                                     | 24.977(2)                                       | 7.3447(15)                                   | 14.101(2)                                    |
| 8.321(4)                                      | 9.1454(9)                                       | 15.015(3)                                    | 22.433(4)                                    |
| 7.027(3)                                      | 19.3903(19)                                     | 6.4840(13)                                   | 14.161(2)                                    |
| 90  | 90  | 90   | 90   |
| 94.826(7)                                     | 129.2530(10)                                    | 111.67(3)                                    | 116.770(2)                                   |
| 90  | 90  | 90   | 90   |
| 4   | 4   | 4  | 24   |
| 866.9(6)                                      | 3429.8(5)                                       | 664.5(2)                                     | 3999.5(11)                                   |
| 1.518   | 1.473   | 1.540  | 1.536  |
| 0.126   | 0.125   | 0.129  | 0.129  |
| 3494  | 11571   | 3372   | 20096  |
| 1264  | 6009  | 653  | 3858   |
| 0.0769, 0.2044                                | 0.0515, 0.1138                                  | 0.0484, 0.1314                               | 0.0964, 0.2170                               |
| 1.064   | 1.022   | 1.078  | 1.083  |

| 3•Form II                                    | 4•H <sub>2</sub> O monoclinic                | 4•pure                                       | 8 Form I (100K)                                   |
|--|--|--|---|
| C <sub>7</sub> H <sub>6</sub> O <sub>4</sub> | C <sub>7</sub> H <sub>8</sub> O <sub>5</sub> | C <sub>7</sub> H <sub>6</sub> O <sub>4</sub> | C <sub>14</sub> H <sub>15</sub> NO <sub>2</sub> S |
| 154.12                                       | 172.13                                       | 154.12                                       | 261.33  |
| Monoclinic                                   | Monoclinic                                   | Triclinic                                    | Monoclinic  |
| <i>P</i> 2 <sub>1</sub> / <i>n</i>           | <i>P</i> 2 <sub>1</sub> / <i>c</i>           | <i>P</i> $\bar{1}$                           | <i>P</i> 2 <sub>1</sub> / <i>n</i>                |
| 298  | 298  | 298  | 100   |
| 5.338(3)                                     | 12.318(3)                                    | 6.8800(8)                                    | 5.1369(5)   |
| 5.486(3)                                     | 3.6448(9)                                    | 8.5444(10)                                   | 17.9280(16)                                       |
| 22.496(11)                                   | 18.182(3)                                    | 17.549(2)                                    | 13.8347(13)                                       |
| 90   | 90   | 77.982(3)                                    | 90  |
| 103.043(8)                                   | 112.516(12)                                  | 85.210(2)                                    | 91.9000(10)                                       |
| 90   | 90   | 85.581(2)                                    | 90  |
| 4  | 4  | 6  | 4   |
| 641.8(5)                                     | 754.1(3)                                     | 1003.6(2)                                    | 1273.4(2)   |
| 1.595  | 1.516  | 1.530  | 1.363   |
| 0.134  | 0.132  | 0.128  | 0.247   |
| 6248   | 6964   | 10622  | 12914   |
| 1268   | 1468   | 3970   | 2485  |
| 0.0480, 0.1155                               | 0.0893, 0.1830                               | 0.0820, 0.1582                               | 0.0388, 0.0945                                    |
| 1.133  | 1.157  | 1.015  | 1.119   |

| 8 Form I (298K)                                   | 8 Form II   | 9 Form I  | 9 Form II   |
|---|---|---|---|
| C <sub>14</sub> H <sub>15</sub> NO <sub>2</sub> S | C <sub>14</sub> H <sub>15</sub> NO <sub>2</sub> S | C <sub>15</sub> H <sub>17</sub> NO <sub>2</sub> S | C <sub>15</sub> H <sub>17</sub> NO <sub>2</sub> S |
| 261.33  | 261.33  | 275.36  | 275.36  |
| Monoclinic  | Monoclinic  | Monoclinic  | Triclinic   |
| <i>P</i> 2 <sub>1</sub> / <i>n</i>                | <i>P</i> 2 <sub>1</sub> / <i>c</i>                | <i>P</i> 2 <sub>1</sub> / <i>c</i>                | <i>P</i> $\bar{1}$                                |
| 298   | 298   | 298   | 298   |
| 5.2133(16)  | 7.6844(6)   | 8.2222(8)   | 7.954(3)  |
| 17.989(5)   | 23.9322(17)                                       | 8.1697(8)   | 8.367(3)  |
| 14.052(4)   | 8.0899(6)   | 21.715(2)   | 12.305(5)   |
| 90  | 90  | 90  | 81.347(5)   |
| 91.659(5)   | 115.0690(10)                                      | 95.0480(10)                                       | 87.854(6)   |
| 90  | 90  | 90  | 64.361(6)   |
| 4   | 4   | 4   | 2   |
| 1317.3(7)   | 1347.62(17)                                       | 1453.0(2)   | 729.5(5)  |
| 1.318   | 1.288   | 1.259   | 1.254   |
| 0.239   | 0.234   | 0.220   | 0.219   |
| 13267   | 13863   | 14612   | 7467  |
| 2626  | 2641  | 2870  | 2835  |
| 0.0738, 0.1767                                    | 0.0424, 0.1107                                    | 0.0478, 0.1249                                    | 0.0434, 0.1182                                    |
| 1.181   | 1.039   | 1.029   | 1.055   |



| 10 Form I   | 10 Form II  | 11  | 12  |
|---|---|---|---|
| C <sub>13</sub> H <sub>11</sub> Cl <sub>2</sub> NO <sub>2</sub> S | C <sub>13</sub> H <sub>11</sub> Cl <sub>2</sub> NO <sub>2</sub> S | C <sub>14</sub> H <sub>14</sub> ClNO <sub>2</sub> S | C <sub>13</sub> H <sub>11</sub> Cl <sub>2</sub> NO <sub>2</sub> S |
| 316.19  | 316.19  | 295.77  | 316.19  |
| Monoclinic  | Monoclinic  | Monoclinic  | Monoclinic  |
| <i>P</i> 2 <sub>1</sub> / <i>n</i>                                | <i>P</i> 2 <sub>1</sub>   | <i>P</i> 2 <sub>1</sub> / <i>n</i>                  | <i>P</i> 2 <sub>1</sub> / <i>n</i>                                |
| 298   | 298   | 298   | 298   |
| 9.495(5)  | 4.9650(8)   | 8.290(3)  | 8.2137(8)   |
| 12.260(6)   | 17.550(3)   | 12.476(5)   | 12.4688(12)   |
| 12.154(6)   | 8.1488(13)  | 13.885(5)   | 14.0076(14)   |
| 90  | 90  | 90  | 90  |
| 97.162(7)   | 102.245(3)  | 98.192(6)   | 101.5720(10)  |
| 90  | 90  | 90  | 90  |
| 4   | 2   | 4   | 4   |
| 1403.7(12)  | 693.88(19)  | 1421.5(9)   | 1405.4(2)   |
| 1.496   | 1.513   | 1.382   | 1.494   |
| 0.607   | 0.614   | 0.412   | 0.606   |
| 13065   | 7110  | 10926   | 14048   |
| 2809  | 2703  | 2836  | 2777  |
| 0.0358, 0.1012  | 0.0544, 0.0939  | 0.0663, 0.1403                                      | 0.0627, 0.1378  |
| 1.056   | 1.057   | 1.079   | 1.336   |

| 13 Form I  | 13 Form II   | 13 Form III  | 14 Form I   |
|--|--|--|---|
| C <sub>12</sub> H <sub>9</sub> Cl <sub>2</sub> NO <sub>2</sub> S | C <sub>12</sub> H <sub>9</sub> Cl <sub>2</sub> NO <sub>2</sub> S | C <sub>12</sub> H <sub>9</sub> Cl <sub>2</sub> NO <sub>2</sub> S | C <sub>13</sub> H <sub>12</sub> ClNO <sub>2</sub> S |
| 302.16   | 302.16   | 302.16   | 281.75  |
| Monoclinic   | Monoclinic   | Monoclinic   | Monoclinic  |
| <i>P</i> 2 <sub>1</sub> / <i>n</i>                               | <i>P</i> 2 <sub>1</sub> / <i>n</i>                               | <i>P</i> 2 <sub>1</sub> / <i>c</i>                               | <i>P</i> 2 <sub>1</sub> / <i>c</i>                  |
| 298  | 298  | 298  | 298   |
| 5.0633(11)   | 5.0365(6)  | 9.4444(10)   | 19.9753(18)   |
| 17.083(4)  | 14.4108(18)  | 12.2349(12)  | 6.1903(5)   |
| 15.300(3)  | 17.988(2)  | 12.3344(12)  | 22.208(2)   |
| 90   | 90   | 90   | 90  |
| 90.485(3)  | 96.856(2)  | 111.4710(10)   | 97.165(2)   |
| 90   | 90   | 90   | 90  |
| 4  | 4  | 4  | 8   |
| 1323.3(5)  | 1296.3(3)  | 1326.3(2)  | 2724.6(4)   |
| 1.517  | 1.548  | 1.513  | 1.374   |
| 0.640  | 0.653  | 0.638  | 0.426   |
| 13467  | 12167  | 11728  | 24906   |
| 2596   | 2294   | 2366   | 4803  |
| 0.0416, 0.1013   | 0.0946, 0.1809   | 0.0447, 0.1141   | 0.0647, 0.1333                                      |
| 1.082  | 1.270  | 1.074  | 1.060   |

| 14 Form II  | 15  | 16   | 17  |
|---|---|--|---|
| C <sub>13</sub> H <sub>12</sub> ClNO <sub>2</sub> S | C <sub>14</sub> H <sub>15</sub> NO <sub>2</sub> S | C <sub>12</sub> H <sub>9</sub> Cl <sub>2</sub> NO <sub>2</sub> S | C <sub>13</sub> H <sub>12</sub> ClNO <sub>2</sub> S |
| 281.75  | 261.33  | 302.16   | 281.75  |
| Monoclinic  | Monoclinic  | Orthorhombic   | Monoclinic  |
| <i>P2<sub>1</sub>/n</i>                             | <i>P2<sub>1</sub>/n</i>                           | <i>Pbca</i>  | <i>P2<sub>1</sub>/c</i>                             |
| 298   | 298   | 298  | 298   |
| 11.083(2)   | 11.1556(8)  | 15.6409(15)  | 10.400(5)   |
| 10.184(2)   | 10.1380(7)  | 7.4161(7)  | 10.989(4)   |
| 24.045(5)   | 24.1724(17)                                       | 23.015(2)  | 11.639(5)   |
| 90  | 90  | 90   | 90  |
| 102.907(3)  | 103.0230(10)                                      | 90   | 98.942(7)   |
| 90  | 90  | 90   | 90  |
| 8   | 8   | 8  | 4   |
| 2645.2(9)   | 2663.5(3)   | 2669.6(4)  | 1314.1(10)  |
| 1.415   | 1.303   | 1.504  | 1.424   |
| 0.439   | 0.236   | 0.634  | 0.442   |
| 26763   | 25971   | 23822  | 12619   |
| 5236  | 5251  | 2360   | 2561  |
| 0.0502, 0.1187                                      | 0.0471, 0.1227                                    | 0.0528, 0.1260   | 0.0671, 0.1425                                      |
| 1.023   | 1.062   | 1.008  | 1.275   |

| 18 Form I  | 18 Form II   | 19   | 20  |
|--|--|--|---|
| C <sub>13</sub> H <sub>12</sub> FNO <sub>2</sub> S | C <sub>13</sub> H <sub>12</sub> FNO <sub>2</sub> S | C <sub>14</sub> H <sub>14</sub> FNO <sub>2</sub> S | C <sub>14</sub> H <sub>14</sub> ClNO <sub>2</sub> S |
| 265.30   | 265.30   | 279.32   | 295.77  |
| Monoclinic   | Monoclinic   | Triclinic  | Triclinic   |
| <i>P2<sub>1</sub>/n</i>                            | <i>P2<sub>1</sub>/c</i>                            | <i>P1</i>  | <i>P1</i>   |
| 298  | 298  | 298  | 298   |
| 8.716(6)   | 9.485(5)   | 8.518(6)   | 8.566(2)  |
| 9.834(7)   | 13.752(8)  | 9.045(7)   | 9.226(2)  |
| 15.410(11)   | 9.822(6)   | 9.189(7)   | 9.307(3)  |
| 90   | 90   | 87.020(9)  | 84.940(3)   |
| 100.176(12)  | 90.881(10)   | 77.933(11)   | 75.128(4)   |
| 90   | 90   | 76.759(11)   | 79.458(4)   |
| 4  | 4  | 2  | 2   |
| 1300.1(16)   | 1281.0(13)   | 674.0(9)   | 698.2(3)  |
| 1.355  | 1.376  | 1.376  | 1.407   |
| 0.254  | 0.258  | 0.249  | 0.419   |
| 10579  | 12074  | 6858   | 7044  |
| 2511   | 2259   | 2657   | 2660  |
| 0.0636, 0.1336                                     | 0.0455, 0.1122                                     | 0.0515, 0.1340                                     | 0.0395, 0.1047                                      |
| 1.054  | 1.071  | 1.059  | 1.043   |

| 21  | 22  | 22•CH <sub>3</sub> NO <sub>2</sub><br>( <i>Pbca</i> Form)   | 22•CH <sub>3</sub> NO <sub>2</sub><br>( <i>P2<sub>1</sub>/c</i> Form)  |
|---|---|---|--|
| C <sub>25</sub> H <sub>16</sub> O <sub>22</sub> S <sub>4</sub><br>796.62<br>Tetragonal<br><i>I4<sub>1</sub>/a</i><br>100<br>21.8492(12)<br>21.8492(12)<br>7.3635(9)<br>90<br>90<br>90<br>4<br>3515.2(5)<br>1.505<br>0.357<br>8258<br>1455<br>0.0634, 0.1436<br>1.005    | C <sub>32</sub> H <sub>26</sub> O <sub>4</sub><br>474.53<br>Triclinic<br><i>P</i> $\bar{1}$<br>100<br>10.1926(10)<br>11.0478(10)<br>13.0960(14)<br>101.849(2)<br>102.082(2)<br>115.675(2)<br>2<br>1224.1(2)<br>1.287<br>0.084<br>12394<br>4633<br>0.0786, 0.1032<br>0.991         | C <sub>34</sub> H <sub>32</sub> N <sub>2</sub> O <sub>8</sub><br>596.62<br>Orthorhombic<br><i>Pbca</i><br>298<br>14.959(3)<br>9.0758(16)<br>22.131(4)<br>90<br>90<br>90<br>4<br>3004.5(10)<br>1.319<br>0.095<br>9523<br>2647<br>0.0582, 0.1060<br>1.003                             | C <sub>34</sub> H <sub>32</sub> N <sub>2</sub> O <sub>8</sub><br>596.62<br>Monoclinic<br><i>P2<sub>1</sub>/c</i><br>298<br>5.2770(9)<br>16.174(3)<br>18.145(3)<br>90<br>95.934(3)<br>90<br>2<br>1540.4(4)<br>1.286<br>0.092<br>14572<br>2703<br>0.0593, 0.1129<br>0.974        |
| 23•CH <sub>3</sub> Cl   | 23•CH <sub>3</sub> NO <sub>2</sub>  | 24  | 25   |
| C <sub>42</sub> H <sub>44</sub> Cl <sub>6</sub> O <sub>4</sub><br>825.47<br>Monoclinic<br><i>P2<sub>1</sub>/n</i><br>298<br>9.992(2)<br>18.203(4)<br>12.043(2)<br>90<br>108.20(3)<br>90<br>2<br>2081.0(7)<br>1.317<br>0.453<br>13916<br>3665<br>0.0718, 0.1725<br>1.037 | C <sub>42</sub> H <sub>48</sub> N <sub>2</sub> O <sub>8</sub><br>708.82<br>Triclinic<br><i>P</i> $\bar{1}$<br>100<br>5.2432(7)<br>12.1351(16)<br>14.5958(18)<br>79.407(2)<br>79.795(2)<br>86.917(2)<br>1<br>898.2(2)<br>1.310<br>0.090<br>6621<br>3159<br>0.0655, 0.1213<br>1.001 | C <sub>24</sub> H <sub>28</sub> N <sub>4</sub> O <sub>8</sub><br>500.50<br>Triclinic<br><i>P</i> $\bar{1}$<br>298<br>7.4783(9)<br>11.7306(13)<br>14.2792(16)<br>87.677(2)<br>77.937(3)<br>83.687(2)<br>2<br>1217.4(2)<br>1.365<br>0.104<br>12791<br>4778<br>0.0468, 0.1174<br>1.043 | C <sub>12</sub> H <sub>12</sub> N <sub>2</sub> O <sub>3</sub><br>232.24<br>Monoclinic<br><i>P2<sub>1</sub>/c</i><br>100<br>11.9491(13)<br>9.0539(10)<br>11.1731(12)<br>90<br>115.0780(10)<br>90<br>4<br>1094.8(2)<br>1.409<br>0.103<br>7276<br>2148<br>0.0351, 0.0904<br>1.052 |

| 26   | 27   | 28  | 29   |
|--|--|---|--|
| $C_{12}H_{12}N_2O_3$<br>232.24<br>Monoclinic<br>$P2_1/c$<br>100<br>8.5521(8)<br>12.7834(12)<br>10.7993(11)<br>90<br>111.6490(10)<br>90<br>4<br>1097.35(18)<br>1.406<br>0.103<br>12031<br>1924<br>0.0348, 0.0906<br>1.081 | $C_{12}H_{12}N_2O_4$<br>248.24<br>Monoclinic<br>$P2_1/n$<br>100<br>9.6416(15)<br>10.5167(16)<br>11.7845(19)<br>90<br>105.398(2)<br>90<br>4<br>1152.0(3)<br>1.431<br>0.109<br>2761<br>1738<br>0.0457, 0.1026<br>1.004 | $C_{12}H_{13}FN_2O_4$<br>268.24<br>Monoclinic<br>$P2_1/c$<br>298<br>7.1711(7)<br>12.8232(13)<br>13.2749(14)<br>90<br>95.314(2)<br>90<br>4<br>1215.5(2)<br>1.466<br>0.121<br>7888<br>2380<br>0.0589, 0.1362<br>1.148 | $C_{12}H_{11}FN_2O_3$<br>250.23<br>Monoclinic<br>$P2_1/c$<br>298<br>12.0905(16)<br>9.0847(12)<br>12.0905(16)<br>90<br>118.3<br>90<br>4<br>1169.2(3)<br>1.421<br>0.114<br>4916<br>2032<br>0.0435, 0.1148<br>1.041 |

| 30   | 31   | 32   | 33   | 34   |
|--|--|--|--|--|
| $C_{12}H_{15}ClN_2O_5$<br>302.71<br>Triclinic<br>$P\bar{1}$<br>298<br>7.9596(10)<br>9.2141(12)<br>10.1006(13)<br>83.020(2)<br>78.551(2)<br>88.151(1)<br>2<br>720.64(16)<br>1.395<br>0.285<br>6953<br>2527<br>0.0900, 0.1873<br>1.183 | $C_{12}H_{11}ClN_2O_3$<br>266.68<br>Monoclinic<br>$P2_1/n$<br>100<br>11.9368(15)<br>8.3774(11)<br>12.6509(17)<br>90<br>109.183(2)<br>90<br>4<br>1194.8(3)<br>1.482<br>0.321<br>7750<br>2094<br>0.0466, 0.1019<br>1.017 | $C_{14}H_{18}N_2O_4$<br>278.30<br>Monoclinic<br>$P2_1/c$<br>298<br>8.7720(9)<br>12.1664(12)<br>14.0288(14)<br>90<br>104.823(2)<br>90<br>4<br>1447.4(3)<br>1.277<br>0.094<br>14306<br>2849<br>0.0493, 0.1195<br>0.954 | $C_{14}H_{16}N_2O_3$<br>260.29<br>Monoclinic<br>$P2_1/c$<br>298<br>11.5274(12)<br>11.9967(12)<br>10.7001(11)<br>90<br>111.328(2)<br>90<br>4<br>1378.4(2)<br>1.254<br>0.089<br>13952<br>2721<br>0.0467, 0.1162<br>1.098 | $C_{19}H_{18}N_2O_8$<br>402.35<br>Orthorhombic<br>$Pccn$<br>298<br>21.8769(11)<br>11.7814(6)<br>14.6796(7)<br>90<br>90<br>90<br>8<br>3783.5(3)<br>1.413<br>0.112<br>36836<br>3691<br>0.0864, 0.1596<br>1.211 |

**X-ray Crystallography:** Reflections were collected on Bruker SMART APEX CCD diffractometer. Mo-K $\alpha$  ( $\lambda = 0.71073$  Å) radiation was used to collect X-ray reflections on all crystals. Data reduction was performed using Bruker SAINT software.<sup>1</sup> Structures were solved and refined using SHELXL-97<sup>2</sup> with anisotropic displacement parameters for non-H atoms. OH and NH hydrogen atoms were located from Fourier map for all crystal structures. All C–H atoms were fixed geometrically. A check of the final CIF file with PLATON<sup>3</sup> did not show any missed symmetry. Crystallographic parameters for all crystal structures are summarized in appendix. All structures are visualized in Mercury 2.2 to see the packing and interactions. Packing diagrams were prepared in X-Seed.<sup>4</sup>

1. *SADABS, Program for Empirical Absorption Correction of Area Detector Data*, G. M. Sheldrick, University of Göttingen, Germany, 1997.
2. *SHELXS-97 and SHELXL-97, Programs for the Solution and Refinement of Crystal Structures*, G. M. Sheldrick, University of Göttingen, Germany, 1997.
3. a) *PLATON, A Multipurpose Crystallographic Tool*, Spek, A. L. Utrecht University, Utrecht, Netherland, 2002; b) A. L. Spek, *J. Appl. Cryst.* **2003**, 36, 7–13.
4. *X-Seed, Graphical Interface to SHELX-97 and POVRay*, L. J. Barbour, University of Missouri-Columbia, Columbia, MO, 1999.

**Neutron Normalization:** The position of hydrogen atom cannot be located accurately in X-ray diffraction. Neutron normalization fixes the D–H distance to its accurate neutron value in X-ray crystal structures. All C–H, O–H and N–H distances are neutron-normalized to 1.083, 0.983 and 1.009 Å in hydrogen bond distance/angle tables.

**FT-Spectroscopy:** Nicolet 6700 FT-IR spectrometer with a NXR FT-Raman Module was used to record IR, NIR and Raman spectra. IR and NIR spectra were recorded on samples dispersed in KBr pellets. Raman spectra were recorded on samples contained in standard NMR diameter tubes or on compressed samples contained in a gold-coated sample holder.

**Thermal Analysis:** DSC was performed on a Mettler Toledo DSC 822e module and TGA was performed on a Mettler Toledo TGA/SDTA 851e module. Samples were placed in open alumina and/or porcelain pans for the TG experiments and in crimped but vented aluminum sample pans for DSC experiments. The typical sample size is 4-6 mg for DSC and 9-12 mg for TGA. Samples were purged by a stream of nitrogen flowing at 150 mL/min for DSC and 80 mL/min for TGA.

**Hot Stage Microscopy:** HSM was performed on a PolythermA hot stage and Heitzsch microscope supplied by Wagner & Munz. A Moticam 1000 (1.3 MP) camera supported by software Motic Image Plus 2.0ML is used to record images. About 1-2 mg of the sample was heated @ 5 K/min.

**Powder X-Ray Diffraction:** Powder XRD of all samples were recorded on a PANalytical 1830 (Philips Analytical) diffractometer using Cu-K $\alpha$  X-radiation ( $\lambda = 1.54056 \text{ \AA}$ ) at 35 kV and 25 mA. Diffraction patterns were collected over  $2\theta$  range of 5-50° at scan rate of 1 °/min. The program Powder Cell 2.3 was used for Rietveld refinement.



---

## ABOUT THE AUTHOR

---

Bipul Ch. Sarma, son of Gobinda Nath Sarma and Ranu Debi, was born in Malikuchi, Nalbari District of Assam, India, in 1979. He received his primary education in Nalbari and completed his secondary school education in Debi Ram Pathsala Higher Secondary School, Nalbari. He then completed his intermediate education from Nalbari College, Assam and B. Sc. from B. Borooah College, Guwahati, Assam. After the completion of his M.Sc. (Organic Chemistry as Special Paper) from Cotton College, Gauhati University, Guwahati, he joined as junior research fellow in a DST sponsored project at Indian Institute of Technology, Guwahati under the supervision of Prof. J. B. Baruah during February 2004 to June 2004 and then he moved to the School of Chemistry, University of Hyderabad to pursue the Ph.D. degree in 2004 under the supervision of Prof Ashwini Nangia. He qualified CSIR-UGC-National Eligibility Test for Junior Research Fellowship (JRF) held in June 2003 and was awarded research fellowship by the Council of Scientific and Industrial Research (CSIR) during 2004-2009 (JRF and SRF). He is the recipient of Dr. K. V. Rao Scientific Society Annual Research Awards for Young Scientist 2009 under the category of Chemistry and Allied Sciences.



---

## RESEARCH PUBLICATIONS

---

1. Polymorphs of 1,1-Bis(4-hydroxyphenyl)cyclohexane and Multiple Z' Crystal Structures by Melt and Sublimation Crystallization.  
**B. Sarma**, S. Roy and A. Nangia  
*Chem. Commun.* **2006**, 4918 – 4920.
2. Tetrakis(4-sulfophenyl)methane dodecahydrate. Reversible and Selective Water Inclusion and Release in an Organic Host.  
**B. Sarma** and A. Nangia  
*CrystEngComm* **2007**, 9, 628 – 631.
3. Coupled Thermal Gravimetric and Infrared Spectroscopic Analysis (TG-IR) in Polymorph Characterization.  
S. Roy, **B. Sarma** and A. Nangia  
*Mettler Toledo Thermal Analysis Newsletter*, **2007**, 1, 9-13.
4. Guest Control in the Self-assembly of H-shaped Host to Cyclopentanoid  $(5,^3_4)$  Net.  
R. Thakuria, **B. Sarma**, and A. Nangia  
*Cryst. Growth Des.* **2008**, 8, 1471 – 1473.
5. Synthron Polymorphism in Dihydroxybenzoic acid  
**B. Sarma** and A. Nangia.  
*Acta Cryst.* **2008**, A64, C449.
6. The Role of  $\pi$ -Stacking in the Composition of Phloroglucinol and Phenazine Cocrystals  
**B. Sarma**, L. S. Reddy and A. Nangia  
*Cryst. Growth Des.* **2008**, 8, 4546 – 4552. (Special Issue on cocrystal and pharmaceutical cocrystals)
7. Synthron Competition and Cooperation in Molecular Salts of Hydroxybenzoic acids and Aminopyridines  
**B. Sarma**, N. K. Nath, B. R. Bhogala and A. Nangia  
*Cryst. Growth Des.* **2009**, 9, 1546 – 1557 (Special Issue on cocrystal and pharmaceutical cocrystals)
8. Supramolecular Networks of H-Shaped Aromatic Phenol Host  
R. Thakuria, **B. Sarma** and A. Nangia  
*New J. Chem.* **2009**, (in press).

9. Polymorphism and Solvent Mediated Phase Transition in Phenylbenzenesulfonamides  
**B. Sarma**, P. Sanphui and A. Nangia  
(Manuscript in preparation)
10. Polymorphs of Isomeric Dihydroxybenzoic Acid  
**B. Sarma** and A. Nangia  
(Manuscript in preparation)
11. Catalytic Oxidative Reactions of Organic compounds by Nitrogen-Containing Copper Complexes.  
N. Barooah, **B. Sarma**, S. Sharma and J. B. Barooah  
*Appl. Organometal. Chem.* 2004, 18, 440 – 445.

